

**A study of an anti-apoptotic modulator present in
*Alcelaphine herpesvirus-1***

Melanie Stowe

**A thesis submitted for the degree of Doctor of
Philosophy in the Faculty of Medicine and Veterinary
Medicine,
University of Edinburgh**

April 2005



Abstract

Malignant catarrhal fever is a fatal lymphoproliferative disease of domestic and wild ruminants. The disease is characterised by lymphocyte migration and proliferation with degeneration of various tissues. This is thought to be responsible for the death of the affected animal. There are two viral causal agents of the disease, *Alcelaphine herpesvirus-1* (AIHV-1) and *Ovine herpesvirus-2* (OvHV-2). AIHV-1 is found naturally in Blue Wildebeest while OvHV-2 is found in sheep. Both cause no apparent disease in the carrier species, however, when they infect a susceptible species, animals develop the disease which is usually fatal. The virulent strain of AIHV-1 has been sequenced and was found to encode eleven putative pathogenesis-associated herpesvirus genes. One of these is contained within open reading frame A9. This encodes a protein that shares a limited amino acid homology to the bcl-2 family of apoptosis regulatory proteins. Apoptosis is a major form of cell death and is characterised by a series of morphological and biochemical changes that take place in the cell. A number of bcl-2 family members have been identified, that can be either anti- or pro-apoptotic. The proteins all possess at least one bcl homology (BH) domain that determines the capacity of the bcl-2 proteins to form homo- or hetero-dimers and/or to bind to proteins not in the bcl-2 family. ORF A9 possesses only one of the BH domains, BH1, which in other proteins has anti-apoptotic activity. The overall aim of this study was to characterise AIHV-1 A9. The specific aims were to determine: if the A9 gene product is functional; when in the viral life cycle A9 is expressed; where in the cell the protein is localised; whether any cellular or viral binding partners can be defined; is the A9 gene expressed in large granular lymphocyte (LGL) T cell lines? Northern blot analyses showed that A9 mRNA was expressed as an early gene in the productive phase of the virus life cycle. The A9 gene product was also shown to protect CHO cells from cis-platin induced apoptosis. The protein encoded by the A9 gene was successfully expressed in *E. coli* and was used to immunise mice and rabbits. Antibodies specific for the A9 protein were generated. However, using these antibodies, the localisation of A9 in CHO cells was inconclusive. A9 mRNA was expressed in LGL T cells from MCF-affected rabbits. To determine binding partners, an expression system involving a tandem affinity purification (TAP) technique was used. Various cDNAs related to the bcl-2 family of proteins were successfully transfected into CHO cells as shown by RT-PCR and immunofluorescence

analysis. However, MADLI analysis of samples failed to identify specific binding partners for A9. A9 vbc1-2 is anti-apoptotic and may function to allow viral replication in infected cells in the productive phase of the life cycle.

Declaration

The work presented in this thesis was carried out at the Moredun Research Institute, Edinburgh. The experimental work and interpretation of the results were undertaken by the author. Contributions to the work in this thesis by colleagues are fully acknowledged in the text.

This work has not been nor is currently being submitted for candidature for any other degree.

Melanie Stowe
Moredun Research Institute
Edinburgh
April 2005

Acknowledgements

I would like to thank the following people for their help during the course of my study and in the preparation of this thesis:

Dr. David Haig for his encouragement and constructive advice.

Dr. Robert Dalziel my university supervisor for his helpful advice and encouragement.

Dr. George Russell for his help with the siRNA and TAP techniques. Furthermore I would like to thank him for his constructive advice and encouragement.

Dr. David Deane for his help with the FPLC, monoclonal antibody production and his useful discussions.

Dr. Harry Wright for his help and for the provision of anti-Bcl-2 rabbit polyclonal antibody.

Miss Jackie Thomson for her assistance performing the caspase-3 assays, continued support and encouragement in and out with the lab.

Miss Iris Campbell for performing the *in vitro* virus infections, the rabbit inoculations and enthusiasm.

Mr. Gareth Young for performing the FACScans.

Mr. Scott Roberts for constructing the pZome-PGK-C vector.

Dr. Thonur Leenadevi for her assistance with RT-PCR on LGL cell lines.

Dr. J.P. Stewart for his kind gift of mtGFP DNA.

Dr. Jeremy Brown for his assistance with the confocal microscopy.

Mr. Kevin McLean for performing the mass spectrometry.

Moredun research Institute for funding this project.

Lastly I would like to thank my parents, my friends and David for their constant support and encouragement throughout this study.

TABLE OF CONTENTS

TITLE	i
ABSTRACT	ii
DECLARATION	iv
ACKNOWLEDGEMENTS	v
TABLE OF CONTENTS	vi
LIST OF ABBREVIATIONS	xiv

CHAPTER 1 GENERAL INTRODUCTION

1.1. Introduction	2
1.2. Herpesviruses	2
1.2.1. Replication of herpesviruses	6
1.2.2. Latency in HSV	8
1.3. Gammaherpesviruses	9
1.3.1. Epstein-Barr virus (EBV)	9
1.3.2. EBV lytic replication	9
1.3.3. EBV latency	11
1.3.4. Murine herpesvirus-68 (MHV-68)	12
1.3.5. Kaposi's sarcoma-associated Herpesvirus (Human herpesvirus-8)	14
1.3.6. KSHV lytic replication	15
1.3.7. KSHV latency	16
1.3.8. Herpesvirus saimiri (HVS)	17
1.3.9. Other gammaherpesviruses of veterinary importance	18
1.4. Malignant catarrhal fever (MCF)	23
1.4.1. Epidemiology	23
1.4.2. Clinical Symptoms	24
1.4.3. MCF Pathology	25
1.4.4. MCF Histopathology	27
1.4.5. Transmission to susceptible species	27
1.4.6. Experimental transmission of MCF	28
1.4.7. <i>Alcelaphine herpesvirus-1</i> (AIHV-1)	29
1.4.8. <i>Ovine herpesvirus-2</i> (OvHV-2)	34
1.4.9. Other viruses implicated in MCF	37
1.4.10. Diagnosis and prevention of MCF	37
1.4.11. Vaccines for MCF viruses	39

2.3.11.	QIAquick gel extraction	76
2.3.12.	Polymerase chain reaction (PCR)	77
2.3.13.	Agarose gel electrophoresis of DNA	78
2.3.14.	Agarose gel electrophoresis including crystal violet	78
2.4. RNA Analysis		79
2.4.1.	Extraction of total cellular RNA	79
2.4.2.	Northern blotting	79
2.4.3.	Reverse transcription polymerase chain reaction (RT-PCR)	81
2.5. Protein Analysis		81
2.5.1.	Sodium dodecylsulphate – polyacrylamide gel electrophoresis (SDS-PAGE)	81
2.5.2.	Protein detection in SDS-PAGE gels	82
2.5.3.	Western blot analysis (immuno-detection of gel-separated proteins)	82
2.5.4.	Measurement of protein concentration	83
2.6. Protein-protein interactions		84
2.6.1.	Tandem affinity purification (TAP)	84
2.6.1.1.	Construction of fusion AIHV-1 and EBV proteins in <i>E. coli</i>	84
2.6.1.2.	Transfection of TAP-tagged fusion DNA into CHO cells	88
2.6.1.3.	Harvesting transfected CHO cells	88
2.6.1.4.	Purification of TAP-tagged proteins	88
2.6.2.	Identification of protein interactions by immunoprecipitation	89
2.7. Anti-A9 antibody production		90
2.7.1.	Construction of recombinant AIHV-1 A9 protein in <i>E. coli</i>	90
2.7.1.1.	Expression of recombinant AIHV-1 A9 protein in <i>E. coli</i>	90
2.7.1.2.	Induction of protein synthesis	92
2.7.1.3.	Harvesting recombinant thioredoxin fusion protein	92
2.7.2.	Affinity Purification of recombinant thioredoxin-A9 fusion protein using ThioBond™ columns	92
2.7.3.	Purification of thioredoxin recombinant protein by electroelution	93
2.7.4.	Immunisation of animals	93
2.7.5.	Production of A9 protein specific monoclonal mouse antibodies	94
2.7.6.	Enzyme linked immuno-sorbent assay (ELISA)	95
2.8. Apoptosis assays		96
2.8.1.	Cells	96
2.8.2.	Induction of apoptosis	96
2.8.3.	Extraction of DNA	97
2.8.4.	Caspase-3 assay	98
2.8.5.	Diff-Quik assay	99

CHAPTER 3	Sequence analysis of ORF A9, production of recombinant A9 viral Bcl-2 and specific antisera	100
3.1. Introduction		101
3.2. Materials and methods		103
3.2.1.	Expression of a GST-A9 fusion protein	103
3.2.2.	Expression of a GST-truncated A9 fusion protein	103
3.2.3.	Solubilisation of proteins	104
3.2.4.	Dialysis of GST-A9 fusion protein	104
3.2.5.	Expression of recombinant thioredoxin-A9 fusion protein in <i>E. coli</i>	104
3.2.6.	Purification of recombinant thioredoxin-A9 protein using ThioBond	104
3.2.7.	Purification of thioredoxin recombinant protein by electroelution	105
3.2.8.	Cleavage of thioredoxin-A9 fusion protein using EnterokinaseMax™	105
3.2.9.	Construction of β -Gal-A9 fusion protein	106
3.2.10.	Production of monoclonal mouse antibodies against recombinant A9 protein	106
3.2.11.	Testing of antisera by ELISA	106
3.2.12.	Isotyping antibodies	107
3.2.13.	Purification of mouse anti-A9 serum 6E1 using IgM-sepharose	107
3.2.14.	Production of polyclonal rabbit antibodies against recombinant A9 protein	107
3.2.15.	Purification of anti-A9 serum using ammonium sulphate precipitation	108
3.2.16.	Transfection of CHO cells with A9 and EBV BHRF1 cDNAs	108
3.2.17.	Indirect immunofluorescence assay	108
3.3. Results		109
3.3.1.	Sequence analysis of ORF A9	109
3.3.2.	Expression of a GST-A9 fusion protein	111
3.3.3.	Expression of thioredoxin-A9 fusion protein in bacteria	114
3.3.4.	Polyclonal antiserum reacts with the Trx-A9 recombinant protein	116
3.3.5.	A9 expression in A9-CHO cells	117
3.3.6.	Monoclonal antibody specific for the A9 protein	118
3.3.7.	Purification of mouse antiserum 6E1 using an anti-mouse IgM column	121
3.3.8.	Detection of AIHV-1 A9 protein in transfected CHO cells	122
3.3.9.	Rabbit polyclonal antiserum reacts with A9 vBcl-2 recombinant protein	124

3.3.10.	Rabbit anti-A9 serum reacts with the A9 protein expressed by CHO cells	125
3.3.11.	Expression of EBV BHRF1 vBcl-2 in CHO cells	126
3.4. Discussion		127
 CHAPTER 4 ORF A9 EXPRESSION IN AIHV-1- INFECTED BOVINE TURBINATE CELLS AND LGL T CELL LINES		130
4.1. Introduction		131
4.2. Materials and methods		135
4.2.1.	Treatment and infection of BT cells	135
4.2.2.	Northern blot analysis of A9 gene expression	135
4.2.3.	Expression of A9 gene in LGLs	136
4.2.4.	Localisation of the A9 proteins in transfected CHO cells	136
4.2.5.	Expression of A9 protein in LGLs	136
4.2.6.	siRNA expression	137
4.2.7.	FACS analysis of rabbit cells	138
4.3. Results		140
4.3.1.	Expression of A9 gene in the lytic virus life cycle	140
4.3.2.	Cellular localisation of A9 protein	142
4.3.3.	Phenotypic analysis of AIHV-1 LGL T cells	145
4.3.4.	Expression of A9 gene in LGL cell lines	151
4.3.5.	Immunofluorescence analysis of A9 expression on AIHV-1 infected LGL T cell lines	153
4.3.6.	Attempts to silence the A9 gene by RNA interference	155
4.4. Discussion		156
 CHAPTER 5 THE APOPTOTIC FUNCTION OF ORF A9 GENE PRODUCT		161
5.1. Introduction		162
5.2. Materials and methods		164
5.2.1.	Cells used	164
5.2.2.	Viability assay	164
5.2.3.	Frequency of cells expressing proteins	164
5.2.4.	Caspase-3 assay	165
5.2.5.	Diff-quick assay	165

5.2.6.	DNA fragmentation assay	165
5.3. Results		166
5.3.1	Frequency of CHO cells expressing BHRF1 or A9	166
5.3.2	Viability assay	166
5.3.3	Diff-quick assay	168
5.3.4	DNA fragmentation assay	171
5.3.5	Caspase-3 assay	173
5.4. Discussion		174
CHAPTER 6	IDENTIFYING PUTATIVE	177
	BINDING PARTNERS OF THE A9 PROTEIN	
6.1. Introduction		178
6.2. Materials and methods		180
6.2.1.	Expression of A9 mRNA analysed by Northern blot	180
6.2.2.	Immunoprecipitation of Bcl-2 proteins	180
6.2.3.	Construction of TAP-tagged fusion in <i>E. coli</i>	180
6.2.4.	Immunostaining of TAP-tagged fusion proteins transfected in CHO cells	180
6.2.5.	Expression of TAP-tagged fusion proteins	181
6.2.6.	Purification of TAP-tagged fusion proteins	181
6.2.7.	Preparing samples for mass spectrometry analysis	181
6.2.8.	Mass Spectrometry	182
6.3. Results		183
6.3.1.	Attempting immunoprecipitation of binding proteins for A9 vBcl-2 in CHO cells	183
6.3.2.	Attempts to immunoprecipitate A9 vBcl-2-binding partners from <i>Cos-1</i> cells	184
6.3.3.	Generation of TAP-A9 and BHRF1 CHO cells	187
6.3.4.	Immunostaining of TAP-A9 fusion protein in CHO cells	187
6.3.5.	Detection of TAP-tagged fusion proteins in CHO cells	189
6.3.6.	Attempts to identify TAP-A9 vBcl-2 and TAP-BHRF1 vBcl-2 binding partners	190
6.3.7.	MALDI/Mass spectrometry analysis of protein bands	191
6.4. Discussion		192
CHAPTER 7	GENERAL DISCUSSION	195

REFERENCES	211
APPENDICES	238
PROCEEDINGS OF MEETINGS	241

FIGURES AND TABLES

FIG 1.1: Schematic diagram of sequence arrangement of HSV-1.	7
FIG 1.2: Comparison of the genetic organisation among some of the gammaherpesviruses.	22
FIG 1.3: MCF kidney and liver histology.	26
FIG 1.4: The Genome Organisation of Alcelaphine Herpesvirus -1.	33
FIG 1.5: Genome Organisation of Ovine Herpesvirus 2.	36
FIG 1.6: Apoptosis can be initiated by ligand binding.	48
FIG 1.7: Comparisons of Bcl-2 protein domains.	52
FIG 1.8: Possible mechanisms of cytochrome <i>c</i> release during apoptosis.	56
FIG 1.9: Possible mechanisms of cytochrome <i>c</i> release during apoptosis.	58
FIG 2.1: Vector pZome-1-C.	86
FIG 2.2: Vector pZome-PGK-C.	87
FIG 2.3: Vector pTrxFus.	91
FIG 3.1: Clustal W analysis of viral and cellular Bcl-2 proteins.	110
FIG 3.2: A9-GST fusion proteins in <i>E. coli</i> lysates detected by Coomassie blue staining.	111
FIG 3.3: Truncated GST-A9 fusion proteins in <i>E. coli</i> lysates detected by Coomassie blue staining.	113
FIG 3.4: GST-A9 fusion proteins in <i>E. coli</i> lysates solubilised in 8M urea detected by Coomassie blue staining.	113
FIG 3.5: Recombinant thioredoxin-A9 fusion protein in <i>E. coli</i> lysates detected by Coomassie blue staining.	115
FIG 3.6: Recombinant thioredoxin-A9 protein purified using Thiobond at various concentrations of β -mercaptoethanol to elute the bound protein detected by Silver staining.	115
FIG 3.7: Western blot of recombinant thioredoxin-A9 fusion protein.	115
FIG 3.8: Western blot of EnterokinaseMax™ digested thioredoxin-A9 fusion protein.	116
FIG 3.9: Northern blot analysis of GAPDH and ORF A9 expression in A9-CHO cells	117
FIG 3.10: Fluorescence images of A9-CHO and UTF CHO cells.	120
FIG 3.11: Antiserum to thioredoxin-A9 purified on an anti-IgM-sepharose column.	121
FIG 3.12: Fluorescent images of CHO cells labelled with anti-A9 and control antibody.	123
FIG 3.13: Western blot analysis of rabbit antibody specific for the A9 protein.	124
FIG 3.14: Fluorescent images of A9CHO cells incubated with serum from an immunised rabbit.	125

FIG 3.15: Reaction of anti-BHRF1 with CHO cells expressing BHRF1 protein and in UTF CHO cells	126
FIG 4.1: siRNA production by the pSuper system.	134
FIG 4.2: Northern blot analysis of GAPDH and ORF A9 expression.	141
FIG 4.3: Confocal microscopy images of A9-CHO cells.	143
FIG 4.4: Cellular localisation of A9.	144
FIG 4.5: FACS profiles	147
FIG 4.6: RT-PCR GAPDH-specific primers	152
FIG 4.7: RT-PCR analysis using ORF A9 specific primers.	152
FIG 4.8: Immunofluorescence analysis of LGL T cells.	154
FIG 4.9: Northern blot analysis of RNA interference of A9 expression	155
FIG 5.1: The percentage of surviving cells after incubation with various doses of cis-platin at various time points throughout the assay.	167
FIG 5.2: CHO cells 24hrs after treatment with 25µM cis-platin stained with the Diff-quick (Dade Behring) staining method.	162
FIG 5.3: The number of apoptotic cells at various time points after incubation with 25µM cis-platin.	170
FIG 5.4: Agarose gel electrophoresis showing typical “DNA laddering” associated with apoptosis	172
FIG 5.5 Caspase-3 apoptosis assay.	
FIG 5.6: The number of apoptotic cells at various time points after incubation with 25µM cis-platin.	168
FIG 6.1: Fluorescent images of A9-CHO cells incubated with serum from rabbit.	183
FIG 6.2: SDS-Page gel of immunoprecipitated CHO cell lysate proteins.	186
FIG 6.3: Immunoprecipitated cell lysate proteins detected by Coomassie blue staining.	186
FIG 6.4: Immunoprecipitated <i>cos</i> cell lysates protein detection by western blotting.	186
FIG 6.5: Immunofluorescence analysis of TAP-tagged transfected CHO cell lines.	188
FIG 6.6: Western blot analysis of TAP-tagged fusion proteins.	189
FIG 6.7: Silver stained gel of TAP purified lysates.	190
FIG 6.8: Mass spectrum of purified samples.	191
FIG 7.1: Sequence alignment based on the predicted secondary structure of AIHV-1 A9 and the observed secondary structure of human Bcl-x _L .	201
FIG 7.2: Predicted structure of the A9 protein.	202
TABLE 1.1: Example of herpesviruses in different subfamilies.	5
TABLE 1.2: AIHV-1 and OvHV-2 ORFs	33
TABLE 2.1: Antibodies and conjugates used in immunostaining.	71
TABLE 3.1: Typical ELISA assay using hybridoma supernates	119
TABLE 3.2: Typical ELISA assay values.	119
TABLE 4.1: Virus titres used in the expression experiment.	135
TABLE 4.2: Selected markers and the use.	139
TABLE 4.3: Detection of cell surface markers on rabbit MCF cell lines.	146
TABLE 6.1: Antibodies and conjugates used.	180

Abbreviations

A	Adenine
AIF	Apoptosis inducing factor
AIHV-1	Alcelaphine herpesvirus-1
ANT	Adenine nucleotide translocator
APS	Ammonium persulphate
ATP	Adenosine triphosphate
BALF	<i>Bam</i> HI 'A' fragment leftward reading frame
BCA	Bicinchoninic acid
Bcl	B cell lymphoma
BH	Bcl-2 homology
BHRF	<i>Bam</i> HI H rightward transcripts
BHV	Bovine herpesvirus-1
BRFL1	<i>Bam</i> HI M leftward transcripts
BSA	Bovine serum albumin
BT	Bovine turbinata
BZLF	<i>Bam</i> HI Z leftward open reading frame
C	Cytosine
CAD	Caspase-activated deoxyribonuclease
CBP	Calmodulin binding peptide
CCPH	Complement control protein homologue
CDK	Cyclin-dependent kinase
CI-ELISA	Competition inhibition enzyme-linked immunosorbent assay
Cis-platin	Cis-platinum dichloroamine II
CHO	Chinese hamster ovary
CPE	Cytopathic effect
CpHV-2	Caprine herpesvirus-2
CO ₂	Carbon dioxide
COX	Cytochrome <i>c</i> oxidase
CTL	Cytotoxic T lymphocyte
dATP	2'-deoxyadenosine 5'-triphosphate
dCTP	2'-deoxycytidine 5'-triphosphate
DDT	Dithiotreitol
dFBS	heat inactivated dialysed foetal bovine serum
DiOC ₆ (3)	3,3'-dihexyloxacarbocyanine iodide
DMSO	Dimethyl sulphoxide
DNA	Deoxyribonucleic acid
dNTP	Deoxynucleoside triphosphate
DHRF	Dihydrofolate reductase
EBER	Epstein Barr virus-encoded small RNA
EBNA	Epstein Barr virus nuclear antigen
EBV	Epstein Barr virus
ECL	Enhanced chemoluminescence
EDTA	Ethylene diaminetetraacetic acid

EGTA	Ethylene Glycol-bis (β -aminoethyl Ether)
EHV	Equine herpesvirus-1
ELISA	Enzyme linked immuno-sorbent assay
FADD	Fas associated death domain
FAS	
FASL	Fas ligand
FBS	Foetal bovine serum
FITC	Fluoresceine isothiocyanate
FLICE	FADD homologous ICE/CED-3-like protease
FLIP	FLICE-inhibitory protein
G	Guanine
G + A	1-glutamic acid + 1-asparagine
GAPDH	Glyceraldehyde 3-phosphate dehydrogenase
GMEM	Glasgow's modified Eagle medium
gp	Glycoprotein
GPCR	G-coupled protein receptor
HAT	Hypoxanthine aminopterin thymidine
HCF	Host cell factor
HCMV	Human cytomegalovirus
H-DNA	High G+C content DNA
HHV-6	Human herpesvirus-6
HHV-7	Human herpesvirus-7
HipHV-1	Hippotrachine herpevirus-1
hrIL-2	recombinant human interleukin-2
HRP	Horseradish peroxide
HSV	Herpes simplex virus-1
HVS	Herpesvirus saimiri
JAK	Janus kinases
JC-1	5,5', 6,6'-tetrachloro-1,1',3,3'-tetraethylbenzimidazolcarbocyanine
Kb	Kilobase
KS	Kaposi's sarcoma
KSHV	Kaposi's sarcoma herpesvirus
ICAD	Inhibitor of caspase-activated deoxyribonuclease
IL	Interleukin
IFN	Interferon
Ig	Immunoglobulin
IMDM	Iscove's modification of Dulbecco's medium
IPA	Isopropanol
IPTG	Isopropyl- β -D-thiogalactopyranoside
IRF	Interferon-responsive factor

l	Litre
LAT	Latency-associated transcript
LANA	Latency associated nuclear antigen
LB	Luria Bertani medium
L-DNA	Low G+C content DNA
LGL	Large granular lymphocyte
LMP	Latent membrane protein
LP	Leading protein
LPD	Lymphoproliferative disease
MCF	Malignant catarrhal fever
MCD	Multicentric Castleman's disease
MHC	Major histocompatible complex
MHV-68	Murine herpesvirus-68
ml	Millilitre
MOPS	Morpholinepropanesulphonic acid
MSX	Methionine sulfoxamine
NF κ B	Nuclear factor κ B
NK	Natural killer
NMR	nuclear magnetic resonance
Oct-1	Cellular octamer binding protein
OD	Optical density
OH	
ori	origin of replication
ORF	Open reading frame
OvHv-2	Ovine herpesvirus-2
PAGE	Polyacrylamide gel electrophoresis
PBS	Phosphate buffer saline
PCR	Polymerase chain reaction
PEG	Polyethylene glycol
PEL	Primary effusion lymphoma
PGK	Phosphoglycerate kinase
PIERCE	Protein assay reagent kit
PKR	Protein kinase R
PLHV-1	Porcine herpesvirus-1
PLHV-2	Porcine herpesvirus-2
PTLD	Posttransplant lymphoproliferative disease
PTP	Permeability transition pore
PS	Phosphatidylserine
RCA	Regulators of complement activation
RNA	Ribonucleic acid
RPMI	Roswell park memorial institute
Rta	R-transactivator
RT-PCR	Reverse transcription PCR

SA-MCF	Sheep-associated MCF
SDS	Sodium dodecyl sulphate
SSC	Standard saline citrate
STAT	Signal transducer and activation of transcription
STP-A	Saimiri transformation protein
T	Thymine
TAE	Tris acetate EDTA
TAP	Tandem affinity purification
TBE	Tris borate EDTA
TCID ₅₀	Tissue culture infective dose
TEMED	Tetramethylethylenediamine
TEV	Tobacco etch virus
TNF	Tumour necrosis factor
TPA	12-O-tetradecanoyl phorbol-13 acetate
TS	Thymidylate synthetase
UTF	Untransfected
UV	Ultraviolet (light)
vCKR	Viral cytokine receptors
VDAC	Voltage dependent anion channel
vFLIP	Viral FLICE inhibitory protein
vMIP-1 α/β	Viral macrophage inflammatory protein 1 α/β
VZV	Varicella zoster virus
X-Gal	5-bromo-4-chloro-3-indolyl- β -D-galactopyranoside
Zta	Z-transactivator
α	Alpha
β	Beta
β -ME	Beta-mercaptoethanol
γ	Gamma
μ g	Microgram
μ l	Microlitre
μ M	Micromolar

Chapter 1

General Introduction

1.1. Introduction

Malignant catarrhal fever (MCF) is an often fatal disease of domestic and wild ruminants, which occurs worldwide (Plowright, 1960; Castro & Daley, 1982; Handley *et al.*, 1995). The disease is usually acute and is characterised by lymphocyte migration and proliferation resulting in the degeneration of various tissues which is thought to be responsible for the demise of affected animals (Reid & Buxton, 1989). MCF is caused by either of two gammaherpesviruses *Alcelaphine herpesvirus-1* (AIHV-1) or *Ovine herpesvirus-2* (OvHV-2) although others have been implicated. AIHV-1 MCF is restricted to Africa and zoological collections, whereas OvHV-2 MCF is seen worldwide. The current hypothesis is that the disease is caused by lymphocytes dysregulated by virus infection that exhibit constitutive non MHC-restricted cytotoxic activity and that destroy multiple tissues *in vivo* (Aiello, 1998; Swa *et al.*, 2001).

1.2. Herpesviruses

The interaction between herpesviruses and their mammalian hosts has been studied in detail (Roizman, 1990). Herpesviruses can infect the host with mild or no apparent symptoms, however, they can also cause fatally incurable diseases. To date there have been over one hundred different herpesvirus species identified. They all share common biological features:

- They express enzymes and other factors that are involved in nucleic acid metabolism (e.g. thymidylate kinase, thymidylate synthetase and dUTPase) as well as a variable number of enzymes that are involved in nucleic acid synthesis (e.g. DNA polymerase, helicase) and protein processing (e.g. protein kinases).
- The synthesis of viral DNA and capsids occurs in the nucleus. Herpesvirus DNA circularises immediately upon the release from capsids into the nuclei of infected cells.
- The production of infectious progeny virus is accompanied by the irreversible destruction of the infected cell.

- Herpesviruses have the ability to establish and remain in a latent phase in the natural host. In cells harbouring latent virus the viral genome takes the form of closed circular molecules, and only a small subset of viral genes are expressed (Roizman *et al.*, 1992).

A typical herpesvirion consists of a core containing linear double stranded DNA, an icosohedral capsid of 100–110nm in diameter and the tegument, which is surrounded by a membrane envelope. Viral glycoproteins protrude from the envelope. The total size of the herpesvirus particle varies between 120-300nm. This variation is thought to be due to the variability in the thickness of the tegument. The double stranded DNA genomes range from 120-230kb and with G+C DNA contents varying from 32-75% (Roizman, 1990).

Herpesviruses are classified into families or subfamilies based on their natural host (Roizman & Baines, 1991). The herpesvirus family *Herpesviridae* has been further classified into three subfamilies *Alphaherpesvirinae*, *Betaherpesvirinae* and *Gammaherpesvirinae* on the basis of the following biological properties.

Alphaherpesviruses have a variable host range, short reproductive cycle (i.e. approximately 12-24 hours) and the ability to spread rapidly in culture. These viruses establish a latent infection in neuronal cells (sensory ganglia). This subfamily contains the genera *Simplexvirus* (e.g. Human simplex virus-1 (HSV-1) and bovine mamillitis (BHV-2)) and *Varicellovirus* (e.g. Varicella zoster virus (VZV or HHV-3) and equine herpesvirus 1 (EHV-1)).

Betaherpesviruses have a restricted host range, relatively long reproductive cycle (i.e. 3-6 days) and spread slowly in culture. Infected cells frequently become enlarged, forming cytomegalia. A latent infection can be maintained in lymphoreticular cells, secretory glands, kidneys and other tissues. This subfamily contains the genera *Cytomegalovirus* (e.g. human cytomegalovirus (HCMV or HHV-5)) and *Muromegalovirus* (e.g. murine cytomegalovirus) and *Roseolovirus* (e.g. human herpesvirus-6 (HHV-6) and human herpesvirus-7 (HHV-7)).

Gammaherpesviruses have a narrow host range. *In vitro* replication occurs in lymphoblastoid cells as well as some types of epithelial and fibroblastic cells. The viruses show specificity for either T or B-lymphocytes and have the ability to establish a latent infection in lymphoid tissue. This family contain two genera *Lymphocryptovirus* (e.g. Epstein-Barr virus (EBV)) and *Rhadinovirus* (e.g. herpesvirus saimiri (HVS)) (Roizman, 1990). Viruses belonging to the subfamilies of herpesviruses are summarised in Table 1.1.

Virus	Natural reservoir	Disease
<i>Alphaherpesviruses</i>		
Herpes simplex virus 1 (HSV-1)	Human	Cold sores, keratitis, ocular disease
Herpes simplex virus 2 (HSV-2)	Human	Genital herpes
Varicella-zoster virus (VZV or HHV-3)	Human	Chicken pox (Varicella) and shingles (zoster)
Bovine Herpesvirus-1 (BHV-1)	Bovine	Infectious bovine rhinotracheitis, genital disease
Porcine Herpesvirus-1 (PLHV-1)	Pigs	Pseudorabies
<i>Betaherpesviruses</i>		
Human cytomegalovirus (HCMV or HHV-5)	Human	Mononucleosis
Human herpesvirus-6 (HHV-6)	Human	Fever and rash in children, mononucleosis in adults
Human herpesvirus-7 (HHV-7)	Human	Roseola infantum
<i>Gammapherpesviruses</i>		
Epstein-Barr virus (EBV or HHV-4)	Human	Infectious mononucleosis, Burkitt's lymphoma
Kaposi's sarcoma Herpesvirus (KSHV or HHV-8)	Human	Kaposi's sarcoma, Primary effusion lymphoma, multicentric Castleman's disease
Bovine Herpesvirus-4 (BHV-4)	Cattle	Conjunctivitis, respiratory infections
Herpesvirus saimiri (HVS)	Squirrel monkey	Lymphoproliferations in cottontail rabbits & new world monkeys
Murine Herpesvirus-68 (MHV-68)	Rodents	Lymphomas, pneumonia (experimental)
Alcelaphine Herpesvirus-1 (AIHV-1)	Wildebeest	Malignant catarrhal fever in cattle
Ovine Herpesvirus-2 (OvHV-2)	Sheep	Malignant catarrhal fever in cattle

Table 1.1 Examples of herpesviruses in different subfamilies

1.2.1. Replication of Herpesviruses

HSV-1 replication has been studied in detail (Roizman, 2001). Infection is initiated when the virus attaches to the cell surface. It has been shown that the most important viral proteins that are involved in this attachment are the envelope glycoproteins gB and gC, these bind to cell surface glycosaminoglycans, preferentially heparan sulphate (reviewed in Rajčáni & Vojvodvá, 1998). The fusion of the viral and cellular membranes is triggered by the interaction of a third glycoprotein, gD with one of several cellular co-receptors. These co-receptors include members of the tumour necrosis factor receptor family, members of the immunoglobulin superfamily nectins (a family of cell adhesion molecules) and 3-O-sulphated heparin sulphates (reviewed in Spear *et al.*, 2000). Fusion of the viral envelope with the host cell membrane requires gB, gD and a gH-gL heterodimer. It has been demonstrated that gB, gD, gH, and gL and the presence of one or more cellular gD receptors are indispensable for mediating fusion (Turner *et al.*, 1998). Fusion of the envelope with the plasma membrane results in the capsid being transported to the nuclear pores to release the DNA into the nucleus. Transcription and replication of the viral DNA and assembly of the new capsids occurs in the nucleus. Viral DNA is transcribed by host RNA polymerase and mRNA is translated in the cytoplasm (Roizman & Sears, 1990). Gene expression in the lytic phase occurs in a chronological order that can be grouped into three categories; immediate early, early and late.

Immediate early transcription of HSV-1 is activated by a virion protein, VP16, which acts through the target sequence TAATGARAT (Sturm *et al.*, 1988). The target sequence is a binding site for the cellular octamer DNA-binding protein, Oct-1. VP16 and host cell factor (HCF) bind to the Oct-1/TAATGARAT complex bringing it into proximity with the preinitiation complex. The immediate early proteins transactivate early gene expression and are required for the synthesis of all other viral-encoded proteins (Roizman & Sears, 1990). The early proteins include enzymes that are required for the replication of the viral genome: a DNA polymerase, a single stranded DNA binding protein, a primosome (complex of proteins that are involved in DNA synthesis), an origin-binding protein and a set of enzymes that are involved in DNA repair. The late

genes are expressed finally and these encode the structural proteins of the virus (Lehman & Boehmer, 1999).

When the viral DNA enters the nucleus it adopts an “endless” configuration, which is consistent with circularisation. The origin of replication can be ori_S , of which there are two copies in the ‘c’-sequences (Ir_S , Tr_S) of the genome, or ori_L of which there is one copy in the U_L region of the genome (fig. 1.1). It has been suggested that HSV-1 DNA replication initiates by a *theta* mechanism, named after the appearance of the DNA resembling the Greek letter θ . Studies have shown that at some stage *theta* replication changes to the rolling circle mode, which is the principal mode of replication. In the rolling circle mode, DNA replication produces long head to tail concatamers (Lehman & Boehmer, 1999).

Recent studies of HSV genome configuration during early infection suggest this model may need to be revised. A study carried out by Jackson and DeLuca (2003) failed to observe circular genomes in wild type HSV-infected cells before the onset of DNA synthesis, which would suggest that circular genomes may not be the initial replication template. They also demonstrated that ICP0 inhibited the formation of circular genomes.

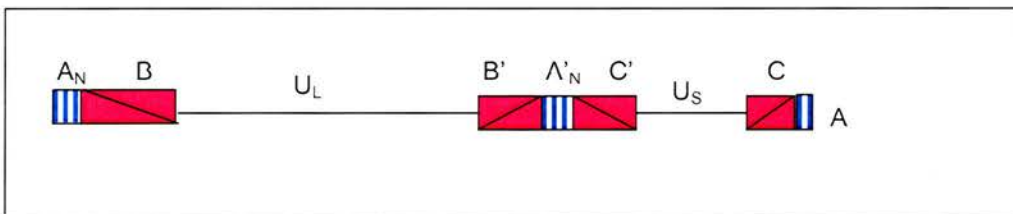


Fig 1.1. Schematic diagram of sequence arrangement of HSV-1. One terminus contains N repeats of sequence A next to a longer sequence B. The other terminus has one directly repeated sequence A next to a sequence C. The terminal sequences are inserted in an inverted form internally (B' A'_N C'). Both the long and short regions can invert, forming four isomers.

1.2.2. Latency in HSV

All herpesviruses are able to establish a latent infection. Latency is defined as a persistent infection where the virus genome is present without the perseverance of infectious virus particles (or viral antigens) (Engels & Ackermann, 1996). HSV has the ability to remain in a latent phase in the human host for its lifetime. The virus remains latent in the sensory nerves innervating the cells infected at the portal of entry, thus avoiding the host immune response. During the latent stage of the virus life cycle the viral DNA is in a circular episomal form and there is limited virus gene expression (Roizman & Sears, 1990). In latently infected neurons, all of the lytic genes are switched off with only the latency-associated transcripts (LATs) detected. There are two major products from these LATs, a 2kb and a 1.5kb RNA (Preston, 2000). LATs are abundant in infected nuclei of the neurons in the host. The number of viral genomes per latently-infected neuron ranges from 10 to 100 (Wagner & Bloom, 1997). Studies have demonstrated that LATs are not essential in the establishment or maintenance of latency or for virus reactivation from latency (Javier *et al.*, 1988; Block *et al.*, 1993; Perng *et al.*, 1994). There are two proposed models describing the functions of LATs. The first is that if present in the nucleus, LATs may inhibit translation of the immediate early gene ICP0, which results in the reduction of lytic gene expression and reduces virus replication and facilitates the establishment of latency (Mador *et al.*, 1998). The second proposes if LATs are in the cytoplasm they may be translated and this results in the stimulation of replication to promote reactivation (Millhouse & Wigdahl, 2000).

LATs have also been shown to have an anti-apoptotic function. Perng and co-workers (1999) were first to observe this and showed that there was an increase in neurovirulence in LAT-mutated virus in rabbits. Since then, numerous studies have identified a possible role of LATs in apoptosis (Perng *et al.*, 2000; Inman *et al.*, 2001; Kent *et al.*, 2003). Fragments of the LAT region were tested for the ability to inhibit apoptosis using an expression plasmid containing 2358bp of the LAT region. It was shown that the region that was being expressed protected the cells from apoptosis induced by various apoptotic agents and by the expression of Bax, a pro-apoptotic protein (Perng *et al.*, 2000; Inman *et al.*, 2001).

1.3. Gammaherpesviruses

1.3.1. Epstein-Barr virus (EBV)

EBV was discovered by Epstein, Achong and Barr in 1964 (Epstein *et al.*, 1964). It is a human gammaherpesvirus that is present in more than 90% of the adult population worldwide. The virus is a member of the genus Lymphocryptovirus and is present as a life-long persistent infection in B-lymphocytes. EBV is associated with several diseases such as infectious mononucleosis, X-linked lymphoproliferative syndrome, Burkitt's lymphoma and Hodgkin's disease.

The EBV genome is 172Kb in length with a G+C DNA content of 60%. EBV was the first herpesvirus to be completely cloned and sequenced (Bankier *et al.*, 1983). The viral genome encodes 100 viral proteins that play roles in viral replication, forming structural components of the virion and modulating the host immune response. Two types of EBV have been identified in the human population: type 1 and type 2. The main differences between the two types can be found in the sequences of EBV nuclear antigen-2 (EBNA-2), EBNA-3A, EBNA-3B and EBNA-3C (Sample *et al.*, 1990). The viral genome is co-linear with other herpesviruses such as VZV, HSV and cytomegalovirus (CMV) (Kieff & Liebowitz, 1990). As with other gammaherpesviruses, EBV possesses homologues to cellular proteins such as the two Bcl-2 homologues encoded by BHRF1 and BALF1. EBV also possesses a homologue of human IL-10, BCRF1, amongst other cytokine genes (Moore *et al.*, 1990). Cellular IL-10 has anti-inflammatory activities mediated by inhibition of macrophage and monocyte synthesis of pro-inflammatory cytokines such as IL-6 and IL-12 (Fiorentino *et al.*, 1991).

1.3.2. EBV lytic replication

The virus infects humans at the oropharyngeal epithelium, which is permissive for virus replication (reviewed in Kieff & Liebowitz, 1990). EBV infects B cells but does not replicate, establishing instead a latent infection. The major envelope

glycoprotein, gp350, binds to the viral receptor CD21 on the surface of the B cell to initiate viral entry (Fingeroth *et al.*, 1984).

The lytic cycle can be induced *in vitro* by the addition of 12-O-tetradecanoyl phorbol-13-acetate (TPA) or other methylation blockers. Following induction of the lytic cycle, the cells exhibit morphological and biochemical changes. These changes result from cytopathology, synthesis of viral DNA in the nucleus, assembly of nucleocapsids, nucleation of the nucleocapsids and the envelopment of the virus, which results in the budding of the virus through the inner nuclear membrane. Virus gene expression occurs as with other herpesviruses in chronological order that can be characterised into three phases; immediate early, early and late.

The immediate early genes products are BZLF1 or Z-transactivator (Zta) and BRFL1 or replication and transcription activator (Rta). Both are key immediate-early transactivators of early EBV lytic gene expression. The expression of these genes leads to the activation of early genes (Takada & Ono, 1989). There are 30 early genes expressed in the lytic phase of the EBV life cycle. Two early EBV genes, BSMF1 and BMRF1, transactivate other early proteins (Cho *et al.*, 1985). Many of the other early genes that are expressed are involved in DNA replication, such as DNA polymerase (BALF5), DNA-binding protein (BALF2), ribonucleotide reductase (BORF2) and thymidine kinase (BXFL1) (Kieff & Liebowitz, 1990). Other early genes that are expressed by EBV include BALF1 and BHRF1. These gene products are both involved in apoptosis. The BHRF1 product has been shown to prevent apoptosis during the lytic cycle (Henderson *et al.*, 1993), whilst the BALF1 product has been shown to be an antagonist to BHRF1. BALF1 acts by negatively regulating the anti-apoptotic activity of BHRF1 (Bellows *et al.*, 2002).

Many of the late genes that are expressed encode structural proteins or proteins that allow virus replication and establishment. Some of the viral glycoproteins are expressed early in the lytic cycle and have a role in antibody-mediated immunity to viral infection. Examples of viral glycoproteins that are expressed are BLLF1 (gp350/220), BALF4 (gp110) and BXLF2 (gp85). Gp110 is an abundantly expressed late EBV protein, that is present in the cell nucleus and in the endoplasmic reticulum, but it is not

a major structural protein (Gong & Kieff, 1990). Gp85 and gp350/220 are found on the virus and in the plasma membrane of lytically-infected cells (Gong & Kieff, 1990). Gp85 is important in the fusion between the virus and the cell membrane, whereas gp350/220 mediates viral binding to the CD21 B-cell receptor (Miller & Hutt-Fletcher, 1988).

1.3.3. EBV latency

As previously stated, EBV persists in B-lymphocytes in the latent state. The virus alters the cell growth cycle so that the cell constantly proliferates. This results in rapid and efficient cell growth and maintenance of the virus. The virus induces immunoglobulin secretion, the expression of B-cell activation markers, DNA synthesis and cell division. Four transcriptional forms of latency have been identified in EBV (Cohen, 2000). These are known as latency I, II, III and IV. Latency I was first identified in Burkitt's lymphoma cells and latency II is found in nasopharyngeal carcinomas (Young *et al.*, 1988). In latency I, only EBNA-1 and Epstein Barr encoded small RNA (EBERs) are expressed. In latency II, EBERs, EBNA-1, latent membrane protein-1 (LMP-1) and LMP-2 are expressed. During latency III, two non polyadenylated RNAs (EBER-1 and EBER-2), six nuclear proteins (EBNA-1, 2, 3A, 3B, 3C and LP) and finally three latent membrane proteins (LMP-1, 2A and 2B) are expressed. A fourth latency stage has been identified in the peripheral blood of healthy individuals that had previously been infected with EBV. It was shown that only EBER was present in all of the individuals tested and in several (but not all those tested) LMP-2 and EBNA-1 was also detected (Tierney *et al.*, 1994).

EBNA-1 is the only protein that has been identified in all types of latency and therefore is believed to have a critical role in maintaining latency. EBNA-1 binds the EBV plasmid origin of latent DNA replication, oriP, to allow the EBV genome to persist as a circular DNA episome (Yates *et al.*, 1984). EBNA-2 is essential for B-lymphocyte growth transformation and transactivates the expression of EBNA1, EBNA3s and LMPs (Abbot *et al.*, 1990; Robertson *et al.*, 1995). EBNA-2 up-regulates the expression of LMP-1 and LMP-2 and other proteins that are involved in the growth and transformation

of B cells (Johannsen *et al.*, 1995). The EBNA 3 proteins also regulate the expression of cellular genes. However, it has been shown that EBNA 3B is not essential for lymphocyte infection *in vitro* (Wang *et al.*, 1990). EBNA-LP has been shown to enhance the ability of EBNA-2 to up-regulate LMP-1 (Yokoyama *et al.*, 2001).

LMP-1 localises in the plasma membrane of infected cells (Mann *et al.*, 1985) and binds several of the tumour necrosis factor receptor-associated factors. This results in the activation of nuclear factor- κ B (NF- κ B) transcription factor, activation of *c-jun*, up-regulation of cellular adhesion molecules, cytokine production and B-cell proliferation. This protein is essential for B lymphocyte growth transformation by EBV (Kaye *et al.*, 1993). LMP-2 prevents the reactivation of EBV from latently-infected cells by blocking tyrosine kinase phosphorylation (Miller *et al.*, 1995). EBER (EBV encoded small RNAs) do not encode proteins. It is thought that these RNAs play a role in oncogenesis and the prevention of apoptosis (Komano *et al.*, 1999).

1.3.4. Murine gammaherpesvirus 68 (MHV-68)

MHV-68 was first isolated from the bank vole (*Clethrionomys glareolus*) in Slovakia (Blaskovic *et al.*, 1980). The MHV-68 genome has been sequenced (Virgin *et al.*, 1997) and is co-linear with those of HVS and KSHV. The genome contains 118,237bp of unique sequence flanked by multiple copies of a 1,213bp terminal repeat. The unique region of the genome has a G+C content of 46% while the terminal repeat sequence has a high G+C content of 78%. The MHV-68 genome is predicted to encode 80 gene products with at least 63 being co-linear with homologous genes in HVS and KSHV. As with other gammaherpesviruses, MHV-68 encodes conserved herpesvirus ORFs (M1 to M14). An example of this is ORF M1. This shows sequence homology to the poxvirus *SPI-1* serpin family of proteins. The poxvirus *SPI-1* protein regulates host cell range by altering apoptosis, regulating inflammatory responses and altering arachidonate metabolism (Brooks *et al.*, 1995; Palumbo *et al.*, 1997). MHV-68 encodes cellular homologues that are involved in apoptosis regulation, cytokine signalling and immune regulation. For example, MHV-68 encodes a cyclin homologue that shows similarities to ORF72 (eclf2) in Herpesvirus saimiri (HVS). ORF72 has homology to

cellular type D cyclins and is thought to associate and regulate cell proliferation (Jung *et al.*, 1994). An IL-8 receptor homologue is also present, which has a homologue in KSHV that induces tumour formation and angiogenesis (Arvanitakis *et al.*, 1997). ORF M11 shows homology with Bcl-2 and has been shown to protect cells against apoptosis (Roy *et al.*, 2000). ORF M3 was the first chemokine-binding protein to be identified in MHV-68. The protein binds to chemokines of the CC, CXC, CX3C and C families and prevents chemokine-induced signal transduction *in vitro* (Parry *et al.*, 2000; van Berkel *et al.*, 2002).

The virus has the ability to establish a productive infection in fibroblast and epithelial cells lines that have been derived from mammalian species including humans (Svobodova *et al.*, 1982). Mice that are infected intranasally with the virus, establish a productive infection in alveolar epithelial cells and mononuclear cells of the lungs causing interstitial pneumonia. The virus then spreads via the lymph nodes to the spleen, where it establishes latency in germinal centre B cells (Sunil-Chandra *et al.*, 1992). Mice with an acute infection usually resolve this within 10-12 days but have a life-long latent infection in lymphoid tissue. Latency in lymphoid tissue is characterised by a transient phase of splenomegaly and lymph node enlargement, which peaks at around 2-3 weeks post-inoculation. It is at this point that the maximum numbers of splenocytes are latently-infected, the numbers of which subsequently decline (Nash & Sunil-Chandra, 1994). One study demonstrated that over a period of three years, 9% of the infected mice developed lymphoproliferative disease (LPD) and high-grade lymphomas. This would suggest that long-term persistence in mice is associated with the development of LPD and high-grade lymphomas (Sunil-Chandra *et al.*, 1994).

The host response to MHV-68 infection in the lungs is characterised by the infiltration of monocytes/macrophages, which occurs during the first three days of infection. However, by day five after infection the number of macrophages decreases and the levels of T cells increase (Nash *et al.*, 1994). It has been suggested that the large number of CD8⁺ T cells that are found in the lungs have an anti-viral role (Ehtisham *et al.*, 1993). Deletion of CD8⁺ T cells before infection leads to uncontrolled virus replication and death (Ehtisam *et al.*, 1993). An antibody response to the virus develops

slowly then rises considerably at two weeks after infection and remains high. However, it has been shown that antibodies are not essential for the suppression of the acute infection (Usherwood *et al.*, 1996).

1.3.5. Kaposi's sarcoma-associated Herpesvirus (Human Herpesvirus-8)

Kaposi's sarcoma-associated Herpesvirus (KSHV) is a gammaherpesvirus that belongs to the *Rhadinovirus* subfamily. The virus is associated with three neoplastic disorders: Kaposi's sarcoma (KS), primary effusion lymphoma (PEL) and multicentric Castleman's disease (MCD).

Early stage KS lesions are composed of small, irregular, endothelial-lined spaces that surround normal blood vessels. They are accompanied by an infiltrate of inflammatory cells. As the disease progresses, a spindle-celled vascular process expands throughout the dermis and these spindle cells form slit-like, vascular channels which contain red blood cells (Weninger *et al.*, 1999). In early KS lesions, only 10% of spindle and endothelial cells are KSHV positive. In late stage nodular lesions, around 90% of spindle cells contain KSHV suggesting that the virus provides a growth advantage to infected cells (Boshoff *et al.*, 1995).

Body cavity-based lymphoma or PEL (Cesarman *et al.*, 1995) is normally found as malignant effusions in the pleural, pericardial or peritoneal cavities without forming significant tumour masses. The majority of PEL patients are HIV positive with advanced immunosuppression. PEL is thought to originate from post-germinal centre B-cells due to the presence of hypermutated immunoglobulin genes (Matolcsy *et al.*, 1998).

MCD is a lymphoproliferative disorder that is characterised by lymphadenopathy, fever and splenic infiltration (Peterson & Frizzera, 1993). The disease is common in HIV-infected individuals where it is often aggressive. KSHV positive MCD cases form a distinct class of MCD, named plasmablastic MCD. A number of patients with KSHV-associated plasmablastic MCD often progress to develop plasmablastic lymphoma (Dupin *et al.*, 2000).

The organisation of the KSHV genome is very similar to other rhadinoviruses such as HVS and MHV-68. The genome is 140.5kb long and is flanked by two terminal repeat regions that have several 801bp repeat subunits of a high (85%) G+C content. As with other herpesviruses, the genome contains genes that are conserved within all herpesviruses and genes that are unique to KSHV. The latter genes have been designated with a K prefix and are numbered sequentially (Schulz, 1998).

Some of the conserved herpesvirus genes that are seen in KSHV genome encode homologues of cellular proteins that are involved in cell proliferation or cell survival. For example, ORF K2 encodes a viral homologue of IL-6, a cytokine that is a functional B cell growth factor and negatively regulates apoptosis; K13 encodes a viral Bcl-2 protein; ORF K9 is a viral interferon regulatory factor protein that blocks IFN and interferon regulatory factor-mediated transcriptional activation. ORF 71 encodes a viral FLICE (FADD homologous ICE) inhibitory protein (vFLIP) that inhibits Fas-mediated apoptosis; ORF 72 encodes v-cyclin that forms a complex with cdk6 that results in the prevention of normal G1 cell cycle arrest. ORF 74 encodes a viral G-coupled protein receptor (GPCR) (Schulz, 1998). GPCR are a large family of receptors that play a fundamental role in cellular communication. These receptors are thought to function in cellular signalling pathways such as degranulation, lymphocyte homing and T-cell activation. GPCR genes have been found in the genomes of poxviruses and herpesviruses. It is thought that these viruses have evolved these genes through long co-evolution with their hosts (Vink *et al.*, 2001).

1.3.6. KSHV lytic replication

During latency, most of the KSHV genome is silent. This is thought to be due to methylation of promoter sequences (Chen *et al.*, 2001). For example, the promoter of ORF 50 is heavily methylated in PEL cell lines. KSHV Rta, encoded by ORF 50, is required to activate the lytic cycle (Lukac *et al.*, 1999). The lytic cycle can be induced *in vitro* using phorbol esters such as TPA either alone or with sodium butyrate. KSHV gene expression has been investigated using DNA array expression profiling in PEL cells stimulated by TPA (Paulose-Murphy *et al.*, 2001). This study demonstrated that

the first set of genes that are expressed after the induction of the lytic cycle are regulators of gene expression such as ORF 50, K8, ORF 57 and ORF 45. Genes that control DNA replication such as DNA polymerase follow this. The genes that are involved in virus structure and maturation are generally expressed later (Jenner *et al.*, 2001, Paulose-Murphy *et al.*, 2001).

1.3.7. KSHV latency

KSHV can become latent in all of the cells that the virus infects, which are (pre- and post-germinal centre) B-cells and endothelial cell precursors. These cell types all have a high proliferative potential that is thought to help the virus propagate its genome within the host. In the latent phase, the viral DNA exists as closed circular episomal DNA. It has been demonstrated that all infected cells express the latent nuclear antigen, viral cyclin (v-cyclin) and vFLIP (Jenner & Boshoff, 2002).

Latency-associated nuclear antigen-1 (LANA-1) possesses a number of functions. Some of these include binding to cellular proteins such as RING3, one of five human homologues of female sterile homeotic (*fsh*) of *Drosophila*, a developmental regulator and as a consequence of this interaction is phosphorylated (Platt *et al.*, 1999). LANA-1 causes RING3 to relocate to nuclear heterochromatin regions, where it is thought that LANA-1 and RING3 have a possible role in the regulation of chromatin structure (Mattsson *et al.*, 2002). LANA-1 has anti-apoptotic activity. When LANA-1 and p53 are over-expressed in p53-null cells, LANA-1 diminishes the apoptotic response (Friborg *et al.*, 1999).

KSHV also encodes a v-cyclin, a homologue of human cyclin D. v-Cyclin phosphorylates the retinoblastoma protein in complex with cyclin-dependent kinase (CDK) 6 and CDK4 (Godden-Kent *et al.*, 1997) to allow the cell cycle to enter in S phase and DNA synthesis. This abolishes cell cycle checkpoints and allows viral DNA to be synthesised.

v-FLIP is a homologue of the cellular protein FLICE-inhibitory protein (FLIP). v-FLIP proteins have been found in other gammaherpesviruses and protect the cells

from many varieties of ligand-receptor-induced apoptosis. The KSHV v-FLIP protein also has the ability to protect cells from Fas-mediated apoptosis (Djerbi *et al.*, 1999).

1.3.8. Herpesvirus saimiri (HVS)

HVS is the prototype of the rhadinovirus subfamily. The virus occurs naturally in squirrel monkeys (*Saimiri sciureus*), which inhabit Central and South American rain forests. The virus was first isolated from primary squirrel monkey kidney cells. However, it persists in peripheral blood lymphocytes. The virus replicates productively in owl monkey kidney cells and induces cell lysis 3-20 days after infection (Fickenscher & Fleckenstein, 1998). It is estimated that over 80% of squirrel monkeys are persistently-infected with the virus (Jung *et al.*, 1999). The virus causes no apparent disease in the host animal. However, it infects New World primates such as tamarin marmosets, owl monkeys, spider monkeys and howler monkeys (Melendz *et al.*, 1969), which develop lymphoproliferative syndromes and leukaemia. Experimentally, HVS causes malignant lymphomas in New Zealand white rabbits (Ablahhi *et al.*, 1985).

The virus has been classified into three subgroups A, B and C based on sequence divergence at the left hand end of the unique L-DNA (Medveczky *et al.*, 1984). The variation has been linked with differences in the ability of the viruses to immortalise T lymphocytes *in vitro* and to produce lymphoma in non-human primates. Viruses of both subgroups A and C immortalise common marmoset T lymphocytes to IL-2 independent proliferation (Szomolanyi *et al.*, 1987). Subgroup C strains also immortalise rabbit and rhesus monkey lymphocytes and can produce lymphoma in rhesus monkeys, as well as in New World primates. The sequence variation is in open reading frames at the left hand end of the genome, which are essential for HVS oncogenicity (Duboise *et al.*, 1998).

Lymphoid cell lines are established by the cultivation of tumour cell tissues from marmosets and owl monkeys experimentally-infected with HVS (Johnson & Jondal, 1981). The cells lines have been cultured continuously for many years. Initially the cell lines produced virus particles, however, this ability was lost after prolonged culture (Marczynska *et al.*, 1973). The cultured cells express many T cell markers and display

cytotoxic activity (Johnson & Jondal, 1981). HVS subgroup C strains are able to transform human T lymphocytes to stable growth *in vitro*. These transformed human T cells do not produce viral particles (Fickenscher *et al.*, 1997).

Albrecht and co-workers (1992) sequenced the genome of HVS. It contains 83 potential genes, with 60 being homologous to other herpesviruses. The genome of HVS encodes 75 ORFs (designated ORF1 to ORF75) and seven genes for small nuclear RNAs. The viral genome consists of a low G+C (34.5%) content unique region that is flanked by a high G+C (70.8%) repeat region (Albrecht *et al.*, 1992). The viral genome includes ORF 72 that encodes a cyclin homologue (Nicholas *et al.*, 1992) and ORF 74, a GPCR homologue (Ahuja & Murphy, 1993). The virus also encodes two potential inhibitors of apoptosis: ORF16, that encodes a homologue of the Bcl-2 protein (Nava *et al.*, 1997); and ORF 71, that encodes a vFLIP. This is anti-apoptotic but is not essential for viral replication, transformation or pathogenicity (Glykofrydes *et al.*, 2000).

1.3.9. Other Gammaherpesviruses of veterinary importance

Equine herpesvirus 2 (EHV-2) is a gammaherpesvirus that is found in horses. EHV-2 is common and can be isolated from leukocytes of “normal” (disease-free) horses. The virus has been implicated in immunosuppression in foals, upper respiratory tract disease, conjunctivitis, general malaise and poor performance (Telford *et al.*, 1995).

The EHV-2 genome is most similar to EBV and HVS as the genome contains the highest level of similarity to proteins specified by HVS and EBV. The viral genome is linear double-stranded DNA and is 184kb in size comprising a unique region of 149kb in size flanked by a 17.5kb direct repeat. The DNA G+C content is 58% in the unique region and 55% in the repeat region (Telford *et al.*, 1995). The genome is co-linear with HVS and EBV and predicted to encode 70 ORFs. Unique genes with no counterparts in HVS were designated with the letter E prefix (E1 to E10). Eight genes in the genome have counterparts in HVS but not in EBV. Four of these have sequence homology (ORFs 10, 11, 70 and 74) and four have positional homology (ORFs 12, 13 and 28) (Telford *et al.*, 1995).

ORF E4 of EHV-2 encodes a protein with 20% identity to the Bcl-x_L protein. Bcl-x_L is an anti-apoptotic protein belonging to the Bcl-2 family of proteins (Bcl-x_L will be discussed in a later section). ORF E4 contains two Bcl homology (BH) domains that are thought to be responsible for anti-apoptotic function (Marshall *et al.*, 1999). The EHV-2 genome contains a gene encoding a homologue of the cytokine IL-10 (ORF E7) and a GPCR encoded by ORF 74. This latter protein was located co-linearly to HVS ORF 74 (Telford *et al.*, 1995). A possible pathological role for EHV-2 is in the reactivation of EHV-1 and EHV-4 from latency (Welch *et al.*, 1982). EHV-1 and EHV-4 cause respiratory infections in young horses. EHV-2 transactivates the immediate-early gene promoter of EHV-1 *in vitro* (Purewal *et al.*, 1992).

Bovine herpesvirus 4 (BHV-4) has been isolated from cattle that show various clinical symptoms such as skin lesions, genital and respiratory diseases, but it has also been isolated from apparently normal healthy cattle (Zimmerman *et al.*, 2001). BHV-4 has been classified as a gammaherpesvirus and has sequence homology to KSHV and HVS (Broll *et al.*, 1999). As with other gammaherpesviruses, BHV-4 possesses apoptosis regulators, vBcl-2 (ORF 16) and a v-FLIP protein (ORF 71) (Wang *et al.*, 1997). However, the genome does not possess a known cytokine or cytokine receptor, GPCR or interleukin receptor within the long unique genome region, in contrast to other gammaherpesviruses such as HHV-8 and EHV-2 (Zimmermann *et al.*, 2001).

Due to the shortage of human organs for transplantation, xenotransplantation is considered as an alternative, particularly using pig organs. However, this has brought into question the possible risk of porcine pathogens transferring to human recipients. A search for porcine herpesviruses identified two gammaherpesviruses of pigs, porcine lymphotropic herpesvirus 1 and 2 (PLHV-1 and PLHV-2). These viruses are widely distributed with a high prevalence in domestic and feral pigs (Ehlers *et al.*, 1999). No disease has been identified in PLHV infection in pigs under natural conditions, however, a porcine gammaherpesvirus has been associated with experimental posttransplant lymphoproliferative disease (PTLD) in miniature swine following allogeneic hematopoietic stem cell transplantation (Huang *et al.*, 2001). The PTLD that was observed was similar to that seen in some humans after tissue transplantation.

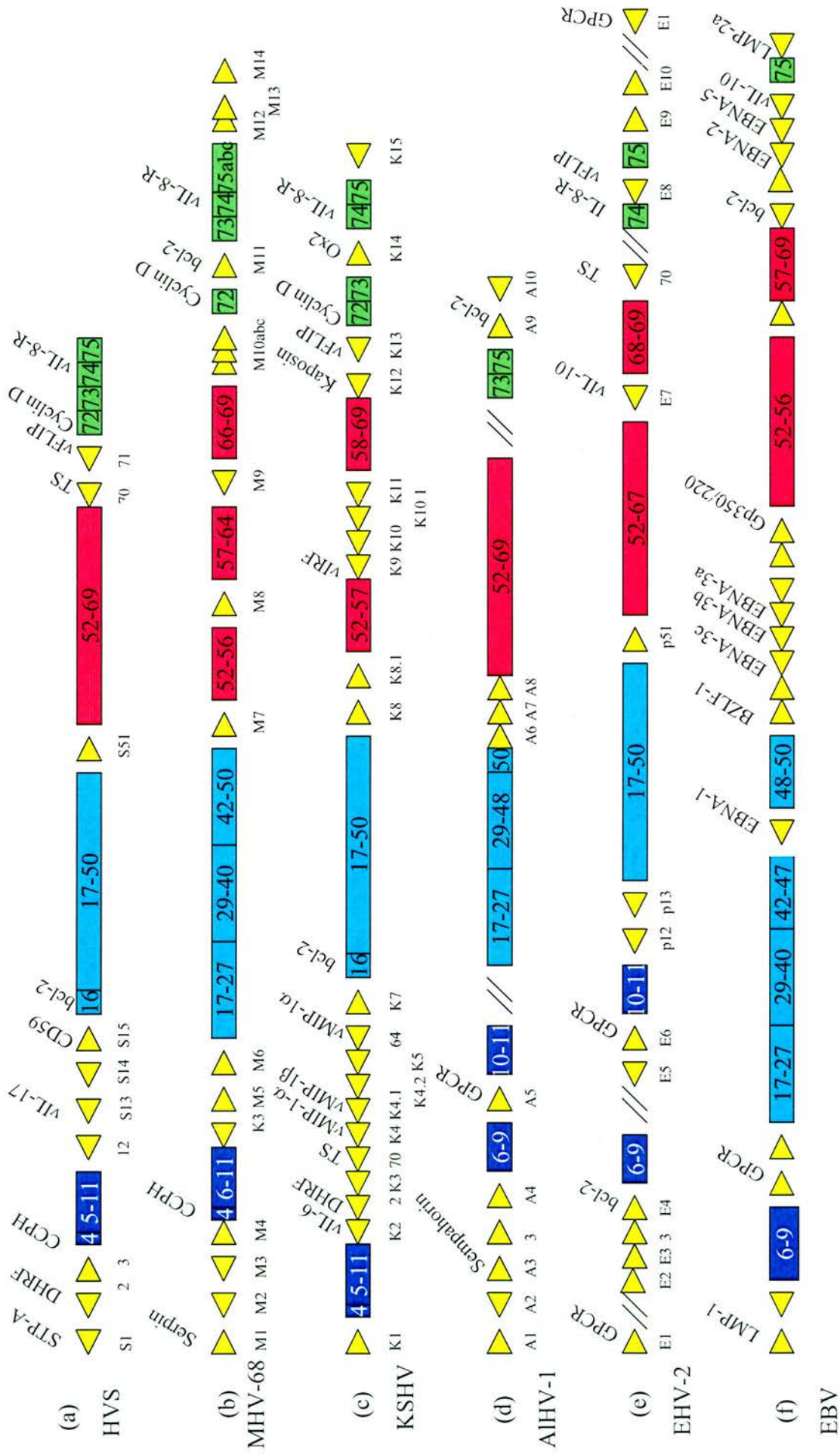
Through amino acid comparisons and phylogenetic analysis of a partial PLHV-1 region of the genome, it appears to have a very similar gene content and arrangement to that of *Alcelaphine herpesvirus-1* (AIHV-1). The genome possesses homologues of genes found in other gammaherpesviruses that may have a role in the pathogenesis of disease. One gene that was identified was E4/BALF1_h. Homologues of this gene are present in EBV and EHV-2. ORF A5/BILF1_h encodes a GPCR. This gene is similar to ORF A5 of AIHV-1, ORF E6 of EHV-2 and ORF BILF1 of EBV all of which encode GPCRs. ORF A8/BLLF1_h is closely related to ORF A8 of AIHV-1 and ORF BLLF1 of EBV (Goltz *et al.*, 2002). BLLF1 mediates the attachment of EBV to B cells via the CD21/CR2 (Tanner *et al.*, 1987) receptor and induces T cell apoptosis (Tanner & Alfieri, 1999).

Fig 1.2 compares the genomic arrangement of a selection of gammaherpesviruses.

Fig. 1.2. Comparison of the genetic organisation among some of the gammaherpesviruses

The genomes of (a) herpesvirus saimiri (HSV) (b) murine gammaherpesvirus 68 (MHV-68), (c) Kaposi sarcoma associated herpesvirus (KSHV), (d) Alcelaphine herpesvirus-1 (AIHV-1), (e) equine herpesvirus 2 (EHV-2), (f) Epstein-Barr virus (EBV) are shown. The genome of EBV has been inverted relative to its conventional orientation. Abbreviations CCPH, complement control protein homologue; DHFR, dihydrofolate reductase; GPCR, G protein-coupled receptor; STP-A, saimiri transformation protein; TS, thymidylate synthetase; vIL-6 viral interleukin 6; vIL-10, viral interleukin 10; vIL17, viral interleukin 17; vIL-8R, viral IL-8 receptor; vIRF, viral interferon-responsive factor; vFLIP, viral FLICE inhibitory protein; vMIP-1 α/β , viral macrophage inflammatory protein 1 α/β . // denotes non-coding regions in the genomes of AIHV-1 and EHV-2. The conserved gene blocks I (blue), II (turquoise), III (red) and IV (green) are shown and the open reading frame designations within these boxes relate to the HVS numbering system. Interspersed between these gene blocks are ORFs that are largely unique to each individual family member and contain several homologues to cellular genes (Adapted from Simas & Efstathiou, 1998).

Fig 1.2 Comparison of the genetic organisation among some of the gammaherpesviruses



1.4. Malignant catarrhal fever

MCF is a systemic disease of cattle and wild ruminants (Castro & Daley, 1982; Plowright, 1990; Handley *et al.*, 1995). To date there are two viruses found to be causal agents of the disease, *Alcelaphine herpesvirus-1* (AIHV-1) and *Ovine herpesvirus-2* (OvHV-2). AIHV-1 is found naturally in Blue Wildebeest (*Connochaetes taurinus*) while OvHV-2 is found in sheep. Both cause no apparent disease in their carrier species. However, when the viruses are transmitted to susceptible species disease can occur, which is often fatal. Experimentally-infected rabbits exhibit similar clinical symptoms and pathology to cattle infected with AIHV-1 and OvHV-2. This provides a very useful experimental model for MCF.

1.4.1. Epidemiology

Mettam (1923) first investigated the association between wildebeest and MCF. Wildebeest could transmit MCF to cattle of all ages by being in close proximity (Plowright *et al.*, 1960; Mushi & Rurangirwa, 1981a). Wildebeest calves are probably the principal source of excreted AIHV-1 that can be contracted by susceptible species. Most adult wildebeest are persistently infected with AIHV-1 (Plowright, 1967). However, it is thought that they may only excrete the virus under certain circumstances, for example severe stress, malnutrition and exposure to high environmental temperatures. The virus can be isolated from the blood of adult wildebeest in late pregnancy (Rweyemamu *et al.*, 1974). Viremia has been demonstrated in pregnant blue wildebeest that were near full-term. This would suggest that some calves are born with infection obtained, *in utero*, while others may acquire the infection shortly after birth (Plowright *et al.*, 1972; Rurangirwa *et al.*, 1982; Barnard *et al.*, 1994). The natural route of infection in cattle is probably through close contact with wildebeest calves. It has been shown that intranasal instillation of cell-free viral suspensions can produce infection in both cattle and rabbits (Mushi & Wafula, 1983). However, natural aerosol infection would realistically take place only over short distances. Viral loads of nasal secretions in wildebeest calves tend to be low (10^3 or 10^2 TCID₅₀/ml) (Mushi & Rurangirwa, 1981a). The virus is thought to replicate in the corneal epithelium and pass

down the nasal duct to the nasal cavity (Mushi & Rurangirwa, 1981a; Rurangirwa *et al.*, 1982). Wildebeest calves over three months old express virus neutralising antibody detectable in their nasal secretions that may affect virus excretion (Mushi *et al.*, 1981). Wildebeest calves can acquire neutralising antibody from colostrum (Reid & Buxton, 1989). Neutralising antibodies in nasal secretions belong to the IgA class and are thought to be induced locally by the virus in the nasal cavity (Mushi and Rurangirwa, 1981a). The production of the IgA antibodies in nasal secretions coincides with the cessation of virus shedding (Rurangirwa *et al.*, 1982).

1.4.2. Clinical Symptoms

The clinical signs of MCF vary between individual animals. However, they can be characterised into three main forms of the disease. These are (1) head and eye, (2) intestinal and (3) neurological forms, which can have a peracute, acute, subacute or chronic course (Reid & Buxton, 1989). The head and eye form of the disease is more commonly seen in cattle, whereas deer develop a chronic form with fatal, haemorrhagic enteritis (Tham, 1997). The incubation period for the disease also varies between animals and can last from a few weeks to several months (Reid & Buxton, 1989).

In all cases of MCF the rectal temperature and pulse rate rises. There is a nasal and ocular discharge that may start as clear and watery but then progresses to mucopurulent (brown coloured secretion) (Reid and Buxton, 1989). This discharge can accumulate and encrust around the nostrils and muzzle and can lead to the nasal passages becoming obstructed, which in turn leads to laboured breathing. In most cases there is congestion, erosion and necrosis of the nasal and oral mucosa and the muzzle (Barnard *et al.*, 1994). Symptoms can also include dullness, inappetance and a decline in milk yield of lactating animals.

Many MCF-affected animals develop ocular lesions that in turn leads to bilateral corneal opacity that can progress to impaired vision or total blindness. The affected animals are often photophobic. Nervous signs such as twitching of the ears, muscle tremors, loss of coordination and aggressive behaviour can be seen in affected animals. Constipation is common in infected cattle and can be persistent. This eventually gives

way to diarrhoea, which can be blood-tinged. In deer with MCF, it is common for the affected animals to have acute diarrhoea from the onset of the disease (Reid and Buxton, 1989). Within four to five days of developing the clinical symptoms of MCF, affected cattle will often die (Barnard *et al.*, 1994).

1.4.3. MCF Pathology

There are various tissues and organs affected by AIHV-1 and OvHV-2 MCF. The most commonly affected are the upper respiratory and digestive tracts, lymph nodes, brain, liver, kidneys and the urinary bladder (Barnard *et al.*, 1994). Lymph node enlargement is seen at the onset of fever. In rabbits infected with AIHV-1, popliteal and submandibular lymph nodes are significantly larger compared to rabbits infected with OvHV-2. In OvHV-2-infected rabbits, severe lesions are seen more commonly in mesenteric lymph nodes. The affected lymph nodes exhibit lymphoid hyperplasia, which is accompanied by an alteration of shape, haemorrhage, oedema and focal necrosis (Reid & Buxton, 1989; Schock, 1996).

In the respiratory tract, lesions can be found in the mouth, pharynx, soft palate and tongue. These may show signs of haemorrhage and focal necrosis of the epithelium, erosions and ulcerations (Reid & Buxton, 1989). Ulceration and haemorrhage of the mucous membranes that cover the nasal septum, turbinates, sinuses and the horn cores can also be seen. In infected rabbits, lesions that are seen in the respiratory tract are more severe in AIHV-1 induced MCF than OvHV-2 MCF (Reid & Buxton, 1989).

The small intestine exhibits a reddened mucosa and small haemorrhages can be seen while the large intestine possesses more obvious mucosal haemorrhaging and erosions (Reid & Buxton, 1989). In AIHV-1 MCF, the spleen and the liver can enlarge to twice the normal size. However, this is not as obvious in OvHV-2 MCF (Reid & Buxton, 1989). The kidneys can also be swollen and contain foci of lesions, which in some cases may be small haemorrhagic foci (Barnard *et al.*, 1994). As shown in fig 1.3 lymphocytes accumulate in the cortex of the kidney. The mucosa of the urinary bladder can exhibit oedema, small haemorrhages, erosions and ulcerations. These lesions are

often associated with the presence of blood in the urine. In the genital tract there can be erosion of the vaginal mucosa (Denholm & Westbury, 1982; Reid & Buxton, 1989).

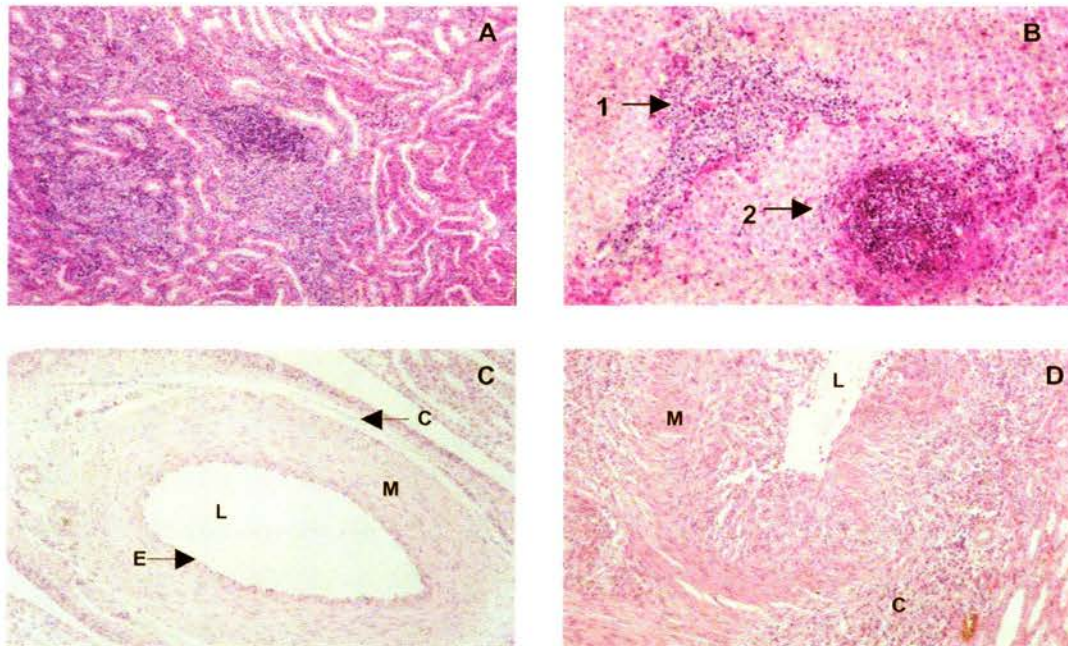


Fig 1.3 MCF, kidney and liver histology. **(A)** H&E staining showing interstitial accumulation of lymphocytes in the cortex of a bovine kidney (infected with OvHv-2). **(B)** H&E staining of a section of deer liver (infected with OvHV-2). Arrow 1 shows lymphocyte accumulation without tissue damage. Arrow 2 shows area of necrosis. **(C)** & **(D)** Vasculitis in deer infected with OvHV-2 MCF. **(C)** Shows a healthy, normal artery with pronounced lumen (L), endothelial lining cells (E), muscle layer (M) and connective tissue (C). **(D)** MCF: Arteritis showing lymphoid cells infiltrating the endothelial lining cells, muscle layer and connective tissue. All pictures taken with magnification x 220.

1.4.4. MCF Histopathology

MCF microscopic lesions can be characterised into four groups: hyperplasia and necrosis in lymphoid organs, interstitial accumulation of lymphocytes in non-lymphoid organs, vasculitis and epithelial degeneration.

Lymphoid hyperplasia exhibits as an increase in the numbers of lymphoblastoid cells in the paracortex of lymph nodes. Focal necrosis also occurs, often follicular in origin. Vasculitis affects the arteries, arterioles, veins and venules (fig 1.3 C&D). This is accompanied by an infiltration of lymphocytes and macrophages (Liggitt & DeMartini, 1980). The blood vessels can become blocked by the increase in numbers of lymphoid cells and the multiplication of endothelial cells (Reid *et al.*, 1979).

1.4.5. Transmission to susceptible species

When cattle and wildebeest are in close proximity, cattle can develop MCF. In most cases the seasonal occurrence of the AIHV-1 MCF disease in cattle is related to the calving season of the wildebeest. In Kenya, MCF usually occurs between April and July following the wildebeest calving season in February to April (Plowright, 1964). However in South Africa, MCF occurs twice, firstly during January to May which coincides with the wildebeest calving season and subsequently between September and November when the wildebeest calves are nine to eleven months old (Barnard *et al.*, 1988). It has been reported that there is a higher incidence of AIHV-1-MCF in East Africa during the months of January through to July, which encompasses the time when the wildebeest calves are born and up until they are 2-3 months old (Plowright, 1990). MCF has also been reported in South Africa between January and May when cattle and wildebeest share grazing and watering places (Barnard *et al.*, 1989). Wildebeest calves younger than three months of age excrete virus into the nasal cavity (Heuschele *et al.*, 1985). It is believed that close contact could facilitate infection transmitted via aerosol droplets, and also that aggressive snorting could produce such aerosols, which would infect cattle (at least over a short distance). The Masai people believe that cattle become infected from either the placenta of the wildebeest or the hair that the wildebeest calves shed (Barnard *et al.*, 1994). However, virus has not been isolated from the placenta

(Rossiter, 1983). A vector (e.g. flies) has been suggested in virus transmission (Barnard & Pypekamp, 1988). However, there is no evidence to support this. It has been demonstrated that African face flies (*Musca xanthomelas*) were able to carry AIHV-1 infected material after feeding on wildebeest tears. They would have to regurgitate into the eyes of cattle within 30 mins for it to be effective. This would appear to be unlikely, and furthermore the amount of virus they carry would be very low (Barnard *et al.*, 1990).

All breeds of cattle (*Bos taurus*) are susceptible to MCF (Plowright, 1990). Other animals such as kudu (*Tragelaphus strepsiceros*), sitatunga (*Tragelaphus spekei*), eland (*Taurotragus oryx*) and roan antelope (*Hippotragus equines*) found in zoological collections are also susceptible to MCF (Wothington & Bigalke, 2001). However, in free-living animals in the wild, MCF has not been reported in these species even when wildebeest and these species come into close contact (Barnard *et al.*, 1994).

The mechanism through which OvHV-2 MCF is passed to susceptible species from sheep still remains unclear. It is known that close contact between sheep and the susceptible species (e.g. cattle) can result in MCF (Plowright, 1990). Shared accommodation with common food and water troughs can result in transmission. As with AIHV-1-MCF, the incidence of OvHV-2-MCF is seasonal and has been associated with the lambing season (Selman *et al.*, 1978).

1.4.6. Experimental transmission of MCF

Rabbits can be easily infected with AIHV-1 or OvHV-2 intraperitoneally or intravenously by inoculation of cells from lymphoid tissues of infected cattle or other rabbits. The incubation period for the disease in rabbits varies from 12 days to several weeks (Reid & Buxton, 1989). The clinical signs and pathology of the disease are similar to that found in AIHV-1-MCF or OvHV-2-MCF in cattle (Schock, 1996). Once infected, IgG and IgM antibodies against the virus appear simultaneously approximately two to six days before the onset of clinical disease. An IgG₂ antibody response is detected 2-4 days later (Rossiter, 1982). Hamsters, guinea pigs, rats and deer are also susceptible to MCF, producing similar symptoms as seen in cattle. However,

inoculated mice produce no symptoms of MCF (Jacoby *et al.*, 1988). MCF is a problem in deer. Members of the Cervidae such as red deer (*Cervus elaphus*), axis deer (*C. axis*), Sika deer (*C. Nippon*), Russa deer (*C. timorensis*), Roe deer (*Capreolus capreolus*), Pere David deer (*Elaphus davidianus*), white-tailed deer (*Odocoileus virginianus*) and black-tailed deer (*O. hemionus columbianus*) are more susceptible than cattle to both AIHV-1 and OvHV-2 MCF (Huck *et al.*, 1961; Reid & Buxton, 1984; Jessup, 1985). When the farming of red deer was first established in Europe and New Zealand, major outbreaks of MCF occurred affecting up to 50% of the herd (Reid *et al.*, 1979). However, it is not now such a severe problem and outbreaks generally occur sporadically affecting individual animals.

1.4.7. Alcelaphine herpesvirus-1 (AIHV-1)

Alcelaphine herpesvirus-1 was first characterized as *Bovine herpesvirus-3* (BHV-3) by the World Health Organisation (WHO, 1976). However, this name was altered to *Alcelaphine herpesvirus-1* to reflect the carrier (or reservoir) species in which the virus is found. Using electron microscopy and morphological characterisation, the virus was identified as a herpesvirus (Plowright *et al.*, 1963; Castro and Daley, 1982). Plowright and co-workers were able to isolate the virus and demonstrated that it was present in the blood of blue wildebeest (*Connochaetes taurinus*) (Plowright *et al.*, 1960). Since then AIHV-1 has been characterised as a gammaherpesvirus belonging to the subfamily Rhadinovirus (Roizman & Sears, 1990). The genome sequence of AIHV-1 was resolved confirming this categorisation (fig. 1.4.) (Ensser *et al.*, 1997).

The two most commonly described isolates of AIHV-1 are WC11 and C500. WC11 was first isolated from blue wildebeest and is cell-free and attenuated (Plowright *et al.*, 1960). The cell-associated and virulent C500 was first isolated from infected cattle (Plowright *et al.*, 1975). After extensive passage of the cells in culture, the virus becomes cell free and attenuated (Wright *et al.*, 2001). As with HVS, the DNA is arranged in blocks separated by non-conserved ORFs. The non-conserved regions, as in other *Rhadinoviruses*, contain homologues of cellular genes. The viral genes were numbered according to their homologues in HVS. The genome consists of 130,608bp of

low G+C content (46.17%) DNA (L-DNA), flanked by 20-25bp repeats of a sequence with a high G+C content (71.83%) (H-DNA) 1113bp-2229bp. The L-DNA contains of approximately 60 conserved herpesvirus ORFs that were arranged co-linearly to HVS. There were eleven conserved herpesvirus ORFs identified which were not present in HVS and have been designated with the letter A prefix (Ensser *et al.*, 1997).

ORF A1 possesses a TATA box-like sequence upstream and a polyadenylation site downstream. ORF A2 has a predicted amino acid sequence with similarity to the transcription factor ATF3 (Ensser *et al.*, 1997). ATF3 is a member of the ATF/CREB family and is a transcriptional repressor (Chen *et al.*, 1996). ORF A3 was found to encode a semaphorin-like protein. Semaphorins are a family of transmembrane and secreted proteins that regulate axonal guidance in the developing nervous system (reviewed in Goshima *et al.*, 2002). It has also been reported that semaphorins have a role in immunoregulation. A human semaphorin has been identified in lymphoid tissues such as lymph nodes, thymus and spleen. The human semaphorin protein exhibits 46% amino acid identity to the AIHV-1 semaphorin (Lange *et al.*, 1998). ORF A4 does not display homology to any sequence in the databases and no function is known, although it contains a putative signal peptide cleavage site and so may be secreted (Coulter *et al.*, 2001). ORF A5 is a homologue of EBV BILF1 and EHV-2 E6. These encode GPCR with seven transmembrane domains. ORF A6 is predicted to encode a protein of 220 amino acids and has a 19.5% amino acid identity to BZLF1 of EBV (Ensser *et al.*, 1997). EBV BZLF1 encodes Zta, a DNA-binding transcriptional activator (Takada & Ono, 1989). ORF A7 shows a weak sequence homology of 17.1% to BZLF2 (Coulter *et al.*, 2001). In EBV this protein encodes a glycoprotein, gp42, which interacts with the β 1 domain of the MHC class II protein (Li *et al.*, 1997). ORF A8 is a positional equivalent of the EBV gene that encodes the glycoprotein gp350/220, however, A8 shows only a limited sequence homology of 16.5% to this protein. The protein is predicted to encode a glycoprotein. ORF A9 encodes a Bcl-2-like protein that may regulate apoptosis. It shares sequence homology in the Bcl-2 homology (BH) 1 domain only (Ensser *et al.*, 1997). ORF A9 will be discussed in more detail in a later section. ORF A10 is predicted to encode a glycoprotein that is 472 amino acids in size (Ensser *et*

al., 1997). The protein is specific to AIHV-1 and may be involved in the attachment and entry of the virus into the cell (Coulter *et al.*, 2001). Virus that has become attenuated by extended passage in cell culture undergoes a variety of genome rearrangements. In some cases the 5' end of the A10 gene is lost and a block of DNA from the middle of the genome is inserted into a position between the 3' end of A10 and the terminal repeat. Therefore, the product of A10 is not expressed in these cells (Handley *et al.*, 1995; Wright *et al.*, 2003). AIHV-1 and OvHV-2 conserved herpesvirus genes and their possible function are listed in table 1.2.

Fig 1.4 The Genome Organisation of Alcelaphine Herpesvirus -1

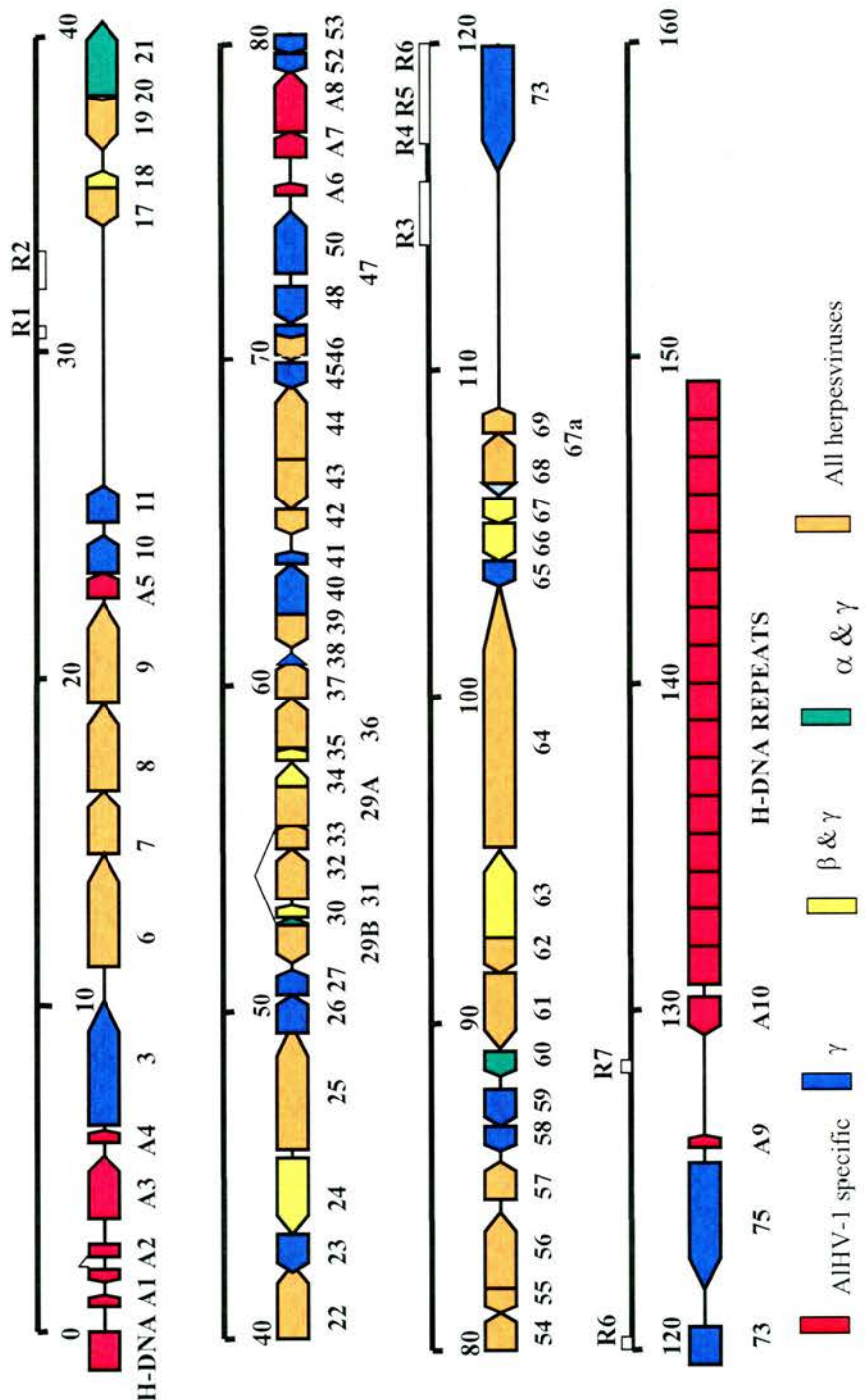


Fig. 1.4 The diagram shows the linearised genome of AIHV-1. The open reading frames are represented as block arrows, which are coloured according to the conservation of the open reading frame among the three subfamilies (α , β and γ) of herpesviruses. Major repetitive regions of the genome are marked R1 to R7. The genome length is shown in Kbp. Adapted from Ensser *et al.*, 1997.

Table 1.2 AIHV-1 and OvHV-2 ORFs

AIHV-1 gene	OvHV-2 gene	Possible function
A1		Unknown
A2	O2	Leucine zipper protein, transcriptional regulator
	O2.5	IL-10 homologue
A3	O3	Semaphorin homologue: cell signalling
	O3.5	Unknown, secreted
A4		Unknown, secreted
A4.5	O4.5	Bcl-2 homologue: cell death regulator
A5	O5	G-protein coupled receptor; intracellular signalling
A6	O6	EBV BZLF1 homologue; transcriptional activator
A7	O7	Viral glycoprotein
A8	O8	Viral glycoprotein
	O8.5	Unknown
A9	O9	Bcl-2 homologue; cell death regulator
A10	O10	Unknown

Table 1.2. AIHV-1 and OvHV-2 ORFs and possible functions (based on sequence homologues).

1.4.8. Ovine Herpesvirus-2 (OvHV-2)

Sheep-associated-MCF (SA-MCF) caused by OvHV-2 was first recognised in Europe (Colson, 1930). Since then it has been recorded worldwide. As yet no free virus has been isolated from domestic sheep. Infection of susceptible cattle and rabbits with virus-infected cells induces MCF, and from various tissues large granular lymphocytes (LGLs) of T-cell (or possibly natural killer (NK) cell) phenotype can be developed and grown in culture (Plowright, 1990; Schock *et al.*, 1998). DNA from these cell lines hybridises to unique regions of AIHV-1 (Reid, 2000), indicating that AIHV-1 and OvHV-2 are related. To determine whether the LGL cell lines supported productive or latent phases of the virus life cycle, an electrophoretic technique was used (Gardella *et al.*, 1984). Gardella gel analysis works on the basis that latent virus is in closed circular episomal form and lytic cycle virus is in linear form. Lysis of infected cells by detergent protease, followed by long electrophoresis times and southern blotting with viral probes, can resolve the linear and circular viral genomes. Such analysis of LGL cell lines has shown that bovine LGL cell lines were predominantly latently-infected (Rosbottom *et al.*, 2002). Rabbit cell lines on the other hand had predominantly linear DNA present in Gardella gels, which would indicate that most of the cells were undergoing productive replication (Rosbottom *et al.*, 2002). LGL cell lines can be used to infect susceptible species (Reid *et al.*, 1983; Swa *et al.*, 2001). The L-DNA genome sequence of OvHV-2 has recently been determined (Rosbottom, 2003) (fig1.5). The predicted amino acid identities of ORF products in comparison to AIHV-1 ranges from 28% (in ORF O6) to 83% (comparing the capsid protein vp23 encoded by ORF 26). The genomic arrangement of OvHV-2 is very similar to that of AIHV-1 (Ensser *et al.*, 1997). Many of the conserved herpesvirus genes that were originally described in AIHV-1 appear to be present in OvHV-2. These include O2, O3, O5, O6, O7, O8 and O9. However, there are also differences, such as the presence of an ORF 49 in OvHV-2, which is not present in AIHV-1. This ORF is not unique to OvHV-2 as it is present in HVS and most other gammaherpesviruses. Other OvHV-2-specific ORFs include O3.5, which is predicted to encode a secreted protein and is in the same position as A4 of AIHV-1. However, their predicted amino acid sequences are very different. OvHV-2 also possesses ORF O2.5,

which is not seen in AIHV-1. This encodes a 182aa protein with homology to IL-10. IL-10 homologues are present in other gammaherpesviruses such as EBV and EHV-2 (Rosbottom, 2003) as well as other viruses such as the betaherpesvirus CMV and parapoxvirus orf virus (Lyttle *et al.*, 1994; Kotenko *et al.*, 2000; Haig *et al.*, 2002). Some of the predicted ORFs and possible functions are shown in table 1.2.

Fig 1.5 Genome Organisation of Ovine Herpesvirus 2

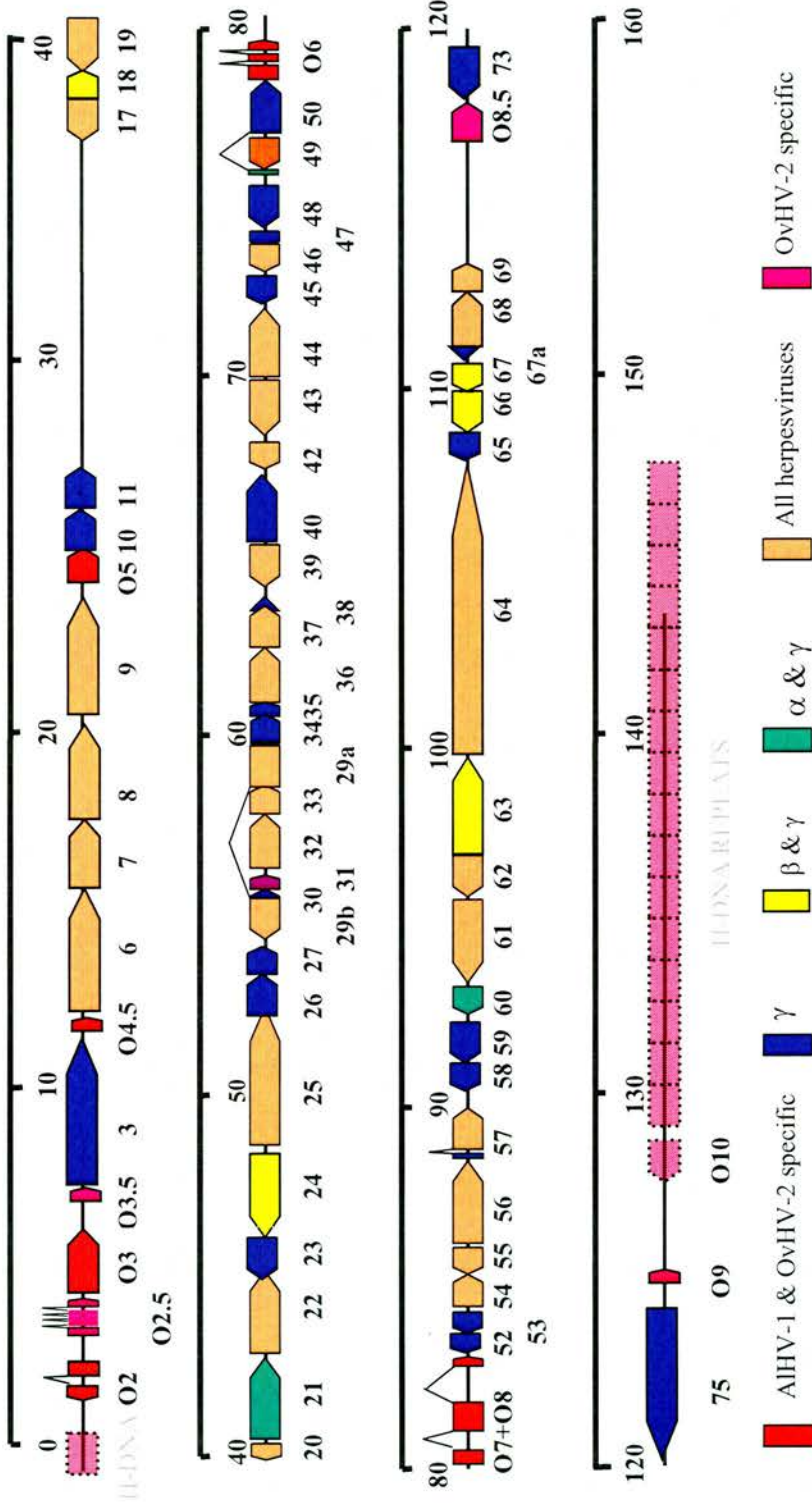


Fig 1.5. The genome organisation of OvHV-2. The diagram shows the linearised genome sequence of OvHV-2 that was cloned into cosmids. The open reading frames are represented as block arrows, which are coloured according to the conservation of the ORF among the three subfamilies (α , β and γ) of herpesviruses. The ORFs unique to OvHV-2 and AIHV-1 are shown in red, whilst the ORFs unique to OvHV-2 only are shown in pink. The genome length is shown in Kbp. ORF 49, shown in orange, is missing in AIHV-1 but is present in HVS, PLHV-1 and other gammaherpesviruses. The sequence not yet cloned, but predicted to be present by comparison with the AIHV-1 genome sequence, is shown in semi-transparent colour. Adapted from Rosbottom, 2003.

1.4.9. Other viruses implicated in MCF

In serological studies, antibodies to AIHV-1 or antigenically related viruses have been detected in species belonging to four subfamilies of *Bovidae*: *Alcelphinae*, *Hippotroginae*, *Caprinae* and *Ovibovinae* (Reid, 2000). Using techniques including serology, DNA alignment and phylogenetic analysis a gammaherpesvirus similar to AIHV-1 was found in goats, and named caprine herpesvirus-2 (CpHV-2). This virus is found worldwide, endemic in goats and is possibly associated with malignant catarrhal fever in Sika deer (Crawford *et al.*, 2002).

A herpesvirus was recovered from cells of a roan antelope (*Hippotragus equinus*) and found to be antigenically related to AIHV-1 and OvHV-2. This gammaherpesvirus was designated hippotragine herpesvirus-1 (HipHV-1). On inoculation into rabbits the virus caused MCF (Reid and Bridgen, 1991).

A virus isolated from Jimela topi and Cape hartebeest was designated *Alcelaphine herpesvirus-2* (AIHV-2) (Seal *et al.*, 1989). A study carried out by Flach and co-workers (2002) showed that scimitar-horned oryx and gemsbok carry their own gammaherpesviruses. Antibodies were present that cross-reacted with AIHV-1 and gammaherpesvirus DNA was detected using primers against herpesvirus DNA polymerase. A herpesvirus was isolated from scimitar-horned oryx and caused MCF when inoculated into rabbits.

1.4.10. Diagnosis and prevention of MCF

There are several methods available to diagnose MCF. Customarily, this has been achieved using post mortem histopathology, history of the herd and the clinical signs that the animal presented with. At present, the laboratory diagnostic tests for virus that are used include virus isolation (AIHV-1) from infected cells, indirect immunofluorescence (using AIHV-1), virus neutralisation and PCR.

The most effective method to isolate the virus is by infecting monolayers of bovine turbinate (BT) cells with either virus-infected cells or free virus. Typical syncytial (multinucleate cell) CPE will develop within 10 to 20 days (Reid & Buxton,

1989) however specificity still needs to be confirmed by indirect immunofluorescence or immunoperoxidase assays (Ferris *et al.*, 1976; Rossiter, 1981).

An indirect immunofluorescence assay is carried out using sera from diseased animals. This can be used in the diagnosis of clinical cases or in identifying latently-infected carriers. AIHV-1 virus is grown in BT cells on a coverslip until 50-70% CPE is reached. A fluorescence test is carried out using serum from the infected animal, BHV-4 is used as a negative control. However, this test is used post mortem and is not particularly sensitive it cross-reacts with other herpesviruses (Rossiter, 1981).

The virus neutralisation test measures serum AIHV-1 and OvHV-2 neutralising antibodies. The test is carried out in 96-well plates using a virus stock of 100 TCID₅₀. The virus is incubated in BT cells for 6 – 9 days and is checked for CPE (Seal *et al.*, 1988). The median virus-neutralising titers of the sera are determined using the method of Karber (1931). Animals considered to have been exposed to the virus usually have serum titres above 1:4. One advantage of this assay is that the antibodies do not cross react with other known bovine herpesviruses. However, the disadvantage is the results take between 12 -14 days to get.

A competitive inhibition enzyme-linked immunosorbent assay (CI-ELISA) was produced using a monoclonal antibody that is specific for a glycoprotein that is conserved between AIHV-1 and OvHV-2 (Li *et al.*, 1994; Li *et al.*, 2001). The assay measures antibody to the virus and is used to determine OvHV-2 in samples.

MCF virus-specific PCR is the preferred method to diagnose MCF (by detecting viral DNA) in a clinical case as it can be used on material obtained antemortem or post mortem (Tham, 1997). It has a high sensitivity and specificity in sheep, goats, wildebeest and all susceptible animals identified so far. PCR is much quicker than virus isolation. The portion of DNA that is amplified for AIHV-1 is ORF 21. This ORF has homology to EBV ORF BXL1 that encodes for thymidine kinase. A study comparing PCR and CI-ELISA showed a 95% agreement. However, this study concluded that PCR was the most reliable method for detecting OvHV-2 MCF in susceptible species (Li *et al.*, 1995).

1.4.11. Vaccines for MCF viruses

Various vaccine strategies have been tried and tested (Plowright, 1968; Rweyemamum *et al.*, 1976; Hamdy *et al.*, 1978; Rossiter 1982) without positive results.

In one study virus isolated from hartebeest and passaged in a BT cell monolayer did not induce MCF in six inoculated cattle (Reid & Rowe, 1973). All developed serum-neutralizing antibody to WC11. Three of the animals were challenged with cell-associated virulent virus isolated from wildebeest and the remaining three were challenged with cell-associated virus that had been passaged in BT cells. The three animals challenged with wildebeest cell-associated virus developed MCF and died, while of the three challenged with BT cell-associated virus only one developed MCF and died. The remaining two animals were then challenged with wildebeest cell-associated virus became viraemic and developed the disease (Reid & Rowe, 1973).

There have been a number of studies carried out with virulent AIHV-1 virus that had been formalin-inactivated or combined with an adjuvant and administered intraperitoneally. These studies produced high levels of neutralising antibodies. However, they provided no resistance to parenteral challenge by cell-associated virulent virus (Plowright *et al.*, 1975). In rabbits vaccinated with inactivated antigens administered intravenously resistance was not produced against the virulent cell associated strain of the virus (Edington & Plowright, 1980).

Keeping reservoir species and susceptible species apart is the current best method of control of MCF. This is particularly important in animals that are kept in captivity. Susceptible species should be segregated from wildebeest, especially during the breeding season and up until the wildebeest calves are at least six months old. If an animal does develop MCF then it should be kept in isolation (Hinchcliff, 2000).

1.5. The host antiviral immune response

The first barrier to virus infection is a host epithelial cell layer. Upon infection of epithelial cells an inflammatory response is initiated. These cells produce cytokines and chemokines involved in inflammation, which is characterised by an increase in blood flow, vascular permeability and leukocyte recruitment to the site of infection

(Roitt *et al.*, 1998). The early response to a virus infection is antigen non-specific and forms part of the innate immune response. Interferon (IFN, type 1 IFN- α/β or type 2 IFN γ) is an important part of host response to virus infection. IFNs stimulate an “anti-viral state” in target cells, to block or impair viral replication, slow the growth of target cells and make them more susceptible to apoptosis (reviewed in Goodbourn *et al.*, 2000). IFNs induce anti-viral mechanisms after binding to their specific receptors on infected cells. This leads to a signal transduction cascade involving Janus kinases (JAK) and signal transducer and activation of transcription (STAT) factors that leads to the transcription of IFN-inducible genes (Goodbourn *et al.*, 2000). The best characterised IFN-inducible components of the antiviral response are protein kinase R (PKR) and the 2'-5' oligoadenylate synthetases. A 67kDa cytosolic PKR protein, binds dsRNA of virus antigen and inhibits the phosphorylation of the α subunit of eIF-2 (a translation initiation factor) after binding virus dsRNA to inhibit viral and cell protein translation thereby inhibiting viral replication (Clemens & Elia, 1997). The 2'-5'-oligoadenylate synthetase activates a latent endonuclease RNase L that degrades viral RNA preventing viral infection (Roitt *et al.*, 1996) and also promotes NF κ B. NF κ B plays an important role in the induction of many immunomodulatory genes, including other cytokines, MHC class I and cell adhesion molecules (Goodbourn *et al.*, 2000). Apoptosis, or programmed cell death, is an innate mechanism that the host uses to eliminate virus-infected cells. It can be induced by a variety of stimuli such as radiation, drug treatment, cytokine withdrawal and infection. Apoptosis will be discussed in detail in a later section.

As well as interferons (IFN $\alpha/\beta/\gamma$), tumour necrosis factor (TNF), natural killer (NK) cells and macrophages are also produced in response to a virus infection. TNF promotes the production of other cytokines and enhances the activation of T and B cells. It can increase the expression of MHC class I and II molecules thereby improving virus antigen presentation (Banyer *et al.*, 2000). Active NK cells can be detected within two days of viral infection (Roitt *et al.*, 1996). IFN activates NK cell cytotoxicity and lysis of virus-infected cells (Biron, 1997).

Complement activation also plays a role in antibody mediated viral immunity by coating the virus, promoting phagocytosis or by directly lysing viruses with lipid membranes (Barber, 2001).

The adaptive immune response is initiated when viral peptides (antigens) are presented by antigen-presenting dendritic cells to antigen-specific T-lymphocytes in a MHC-restricted manner. The adaptive immune response is characterised by virus-antigen specificity and immunological memory. Antigen-specific B-lymphocytes develop into plasma cells that secrete antibodies, whereas T-lymphocytes either assist B-lymphocytes to produce virus-specific antibodies or directly attack and kill virus-infected cells (e.g. cytotoxic T-cells (CTL)). Antigen-presenting dendritic cells present antigens on the surface of the cell in association with the major histocompatibility complex gene derived proteins (MHC class I and II). The MHC class I molecule consists of a polymorphic transmembrane heavy chain associated with a non-polymorphic light chain and a peptide derived from proteolysis of cytoplasmic proteins. By transferring these peptides from the cytoplasm to the cell surface, the MHC class I antigen presentation system provides CTL's with a means of inspecting the intracellular environment (Heemels & Ploegh, 1995; York & Rock, 1996). These protein complexes bind antigen less specifically than the antigen receptors on T-and B-lymphocytes but ensure that T-and B-lymphocytes recognise the antigen efficiently in order that foreign as opposed to self-antigens are preferentially recognised. Memory exhibited as a vigorous immune response involving large numbers of antigen-specific lymphocytes is produced rapidly after subsequent infection (Haig, 2001).

CTL's use perforin and granzymes or/as well as FAS-FASL mediated mechanisms to induce death in virus-infected cells. Natural killer cells also secrete processed granzymes that can enter the target cells through repair endocytosis. These processes lead to activation of pathways that eventually lead to apoptosis of infected target cells (Barber, 2001).

1.5.1. Immune evasion mechanisms adopted by herpesviruses

As the host animal has evolved mechanisms to attempt to prevent the virus from establishing, the virus has itself evolved mechanisms to evade the immune system. Such strategies include interference with/or avoidance of the innate and adaptive immune responses (Haig, 2001). For example, by interfering with the host apoptosis response (Vossen *et al.*, 2002), interferon response (Goodbourn *et al.*, 2000) and aspects of the adaptive immune response.

One way in which the virus overcomes the immune system to interfere with antigen processing and presentation. This is the mechanism by which the host recognises foreign peptides and activates CD8⁺ T cells or CD4⁺ T cells to establish an anti-viral immune response. For example, EBV encodes a nuclear antigen (EBNA)-1 that is able to avoid CTL detection and encodes a mechanism to inhibit the generation of epitopes (Levitskaya *et al.*, 1995), HSV encodes a cellular protein 47(ICP47) that binds to the transporter associated with antigen presentation and inhibits transporter associated with antigen presentation-mediated peptide translocation across the ER membrane (Fruh *et al.*, 1995). HCMV possess pp65 that modulates the processing of another HMCV protein. These proteins prevent peptide generation and transport (Alcami & Koszinowski, 2000).

Viruses have also evolved strategies to counteract the complement system. It has been shown that herpesviruses such as HSV and VZV can inhibit the classical complement activation pathway by avoiding complement binding to antibody-antigen complexes. This removes the antibody-antigen complexes from the cell surface of the infected cell or by expressing Fc receptors (Dowler & Veltri, 1984). Another way in which they can bypass the complement pathway is by expressing proteins with functional similarities to regulators of complement activation (RCA) proteins and other complement regulators in order to protect their lipid envelopes and the membranes of the infected cells (Favoreel *et al.*, 2003). An example of this can be seen with HVS, which encodes two proteins that share amino acid homology with complement regulators. ORF4 encodes a protein with homology to decay-accelerating factor (CD55) and has been found to inhibit C3 convertase activity. ORF15 encodes a protein with homology

to CD59, the terminal product of the complement cascade, the membrane attack complex. Finally the viruses can incorporate the host complement control proteins into their viral envelope and so can upregulate the expression of these proteins in the infected cells (Favoreel *et al.*, 2003). HCMV has been found to upregulate CD55 (a protein that can protect cells from complement mediated lysis) and CD46 (protein that is involved in the regulation of complement activation). Functional studies revealed that the upregulation of CD55 resulted in the suppression of the alternative complement pathway and an increase in resistance to complement-mediated lysis.

Herpesviruses can also interfere with the interferon response by blocking IFN-induced transcriptional responses and the janus kinase/signal transducers and activators of transcription factors. This can be achieved by inhibiting PKR activation and the phosphorylation of eIF-2 α .

Herpesviruses can reduce the inflammatory response. This is demonstrated in EBV and CMV, which possess homologues of mammalian IL-10, a cytokine with anti-inflammatory activity (Zdanov *et al.*, 1997).

Herpesviruses can modulate the activity of chemoattractant cytokines that regulate leukocytes trafficking to sites of infection. They can also encode cytokine receptors (vCKR). For example, HCMV and HHV-6 encode vCKR's. However, their function is unknown. The viral envelope protein, gp350, in EBV induces the expression of the IL-1 receptor antagonist, which inhibits the activity of IL-1. IL-1 is important in inflammatory responses (Roberge *et al.*, 1996).

1.5.2. Viral initiation and prevention of apoptosis

Multicellular organisms have a variety of strategies to defend themselves from viral infection. On infection of many cell types, cytokines such as IL-1 and TNF are produced, which in turn activate and recruit macrophages, NK cells and neutrophils. These cells can induce phagocytosis and help to clear the viral infection. Apoptosis is another anti-viral strategy. If the cell can commit suicide before the virus has replicated or before large amounts of virus are produced this will protect surrounding cells. The second line of defence, adaptive immunity, is mediated through humoral and cell

mediated immune responses. This line of defence involves cytotoxic T cells, antibodies and cytokines.

Virus replication can trigger apoptosis directly or provoke the recognition by CTLs and NK cells. CTLs can trigger receptor-mediated apoptosis either by the release of soluble factors such as TNF or by direct cell-cell contact via membrane-bound Fas ligand (FasL). Engagement of both of these factors leads to the recruitment of cytoplasmic components, which can eventually lead to caspase activation (this will be discussed later in the chapter). The attachment and entry of the host cell can trigger apoptosis. For example, even non-infectious virus particles of HSV-1 can induce apoptosis in HeLa cells (Galvan & Roizman, 1998). Therefore, it would appear that viral entry can trigger apoptosis in susceptible cells unless anti-apoptotic proteins are expressed to prevent the apoptotic pathway.

The lytic granule-mediated mechanisms are the major pathway by which CTL eliminate virus-infected cells (Kagi *et al.*, 1995). The major factors of this pathway include perforin and granzymes A and B. Perforins function by allowing granzymes to redistribute from the endosomal compartment to the cytoplasm and nucleus. Both granzyme A and B can induce apoptosis in the target cell however, they can do this in different ways (Russell & Ley, 2002). Granzyme B-mediated apoptosis involves the cleavage of Bid by granzyme B to activate the mitochondria pathway (which will be discussed later in this chapter) (Sutton *et al.*, 2000).

When viruses infect cells their proteins disturb normal cell physiology and provide upstream signals that trigger a death response. There are a number of checkpoints that trigger apoptosis in host cells such as the attachment and entry of viruses in the host cell, IFN production, mitochondrial sensors, activation of p53 and the inundation of viral proteins in the ER (reviewed in Everett & McFadden, 1999).

Initiation of the Fas and TNF pathway occurs by the binding of the receptor and ligand on the cell surface this results in the stimulation of the Fas induced apoptosis pathway, which is described in section 1.5.2. Therefore many viruses have evolved proteins that prevent this pathway from being initiated, for example Adenoviruses express protein E3-10.4K and E3-14.5K these proteins reduce the presentation of Fas

molecules on the surface of the cell. This reduction results in the resistance to Fas-mediated cell death. These proteins also confer some resistance to TNF-mediated apoptosis (Dimitrov *et al.*, 1997; Shisler *et al.*, 1997).

PKR is one activator of IFN and PKR gene expression is in turn upregulated by IFN. The enzyme becomes activated by dsRNA binding two dsRNA binding motifs in its amino terminus, to promote dimerisation, this stimulates trans-autophosphorylation. The phosphorylated dimeric PKR recognises the eukaryotic translation initiation factor-2 (eIF-2). Therefore for a virus to overcome this pathway and produce a successful infection it has to evolve mechanisms to inhibit PKR function. KSHV expresses a protein vIRF2 (ORF K11.1) that binds and inactivates PKR thereby preventing the initial activation of IFN, by this particular pathway (Burysek & Pitha, 2001). It has also been demonstrated in other viruses, for example, the hepatitis C virus expresses a protein NS5A, this protein binds and inhibits PKR (Gale *et al.*, 1997). Hepatitis C virus also expresses an envelope protein, E2, this has been shown to inhibit kinase activity thereby blocking the inhibitory effect that PKR has on protein synthesis (Polak *et al.*, 1997).

Activation of p53 is a mechanism that the host cell uses to induce apoptosis upon viral infection. p53 can be activated by many different types of DNA damage such as double-stranded breaks in DNA by γ -irradiation, the presence of DNA repair intermediates and chemical damages to DNA. Unscheduled DNA replication and viral gene expression can lead to the activation of transcription factor p53. In the cell cycle p53 activation leads to the transcription of p21. p21 binds to a number of cyclin and Cdk complexes to stop DNA replication (El-Deiry *et al.*, 1993). The mechanism by which p53 induces apoptosis still remains unclear. It is known that p53 targets genes that are involved in apoptosis such as Bax, Fas and NF κ B (Bennet *et al.*, 1998; Gottlieb & Oren, 1998; Ryan *et al.*, 2000). Many viruses have evolved proteins to counter the effects of p53, for example adenoviruses express proteins, E1B-55K that act as p53 antagonists. E1B-55K binds and inactivates p53 (Alcami & Koszinowski, 2000). HHV-8 also encodes a p53 inhibitor, LANA. Human papilloma virus encodes a protein E7 that induces p53-induced apoptosis, however, it also encodes a protein, E6, which binds p53 and proteolytically degrades it (Tortorella *et al.*, 2000).

1.5.4. Apoptosis

Apoptosis can be triggered by a variety of stimuli. It is a major form of cell death and one way in which the host can limit viral proliferation. Therefore, herpesviruses have developed strategies to prevent apoptosis by expressing proteins that block cell death. This can be carried out by encoding homologues of cellular anti-apoptotic Bcl-2 proteins, blocking signals triggered by activation of TNFR family members and inactivating IFN-induced PKR and the tumour suppressor p53. One example of this can be seen in HHV-8, K13 protein, which encodes a vFLIP protein. This protein interacts with Fas associated death domain (FADD) or FLICE and inhibits the recruitment of FLICE, which initiates the caspase cascade.

Some of the gammaherpesviruses that have been sequenced encode a vFLIP and at least one Bcl-2 homologue, suggesting that these are important proteins in the viral life cycle and/or in pathogenesis. The cellular Bcl-2 family and FLIP are key regulators of apoptosis suggesting that it is an important anti-viral defence mechanism.

There are two major forms of cell death: apoptosis and necrosis. The features that are normally seen in cells that are undergoing necrosis are clumping of the nuclear chromatin, dilation of the endoplasmic reticulum and dispersal of ribosomes. These factors are followed by the swelling of the mitochondria, and progress to the rupturing of nuclear, organelle and the plasma membranes. The eventual result is that phagocytic cells ingest and degrade the debris (Wyllie *et al.*, 1980).

The onset of apoptosis is characterised by the shrinking of the cell and the condensation of nuclear chromatin into sharply defined masses that marginate against the shrinking nuclear membranes. The cellular phospholipid bilayer is disrupted and leads to the phospholipid, phosphatidylserine, being exposed on the outer leaf of the plasma membrane and the activation of an endonuclease, which cleaves genomic DNA. The precise endonuclease is still unknown. Work carried out by Enari and co-workers (1998) showed that a caspase-activated deoxyribonuclease (CAD) and its inhibitor (ICAD) exist as a complex. After apoptotic stimuli, ICAD is cleaved from the complex allowing CAD to enter the nucleus and degrade chromosomal DNA. However, others

have found various other nucleases that could also be considered as candidates (Zhang *et al.*, 1998; Sakahira *et al.*, 1998, Wyllie, 1998) it would therefore appear that the apoptosis-associated nuclease is not sequence specific and no one nuclease is involved entirely (Wyllie, 1998). The nucleus condenses further and breaks up, with double membranes surrounding the nuclear fragments. The whole cell breaks down into membrane bound apoptotic bodies, which are spherical or ovoid in shape. The apoptotic bodies are rapidly phagocytosed by healthy neighbouring cells such as macrophages (Wyllie *et al.*, 1980).

Apoptosis can be broadly categorised into three stages: activation, execution and disposal. Activation can be caused by an external stimulus delivered through surface receptors or an internal stimulus such as the action of a drug, toxin or radiation. The execution phase is a regulatory cascade which when initiated leads to the biochemical and morphological changes characteristic of apoptosis. It is during this phase that the cell is committed to apoptosis. The final phase, disposal, involves the removal of the resulting apoptotic bodies by phagocytic cells such as macrophages.

There are two main pathways that initiate apoptosis; firstly through ligand binding and secondly by loss of suppressor activity. Death receptors can play a role in initiating apoptosis when a cell loses contact with its surroundings or incurs irreparable internal damage. These receptors belong to the tumour necrosis factor (TNF) receptor gene superfamily. One of the most studied and well-characterised death receptors is Fas (also known as CD95 or Apo 1) (Ashkenazi & Dixit, 1998). Fas is a cell surface protein and is a receptor for Fas ligand (FasL). Fas L is a homotrimeric molecule that binds to three Fas molecules. Fas ligation leads to the clustering of the receptor death domains. An adaptor protein called FADD (Fas-associated death domain) binds through its own death domain. FADD also contains a death effector domain that binds to an analogous domain repeated in tandem within the pro-enzyme form of caspase-8 (also known as FLICE). Caspase-8 is self-cleaved after binding to FADD and activates downstream effector caspases such as caspase-9 to induce apoptosis (fig 1.7) (Ashkenazi & Dixit, 1998).

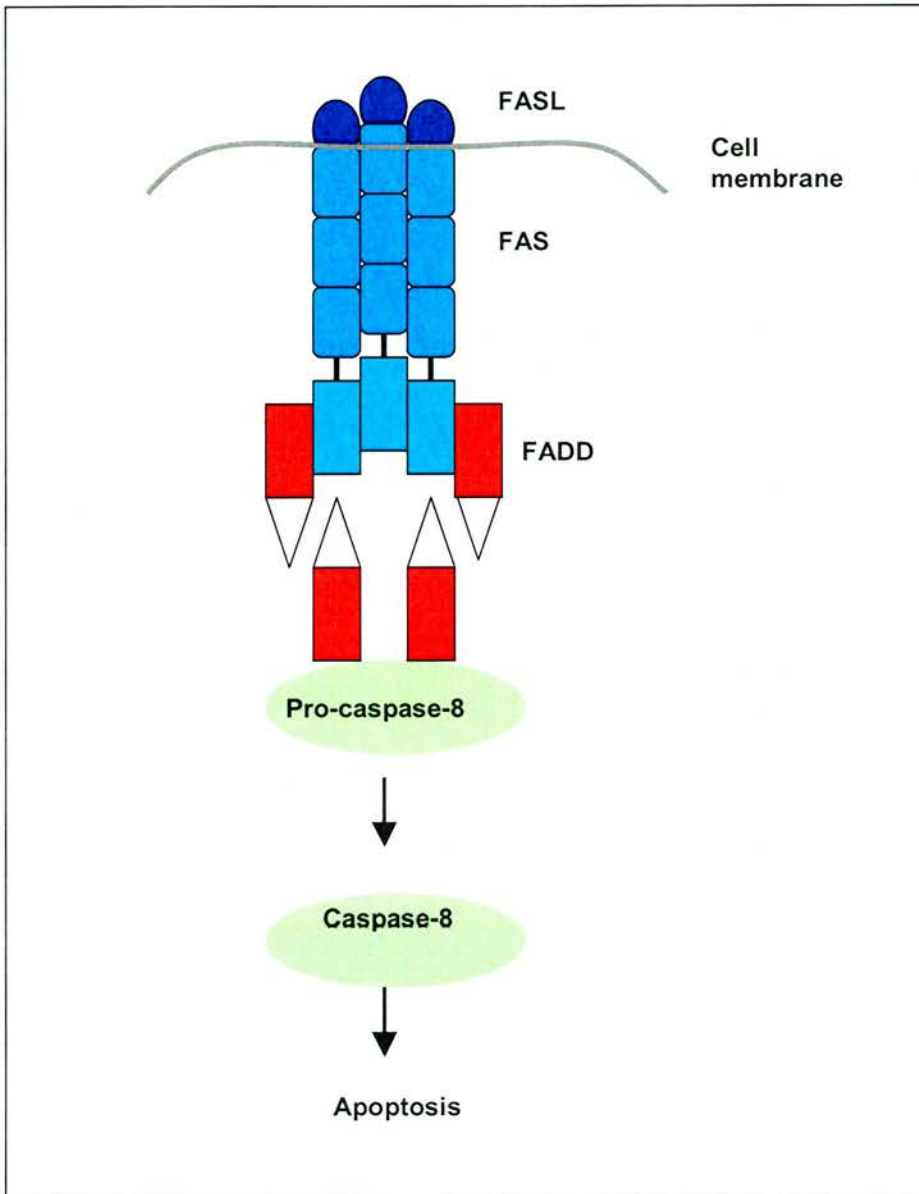


Fig 1.6. Apoptosis can be initiated by ligand binding. Fas binds to FasL which in turn binds to Fas associated death domain (FADD). This results in the self-cleavage of pro-caspase-8 to caspase-8, which activates the series of caspase cascades. The second pathway for initiation of apoptosis involves the loss of suppressor activity in response to a variety of cellular stresses such as DNA damage, protein kinase inhibition or loss of survival signalling, e.g. when cytokines are not available. This pathway is

often called the mitochondrial-dependent pathway and involves members of the Bcl-2 family of proteins. The mechanism of how apoptosis is initiated in this pathway still remains unclear. Possible mechanisms will be discussed in detail in a later section.

Apoptosis is accomplished by specialised cellular machinery which is highly conserved in different species (Thornberry & Lazebnik, 1998). Cytosolic Aspartate-Specific Proteases, also known as caspases, are responsible for the deliberate disassembly of a cell into apoptotic bodies. Caspases exist as an inactive form in the cytosol as a single polypeptide chain (Green & Kroemer, 1998). They all share similarities in amino acid sequence, structure and substrate specificity. All procaspases contain a highly homologous protease domain that can be divided into two subunits, a large subunit of 20kDa and a small subunit of approximately 10kDa. Each procaspase also contains a prodomain or NH₂-terminal peptide of variable length (Chang & Yang, 2000). It is believed that oligomerisation of procaspases is the mechanism of initiating caspase activation. However, effector procaspases are activated most commonly by initiator caspases and also by other proteases (Chang & Yang, 2000). Caspases cleave after aspartic acid residues with recognition of at least four amino acids essential for efficient catalysis. Caspases-6, 7 and 3 are directly implicated with the execution of apoptotic cells, while caspases-8, 10, 9 and 2 are initiator caspases which function as signalling molecules. Caspases are also involved in the cleavage of pro-apoptotic Bcl-2 proteins to produce a fragment that promotes apoptosis (Thornberry & Lazebnik, 1998). Bid, a pro-apoptotic Bcl-2 family member is cleaved by the initiator caspase-8 following death receptor activation (Li *et al.*, 1998).

The final stage in apoptosis is the disposal of the apoptotic body that is formed in apoptosis. During apoptosis the plasma membrane is disrupted leading to the exposure of phosphatidylserine on the plasma membrane. Phosphatidylserine is one receptor that phagocytic cells use as a signal of an apoptotic cell (Fadok & Chimini, 2001). The apoptotic cells are enveloped by pseudopodia that are extended by the phagocyte. Binding and engulfment is achieved by one or more membrane receptors such as CD14 (Devitt *et al.*, 1998), SR-A (Platt *et al.*, 1996) and CD36/vitronectin receptor. Internalisation of the apoptotic cell involves the reorganisation of some of the

cytoskeleton through adaptor molecules. The internalised apoptotic material is phagocytosed by dendritic cells, taken into the MHC class I pathway and presented to CTLs (Platt *et al.*, 1998).

1.5.5. Measuring Apoptosis

The process of apoptosis involves many changes in cell morphology as discussed previously. The process of cell shrinkage, increased cytoplasmic density, chromatin condensation and the segregation into sharply circumscribed masses to produce apoptotic bodies can be detected by electron microscopy (Kerr *et al.*, 1972). Confocal laser-scanning microscopy can also be used to analyse the morphological changes that take place (Smith *et al.*, 1992). By using DNA dyes such as propidium iodide and Hoechst 33342, the condensed chromatin and nuclear fragmentation that takes place can be examined.

During apoptosis, the DNA is cleaved by an endonuclease as described previously. This results in multiple fragments of 185bp being produced (Wyllie, 1980). These fragments can be analysed by agarose gel electrophoresis to show the typical “DNA-ladder” configuration (Compton & Cidlowski, 1986). The sensitivity of this assay can be increased by labelling free 3' OH ends of the nicked DNA with ³²P-dATP or ³²P-dCTP before agarose gel electrophoresis (Rosl, 1992).

Flow cytometric analysis, based on the morphological and cell phenotypic changes that take place (e.g. DNA fragmentation, DNA loss and membrane changes) can be used to make quantitative measurements of apoptosis. Apoptotic cells exhibit lower forward scatter and higher side scatter values than viable cells due to changes in size and granularity of the cells (Sgonc & Wick, 1994).

During apoptosis, the plasma membrane undergoes several changes. The phospholipid bilayer is disrupted which leads to the exposure of phosphatidylserine from the inner to the outer leaflet of the plasma membrane. This can be detected by annexin V, which binds to phosphatidylserine in the presence of calcium. To discriminate apoptotic cells from necrotic cells, propidium iodide is used in conjunction with annexin

V. This assay gives an early detection of apoptosis, but the disadvantage of this assay is the inability to distinguish between late apoptotic cells and necrotic cells.

A major event in apoptosis is the loss of mitochondrial membrane potential. This can be measured by staining the mitochondria with cationic, lipophilic fluorochromes such as 5,5',6,6'-tetrachloro-1,1',3,3'-tetraethylbenzimidazolcarbocyanine (JC-1), 3,3'-dihexyloxacarbocyanine iodide (DiOC₆(3)) or rhodamine 123. In apoptotic cells the incorporation of these dyes is reduced (Zamzami *et al.*, 1995).

1.6. Bcl-2 family of proteins

The Bcl-2 family is one of the most important families of regulatory proteins involved in apoptosis. The prototype of the family, the Bcl-2 proto-oncogene, was discovered at the chromosomal breakpoint of t(14:18) in human B-cell lymphomas (Bakhshi *et al.*, 1985). It was found to inhibit cell death rather than promote cell proliferation. Since this discovery, a number of Bcl-2 family members have been discovered that act as both anti- and pro-apoptotic proteins. The proteins all contain at least one of four domains known as Bcl homology (BH) domains as well as a transmembrane domain at the carboxy terminus. BH domains are important as they determine the capacity for the Bcl-2 proteins to form homo- or hetero-dimers or to bind proteins outside the Bcl-2 family (Tsujimoto & Shimizu, 2000). The Bcl-2 proteins can be roughly divided into three categories (fig 1.7):

- Anti-apoptotic members such as Bcl-2, Bcl-x_L, and Bcl-w share sequence homology within all four domains BH1, BH2, BH3 and BH4.

- Pro-apoptotic members such as Bax, Bad and Bak share sequence homology in BH1, BH2 and BH3, but do not possess the BH4 domain.
- ‘BH3 only proteins’ such as Bik, Bid and Bim are pro-apoptotic and as the name suggests, share sequence homology only in the BH3 domain (Adams & Cory, 1998; Tsujimoto & Shimizu, 2000). These proteins cannot homodimerise, but can form heterodimers with anti-apoptotic members (Kelekar & Thompson, 1998).

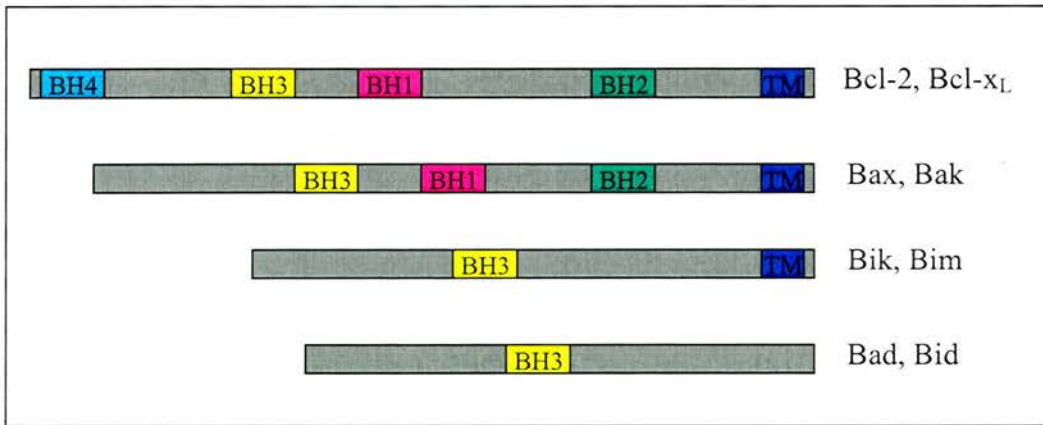


Fig 1.7. Comparisons of Bcl-2 protein domains. Anti-apoptotic proteins such as Bcl-2 and Bcl-x_L share sequence homology with all four domains. Pro-apoptotic members such as Bax and Bak share sequence homology in BH1, BH2 and BH3. Other pro-apoptotic members called the BH-3 only members contain only the BH3 domain. Pro-apoptotic members such as Bik and Bim possess the transmembrane domain while others such as Bad and Bid do not.

The BH1 and BH2 domains are important for Bcl-2 and Bcl-X_L to interact with pro-apoptotic proteins in order to prevent apoptosis (Borner *et al.*, 1994). The BH1 domain possesses a conserved “NWGR” sequence motif has a vital role in preventing apoptosis and facilitates the heterodimerisation of other Bcl-2 family members. However, mutational studies have shown that this sequence is not essential in homodimerisation (Yin *et al.*, 1994).

The BH3 domain appears to play a fundamental role in the induction of apoptosis. Through a series of mutagenic studies, this domain was shown to be key for pro-apoptotic proteins (Reed, 1998). It allows the pro-apoptotic proteins to interact with and antagonize anti-apoptotic proteins (Yang *et al.*, 1995). The introduction of the BH3 domain from Bax into Bcl-2 (anti-apoptotic) converts the protein to a pro-apoptotic protein (Hunter & Parslow, 1996). Mutations in the BH3 domain that affect heterodimerisation and apoptotic activity have been shown to occur at leucine at position 1 and aspartic acid at position 6 of the BH3 domain (Kelekar & Thompson, 1998).

The BH4 domain is highly conserved throughout the anti-apoptotic proteins. If this domain is deleted from Bcl-x_L it loses its apoptotic function, suggesting that the BH4 domain is vital for apoptotic behaviour. This domain binds to proteins not in the Bcl-2 family, but have a role in apoptosis involving mediators such as Raf1, ced4 and calcineurin (Huang *et al.*, 1998; Shibasaki *et al.*, 1997; Wang *et al.*, 1994). The BH4 domain may be essential for Bcl-2/Bcl-x_L prevention of apoptotic mitochondrial changes (Shimizu *et al.*, 2000). The BH4 domain interacts with the voltage-dependent anion channel (VDAC) (Boya *et al.*, 2001).

1.6.1. Bcl-x_L structure

The structure of Bcl-x_L has been examined in detail by X-ray crystallography and nuclear magnetic resonance (NMR). The protein consists of seven amphipathic α -helices which are joined by flexible loops (Reed, 1998). There are two main α -helices (α 5 and α 6). Studies have demonstrated that lying upstream of α 5 is the BH1 domain. The BH2 domain can be found in the distal region of α 6. These two central helices are predominantly hydrophobic. The BH3 domain has been shown to be on α 2 (Reed,

1998). A hydrophobic cleft is formed at the surface of the Bcl-x_L protein by the BH1, BH2 and BH3 domains (Muchmore *et al.*, 1996; Reed, 1998). This is the binding site for the BH3 domain of Bak (Muchmore *et al.*, 1996). The Bcl-x_L protein shares structural similarity with the pore-forming diphtheria toxin. These toxins form pores which act as channels for ions and small proteins (Motyl, 1999; Antonsson & Martinou, 2000). This suggests that Bcl-x_L proteins may form pores in the endoplasmic and mitochondrial membranes and may be regulated by signals dependent on voltage and pH (Motyl, 1999).

1.6.2. Bid structure

The structure of the pro-apoptotic protein Bid was determined by heteronuclear NMR spectroscopy. The structure of this protein was very similar to that of Bcl-x_L. It consists of eight helices that are arranged into three layers. As with Bcl-x_L there are two central helices (α F and α G) that are surrounded by amphipathic helices on either side. This protein, however, does not form the cleft that allows the BH3 domain to bind (McDonnell *et al.*, 1999).

1.6.3. Possible mechanisms of cytochrome c release

The anti-apoptotic proteins are found within the cytoplasmic region of the mitochondrial membrane, endoplasmic reticulum and nuclear envelope (Adams and Cory, 1998; Gross *et al.*, 1999). Most pro-apoptotic family members are found in the cytosol or cytoskeleton before the induction of apoptosis. An exception is Bak, which is an integral protein of the mitochondrial membrane (Gottlieb, 2000). After the induction of apoptosis, the BH3-only proteins undergo post-translational changes, which allow them to target membranes, especially the mitochondrial membrane (Gross *et al.*, 1999).

Mitochondria play an essential role in the regulation of apoptosis by releasing apoptogenic factors such as cytochrome *c* and apoptosis inducing factor (AIF) (Liu *et al.*, 1996; Yang *et al.*, 1997; Kluck *et al.*, 1997). The actual mechanism by which cytochrome *c* is released is the subject of a long-standing debate and remains unresolved

(Skulachev, 1996; Vander Heiden *et al.*, 1997). Bax and other pro-apoptotic proteins promote the release of cytochrome *c*.

One theory behind the release of cytochrome *c* is that Bcl-2 family members aggregate to form a pore that is large enough to allow the passage of cytochrome *c*. This was suggested by structural similarity between Bcl-x_L and a bacterial pore-forming toxin (diphtheria toxin). *In vitro*, Bcl-2 family members are able to form ion-conducting pores in artificial bilayers (Schendel *et al.*, 1997). Bid is proteolysed by caspase 8 and the C-terminal portion (tBid) interacts with the mitochondria membrane (Li *et al.*, 1998; Desagher *et al.*, 1999; Gilmore *et al.*, 2000). Bax and Bak are thought to undergo a conformational change after they have interacted with tBid. In the cytosol, where Bax is normally found, the protein exists as a monomer. However, upon activation by tBid, Bim or by BH3 domains of BH3-only proteins, Bax changes conformation, translocates and inserts itself into the outer mitochondrial membrane. After induction by similar proteins, Bax can homo-oligomerise to form a complex that creates a large pore-forming channel (Fig 1.8). A model that has been proposed is that Bcl-x_L may bind to Bax in order to prevent Bax proteins from entering the mitochondrial membrane and thereby preventing the initiation of apoptosis (Harris & Thompson, 2000).

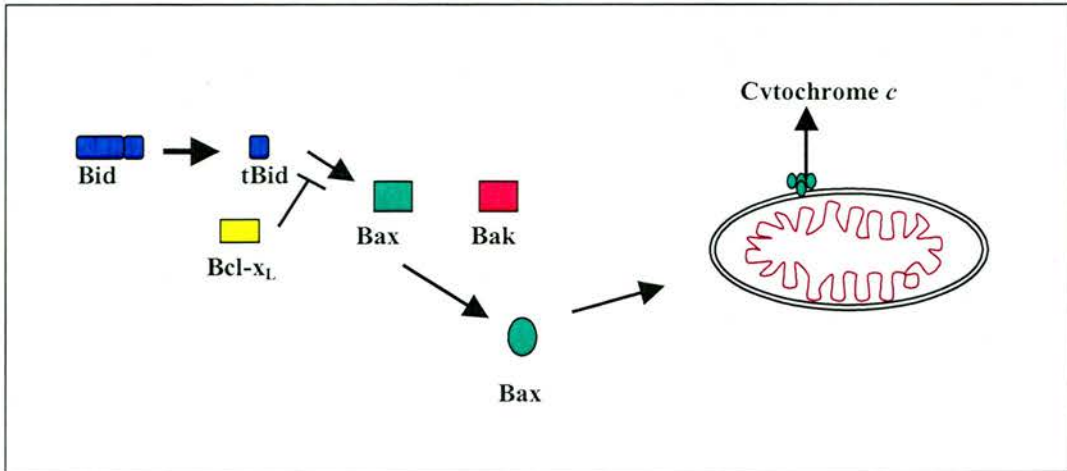


Fig 1.8. Possible mechanism of cytochrome *c* release during apoptosis. The pro-apoptotic Bcl-2 member, Bid is cleaved to, tBid. tBid can interact with Bax and Bak to change their conformation. Bax translocates from the cytosol to the mitochondrial membrane where it oligomerises and inserts into the membrane to form a pore to allow the release of cytochrome *c*. Anti-apoptotic members such as Bcl-x_L can prevent this translocation by binding to the BH3 domain of pro-apoptotic proteins.

A second theory is that the opening of the permeability transition pore (PTP) allows the release of cytochrome *c*. The PTP is a large multi-protein complex that can form a large channel between the cytosol and the mitochondrial matrix. The PTP is comprised of the voltage dependent anion channel (VDAC) (found in the outer membrane), the adenine nucleotide translocator (ANT) (found in the inner membrane), creatine kinase, hexokinase and cyclophilin D. Voltage, matrix pH, oxidative stress, electron flow, cyclophilin D and ANT can regulate the opening of the pore (Gottlieb, 2000). The outer membrane is permeable to solutes of up to 5kDa, allowing the exchange of respiratory chain substrates between the intermembrane space and the cytosol. Inner membrane impermeability is essential for the maintenance of the electrochemical potential (Van Loo *et al*, 2002). This model proposes that Bax can interact with the VDAC and the ANT to form a large hybrid channel (fig 1.9). Using isolated mitochondria and recombinant Bcl-2 family members it was also shown that the VDAC channel is a target for the Bcl-2 family members. Bcl-x_L closes the VDAC channel in liposomes while pro-apoptotic proteins such as Bax and Bak can open the VDAC channel to allow the passage of cytochrome *c* (Tsujimoto & Shimizu, 2000). Recent experiments using co-immunoprecipitation have shown that Bcl-x_L and VDAC interact. Other work showed that the BH4 domain of both Bcl-2 and Bcl-x_L was able to inhibit VDAC-dependent cytochrome *c* release (Harris & Thompson, 2000).

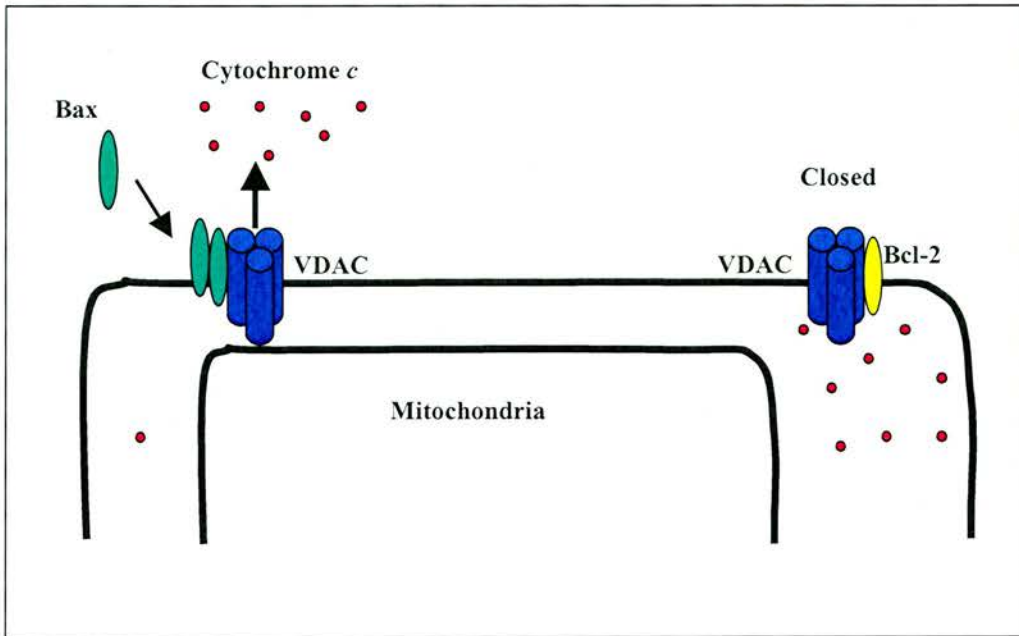


Fig 1.9. Possible mechanisms of cytochrome *c* release during apoptosis. The pro-apoptotic Bcl-2 member Bax can translocate to the mitochondria where it can open the voltage dependent anion channel to allow the release of cytochrome *c* by binding the voltage dependent anion channel. Bcl- x_L can also bind to the voltage dependent anion channel and prevent it from opening.

1.6.4. After the release of cytochrome c

Once cytochrome c has been released it exerts its effects by acting as a co-factor for the assembly of a large caspase-activating complex in the cytosol called the apoptosome. The apoptosome was discovered by Wang and colleagues through a cell-free system that was based on cytosolic extracts in HeLa cells (Liu *et al.*, 1996).

Once cytochrome c has been released from the mitochondria it binds to Apaf-1. Apaf-1 is a cytosolic protein that contains a caspase-recruitment domain (CARD), a nucleotide-binding domain (a similar domain that is found in the *C. elegans* protein CED-4) and multiple WD-40 repeats (Zou *et al.*, 1997). Apaf-1 binds to dATP, which triggers oligomerisation to form the apoptosome. The apoptosome complex is a wheel-like structure consisting of a central hub, connected to seven radial spokes. It is predicted to be composed of seven Apaf-1 CARD domains. The nucleotide-binding domain promotes oligomerisation and also forms spokes projecting outwards from the hub, connecting the core of the apoptosome to the Y-shaped tail formed by a bundle of WD-40 repeats (Acehan *et al.*, 2002).

The CARD domain of Apaf-1 becomes exposed in the apoptosome, this results in the recruitment of procaspase-9 to the complex. The recruitment of procaspase-9 initiates the auto activation of pro-caspase 9 to caspase 9. Only activated caspase-9 has the ability to efficiently cleave and activate downstream executioner caspases such as caspase-3 and -7 (Slee *et al.*, 1999). Upon activation caspase-3 then processes and activates caspases-2 and -6 followed by the activation of caspases-8 and 10 (by caspase-6) (Braton *et al.*, 2001).

Simultaneous with cytochrome c release Smac/Diablo, a 25kDa mitochondrial protein is also released from mitochondria into the cytosol during apoptosis. Upon import into the mitochondria a 55 amino acid mitochondrial targeting sequence is removed to produce a mature Smac molecule. The first four amino acid of the mature Smac molecule binds to BIR (baculovirus IAP (inhibitor of apoptosis protein)) (Du *et al.*, 2000). The IAP family are a group of intracellular proteins that contain BIR domains that inhibit active caspases (Chai *et al.*, 2000). Therefore when cytochrome c and Smac are released from the mitochondria, cytochrome c binds to Apaf-1, however,

this pathway can be terminated when IAPs bind and inhibit activated caspases. Therefore, Smac binds IAPs preventing this pathway from occurring (Braton *et al.*, 2001).

1.6.5. Viral bcl-2 homologues

The Bcl-2 family of proteins play an important role in apoptosis. Viruses have evolved Bcl-2 homologues to help evade the host immune response. The first viral Bcl-2 homologue was identified in cells which had been infected with adenovirus. The viral protein E1B 19K was required to prevent the destruction of the host cell and viral DNA and also enhanced the cytopathic effects during productive virus infection (Pilder *et al.*, 1984). Since this discovery, a number of viruses that have been sequenced have been found to possess at least one Bcl-2 homologue. In all of the gammaherpesviruses that have been sequenced a Bcl-2 homologue is present.

From the sequences of the viral Bcl-2 homologues it would appear that none of these possess the unstructured loop that is present in both cellular Bcl-2 and Bcl-x_L. However, they do contain a hydrophobic region within the carboxy terminus of the protein. It is thought that intracellular membrane localisation is mediated by this hydrophobic region (Cheng *et al.*, 1997). It would appear that the gammaherpesviruses have hijacked cellular Bcl-2 homologues in order to play an important role in the virus life cycle.

HHV-8 possesses a Bcl-2 homologue which protects against Sindbis virus-induced apoptosis. The gene product was found to possess amino acid sequence homology within two BH domains BH1 and BH2, but overall it only shares around 15-20% sequence similarity with other Bcl-2 family members (Cheng *et al.*, 1997). The gene contains the "NGWR" sequence that has been shown to be important for the prevention of apoptosis and heterodimerisation with other Bcl-2 family members (Yin *et al.*, 1994). The conserved caspase cleavage site present in human Bcl-2 is absent in the viral protein. The protein also lacks the unstructured loop that can be seen in cellular Bcl-2 proteins (Huang *et al.*, 2002). The KSHV Bcl-2 protein localises to organelle membranes in the same way as human Bcl-2, i.e. mainly the mitochondrial membrane,

but it can also be found in the ER and golgi apparatus (Sarid *et al.*, 1997). This protein can prevent early apoptotic cell death in cells that are infected with the virus and may also be involved in the development and growth of transformed cells in concert with the human Bcl-2 protein (Widmer *et al.*, 2002).

The MHV-68 Bcl-2 homologue, encoded by ORF M11, protects cells such as murine epithelial, HeLa and BHK cells from TNF- α induced apoptosis (Wang *et al.*, 1999; Bellows *et al.*, 2000; Roy *et al.*, 2000). Investigations carried out by Gangappa and co-workers (2002) demonstrated that the M11 gene was required for reactivation from latency. Using a M11 deficient virus establishment of latency did not require the virus Bcl-2 homologue, nor was it required for replication during an acute infection (Gangappa *et al.*, 2002).

EBV possesses two bcl-2 homologues, BHRF1 (*Bam*H1 rightward reading frame) and BALF1 (*Bam*H1 'A' fragment leftward reading frame 1). The first to be described was BHRF1 (Khanim *et al.*, 1997). It was found to contain both BH1 and BH2 domains, which as previously stated bind to pro-apoptotic proteins to inhibit apoptosis. The BHRF1 product encodes a 17kDa protein that protects against chemotherapeutic drugs- and gamma radiation-induced apoptosis (McCarthy *et al.*, 1996; Khanim *et al.*, 1997; Dawson *et al.*, 1998) and is also expressed as an early lytic gene (Bellows *et al.*, 2002). It has been suggested that BHRF1 may function to increase the life span of the cells undergoing viral replication (Marshall *et al.*, 1999). The second Bcl-2 homologue found in EBV was BALF1, which has the BH1 and BH2 domains and is expressed early during the lytic phase of the viral life cycle. However, Bellows and co-workers (2002) showed that BALF1 failed to protect cells against Sindbis virus-induced apoptosis. Using co-immunoprecipitation studies it was found that the BALF1 product directly bound to the BHRF1 product and KSHV Bcl-2 to inactivate their anti-apoptotic function (Bellows *et al.*, 2002). The protein has been found to localise at the mitochondria membrane, as with cellular Bcl-2 proteins (Hickish *et al.*, 1994). Both BHRF1 and BALF1 were dispensable for efficient B-cell immortalization when deleted from the virus genome as individual knockouts. However, when deleted as a double knockout the EBV mutants are unable to

immortalize B-cells. The conclusion was that the viral Bcl-2 proteins protected infected cells until latency was established (Altmann & Hammerschmidt, 2003).

1.7. Thesis Objectives and strategies

AIHV-1 expresses eleven conserved herpesvirus genes that are not seen in other herpesviruses. Some may be homologues of cellular proteins that the virus has 'adopted' to allow itself to establish a life cycle and remain persistent in the host. The detailed mechanism underlying the pathogenesis of AIHV-1 still remains unknown and it is thought that these conserved genes that are found in AIHV-1 are involved in the unique pathogenesis of the disease. The overall aim of this study was to characterise the A9 gene that is present in AIHV-1 to determine if it functions as an anti-apoptotic effector, and if so, determine the mechanism the virus uses to evade the host apoptotic response.

Specific objectives:

The main objectives of this study were:

- To determine if the Bcl-2 protein present in AIHV-1 was anti-apoptotic.
- To determine where in the cell viral Bcl-2 localised.
- To determine when in the virus life cycle the A9 gene was expressed.
- To detect and characterise cellular or viral binding partners for the viral A9 Bcl-2 protein.
- To eliminate A9 expression in A9-transfected cell lines

Chapter 2

Material and Methods

2.1 Animals and viruses

2.1.1 Animals

2.1.1.1 Mice

Female BALB/c mice, 2-3 months of age were used for the preparation of monoclonal antibodies. Mice were group-housed and supplied with proprietary food and water *ad libitum*.

2.1.1.2 Rabbits

Specific pathogen-free 3–12 month old New Zealand white rabbits (Harlan, UK) of either sex were used for the preparation of polyclonal antibodies and in the production of large granular lymphocytes (LGL). Rabbits were housed in individual cages and supplied with proprietary food and water *ad libitum*.

2.1.2 Viruses

The WC11 strain of AIHV-1, first isolated from a blue wildebeest, has been extensively passaged in culture and is a cell-free, attenuated virus (Plowright *et al.*, 1960; Plowright, 1968; Wright *et al.*, 2003). The C500 strain of AIHV-1 was first isolated from an infected ox (Plowright *et al.*, 1975; Wright *et al.*, 2003). The virus is mainly cell-associated and virulent when cultured in bovine turbinate (BT) cells for a short time (i.e. up to passage number 5) thereafter becoming cell-free and attenuated (i.e. does not cause disease when inoculated into rabbits or cattle).

2.1.3 Inoculation of rabbits with AIHV-1 virus

Rabbits were inoculated intravenously with the virulent C500 low passage cell-associated strain of AIHV-1. Approximately 3×10^6 (in 1ml) of C500 low passage AIHV-1-infected BT cells were used to inoculate rabbits. The rectal temperature was recorded each day and the animals euthanased after 2 days of febrile response ($>40^{\circ}\text{C}$).

Rabbit spleen, mesenteric and popliteal lymph nodes were removed aseptically from infected rabbits for further study. LGL cell lines were established from these tissues as described in section 2.2.1.

2.2 Cell Culture

2.2.1 Preparation of large granular lymphocyte (LGL) cell lines

Rabbit spleen, mesenteric and popliteal lymph nodes were removed aseptically from infected rabbits after 2 days of febrile response. The tissue was chopped finely with scissors in the presence of Iscove's modification of Dulbecco's medium (IMDM) (Gibco, BRL) supplemented with 10% (v/v) foetal bovine serum (FBS), 200U/ml penicillin, 200µl/ml streptomycin and 350U/ml recombinant human interleukin-2 (hrIL-2) (Chiron UK Ltd). Cell suspensions were passed through stainless steel sieves and set up in 25cm² flasks (Costar UK Ltd) and maintained as described in section 2.2.2. The LGL cell line used in this study was BJ2590.

2.2.2 Cell maintenance

Maintenance of MCF LGL cell lines was based on methods previously determined by Reid *et al.*, 1989. Briefly, all MCF LGL cell lines were grown in 25cm² flasks and maintained in IMDM containing 350U/ml of hrIL-2 for optimum growth. Half of the medium was replaced with fresh medium containing fresh IL-2 once a week.

Chinese hamster ovary (CHO) fibroblast cells were maintained in Glasgow's modified Eagles medium (GMEM) (Sigma) containing 1mM sodium pyruvate (Gibco BRL), 100µM non-essential amino acids (Gibco BRL), G + A (0.74µM l-glutamic acid and 0.9µM l-asparagine) and nucleosides (26µM adenosine, 24µM guanosine, 28µM cytidine, 28µM uridine, 10µM thymidine) supplemented with 7.5% (v/v) heat-inactivated foetal bovine serum (FBS). CHO cells that had been transfected with the pEE14 constructs (see section 3.2.16) were maintained in glutamine-free GMEM

supplemented with 7.5% (v/v) heat inactivated dialysed FBS (dFBS) and 25 μ M methionine sulfoxamine (MSX).

pEE14 contains a glutamine synthetase gene that confers on transfected CHO cells resistance to MSX. CHO cells transfected with pEE14 were maintained in GMEM containing no glutamine and MSX selection was applied to select for pEE14-transfected CHO cells.

CHO cells that had been transfected with pZome-C or pZome-PGK-C constructs (see section 2.6.1.2) were maintained in GMEM supplemented with 7.5% (v/v) FBS, 2% (v/v) glutamine and puromycin. These vectors contain a puromycin resistance gene that is only expressed in transfected cells. Therefore, maintaining these cells with puromycin pressure selects for puromycin-resistant transfected cells. After carrying out titration experiments, the optimum concentration of puromycin was 6 μ g/ml. Cells were incubated in 25cm², 75cm² or 225cm² flasks (Costar UK Ltd) in a humidified atmosphere of 5% CO₂ in air at 37°C.

Bovine turbinate (BT) cells were maintained in IMDM supplemented with 10% heat-inactivated FBS. Cells were passaged twice a week.

2.2.3 Cell passage

For adherent cell lines, medium was removed from the flask and cells washed twice with warm (37°C) PBS. Cells were removed from the flasks using trypsin (0.25%)/versene (0.02%) incubated at 37°C, in a humidified atmosphere of 5% CO₂ in air for 2 mins. The flask was gently tapped to remove any bound cells and a small volume of medium containing FBS was added to neutralise the trypsin. Cells were passaged twice a week and maintained with the selective pressure where appropriate (see section 2.2.2).

2.2.4 Cryopreservation

Cells were grown in 225cm² cell culture flasks until near confluent. They were pelleted by centrifugation at 254 x g for 5 mins. Cell pellets were resuspended in growth medium, supplemented with 50% (v/v) FBS and 10% (v/v) dimethyl sulphoxide

(DMSO) to give a concentration of 5×10^6 cells/ml. The suspension was transferred into a cryotube (Nunc Inc.) and then placed in a Cryo freezing container (Nalge Nunc International) to provide reproducible, slow cooling. The container was stored at -70°C for 24 hrs and tubes were transferred to a liquid nitrogen tank for storage until required.

Cells removed from frozen storage were thawed rapidly in a 37°C water bath and the suspension diluted in 10ml of warm culture medium. Cells were washed and centrifuged at $254 \times g$ for 5 mins. The cell pellet was resuspended in 20ml of culture medium and set up in a 162cm^2 flask (Costar Ltd, UK).

2.2.5 Determination of cell morphology by Leishman's staining

Cell suspensions, $200\mu\text{l}$, at a density of 1×10^6 cells/ml, were centrifuged, using a cytopsin 3 machine (Shandon), onto slides and the cell morphology was revealed using Leishman's stain (BDH Laboratory Supplies, UK). Slides were incubated in undiluted Leishman's stain for 2 mins followed by an incubation of 10 mins with Leishman's stain diluted 1:2 with tap water. Cells were rinsed with water, allowed to dry and mounted with Shandon mounting media (Thermo Shandon Ltd). Cells were then examined by light microscopy using a BH-2 Olympus microscope (Olympus).

2.2.6 Determination of cell growth and viability

A $50\mu\text{l}$ sample of cells was mixed with an equal volume of 0.1% (w/v) nigrosine (Merck Ltd), 2% (v/v) FBS in water. Dead cells were identified by the entry of nigrosine into the cells, whereas live cells excluded the dye. Live and dead cells were counted in a haemocytometer. The density of live cells and percentage viability (i.e. $[\text{number of live cells} / (\text{number of live} + \text{dead cells})] \times 100$) were calculated.

2.2.7 Stable and transient transfection of genes and cDNAs into cells

DNA-mediated gene/cDNA transfer (transfections) into cells was carried out using lipofectamine (Invitrogen). This allows for functional and protein analyses to be carried out on the transfected cells expressing recombinant protein. Stable transfections were carried out to create long-term selected cell lines, whereas transient transfections

were carried out to provide a rapid expression system. Lipofectamine™ 2000 reagent is a cationic lipid that provides high transfection efficiency and protein expression levels. The protocol used was as described by the manufacturer (Invitrogen). The day before a stable transfection, CHO cells were seeded in a 6 well plate (Costar UK Ltd) at a concentration of 2×10^5 cells/ml with 2ml of cell suspension added to each well. In the case of transient transfections cells were set up in 8 well chamber slides (Lab-Tek) at a concentration of 1×10^5 cells/ml with 200µl of cell suspension added into each well. Cells were incubated at 37°C, in a 5% CO₂ in air atmosphere and allowed to grow to approximately 90% confluency. Purified plasmid DNA (2µg for stable transfections and 0.2µg for transient transfections), containing the gene to be expressed, was diluted in 250µl or 50µl of GMEM (Sigma) (containing no serum or antibiotics) for stable and transient transfections respectively. This was mixed briefly by pipetting. Lipofectamine (4µl or 0.4µl of stock suspension) was diluted in 250µl or 50µl GMEM containing neither serum nor antibiotics. Both mixtures were incubated separately at room temperature for 5 mins. The diluted lipofectamine and diluted DNA were then mixed together and incubated at room temperature for 20 mins. The lipofectamine-DNA complex (500µl or 100µl total volume) was then added to CHO cells and mixed by gently rocking the plate. Cells were incubated at 37°C, in a humidified atmosphere of 5% CO₂ in air for 24 hr. Thereafter, for stable transfections CHO cells were passaged 1:10 and were continuously maintained in medium with the appropriate selective pressure to maintain expression of the gene of interest. Transient transfected CHO cells were incubated at 37°C and 5% CO₂ for 24-72 hrs to allow for gene expression without selection.

2.2.8 Preparation of cell lysates

CHO cells (approximately 10^7) were washed *in situ* twice with warm PBS and then removed from the flasks by scraping with a cell-scraper (Costar UK Ltd). Cells were removed from the flasks and pelleted by centrifugation at 254 x g for 5 mins. Supernates were removed, and 1ml cold lysis buffer (1% (v/v) Triton X-100 or 1% (v/v)

NP-40, 20mM Tris pH7.2, 150mM NaCl) containing protease inhibitors (0.02mg/ml pancreas-extract inhibitor, 0.02mg/ml chymotrypsin inhibitor, 0.0005mg/ml metalloprotease inhibitor, 0.002mg/ml trypsin inhibitor, 0.33mg/ml papain inhibitor were used in the form of a CompleteTM protease inhibitor tablet, (Roche)) was added to cell pellets and mixed by vortexing for 10 secs. Lysates were incubated on ice for 20 mins, passed through a 26G needle and returned to ice for a further 20 mins. Cellular debris was removed from lysates by centrifugation at 17,900 x g for 15 mins.

2.2.9 Immunostaining of cells

Cells were seeded at a density of 1×10^5 cells/ml in 8 well chamber slides (Lab-Tek) with 200 μ l of the cell suspension into each well and incubated at 37°C, 5% CO₂ in air for 48 hrs. Cells were washed with warm PBS and fixed by immersion in ice cold acetone or 1% (w/v) paraformaldehyde in PBS for 10 mins. Cells were washed in PBS then placed into a moist box and blocked with 50 μ l of normal goat serum (DAKO) (1:40), donkey serum (1:10) or normal swine serum (1:10) (the serum used was from the species of animal that the secondary antibody was raised in) for 1 hr at 37°C to prevent non-specific binding. Cells were then washed twice with PBS for 5 mins each time and then incubated with the primary antibody in PBS for 1 hr at 37°C (antibodies used and concentrations are shown in table 2.1). Controls were incubated for 1 hr at 37°C in PBS with normal serum (DAKO) (1:1000). Cells were washed twice in PBS for 5 mins before incubation with a secondary conjugate (see table 2.1) for 1hr at 37°C. Cells were washed twice with PBS for 5 mins each time and if necessary were incubated in tertiary conjugate (see table 2.1) at 37°C for 1hr. Cells were washed with PBS, air dried and mounted using Mowiol (Mowiol 4-88 (Sigma), 30% (v/v) Glycerol, 0.2M Tris pH8.5, 2.5% (w/v) DABCO (Sigma)) mounting media. After labelling, the cells were examined using an Olympus BX50 microscope (Olympus) using a blue (NB) filter (to examine FITC conjugates) at 470-490nm or using a green (NG) filter (to examine TRITC conjugates) at 530-550nm.

Antigen	Primary*	Secondary	Tertiary
AIHV-1 A9	Rabbit sera, 162 & 163 1:500	Anti-rabbit biotin conjugate (DAKO), 1:500	Streptavidin FITC conjugate (DAKO) 1:75
AIHV-1 A9	Rabbit sera, 162 & 163 1:500	Swine anti-rabbit TRITC conjugate (DAKO) 1:75	NA
AIHV-1 A9	Mouse monoclonal 6E1 & 6G8 1:500	Goat, anti-mouse FITC conjugate (DAKO) 1:75	NA
EBV BHRF1	Mouse monoclonal antibody (Clone MAB818, Chemicon) 1:1000	Goat, anti-mouse FITC conjugate (DAKO) 1:75	NA

Table 2.1 Antibodies and conjugates used in immunostaining. Dilutions used and suppliers are shown. FITC= Fluoresceine isothiocyanate. TRITC= tetramethyl rhodamine isothiocyanate. * See section 2.7 for description of the preparation of the different antibodies.

2.2.10 Confocal Microscopy

Confocal microscopy was used to analyse the cellular location of the A9 protein. Cells were prepared and fluorescently stained as described in section 2.2.9. Fluorescent images were acquired using an MRC-600 confocal laser scanning microscope (CLSM: Bio-Rad Laboratories) mounted on an Axiovert 100 inverted microscope equipped with Plan-Apochromat® objective lenses (Carl Zeiss). Fluorophores were excited sequentially using the 488 nm (FITC) and 568 nm (Rhodamine) lines from a 15 mW Kr/Ar laser (Bio-Rad Laboratories).

2.3 Molecular Biology Techniques

2.3.1 Digestion of DNA with Restriction Enzymes

Restriction enzymes were obtained from Invitrogen, New England Biolabs, Promega or Roche and were used with the supplied buffers according to the manufacturer's instructions. Restriction enzyme digests were typically carried out for 2 hrs at 37°C in a 20-200µl volume, using 10 units enzyme per 1-10µg of DNA. Digestion was analysed using agarose gel electrophoresis (as described in section 2.3.13).

2.3.2 Ligation of DNA

Ligation of DNA was performed using T4 DNA ligase (Roche). Ligation reactions were set up in a total volume of 20µl containing 100ng of linearised plasmid DNA and varying amounts of insert DNA depending on size, such that the molar ratio of plasmid to insert DNA was 1:4. The reactions contained 2µl of 10 x DNA ligase buffer (660mM Tris/HCl, 50mM MgCl₂, 10mM ATP, pH 7.5) and 2 units of T4 ligase. All ligation experiments included negative controls whereby insert DNA was omitted from the reaction in order to check for self-ligation of the plasmid. Ligation reactions were performed overnight at 4°C.

2.3.3 TA Cloning using pGEM-T Easy Vector

PCR products were cloned into pGEM-T Easy TA cloning vector (Promega) according to the manufacturer's instructions. A ligation reaction was set up in a total volume of 10µl to contain; 1 x Rapid Ligation Buffer, 50ng pGEM-T Easy Vector, 3µl PCR product and 6 Weiss units T4 DNA ligase. The reaction was incubated at room temperature for 1 hr and a 2µl aliquot used to transform *E. coli* JM109 strain. After transformation, bacteria were plated out onto LB-Amp plates to which 100µl per plate (0.1M stock) isopropyl-β-D-thiogalactopyranoside (IPTG) and 20µl per plate (50mg/ml stock) 5-bromo-4-chloro-3-indolyl-β-D-galactopyranoside (X-Gal) had been added.

2.3.4 Preparation of competent *E. coli*

JM109 competent cells were used for the transformation of plasmid DNA by heat shock. The bacteria were grown in sterilised Luria-Bertani (LB) medium (Sambrook *et al.*, 1989) with the addition of appropriate antibiotics. Agar plates were made with 15g/l bacteriological agar (ICN Biochemicals) in LB medium.

An aliquot, 10 μ l, of frozen *E. coli* cells stocks were streaked onto LB plates containing 50 μ g/ml ampicillin and incubated at 37°C overnight. A bacterial colony was picked with an inoculating loop and grown in 10ml of LB broth containing 50 μ g/ml ampicillin in an orbital shaker (HT, Infors, AG) at 37°C overnight. An aliquot, 2.5ml, of overnight culture was added to 500ml of LB broth containing 50 μ g/ml ampicillin and incubated in an orbital shaker at 37°C until the O.D₆₀₀ was 0.2. Bacteria were pelleted by centrifugation at 4000 x g for 10 mins at 4°C. The bacterial pellet was resuspended in 250ml of ice-cold sterile 0.1M calcium chloride (CaCl₂) and left on ice for 20 mins. The mixture was centrifuged at 4000 x g for 10 mins at 4°C, and the pellet was resuspended in 5-20ml of CaCl₂. Sterile glycerol was added to a final concentration of 10% and the cells were split into 0.5ml aliquots and stored at -70°C until required.

2.3.5 Transformation of competent *E. coli* with plasmid DNA

E. coli strain JM109 was used as a standard strain for the expression of high yields of recombinant proteins except that strain GI724 was used for vector pTRXFUS (Invitrogen). A 50 μ l aliquot of competent bacterial cells GI724 or JM109 as required was thawed on ice. The ligation reaction or purified plasmid DNA (approximately 50ng total DNA) was added and the mixture was held on ice for 30 mins, after which it was heat-shocked at 42°C for 2 mins. Transformed GI724 cells were spread on low tryptophan RMG-agar (16.7mM Na₂HPO₄, 22mM KH₂PO₄, 8.5mM NaCl, 18.7mM NH₄Cl, 1mM MgCl₂, 2.0 % (w/v) Casamino acids, 1.5% (w/v) agar) (Invitrogen) plates containing 100 μ g/ml ampicillin and 0.5% (w/v) glucose then incubated at 30°C overnight to inhibit tryptophan-induced protein expression. Transformed JM109 cells

were spread on LB plates containing 100µg/ml ampicillin and incubated at 37°C overnight.

2.3.6 Selection and growth of ampicillin resistant colonies

Single ampicillin-resistant colonies were inoculated into 1ml RM medium (16.7mM Na₂HPO₄, 22mM KH₂PO₄, 8.5mM NaCl, 18.7mM NH₄Cl, 1mM MgCl₂, 0.2% (w/v) Casamino acids) (Invitrogen) for GI724 cells, or LB-broth (1% (w/v) Tryptone, 1% (w/v) yeast extract, 0.5% (w/v) NaCl) for JM109 cells containing 100µg/ml or 50µg/ml ampicillin respectively. GI724 cells were incubated at 30°C, while JM109 cells were grown at 37°C. Cells were incubated overnight with constant agitation in an orbital shaker.

2.3.7 Storing bacterial cultures as glycerol stocks

Glycerol stocks were made by growing *E. coli* bacterial cultures in LB broth containing 50µg/ml ampicillin to log phase and adding glycerol to 30% (v/v), before mixing and storing at -70°C.

2.3.8 Quantification of nucleic acids

DNA and RNA were quantified by spectrometry. Nucleic acid samples were diluted in distilled water or TE buffer. Using distilled water or TE (10mM Tris-Cl, pH 7.5, 1mM EDTA) buffer as a reference, the OD₂₆₀ and OD₂₈₀ were determined using a Cecil CE 2041, 2000 series spectrophotometer. The nucleic acid concentration was determined by using the following formula:

$$\text{OD}_{260} \text{ reading} \times \text{dilution factor} \times A = \mu\text{g/ml nucleic acid}$$

(where A = 50 for double stranded DNA and 40 for single stranded RNA)

The purity of the test sample was estimated using the OD 260.280 ratio which gives an indication of contamination by protein (with peak absorbance at 280nm).

Pure preparations of DNA and RNA have ratios of 1.8 and 2.0 respectively.

2.3.9 Small scale preparation of plasmid DNA (mini-preps)

Small scale preparations of plasmid DNA were used for initial characterisation of cloned DNA fragments. The method used is as described by the manufacturer's protocol (QIAprep plasmid minipreps, Qiagen). A single bacterial colony was picked and grown in 10ml of LB broth containing 50µg/ml ampicillin in an orbital shaker at 37°C overnight. Bacterial cells were pelleted by centrifugation at 4000 x g for 10 mins at room temperature. The pellet was resuspended in 250µl of buffer P1 (resuspension buffer containing RNase) and transferred to a microcentrifuge tube. This was followed by the addition of 250µl of buffer P2 (lysis buffer) and mixing by inversion of the tube. Genomic DNA and proteins were precipitated by the addition of 350µl of buffer N3 (neutralising buffer) mixed by inversion and then centrifuged in a microcentrifuge at 17900 x g for 10 mins. The supernatant was transferred into a QIAprep spin column (Qiagen) and centrifuged at 17900 x g for 30-60 secs. Unbound material was discarded, the column was washed with 0.5ml of buffer PB (to remove trace nuclease activity) and centrifuged at 17900 x g for 30-60 secs. The column was washed with 0.75ml of buffer PE (containing ethanol) and centrifuged at 17900 x g for 30-60 secs (to remove residual wash buffer), unbound material was discarded and the column centrifuged for a further 1 min at 17900 x g. The QIAprep column was placed into a fresh Micro-centrifuge tube and DNA was eluted by the addition of 50µl of buffer EB (10mM Tris-Cl pH7.5, 1mM EDTA) and centrifuged for 1 min. DNA was stored at -20°C until required.

2.3.10 Large scale preparation of DNA (Maxi-preps)

The method used was as described by the manufacturer's protocol (Qiagen) an alkaline lysis followed by ion-exchange chromatography. A single colony of bacteria was picked using an inoculating loop and grown in 10ml of LB broth containing 50µg/ml or 100µg/ml ampicillin in an orbital shaker at 37°C overnight. 5ml of the overnight culture was incubated in 500ml of LB broth overnight. *E. coli* cells were pelleted by centrifugation at 6000 x g for 15 mins at 4°C. The pellet was resuspended in 10ml of buffer P1 (50mM Tris-Cl, pH 8, 10mM EDTA, 100g/ml RNase A), 10ml of

buffer P2 (200mM NaOH, 1% (w/v) SDS) was added and incubated at room temperature for 5 mins. Chilled buffer P3 (3M potassium acetate pH 5.5), 10ml, was added, mix by inverting tube and incubated on ice for 20 mins. The solution was centrifuged at 1380 x g for 10 mins and the supernatant was filtered through 3M filter paper (Whatman). The QIAgen tip-500 (Qiagen) was equilibrated by applying 10ml of buffer QBT (750mM NaCl, 50mM 3-N-morpholino propanesulphonic acid (MOPS) (20mM MOPS, 5mM Sodium acetate pH8.0, 1mM EDTA pH8.0) pH7, 15% (v/v) isopropanol, 0.15% (v/v) Triton X-100) and allowed to empty under gravity flow. Supernatant was applied to the QIAgen tip and allowed to enter the resin by gravity. The QIAgen tip was washed twice with 30ml of buffer QC (1M NaCl, 50mM MOPS pH7, 15% (v/v) isopropanol). DNA was eluted with 15ml of buffer QF (1.25M NaCl, 50mM Tris-Cl pH8.5, 15% (v/v) isopropanol). DNA was precipitated by adding 10.5ml of isopropanol, mixing and centrifuging at 15300 x g for 30 mins at 4°C. The DNA pellet was washed with 5ml of 70% (v/v) ethanol and centrifuged at 15000 x g for 10 mins. The supernatant was removed and the DNA pellet was dried gently at room temperature before resuspending in 100µl of TE buffer. The DNA was stored at -20°C until required.

2.3.11 QIAquick Gel Extraction

QIAquick gel extraction was used to purify PCR products prior to cloning. The protocol used was as described in the manufacturers instructions (QIAquick gel extraction kit, Qiagen). DNA fragments were excised in the minimum volume from agarose gels using clean, sharp scalpels. Gel slices were weighed and three volumes of buffer QG were added to every one volume of gel. The mixture was incubated at 50°C for 10 mins in order to dissolve the gel pieces. One gel volume of isopropanol was added to the samples and mixed, the samples were transferred to QIAquick spin columns (Qiagen). The columns were centrifuged at 17900 x g for 1 min to bind DNA to the column. Unbound material was discarded and 0.5ml of buffer QG was applied to the column. The column was centrifuged at 17900 x g for 1 min to remove all traces of agarose solution. The column was washed using 0.75ml of buffer PE and centrifuged at

17900 x g for 1 min. Unbound material was discarded and the column was further centrifuged at 17900 x g for 1 min to remove any residual ethanol from buffer PE. The column was placed into a fresh microfuge tube and DNA was eluted from the column with 50µl of buffer EB by centrifugation at 17900 x g for 1 min. Purified DNA was stored at -20°C until required.

2.3.12 Polymerase chain reaction (PCR)

PCR was used for two purposes in this study: either in the production of DNA fragments for cloning or in conjunction with reverse transcription to examine the expression of AlHV-1 genes. Both procedures were carried out in the same way. PCR amplification was performed using the ExpandTM long template PCR system (Roche). The reaction was set up in a total volume of 50µl as follows, 0.75µl of Taq DNA polymerase, 5µl 10 X PCR buffer (Roche buffer 3 containing 22.5mM MgCl₂, and detergents, pH 9.2), 0.5µl of each primer at 0.2pmol, 2-4µl of template DNA, 2µl of 10mM dNTP's and distilled water. A negative control was prepared that included all components, except that template DNA was replaced with water. The reaction was gently mixed and a layer of mineral oil was added to the top of the reaction mixture to prevent evaporation. PCR was carried out in thin walled 0.5ml Micro-centrifuge tubes in a Hybaid Omingene thermal cycler (Hybaid Ltd). All primers used in this study are shown in appendix 2.1.

PCR reactions involved one cycle of denaturation at 93°C for 2 mins. A further 10 cycles consisting of denaturation at 93°C for 20 secs, annealing temperature for 30 secs and elongation stage at 68°C for 2 mins. The next 25 cycles involved the same conditions for denaturation and annealing and an elongation step of 5 mins. A final cycle involved the same conditions for denaturation and annealing followed by an elongation step of 7 mins.

Annealing temperatures varied depending on the PCR primers used. All primers were obtained from MWG-Biotech. Annealing temperatures were calculated using the following formula:

$[(\text{Number of Gs} + \text{Cs}) \times 4] + [(\text{Number of As} + \text{Ts}) \times 2] = \text{annealing temperature}$ (Suggs *et al.*, 1981), (where G = guanine; C = cytosine; A = adenine; T = thymine). If a restriction endonuclease recognition site was incorporated in the oligonucleotide primer, its sequence was not used in the above equation.

2.3.13 Agarose gel electrophoresis of DNA

DNA fragments were analysed using conventional agarose gel electrophoresis. Agarose concentration varied between 0.5-2% (w/v) depending on size of DNA fragment, electrophoresis buffer used was 1 X TBE (45mM Tris/borate, 1mM EDTA pH7.3). Electrophoresis was generally carried out at 100V for 30-45 mins. Ethidium bromide was added to a final concentration of 0.5µg/ml and DNA was visualised by fluorescence under UV illumination. A record was obtained by photographing the gels using the Imagemaster® VDS (Pharmacia Biotech). The sizes of DNA fragments were determined by comparison with known standards (1kb DNA markers, Promega).

2.3.14 Agarose gel electrophoresis including crystal violet

Crystal violet allows the viewing of DNA fragments by white light instead of UV, reducing DNA damage thus increasing the chances of successful cloning (Hartman, 1991). Agarose (1% w/v) was dissolved in 1 x TAE (40mM Tris acetate, 1mM EDTA pH 7.2). Before pouring the gel, crystal violet (Sigma) was added to a final concentration of 0.8µg/ml. The same concentration was also used in the TAE running buffer. Electrophoresis was carried out at 100V for 30-45 mins. DNA fragments were viewed on a white light box (Artwork Light box 2418), DNA bands were extracted from gels using clean sharp scalpels and purified using QIAquick gel extraction kit (Qiagen) (see section 2.3.11).

2.4 RNA Analysis

RNA analysis was used to determine when in the productive phase of the virus life cycle various genes were expressed or to determine if the gene was being expressed.

2.4.1 Extraction of total cellular RNA

Control (non-infected) and AIHV-1-infected BT cells were pelleted and media removed. Cells (approximately 1×10^7 cells) were homogenised in 10ml of RNA extraction buffer (4M guanidinium isothiocyanate, 25mM sodium citrate pH 7.0, 0.5% (w/v) sarcosyl, 0.72% (v/v) β -ME). The lysates were incubated at room temperature with agitation on a Rotatest shaker (Luckham) for 20 mins and then stored at -20°C until required. The lysates were transferred to a 50ml tube (Falcon) and 0.1 volumes of 3M sodium acetate pH 4.8, was added followed by 1 volume of water-saturated phenol and 0.2 volumes of chloroform. The mixture was vortexed, incubated for 5 mins at room temperature and then incubated on ice for 10 mins. The solution was centrifuged at $9800 \times g$ for 30 mins. The upper phase (aqueous layer) was transferred to a fresh tube and 1 volume of isopropanol was added, the mixture was stored at -20°C overnight. RNA was pelleted by centrifugation at $7700 \times g$ for 30 mins. The RNA pellet was resuspended in 0.5ml of RNA extraction buffer, 0.5ml of isopropanol was added and the samples were centrifuged at $17900 \times g$ (Microcentrifuge 113, Sigma) for 10 mins. The pellet was washed with 0.5ml of 70% (v/v) ethanol, vortexed, centrifuged at $17900 \times g$ for 10 mins. Samples were resuspended in 100 μl of sterile distilled water and stored at -20°C until required.

2.4.2 Northern blotting

RNA was analysed using agarose gel electrophoresis. Gels contained agarose (1% (w/v)) and 5% (v/v) formaldehyde in MOPS (electrophoresis buffer). Electrophoresis was carried out at 100V for 30-60 mins. RNA was visualised by

ethidium bromide fluorescence under UV illumination. A record was obtained by photographing gels using the ImageMaster® VDS (Amersham Pharmacia).

The MOPS/formaldehyde gel was washed twice for 20 mins in 10 x standard saline citrate (SSC) (1.5 NaCl, 0.15M tri-Sodium citrate) with agitation on a Rotatest shaker (Luckham). RNA was transferred to a nylon membrane (Hybond N, Amersham Pharmacia) by capillary transfer. The gel and membrane were sandwiched between several sheets of 3mm filter paper (Whatman) and topped with a paper towel stack with a weight on top which was placed on a bridge of three sheets of 3mm filter paper (Whatman) with 10 x SSC and incubated overnight. RNA was fixed to the membrane after drying at room temperature by UV cross-linking using a Hybaid cross-linker (Hybaid) for 1 min according to manufacturers instructions. Membranes were stored at room temperature wrapped in Saran wrap and stored in dark until required or used in hybridisation.

For probe labelling, DNA was diluted to a concentration of 2.5-25ng in 45µl of TE buffer. DNA was denatured by heating to 95-100°C for 5 mins in a boiling water bath, cooled on ice for 5 mins and centrifuged at 17900 x g for 30 secs. Denatured DNA was transferred to a Rediprime reaction tube (Amersham Bioscience) and 5µl of Redivue [³²P]dCTP (Amersham Pharmacia) was added to the Rediprime reaction tube and thoroughly mixed by pipetting until a colour change was observed. The labelling reaction was incubated at 37°C for 2 hrs, heated to 95-100°C for 5 mins and then cooled immediately on ice for 5 mins. The northern blot membrane was washed in 2 x SSC for 5 mins at room temperature. The probe was then added to sufficient 'rapid-hyb' buffer (10-20ml)(Amersham Biosciences) to cover the northern blot membrane and hybridised overnight in a hybridisation oven at 65°C.

After hybridisation, unbound probed and non-specifically bound probe were removed by washing the membrane twice in 2 x SSC containing 0.2% (v/v) SDS for 5 mins at room temperature, then a further wash at 65°C for 2 hrs. The membrane was then wrapped in Saran wrap and exposed to X-ray film (Kodak X-Omat AR, Sigma) at -70°C overnight.

2.4.3 Reverse transcription polymerase chain reaction (RT-PCR)

RT-PCR was used to produce cDNA to examine the expression of genes. RT-PCR was carried out as described by the manufacturers protocol (RETROscript Kit, Ambion). A reaction containing 1µg total cellular RNA and 2µl (1.25µM) Random decamers was made up to 12µl with sterile nuclease-free water and mixed briefly, centrifuged at 17900 x g for 30 secs and heated at 75°C for 3 mins. Samples were 'pulse-centrifuged' and placed on ice and the following components were added; 10µl 10 X RT Buffer (500mM Tris-HCl, pH 8.3, 750mM KCl, 30mM MgCl₂, 50mM dithiothreitol (DTT)), 4µl dNTP (2.5mM each dNTP) mix, 1µl RNase inhibitor, 1µl reverse transcriptase (RETROscript Kit, Ambion). The components were mixed, centrifuged at 17900 x g for 30 secs, incubated at 42°C for 1 hr, and then at 92°C for 10 mins. Samples were then ready to be used for PCR amplification (as described in section 2.3.12) or stored at -20°C until required.

2.5 Protein Analysis

2.5.1 Sodium dodecylsulphate – polyacrylamide gel electrophoresis (SDS-PAGE)

The separation of proteins was performed by discontinuous polyacrylamide gel electrophoresis under reducing conditions using the method described by Laemmli (1970) in the Mini Protean II system (Biorad). Samples were boiled in an equal volume of reducing Laemmli sample buffer (100mM Tris pH6.8, 200mM DTT, 4% (w/v) SDS, 0.2% (v/v) bromophenol blue, 20% (v/v) glycerol) prior to loading onto gels. Proteins were separated on 10%, 12%, or 15% (depending on the molecular weight range to be separated) acrylamide gels made up in separating gel buffer (0.375M Tris-HCl pH 8.8, 1% (w/v) SDS, 0.1% (v/v) tetramethylethylenediamine (TEMED), 0.1% (w/v) ammonium persulphate (APS)), overlaid with 4% acrylamide made up in stacking buffer (0.15M Tris-HCl pH 6.8, 0.5% (w/v) SDS, 0.2% (v/v) TEMED, 0.2% (w/v) APS).

Electrophoresis was carried out at 200V for 45-60 mins in tank buffer (25mM Tris, 192mM Glycine, 0.1% (w/v) SDS).

2.5.2 Protein detection in SDS-PAGE gels

Separated proteins were detected by Coomassie brilliant blue R concentrate (Sigma Aldrich) or by silver staining.

For Coomassie staining of proteins, gels were incubated in the Coomassie brilliant blue R concentrate for 1 hr with agitation followed by three washes in destain (10% (v/v) methanol, 10% (v/v) Glacial acetic acid in water) for 30 mins each wash.

For more sensitive detection, silver staining was used. Firstly, the gels were fixed in 50% (v/v) methanol, 10% (v/v) glacial acetic acid in water for 20 mins followed by two washes in 5% (v/v) methanol, 7% (v/v) glacial acetic acid in water for 10 mins each. After a 10 mins wash in distilled water, proteins were reduced in DTT (5 μ g/ml in water) for 15 mins with agitation on a Rotatest shaker (Luckham) and gels were washed again in distilled water for 10 mins. Gels were stained in 0.1% (w/v) silver nitrate in water for 20 mins followed by a quick rinse with distilled water. Protein bands were visualised by incubation with 0.3M sodium carbonate, 0.02% (v/v) formaldehyde in water for 5-10 mins. The reaction was stopped by the addition an equal volume of 0.1% (w/v) citric acid in water.

2.5.3 Western blot analysis (immuno-detection of gel-separated proteins)

Gel-separated proteins were electrophoretically-transferred from gels to nitro-cellulose membranes (Amersham Pharmacia). The gel and membrane were sandwiched between several sheets of 3mm filter paper (Whatman) soaked in transfer buffer (25mM Tris, 200mM Glycine, 5mM SDS) and then placed in a semi-dry blotting apparatus (Sigma). A tube was rolled over the surface of the filter paper to exclude all air bubbles from between layers. The transfer of proteins was carried out at 70mA per gel (2mA/cm² of gel) for 1 hr. After transfer, the membrane was blocked with 4% (w/v) non-fat milk (Marvel) in wash buffer (0.5M NaCl, 0.5% (v/v) Tween 80 in PBS) for 45-90 mins. The membrane was incubated in primary antibody in wash buffer for 1 hr then

HRP-conjugated secondary antibody (Dako) in wash buffer for 1 hr at room temperature. Between blocking, primary and secondary antibody stages, the membrane was thoroughly washed in wash buffer for at least 20 mins with constant agitation on a Rotatest shaker (Luckham). After a final wash, bound HRP-antibody-antigen complexes were detected by treating blots with the enhanced chemiluminescence (ECL) reagent (Amersham International) according to manufacturer's instructions, and exposure to Hyperfilm ECL (Amersham International) for 10-60 sec before development.

2.5.4 Measurement of protein concentration

Protein concentrations in samples were determined using the Bicinchoninic acid (BCA) Protein Assay Reagent Kit (PIERCE) according to the manufacturer's protocol. The BCA Protein assay reagent kit includes: BCA Reagent A; 500ml, containing sodium carbonate, sodium bicarbonate, bicinchoninic acid and sodium tartate in 0.1M sodium hydroxide, BCA reagent B, 25ml containing 4% (w/v) cupric sulphate and albumin standard, 2mg/ml.

A standard curve was generated using a range of bovine serum albumin (BSA) concentrations, 0.05-2.0mg/ml, made up in PBS. Each test sample, 10 μ l in PBS, was pipetted into duplicate wells of a 96-well flat-bottomed plate (Costar UK Ltd). To each well 200 μ l of the working reagent (50 parts BCA reagent A with 1 part BCA reagent B) was added and the plate was incubated at 37°C for 30 mins. A colour change was detected by the absorbance at 562nm on a DYNEX MRXII microplate reader (DYNEX). The protein concentration was calculated using the standard curve of BSA concentration against O.D.₅₆₂.

2.6 Detecting protein-protein interactions

2.6.1 Tandem affinity purification (TAP)

2.6.1.1 Construction of AIHV-1 and EBV fusion proteins in *E. coli*

TAP-tagged fusions were made in the pZome-C retroviral vector (Cellzome) (Fig 2.1). An A9 fragment was amplified by PCR (see section 2.3.12) from AIHV-1 DNA using PCR primers bclahvF and bclahvR (appendix 2.1). The PCR product was then cloned into pGEM-T Easy (Promega) (see section 2.3.2). After sequencing to verify accurate amplification the A9 gene fragment was prepared by digestion with *NcoI*. Digested fragments were purified by agarose gel electrophoresis in the presence of crystal violet (see section 2.3.14) and the Qiaquick gel extraction kit (as described in section 2.3.11). The purified A9 fragment and *NcoI* cut pZome-C plasmid DNA were ligated (as described in section 2.3.2). Clones carrying the A9 fragment in the correct orientation were digested with *BamHI* to remove 30bp of residual DNA carried over from the pGEM-T vector. DNA was sequenced to check that the vector-insert junctions were correct.

The PGK promoter sequence was amplified by PCR from another vector, pSuper (Oligoengine), to contain an *EcoRI* site at the 5' end and a *HindIII* site at the 3' end (as described in section 2.2.12) and was ligated into the pGEM-T Easy vector as described above. The original SV40 promoter was removed from the pZome vector by digesting with *EcoRI* and *HindIII* (as described in section 2.3.1) and replaced with the PGK promoter excised from pGEM-T Easy. The A9 fragment was recloned into the pZome-PGK-C vector, as described above (Fig 2.2).

Epstein Barr virus Bcl-2 homologue BHRF1 was used as a control in this study. This Bcl-2 homologue was chosen as it has been shown to bind to Bax and Bak (Marshall *et al.*, 1999). BHRF1 was amplified by PCR (see section 2.3.12) from EBV DNA using PCR primers BHRF1F and BHRF1R (appendix 2.1). The PCR product was cloned into the pGEM-T Easy vector (section 2.3.6). After sequencing to verify accurate amplification, the BHRF1 gene fragment was prepared by digestion with *NcoI*.

The digested fragment was purified as described above and ligated into the pZome-PGK-C retroviral vector.

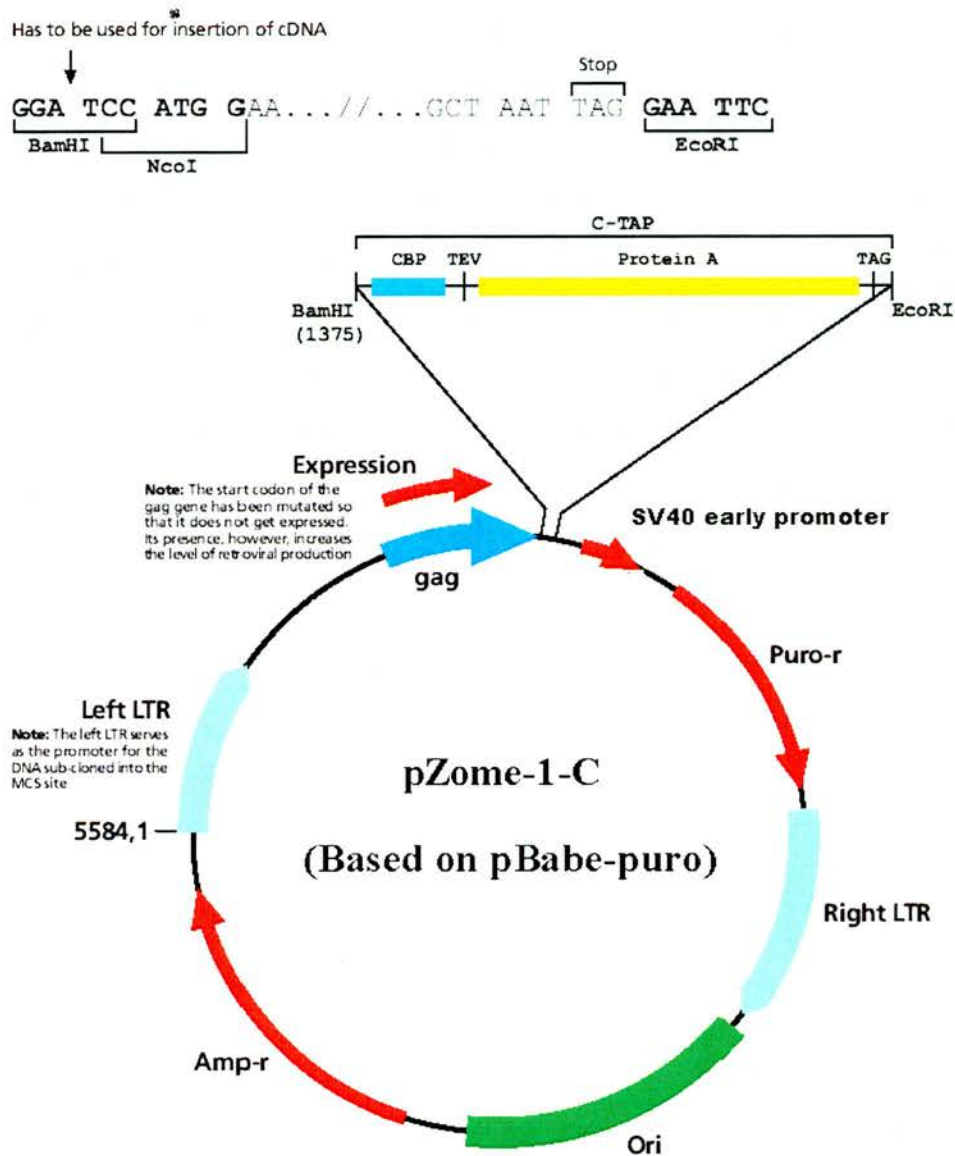


Fig 2.1. Vector pZome-1-C was obtained from Cellzome.

The plasmid directs the synthesis of the TAP-tag protein under the control of the retroviral LTR promoter. It also contains the ampicillin resistance gene for the selection of plasmid containing bacterial colonies and the puromycin resistance gene for the selection of plasmid containing transfected mammalian cells, which is transcribed from the SV40 promoter. CBP denotes the calmodulin binding protein and TEV denotes the tobacco etch virus cleavage site.

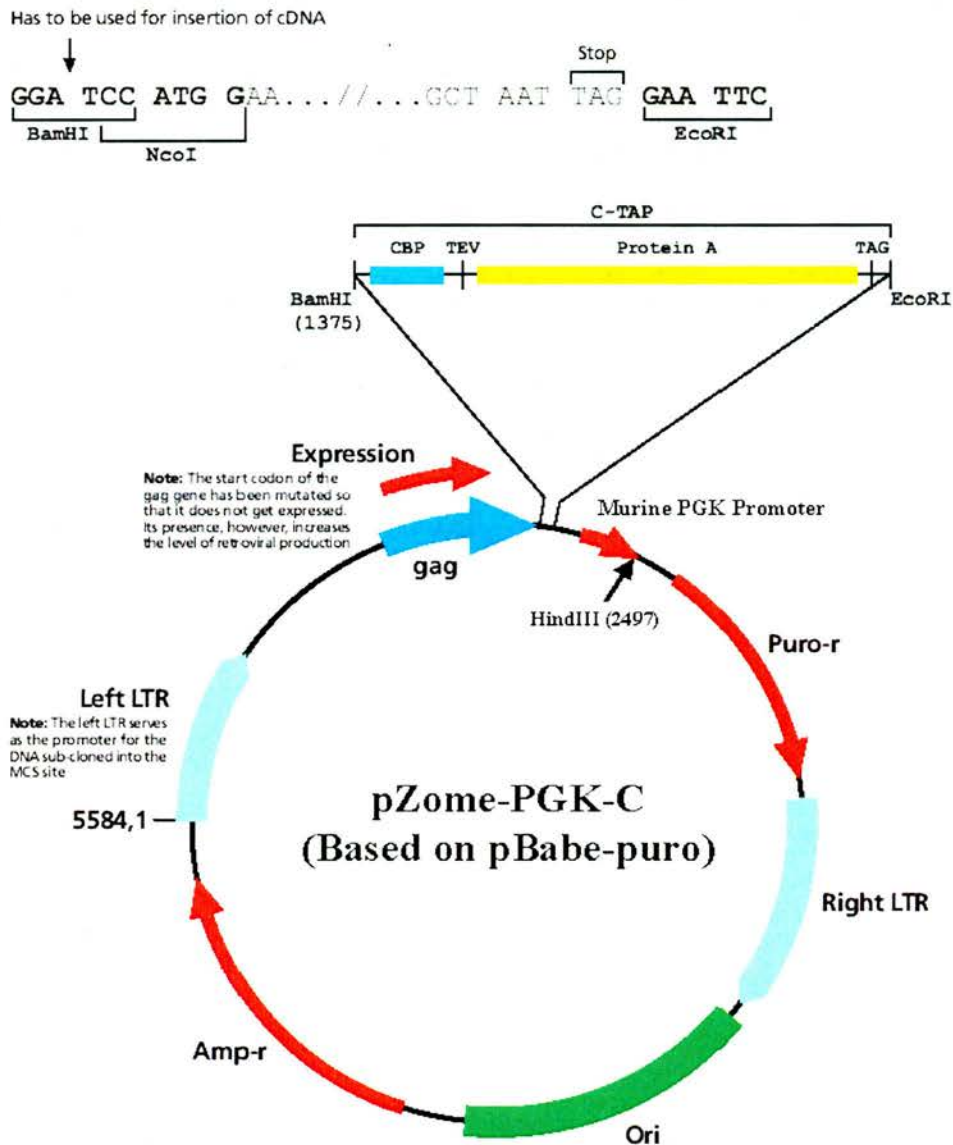


Fig 2.2. Vector pZome-PGK-C.

The plasmid directs the synthesis of the TAP-tag protein under the control of the retroviral LTR promoter. It also contains the ampicillin resistance gene for the selection of plasmid containing bacterial colonies and the puromycin resistance gene for the selection of plasmid containing transfected mammalian cells, which is transcribed from the murine PGK promoter. CBP denotes the calmodulin binding protein and TEV denotes the tobacco etch virus cleavage site

2.6.1.2 Transfection of TAP-tagged fusion DNA into CHO cells

Purified p-Zome-PGK-C vector DNA containing the required insert (2 μ g) was stably-transfected into CHO cells using the lipofectamine™ 2000 reagent (as described in section 2.2.7). The following day, transfected CHO cells were passaged 1:10 and selected in the presence of puromycin (6 μ g/ml). In order to purify the TAP-tagged proteins, transfected CHO cells were grown to high cell density in triple-layer flasks (TPP) with 6 μ g/ml of puromycin added.

2.6.1.3 Harvesting transfected CHO cells

For TAP-tag analysis, 10⁹ to 10¹⁰ cells were harvested from triple-layer flasks. Transfected CHO cells were washed twice with warm (37°C) PBS to remove excess serum, removed from the flasks using trypsin/versene and incubated at 37°C, 5% CO₂ in air for 2 mins. The flasks were gently tapped to remove any bound cells and the trypsin was neutralised in 20ml GMEM supplemented with 7.5% (v/v) FBS and 2% (v/v) glutamine. Cells were pelleted by centrifugation at 1500 x g for 5 mins at 4°C. The remaining steps were carried out at 4°C unless stated. Pelleted cells were resuspended in 5ml of PBS and centrifuged at 1500 x g for 5 mins. Cells were lysed in 0.5ml of lysis buffer per 10⁷ cells, (20mM Tris pH 7.5, 0.15M NaCl, Complete® protease inhibitor tablet (Roche)) frozen, and thawed three times using dry ice. The lysate was centrifuged at 16000 x g for 10 mins. The supernatant was transferred to a fresh tube and NP-40 added to give a final concentration of 0.1% (v/v). The pellet was resuspended in 1.5ml of lysis buffer containing 0.1% (v/v) NP-40. This protein pellet was further solubilised by three freeze- thaw cycles, centrifuged at 17900 x g for 10 mins and both soluble and pellet-derived fractions were stored at -20°C until required.

2.6.1.4 Purification of TAP-tagged proteins

The protocol was adapted from Cox *et al.*, 2002. IgG sepharose (Amersham International), 200 μ l, was transferred to a 0.8 X 4cm disposable Poly-Prep column (Bio-Rad). The sepharose was washed with 10ml of IPP150 buffer (10mM Tris-Cl pH 8.0,

150mM NaCl, 0.1% (v/v) NP-40) and protein lysates were transferred to the column containing washed beads and rotated for 2 hrs to allow proteins to bind via the Protein A domains. Unbound proteins were eluted under gravity and the Sepharose washed three times with 10ml IPP150. The column was then washed with 10ml TEV cleavage buffer (10mM Tris-Cl pH 8.0, 150mM NaCl, 0.1% (v/v) NP-40, 0.5mM EDTA, 1mM DTT) and bound TAP-tagged proteins were released from the IgG column by incubation with 1ml TEV cleavage buffer containing 10units of TEV protease (Invitrogen) and rotated for 2 hrs at room temperature. Proteins were eluted under gravity and mixed with 3ml of IPP150 calmodulin-binding buffer (10mM Tris-Cl pH 8.0, 10mM β -mercaptoethanol, 150mM NaCl, 1mM magnesium acetate, 1mM imidazole, 2mM CaCl_2 , 0.1% (v/v) NP-40) with a final CaCl_2 concentration of 3mM. The mixture was added to 200 μ l of calmodulin beads (Stratagene) that had been washed with 10ml of IPP150 calmodulin binding buffer. Protein and calmodulin beads were mixed by rotating at 4°C for 1 hr. Unbound material was eluted under gravity and the column was washed with 30ml of IPP150 calmodulin-binding buffer. Bound proteins were eluted in 1ml of IPP150 calmodulin elution buffer (10mM Tris-Cl pH 8.0, 10mM β -mercaptoethanol, 150mM NaCl, 1mM magnesium acetate, 1mM imidazole, 2mM EGTA, 0.1% (v/v) NP-40).

The eluted proteins were concentrated using microcons (Millipore) at 17900 x g until the samples occupied a total volume of 50 μ l. The concentrated eluted fractions were stored at -20°C until further analysed (see below).

2.6.2 Identification of protein interactions by immunoprecipitation

Cell lysates (1ml) were prepared as described in section 2.2.8, pre-cleared with 0.25 μ g of normal rabbit serum and 20 μ l of protein A/G-agarose (Santa-Cruz) to remove the binding of non-specific proteins and incubated at 4°C for 30 mins. The suspension was pelleted by centrifugation at 1000 x g for 30 sec, and the supernatant was transferred to a fresh micro-centrifuge tube. The cell lysate was then incubated with an appropriate primary antibody for 2 hr at 4°C by rotating. Protein A/G-agarose (20 μ l) was added to the suspension and incubated at 4°C overnight. The pellet was collected

by centrifugation at 1000 x g for 5 mins at 4°C, the supernatant was discarded, and the pellet washed 3 times with 1ml PBS. The pellet was finally resuspended in 40µl of 2 x reducing sample buffer and analysed by electrophoresis.

2.7 Anti-A9 Antibody Production

For the production of anti-A9 Bcl-2, a thioredoxin fusion protein was used as an antigen. *E. coli* strain GI724 was used to properly regulate expression of the fusion protein. The bacterial cells were grown in RM medium, then transferred to induction medium. Protein expression was induced by the addition of tryptophan.

2.7.1 Production of recombinant AIHV-1 A9 protein

2.7.1.1 Expression of recombinant AIHV-1 A9 protein in *E. coli*

Thioredoxin fusion proteins were prepared in the ThioFusion™ Expression System (Invitrogen). The vector pTrxFus (Invitrogen) contained the following restriction sites – *KpnI*, *SmaI*, *BamHI*, *XbaI*, *AccI*, *Sall*, *PstI* that could be used to place the thioredoxin open reading frame upstream of a cloned gene (fig 2.3).

An DNA fragment encoding the A9 gene excluding the transmembrane domain was amplified by PCR (see section 2.3.12) from AIHV-1 DNA using primers Y4233 and Y4234 (appendix 2.1). The PCR product and pTrxFus DNA was digested with *KpnI* and *XbaI* and ligated together (as described in section 2.3.2).

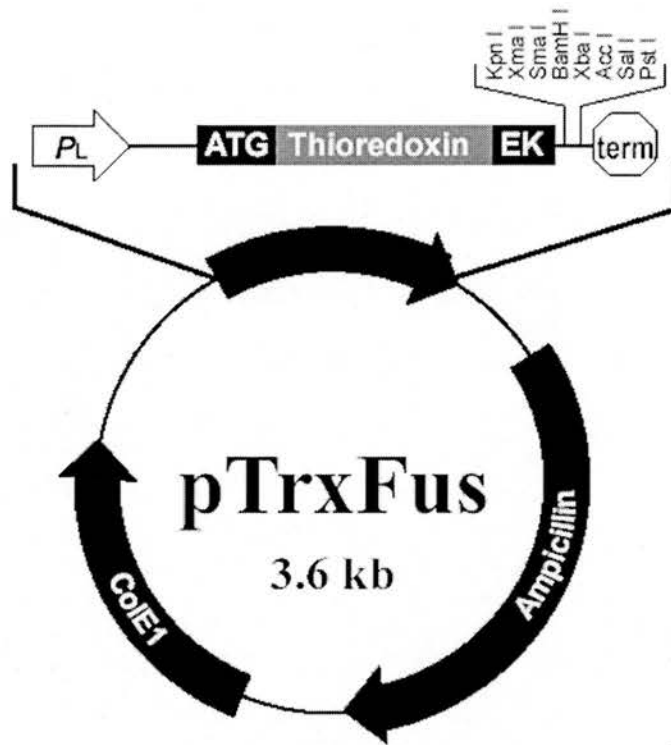


Fig 2.3. pTrxFus vector was obtained from Invitrogen.

This vector uses the P_L promoter from bacteriophage λ to drive expression. Expression is induced by the addition of tryptophan, which shuts down *cl* repressor synthesis to allow the transcription from the P_L promoter. The vector also contains an ampicillin resistance gene to aid selection of transformed *E. coli*.

2.7.1.2 Induction of protein synthesis

E. coli GI724 transformed with thioredoxin fusion constructs were inoculated into 10ml RM medium (Invitrogen thiofusion expression system) containing 100µg/ml ampicillin. An aliquot, 5ml, of overnight culture was added to 100ml of induction medium (42mM Na₂HPO₄, 22mM KH₂PO₄, 8.6mM NaCl, 18.7mM NH₄Cl, 2 % (w/v) Casamino acids, 8% (w/v) dextrose, 100µg/ml ampicillin) and incubated in an orbital shaker for 2½ hrs at 30°C. Thioredoxin fusion protein expression was induced by the addition of tryptophan to 1mM (Sigma) and incubated at 37°C for 2½ hrs in an orbital mixer. Cells were centrifuged at 1080 x g for 10 mins and the bacterial pellet stored at -20°C until required.

2.7.1.3 Harvesting recombinant thioredoxin fusion protein

E. coli cell pellets were resuspended in 15ml of PBS containing a protease inhibitor cocktail tablet (Complete®, Roche) and 100µl of lysozyme (Sigma) (10mg/ml). Cells were lysed by sonication using a sonication probe (Jenson) for 1 min. Soluble and insoluble proteins were separated by centrifugation at 13000 x g for 30 mins. Insoluble pellets were solubilised in 45µl reducing Laemmli sample buffer (see section 2.5.1) and heated in a boiling water bath for 5 mins. An equal volume of 2 x reducing Laemmli sample buffer was added to 10µl of supernatant and 20µl of pellet. The proteins were analysed by SDS-PAGE electrophoresis (see section 2.5.1) and the gel was stained by Coomassie blue to detect the presence of recombinant protein.

2.7.2 Affinity Purification of recombinant thioredoxin-A9 fusion protein using ThioBond™ columns

The ThioBond™ resin was used in the affinity purification of thioredoxin fusion proteins. All fusions expressed from the pTrxFus plasmid contain vicinal dithiols while other proteins are washed away. The purified thioredoxin fusion proteins were eluted using β-mercaptoethanol (β-ME).

The method used was as described in the manufacturer's instructions (Invitrogen). ThioBond™ resin (Invitrogen) was equilibrated using equal volumes of running buffer (PBS, 1mM EDTA) containing 20mM β -ME. Fresh running buffer containing 20mM β -ME was added and incubated for 30-60 mins. The resin was allowed to settle and supernatant removed. The resin was then washed three times with running buffer (without β -ME), before incubating for 1hr with the cell lysate. The complex was then applied to a column and unbound protein collected. The resin was washed in running buffer containing 1mM β -ME. Recombinant thioredoxin-A9 fusion protein was eluted using running buffer containing 200mM β -ME. Samples were collected in 1ml fractions and stored at -20°C for future use. The column was regenerated using running buffer and stored at 4°C until required.

2.7.3 Purification of thioredoxin recombinant protein by electroelution

Crude *E. coli* lysate, 200 μl , was prepared in the same volume of 2 x Laemmli sample buffer. Proteins were visualised during separation by Coomassie blue staining of SDS-PAGE gels (see section 2.5.2.). Recombinant thioredoxin-A9 proteins were excised from gels using a clean scalpel.

Gels containing the excised protein bands were roughly chopped and placed in the cathode (-ve/upper) chamber of a Biorad electroelution unit. Both chambers and the tank unit were filled with tank buffer (25mM Tris, 200mM Glycine, 5mM SDS). A current of 50mA was applied for approximately 30 mins or until all the blue dye (protein) had moved from the upper to the lower chamber. Electroeluted material was collected, washed in Vivaspin concentrators (with a 10kDa cut-off membrane) (Vivascience) with PBS and stored at 4°C until required.

2.7.4 Immunisation of animals

Mice were immunised subcutaneously with an emulsion of complete Freund's adjuvant (Difco Laboratories), 200 μl , mixed with an equal volume of antigen (purified recombinant thioredoxin-A9 protein, 26 μg). Four weeks later, mice were re-immunised

intraperitoneally using an emulsion of Freund's incomplete adjuvant, 50µl, with an equal volume of antigen (31µg). Serum was tested after the second immunisation for the presence of specific antibody by Western blot (see section 2.5.3). The mice were re-immunised intraperitoneally four weeks later with 50µl of Freund's incomplete adjuvant with an equal volume of antigen (31µg). Animals were euthanased by cervical dislocation and the spleen was collected for hybridoma production.

For the production of polyclonal antibodies, rabbits were immunised intramuscularly with an emulsion of complete Freund's adjuvant mixed with an equal volume of antigen (electroeluted recombinant thioredoxin-A9 protein) (containing 75µg). Four weeks later, animals were re-immunised subcutaneously with an emulsion of Freund's incomplete adjuvant with an equal volume of antigen (containing 75µg). Animals were ex-sanguinated under halothane anaesthesia and the serum was collected for antibody.

2.7.5 Production of A9 protein specific monoclonal mouse antibodies

NSO mouse myeloma cells were removed from liquid nitrogen (see section 2.2.4) and cultured one week prior to fusion. NSO mouse myeloma cells (ECCAC, UK) were recovered from cell culture by gently tapping the cell culture flask. Cells were transferred into 50ml tubes and centrifuged at 238 x g for 5 mins with the pellet being resuspended in 20ml of NSO growth medium (Rosewell Park Memorial Institute (RPMI) medium with L-glutamine (Gibco), 5mM N'-[2-hydroxyethyl] piperazine-N'-[2-ethanesulphonic acid] (HEPES, Sigma), 1.5% (w/v) L-Glutamine, (10000U) Penicillin/Streptomycin) containing 10% (v/v) FBS.

Mouse macrophages from non-immunised Balb/c mice were used as feeder cells. Ice-cold PBS containing penicillin (200U/ml) and streptomycin (200µl/ml) was injected into the peritoneal cavity. The body was massaged and the PBS was withdrawn using a syringe. The suspension was centrifuged at 500 x g for 10 mins, washed twice with PBS and a cell count was carried out. The cell pellet was resuspended to a concentration of $2-5 \times 10^4$ cells/ml in plating out medium (NSO medium containing 20% (v/v) FBS, OPI

media supplement (0.15g/l oxaloacetate, 0.05g/l pyruvate, 0.0082g/l bovine insulin) (1:50, Sigma) and hypoxanthine aminopterin thymidine (HAT) (1:50, Sigma)) and plated out at 75µl/well in 96 well plates. The plates were incubated overnight at 37°C in a humid 5% CO₂ in air atmosphere.

Immunised spleen was recovered and rinsed well with medium containing streptomycin (200µl/ml) and penicillin (200U/ml). The spleen was placed in a 90mm² petri dish (Bibby Sterilin Ltd) and cells were flushed out by using syringes with 26G needles. RPMI containing 10% (v/v) FBS (10ml) was injected into the spleen to displace cells into the surrounding medium. The spleen was teased apart by the action of the needles to completely release spleen cells. The medium was transferred to a universal and the debris allowed to settle. The supernatant was removed and the cells pelleted at 254 x g for 5 mins. The cell pellet was resuspended in ice cold 0.17M NH₄Cl (5ml) and placed on to ice for 10 mins. The cells were washed twice with medium without serum and resuspended in serum-free medium.

NSO cells were added to the spleen cells to give a fusion ratio of 1:5 (NSO:spleen). The cell suspension was centrifuged at 254 x g for 5 mins. The supernatant was removed and the cell pellet was resuspended in 1ml of warm polyethylene glycol (PEG) solution (Sigma). Serum-free medium (10ml) was slowly added to the fusion mixture and the cells centrifuged at 185 x g for 5 mins. The cell pellet was resuspended in 10ml of plating-out medium and the cell suspension was added to 80ml of plating-out medium. Cells were dispensed (125µl/well) to plates containing macrophage feeder cells and incubated at 37°C in a humid 5% CO₂ in air atmosphere. Supernatant material was tested for reactivity to the thioredoxin-A9 fusion protein by ELISA (see section 2.7.6).

2.7.6 Enzyme linked immuno-sorbent assay (ELISA)

ELISA's were used to measure the antibody from hybridoma clones specific for the A9 protein.

96 well ELISA plates (M129B, Greiner Laborotechnik) were coated with 50µl/well of either thioredoxin protein (control) or recombinant thioredoxin-A9 fusion

protein (0.5µg/ml) in 0.1M carbonate buffer pH 9.6 at 4°C overnight. Plates were washed three times with wash buffer (PBS containing 0.05% (v/v) Tween 20[®] (Sigma)), then non-specific binding sites were blocked for 1 hr at room temperature with 100µl per well 4% (v/v) FBS and washed again three times in wash buffer. Plates were incubated with 50µl per well of hybridoma supernatant at neat, 1:5, 1:10 and 1:20 dilutions for 1 hr and then washed three times with wash buffer. Secondary antibody, goat anti-mouse-HRP conjugate (DAKO) was added at a dilution of 1:2000 for 1 hr. All dilutions were in wash buffer. The plates were washed three times with wash buffer and the colour reaction was allowed to develop with the addition of 50µl per well of SureBlue[™] TMB Microwell Peroxidase (KPL) for 10-15 mins. The reaction was terminated by the addition of 50µl of 2.5M H₂SO₄ per well. The optical density of the reaction mixture was measured using a MRX Microplate reader (Dynex Technologies) equipped with a 492nm filter.

2.8 Apoptosis assays

2.8.1 Cells

Apoptosis assays were carried out with A9-transfected CHO cells. BHRF1 cDNA from EBV was used as a positive Bcl-2 control and an ovine interferon (IFN) transfected CHO cell line that was resistant to MSX selective pressure but did not produce IFN was used as a transfection control (Graham *et al.*, 1995). Untransfected (UTF) cells were used as a negative control. Cells were set up in GMEM supplemented with 2% (v/v) dialysed FBS.

2.8.2 Induction of apoptosis

CHO cells were seeded 24hrs before incubation with (25µM) Cis-platinum dichloroamine II (cis-platin) (Sigma). This dose was based on a dose-response experiment. Cis-platin has been shown to induce apoptosis by binding to the purine bases on DNA and causing the DNA helix to kink (Jamieson & Lippard, 1999). This

results in slower DNA replication which induces apoptosis. Cells were incubated with cis-platin for 3 hrs at 37°C, 5% CO₂ in air in an incubator. Media was removed from cells and fresh medium was added. Samples were analysed using the appropriate apoptosis assay (see below) at 24, 48 and 72hrs after incubation with cis-platin.

2.8.3 Extraction of DNA

DNA was extracted from CHO cells to analyse the DNA and identify if the typical “DNA laddering” that is observed in apoptotic cells was produced in cells treated with cis-platin.

CHO cells were cultured in 35mm² petri dishes (Nalgene) at a concentration of 3 x 10⁵ cells/ml with 1.5ml of cell suspension added to each dish. After 24 hrs, apoptosis was induced using cis-platin.

At 24, 48, and 72 hrs after treatment with cis-platin, the media was removed from cells. The cells were washed with warm (37°C) PBS and removed from the petri dish by incubating for 2 mins at 37°C with trypsin (0.25%) /versene (0.02%). Trypsin was neutralised with the addition 200µl of GMEM containing 7.5% (v/v) FBS. Cells were pelleted by centrifugation at 100 x g for 10 mins and washed with 500µl of PBS to remove residual serum. Cells were pelleted by centrifugation at 100 x g for 10 mins and resuspended in 200µl of PBS. DNA was extracted from the cells using Easy-DNA kit (Invitrogen) according to the manufacturers protocol. Cells were lysed using 350µl of solution A (lysis buffer), vortexed and incubated at 65°C for 10 mins. 150µl of solution B (precipitation solution) was added to the lysate (to precipitate proteins and lipids). This was vortexed, and 500µl of chloroform was added to the samples, which were vortexed again and centrifuged at 17900 x g for 20 mins. The upper phase of the solution was transferred into a fresh micro-centrifuge tube (1.5ml) and 1ml of 80% (v/v) ice-cold ethanol was added, vortexed and incubated on ice for 30 mins. The samples were centrifuged at 17900 x g for 10 mins, the ethanol removed and replaced with 500µl of ice-cold 80% (v/v) ethanol. The tubes were inverted five times and centrifuged at 17900 x g for 5 mins. The DNA pellet was resuspended in 20µl of TE buffer containing

0.5µl of 2mg/ml RNase. DNA was incubated at 37°C for 30 mins. Loading buffer (30% (v/v) glycerol: TE, 0.25% (w/v) bromophenol blue) (6µl) was added to a sample of DNA for analysis by agarose gel electrophoresis (section 2.3.13).

2.8.4 Caspase-3 assay

Cells were cultured at a concentration of 5×10^4 cells/ml in GMEM supplemented in 2% (v/v) FBS. The cell suspension, 1ml (5×10^4 cells) was added to a 24 well plate (Costar). After 24 hrs, apoptosis was induced using cis-platin as described in section 2.8.2.

The assay was carried out 24, 48 and 72 hrs after incubation with cis-platin. The media was removed from the cells and retained. The cells were washed with 1ml of warm (37°C) PBS and removed from the 24 well plate. The PBS was retained and the cells were removed from the plate by incubating for 2 mins at 37°C with trypsin (0.25%) / versene (0.02%). Trypsin was neutralised with the addition of 500µl of GMEM containing 7.5% (v/v) FBS. Cells were pelleted by centrifugation at 100 x g for 5 mins and resuspended in 500µl of PBS. Cells pelleted by centrifugation at 100 x g for 4 mins. The supernatant was removed and the cells were resuspended in 50µl of ice-cold lysis buffer (10mM HEPES pH 7.4 (Sigma), 42mM potassium chloride, 5mM magnesium chloride, 1mM DTT, 1µg/ml Pepstatin A (Sigma), 1µg/ml Leupeptin (Sigma), 5µg/ml Aprotinin (Sigma), 0.1% Triton X-100). Cells were incubated on ice for 10 mins, vortexed and pelleted by centrifugation at 17900 x g for 4 mins. The supernatant was removed and stored at -20°C until required.

10µl of lysate was added in triplicate to a 96 well flat bottom plate (Costar). To this 150µl of caspase assay buffer (20mM HEPES pH 7.4, 1mM EDTA, 10% sucrose, 5mM DTT, 0.1% CHAPS, 13.3µM N-Acetyl-Asp-Glu-Val-Asp-7-ami-do-4-methylcoumarin (Av-DEVD-AMC)) and the plate was sealed and incubated at 37°C for 5 hrs. The results were obtained using a fluorescent plate reader (Cytofluor Series 4000, Perspective Biosystems) with an excitation filter set at 395nm and an emission filter set at 490nm. The results were read in relative fluorescent units (RFU).

2.8.5 Diff-quick® assay

The diff-quick (Dade Behring) reagents stained cells in such a way that morphological evidence of apoptosis can be visualised by light microscopy. This assay detects changes that occur in cell morphology during apoptosis. In cells that are healthy, the nuclei and cytoplasm can be seen. However, in cells that are undergoing apoptosis the cells round up and the nuclei are darkly stained.

CHO cells were cultured at a concentration of 1×10^5 cells/ml in GMEM supplemented with 2% (v/v) FBS. The cell suspension, 200 μ l, (2×10^4 cells) was added to each well of an eight well chamber slide (Lab-Tek). After 24 hrs, apoptosis was induced using cis-platin as described in section 2.8.2.

The assay was carried out 24, 48 and 72 hrs after incubation with cis-platin. Cells were washed once with warm (37°C) PBS. Cells were fixed by immersion in Fast green in methanol, 0.002g/l for 10 secs. Cells were then stained by immersion in stain 1 (Eosin G in phosphate buffer pH 6.6, 1.22g/l) for 10 secs followed by immersion in stain 2 (Thiazine dye in phosphate buffer pH 6.6, 1.1g/l) for 10 secs. The excess dye was removed by washing slides in distilled water. The slides were air-dried and mounted using Shandon mounting media (Shandon). The cells were examined under a light microscope. A sample of 200 cells was counted from each well to determine whether the cells were pyknotic or healthy.

Chapter 3

Sequence analysis of ORF A9, production of recombinant A9 viral Bcl-2 and specific antisera

3.1 Introduction

The AIHV-1 genome has been sequenced and contains eleven 'unique' genes (Ensser *et al.*, 1997). Many of these genes were found to have homology with cellular counterparts, one of which is contained within ORF A9. This encodes a possible apoptosis-inhibitory protein, based on predicted amino acid comparisons. Many herpesviruses express at least one Bcl-2 homologue that have been proven to be anti-apoptotic.

In this study, the expression of ORF A9 in bacteria and the production of mouse monoclonal and rabbit polyclonal antibodies specific for AIHV-1 A9 are described.

The A9 gene was amplified by PCR and cloned into the expression vector pGEX-3X that expresses recombinant proteins as a Glutathione S-transferase (GST) fusion protein. Expression is repressed, under normal conditions, by the product of the LacI^q gene. Repression is removed by the addition of the inducer isopropyl β -D thiogalactosidase (IPTG), a lactose analogue. The plasmid directs the synthesis of the fusion protein under the control of the IPTG inducible *tac* promoter. This is a strong promoter that can result in high levels of expression of the fusion protein. The plasmid also contains the ampicillin resistance gene for the selection of plasmid-containing colonies.

The cloned A9 gene was also inserted into the expression vector, pTrxFus that expresses recombinant proteins as thioredoxin fusion proteins. This vector uses the P_L promoter from bacteriophage λ to drive expression and has been shown to be one of the most efficient promoters for bacterial expression (Buell *et al.*, 1986). The bacteriophage λ *cI* repressor binds to the operator region in front of the P_L promoter and controls the level of transcription from this promoter. When cells are grown in tryptophan-free medium, the *cI* repressor gene is transcribed and the *cI* protein binds to the P_L promoter preventing transcription. Expression is induced by the addition of tryptophan, which shuts down *cI* repressor synthesis to allow the transcription from the P_L promoter. The vector also contains an ampicillin resistance gene to aid selection of transformed *E. coli*. The thioredoxin expression system was used as it has been proven to express high levels of soluble fusion proteins (Holmgren, 1985; La Villie *et al.*, 1992). Both the GST and Trx systems are useful in the identification of the recombinant proteins as (in the

absence of A9 specific antibodies) monoclonal antibodies for both are available commercially.

The thioredoxin fusion protein was used as an antigen to raise specific anti-sera in mice and rabbits. This chapter describes the purification of the thioredoxin fusion protein by affinity chromatography and the purification of the antibodies that were produced. These reagents were then used to detect the presence of A9 protein in transfected CHO cell lines and LGL cell lines.

The objectives of this part of the work were:

- To analyse ORF A9 predicted amino acid sequence for homology to the Bcl-2 family of proteins.
- To express A9 protein and raise specific antisera.

3.2 Materials and Methods

3.2.1 Expression of a GST-A9 fusion protein

A9 DNA was amplified by PCR from WC11 AIHV-1 DNA using PCR primers; 5 Bcl Gex and 3 Bcl Gex (appendix 2.1). The purified product was purified and digested with *Not1* and *Sal1*. The PCR product was ligated into pGEX-3X in frame with GST, using the *Not1* and *Sal1* sites. The ligated DNA were transformed in *E. coli* strain BL2 and streaked out onto LB agar overnight. A colony of bacteria was picked using an inoculating loop and grown overnight in 10ml LB broth. The bacteria were pelleted by centrifugation at 4000 x g for 10 mins. The pellet was lysed by the addition of lysis buffer (50mM Tris, 10mg/ml lysozyme) followed by sonication using a sonication probe (Jensons) for 30 secs. The insoluble and soluble proteins were separated by centrifugation at 16 000 x g for 30 mins. Both the insoluble and soluble proteins were run on a 15% SDS-PAGE gel (as described in section 2.5.1). Proteins were detected by Coomassie blue staining.

3.2.2 Expression of a GST-truncated A9 fusion protein

PCR was used to amplify the A9 gene excluding the hydrophobic transmembrane domain. PCR primers 5 Bcl Gex and 3 Bcl GexT (appendix 2.1) were used. The PCR product was purified, digested with *Not1* and *Sal1* and ligated into pGEX-3X in frame with the GST as described in section 3.2.1. The fusion protein was generated and expressed as described in section 3.2.1.

3.2.3 Solubilisation of proteins

Where indicated, the protein pellets were resuspended in 8M urea and incubated overnight. The soluble and insoluble fractions were separated by centrifugation at 16 000 x g for 45 mins. The supernatant material was analysed by electrophoresis on a 12% SDS-PAGE gel (as described in section 2.5.1). Proteins were detected by Coomassie blue staining.

3.2.4 Dialysis of GST-A9 fusion protein

Samples were dialysed to remove excess urea. The dialysis tubing was prepared by washing in running water for 3-4 hrs. The sulphur compounds were removed from tubing by heating in a 0.3% (w/v) solution of sodium sulphide at 80°C for 1 min. The tubing was then washed in hot water (60°C) for 2 mins, followed by an acidification step of 0.2% (v/v) sulphuric acid then rinsed in hot water to remove the acid. Proteins were pipetted into the dialysis tubing and dialysed overnight in PBS. The soluble and insoluble proteins were separated by centrifugation at 16,000 x g for 45 mins. Proteins were analysed by Coomassie blue staining of a 12% SDS-PAGE gel.

3.2.5 Expression of recombinant thioredoxin-A9 fusion protein in *E. coli*

DNA encoding the A9 gene excluding the hydrophobic transmembrane domain was amplified by PCR using primers Y4233 and Y4234 (appendix 2.1). The PCR product was purified, digested using *Kpn1* and *Xba1* and ligated into the pTrxFus expression vector. The construct was transformed into the GI724 strain of *E. coli* (as described in section 2.3.4). Bacterial colonies were analysed for the A9 sequences inserted into pTrxFus (by mini-preps, as described in section 2.3.9) and restriction analysis of the plasmid DNA using *Kpn1* and *Xba1* (as described in section 2.3.1). Positive samples were tested for the expression of thioredoxin fusion proteins. Protein expression was induced by the addition of tryptophan to a final concentration of 1mM and then cultured for a further 3 hrs as described in section 2.6.2.2. Recombinant thioredoxin-A9 fusion proteins were harvested from *E. coli* by lysis as described in section 2.6.1. Proteins were separated by electrophoresis and detected by Coomassie blue staining. Western blotting was also used to identify recombinant thioredoxin-A9 fusion proteins (as described in section 2.5.3). Mouse monoclonal anti-thioredoxin (Invitrogen) was used at a concentration of 1:5000 followed by incubation with anti-mouse-HRP (DAKO) at a concentration of 1:2000.

3.2.6 Purification of recombinant thioredoxin-A9 protein using ThioBond

Recombinant thioredoxin-A9 fusion proteins were purified using ThioBond™ resin (Invitrogen) (section 2.6.2). Thioredoxin-A9 fusion proteins were eluted using β -mercaptoethanol and analysed by electrophoresis. Proteins were visualised by silver

staining of SDS-PAGE gels. Eluted proteins were concentrated using 10kDa centricons (Millipore). β -mercaptoethanol was removed from eluted proteins by dialysis with PBS in centricons to a final volume of 500 μ l.

3.2.7 Purification of thioredoxin recombinant protein by electroelution

Recombinant thioredoxin-A9 proteins were separated by Serva Blue R (Coomassie blue R) in the upper tank buffer to visualise the proteins bands in the gel during separation. Samples in non-reducing Laemmli sample buffer were loaded into a single large well on a Biorad Mini Protean II system using a 1.25mm comb. Up to 400 μ l total volume was loaded per gel. The upper tank was filled with cathode buffer (3.08g/l Tris, 14.4g/l Glycine, 0.05% (w/v) SDS, 24mg/l Serva Blue (Sigma) and the lower tank filled with tank buffer as for a traditional SDS-PAGE. Once identified, the relevant protein band was excised from the gel. Gels containing the excised protein bands were roughly chopped and placed in the cathode (-ve/upper) chamber of a Biorad electroelution unit. Both chambers and the tank unit were filled with tank buffer (25mM Tris, 200mM Glycine, 5mM SDS). A current of 50mA was applied for approximately 30 mins or until all the blue dye (protein) had moved from the upper to the lower chamber. Electroeluted material was collected, washed in Vivaspin concentrators (with a 10kDa cut-off membrane) (Vivascience) with PBS and stored at 4°C until required.

3.2.8 Cleavage of thioredoxin-A9 fusion protein using EnterokinaseMaxTM

The cleavage of thioredoxin-A9 fusion protein using EnterokinaseMaxTM was carried out as described in the manufacturer's protocol (Invitrogen). The digestion was set up as follows: 20 μ g of thioredoxin-A9 fusion protein, 3 μ l 10 x EKMaxTM buffer, 4 μ l EKMaxTM and deionised water was added to make a final volume of 30 μ l. The digestion was mixed and incubated at 4°C overnight. Samples were boiled in an equal volume of reducing Laemmli sample buffer and electrophoresis was carried out as described in section 2.5.1.

3.2.9 Construction of β -Gal-A9 fusion protein

A9 DNA was amplified by PCR (see section 2.3.12) from AIHV-1 WC11 DNA using primers 5pMSBCL and 3pMSBCL (appendix 2.1). The PCR product and pMS plasmid DNA was digested with *Hind*III and ligated together (as described in section 2.3.2).

E. coli JM109 transformed with the β -Gal fusion constructs were inoculated into 10ml L-broth containing ampicillin (100mg/ml). An aliquot, 5ml, of overnight culture was added to 100ml of L-broth containing ampicillin (100mg/ml) and incubated in an orbital shaker for 3 hrs. β -gal fusion protein expression was induced by the addition of IPTG to 1mM (Sigma) and incubated for 3 hrs. Cells were centrifuged at 1080 x g for 10 mins and the bacterial pellet stored at -20°C until required. The bacterial pellets were resuspended in 15ml of PBS containing a protease inhibitor cocktail tablet (Complete®, Roche) and 100 μ l of lysozyme (10mg/ml, Sigma). Cells were lysed by sonicating using a sonication probe for 1 min. Soluble and insoluble proteins were separated by centrifugation at 13000 x g for 30 mins. Insoluble pellets were solubilised in 45 μ l reducing Laemmli sample buffer (see section 2.5.1) and heated in a boiling water bath for 5 mins. Proteins were detected by western blot analysis using mouse anti-A9 serum.

3.2.10 Production of monoclonal mouse antibodies against recombinant A9 protein

For the preparation of monoclonal mouse antibodies, two mice were immunised with purified thioredoxin-A9 fusion protein as described in section 2.7.4. Monoclonal antibodies against the recombinant A9 protein were produced as described in section 2.7.5.

3.2.11 Testing of antisera by ELISA

To test the reactivity of supernatant from hybridomas that had been produced, recombinant thioredoxin-A9 fusion protein was coated on ELISA plates (M129B, Greiner Laborotechnik) and an ELISA was carried out as described in section 2.7.6. Positive samples against recombinant thioredoxin-A9 protein were analysed further by repeating the ELISA using thioredoxin protein at a concentration of 2 μ g/ml as described

in section 2.7.6. Those that were positive for the recombinant thioredoxin-A9 protein and negative for the thioredoxin protein on its own were considered positive for A9.

3.2.12 Isotyping antibodies

Antibodies 6E1 and 6G8 were isotyped with respect to immunoglobulin class/subclass using the IsoStrip mouse monoclonal antibody isotyping kit (Roche) according to the manufacturer's protocol. Hybridoma supernatant was diluted 1:10 and pipetted into a development tube. The tube was incubated at room temperature for 30 sec and then agitated in order to completely resuspend the coloured latex. A strip was inserted into the development tube and incubated for 5-10 mins to allow bands to develop.

3.2.13 Purification of mouse anti-A9 hybridoma supernatant, 6E1 using IgM-sepharose

Hybridoma supernatant 6E1 was purified on an anti-mouse IgM sepharose column (Sigma) by Fast performance liquid chromatography (FPLC). The hybridoma supernatant was filtered through a 0.45µm filter. A small column (2ml) of anti-mouse IgM sepharose was packed and washed thoroughly with PBS. 6E1 supernatant was loaded on to the column and unbound proteins were collected. The O.D.₂₈₀ was monitored for all fractions collected, to detect proteins. The column was washed with PBS until the O.D.₂₈₀ returned to baseline and unbound proteins were eluted. IgM antibody was eluted from the column using elution buffer (0.5M Glycine, 0.15M NaCl pH 2.8) at a rate of 1.5ml/min. Eluted protein samples were detected by a rise in O.D.₂₈₀, the relevant fractions collected and immediately neutralised with 1M Tris, pH 8.0. Samples were pooled together and stored at -20°C for future use. The column was cleaned and washed with several cycles of PBS.

3.2.14 Production of polyclonal rabbit antibodies against recombinant A9 protein

For the preparation of polyclonal antibodies, two rabbits were immunised with electroeluted thioredoxin-A9 fusion protein. The antigen was prepared as described in section 2.7.3. Electroeluted thioredoxin-A9 fusion protein was concentrated using

centricons (centrifugal concentrators with a 10kDa cut-off membrane) (Millipore) to a final volume of 1.5ml. The protein concentration was determined and this material was divided between the two rabbits for each set of inoculations.

3.2.15 Purification of anti-A9 serum using ammonium sulphate precipitation

Anti-A9 rabbit serum was centrifuged at 3,000 x g for 30 mins. Supernatant was transferred to a beaker and an equal volume of saturated ammonium sulphate was added slowly. The solution was placed on ice for 1-2 hrs and centrifuged at 3,000 x g for 30 mins. The supernatant was removed and the pellet was resuspended in 15ml of 1X PBS. The solution was dialysed in PBS overnight.

3.2.16 Transfection of CHO cells with A9 and EBV BHRF1 cDNAs

CHO cells were stably-transfected with 2 μ g of the plasmid construct pEE14-A9 or pEE14-BHRF1 using Lipofectamine 2000™ (4 μ l) (as described in section 2.2.7) to produce A9-CHO and BHRF1-CHO cells respectively. Transfections were carried out in 6 well plates (Nunc) with a total volume of 500 μ l of transfection complex being added to each well.

3.2.17 Indirect immunofluorescence assay

CHO cells were seeded at a density of 1x 10⁵ cells/ml in 8 well chamber slides with 200 μ l of cell suspension added to each well. Immunofluorescence was carried out as described in section 2.2.9. Cells were fixed with ice-cold acetone, washed with PBS and incubated with the positive samples in the ELISA at the following dilutions: neat, 1:5, and 1:10. This was followed by incubation with goat, anti-mouse-FITC (1:75).

Rabbit antisera, 162 and 163 were used at a dilution of 1:500. A secondary conjugate of goat anti-rabbit-biotin was used (1:500) followed by a tertiary conjugate of streptavidin-FITC (1:75). Cells were examined using an Olympus BX50 microscope (Olympus) using a blue (NB) filter at 470-490nm.

3.3 Results

3.3.1. Sequence analysis of ORF A9

Analysis of the predicted amino acid sequence of ORF A9 from C500 low passage AIHV-1 using the blastp program revealed 33% amino acid identity with human Bcl-w. Bcl-w is an anti-apoptotic member of the Bcl-2 family of proteins. The area of homology between A9 and Bcl-w is concentrated in one region, the BH1 domain.

The predicted mass of the A9 protein is 19kDa. This is smaller than human Bcl-2 which has a mass of 26kDa. The viral Bcl-2 homologues that are present in the sequenced gammaherpesviruses are all smaller molecules than their cellular counterparts. This is probably due to the lack of some BH domains. For example, the Bcl-2 homologue present in HHV-8 has a molecular weight of 19kDa and contains only BH1, BH2 and the transmembrane domain.

The AIHV-1 A9 predicted amino acid sequence was compared to viral and cellular Bcl-2 family members by Clustal W analysis (fig. 3.1). The analysis showed that AIHV-1 A9 has a highly conserved BH1 domain and transmembrane domain while other Bcl-2 family domains (BH2-4) could not be identified. Within the BH1 domain of the Bcl-2 family members there is a conserved sequence, NWGR. Part of this sequence is present in AIHV-1 A9, where the sequence is HWGR. The A9 protein sequence possesses the conserved glycine residue that is essential in anti-apoptotic activity (Yin *et al.*, 1994).

From the recent genome sequence of OvHV-2 (Stewart & Rosbottom, personal communication) the Bcl-2 homologue (ORF O9) also possessed a BH1 domain and transmembrane domain but lacked the three remaining Bcl-2 family domains. Interestingly the OvHV-2 Bcl-2 homologue does possess the conserved sequence NWGR. The greatest similarity in this analysis was between AIHV-1 A9 and OvHV-2 O9 sequences.

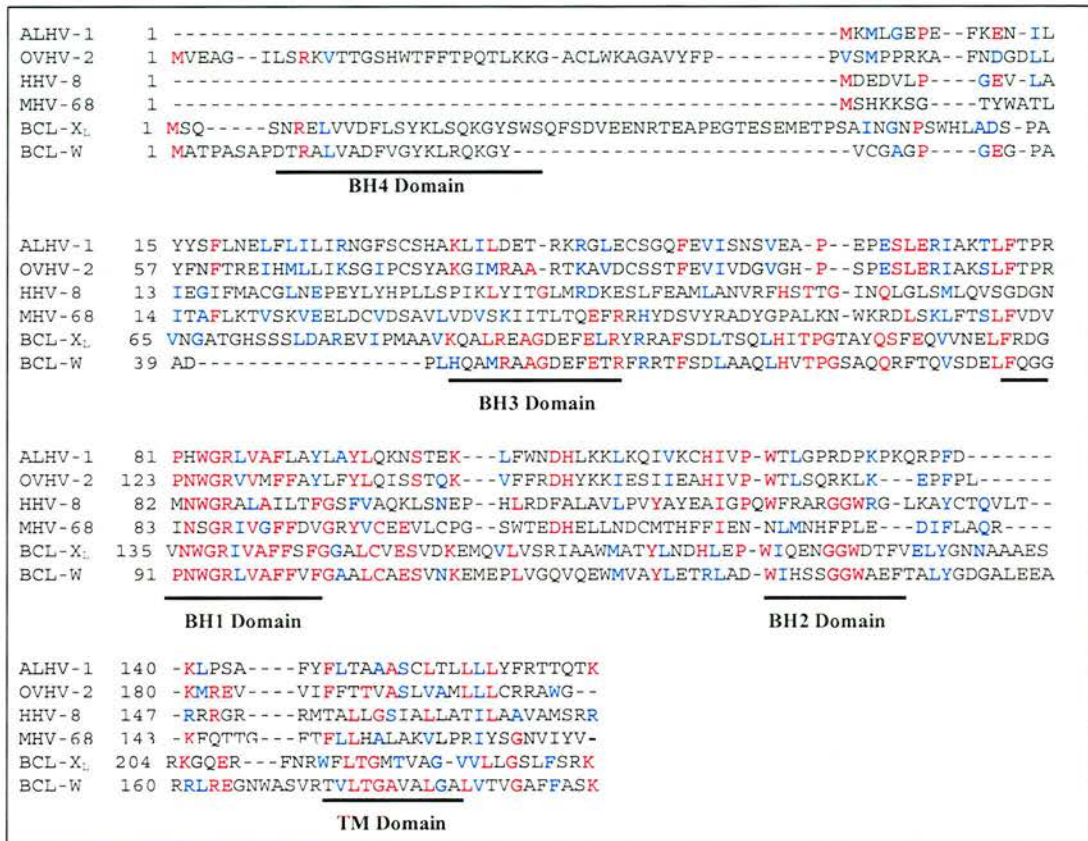


Fig. 3.1. Clustal W analysis of viral and cellular Bcl-2 proteins. The amino acid sequences of viral and cellular Bcl-2 proteins (AlHV-1 (Ensser *et al.*, 1997), OvHV-2 (Stewart & Rosbottom, personal communication), HHV-8 (Cheng *et al.*, 1983), MHV-68 (Virgin *et al.*, 1997), Bcl-x_L (Boise *et al.*, 1993), Bcl-w (Gibson *et al.*, 1996)) were aligned and displayed using the BOXSHADE program. Identical residues are in red while similar residues are blue. The position of the Bcl homology (BH) domains and the transmembrane domain are also marked on the diagram.

3.3.2 Expression of a GST-A9 fusion protein

Primers (pGex5 and pGex3 as shown in appendix 2.1) were designed to amplify the A9 gene from WC11 AIHV-1 DNA. The amplified DNA was ligated into pGEX-3X in frame with the GST fusion protein using the *Not*I and *Sal*I sites. The construct was transformed into *E. coli* bacteria and the transformants were checked for the presence of inserted A9 DNA. Samples positive for A9 inserts were analysed for the expression of the GST-A9 fusion protein. Expression of the GST-A9 fusion protein was induced by the addition of IPTG. Both the cell supernatant and pellet were then analysed by electrophoresis on a 15% SDS-PAGE gel. Recombinant proteins were detected using Coomassie blue stain (fig. 3.2). A dominant protein that had an approximate size of 45kDa in the pelleted fraction was observed. The predicted size of the A9 protein was 19kDa and the GST protein was 26kDa, therefore the 45kDa protein band was the correct size to be the GST-A9 fusion protein. However, since the protein was present in the pellet and not in the supernatant, the protein was insoluble.

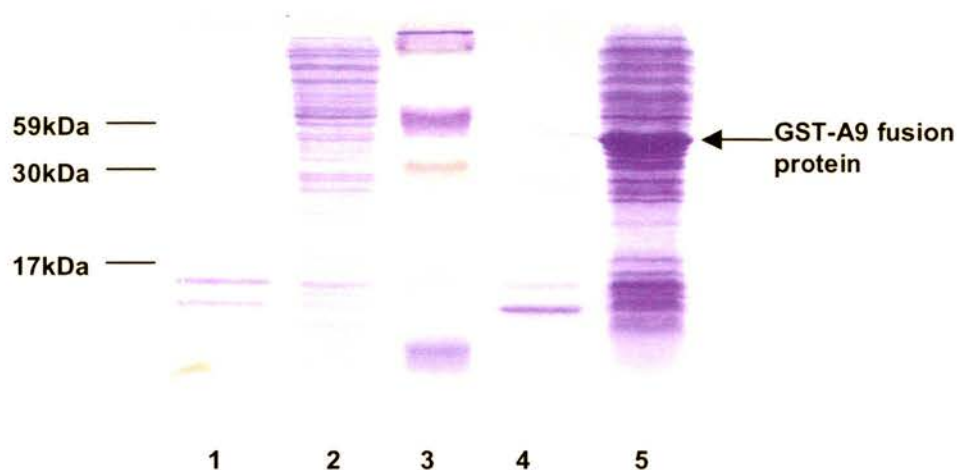


Fig. 3.2. A9-GST fusion proteins in *E. coli* lysates detected by Coomassie blue staining. **1)** Uninduced cell supernatant, **2)** Induced cell supernatant, **3)** Kaleidoscope molecular mass markers (Bio-rad), **4)** Uninduced cell pellet, **5)** Induced cell pellet.

The GST-A9 fusion protein was insoluble, possibly due to the hydrophobic transmembrane domain present in the A9 protein. Therefore, primers were designed to amplify a fragment of the A9 gene that excluded the hydrophobic transmembrane domain. A 456bp A9 DNA fragment was amplified by PCR using primers 5 Bcl Gex and 3 Bcl Gex T (appendix 2.1). The PCR product was ligated in pGEX-3X in frame with the GST fusion protein using *Not1* and *Sal1* sites. Fig. 3.3 shows faint bands corresponding to the truncated GST-A9 fusion protein were detected in the supernatant. However, the dominant band was present in the pellet, indicating that the protein was still insoluble.

To further attempt to solubilise the recombinant GST-A9 fusion protein, pellets were resuspended in 8M urea. Fig. 3.4, shows that 8M urea solubilised the proteins in the pellet. However, the protein could not be purified using glutathione sepharose, possibly due to excess urea. Samples were dialysed overnight in PBS to remove the urea. The soluble and insoluble materials were separated by centrifugation and analysed by electrophoresis. Proteins were detected by Coomassie blue staining on a 12% SDS-PAGE gel. Faint bands corresponding to GST-A9 were observed in supernatant samples, however, a dominant band was observed in the pellet. Thus, removal of the urea by dialysis led to protein becoming insoluble once more. Attempts to purify the GST-A9 protein using glutathione beads were unsuccessful. It was decided to use an alternative fusion protein.

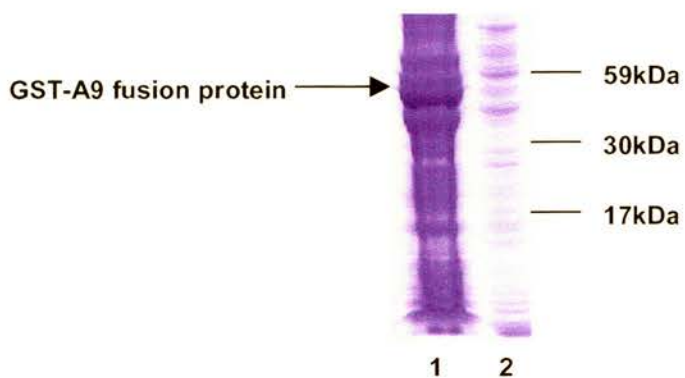


Fig. 3.3. Truncated GST-A9 fusion proteins in *E. coli* lysates detected by Coomassie blue staining. 1: Truncated A9-GST fusion protein. Cell lysate, pellet. 2: Truncated A9-GST fusion protein. Cell lysate, supernatant.

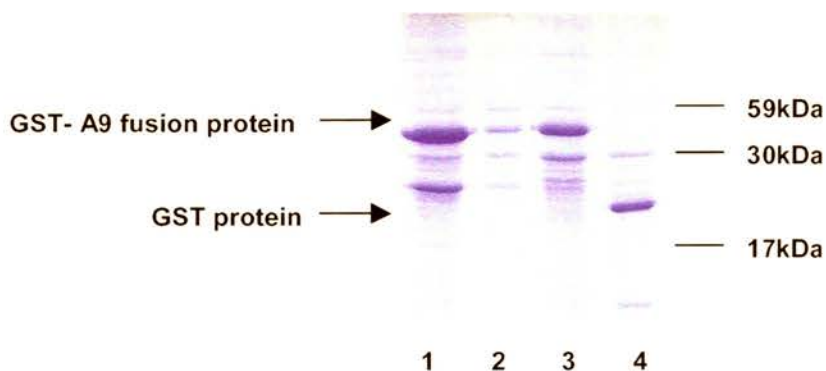


Fig. 3.4. GST-A9 fusion insoluble protein pellets in *E. coli* solubilised in 8M urea detected by Coomassie blue staining. 1: Induced truncated A9-GST. Cell lysate supernatant. 2: Uninduced truncated A9-GST. Cell lysate supernatant. 3: Induced A9-GST. Cell lysate supernatant. 4: Induced GST. Cell lysate supernatant.

3.3.3 Expression of thioredoxin–A9 protein in bacteria

Primers, Y4233 and Y4234 were designed to amplify ORF A9 from WC11 AIHV-1 DNA. A9 DNA was ligated into the *Kpn*I and *Xba*I sites of the pTrxFus plasmid. The construct was transformed into *E. coli* bacteria and transformants were checked for the presence of inserted A9 DNA. Samples positive for the A9 insert were analysed for the expression of thioredoxin fusion protein. Expression of the thioredoxin fusion protein was induced by the addition of tryptophan. Fig. 3.5 shows a dominant band around 30kDa. The predicted size of the A9 protein is 19kDa and the thioredoxin protein is 11kDa, which is consistent with the dominant band being the thioredoxin-A9 fusion protein. The protein was present in the supernatant indicating that it is soluble.

ThioBond™ resin was used to purify the recombinant thioredoxin-A9 protein from crude cell lysate. The fusion protein was eluted using β -mercaptoethanol. The SDS-PAGE gel analysis (fig. 3.6) shows that the optimum concentration to elute the fusion protein was 100-200mM β -mercaptoethanol. Proteins were detected by Silver staining. Western blot analysis using an anti-thioredoxin antibody confirmed the presence of recombinant thioredoxin-A9 protein (fig. 3.7).

This material was used to immunise rabbits as described in section 2.7.4.

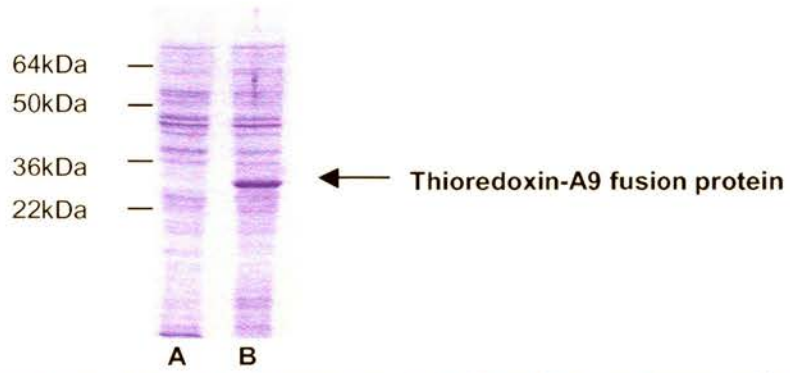


Fig 3.5. Recombinant thioredoxin-A9 fusion protein in *E. coli* lysates detected by Coomassie blue staining. **A:** Trx-A9 uninduced **B:** TRX-A9 induced

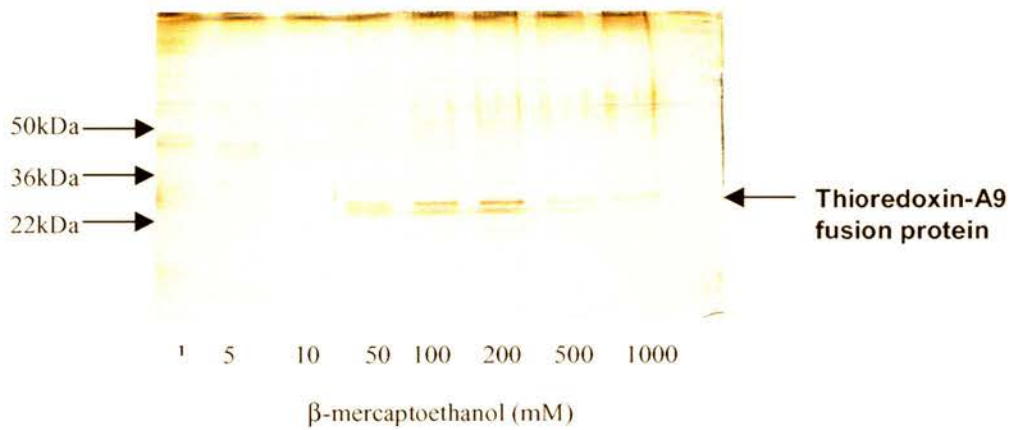


Fig. 3.6. Recombinant thioredoxin-A9 protein purified using Thiobond and various concentrations of β -mercaptoethanol to elute the bound protein. Detected by Silver staining.

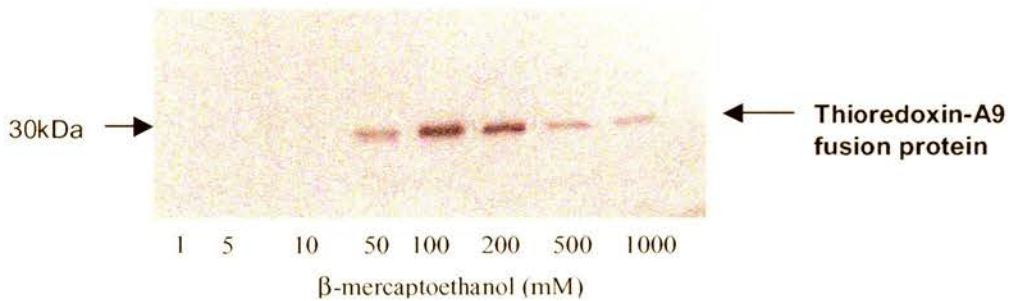


Fig. 3.7. Western blot of recombinant thioredoxin-A9 fusion protein purified using various concentrations of β -mercaptoethanol probed with anti-thioredoxin monoclonal antibody followed by goat, anti-mouse-HRP conjugate.

3.3.4 Polyclonal antiserum reacts with the Trx-A9 recombinant protein

Recombinant thioredoxin-A9 fusion protein was digested with EnterokinaseMax™. This allowed the cleavage of the A9 protein from the thioredoxin fusion protein. Western blot analysis was used to determine if there was antibody to the A9 protein in antiserum from the tail bleed of immunised mice after the first challenge compared with an anti-thioredoxin antibody to detect thioredoxin-A9 (fig. 3.8). A thioredoxin-specific band was observed with the mouse serum. However, an A9 vBcl-2 specific band was also identified at the predicted molecular weight of the A9 protein (19kDa). The mice were re-immunised to boost the anti-A9 response and to allow the production of monoclonal antibodies.

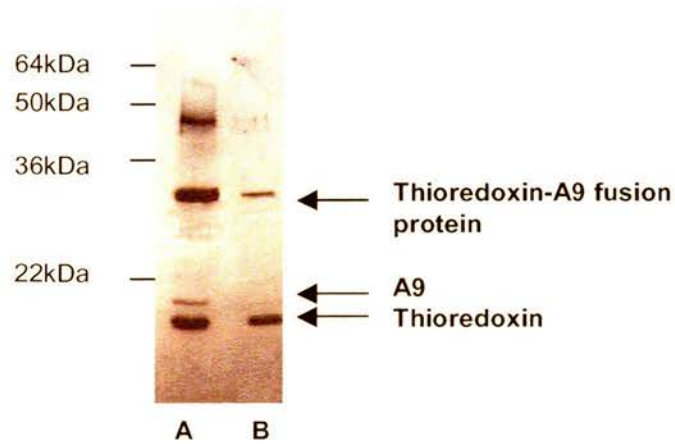


Fig. 3.8. Western blot of EnterokinaseMax™ digested thioredoxin-A9 fusion protein. A: Antiserum from immunised mouse. **B:** Anti-thioredoxin antibody.

3.3.5 A9 expression in A9-CHO cells

The expression of A9 in A9-CHO cells was investigated by Northern blot analysis. Fig 3.9A shows the result of the Northern blot analysis with an A9 probe. A9 mRNA was detected in the transfected cells but as expected not in the UTF CHO cells. Fig. 3.9B shows the result of the Northern blot analysis with control GAPDH labelled probe. Both UTF and A9-CHO cells showed a GAPDH product. This indicated that the RNA was intact and the gel was loaded with equivalent amounts of RNA. Northern blot analysis revealed that A9 mRNA was expressed in A9-CHO cells.

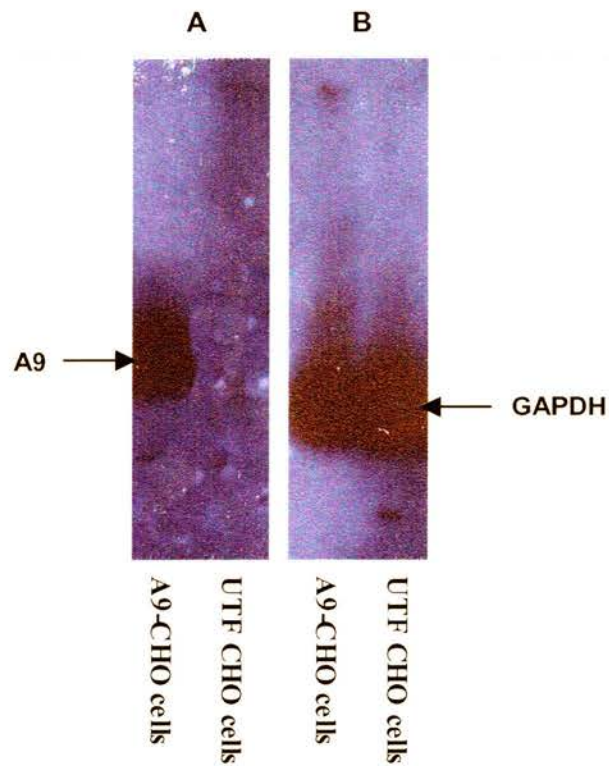


Fig. 3.9. Northern blot analysis of GAPDH and ORF A9 expression in A9-CHO cells. RNA samples were obtained from A9-CHO cells. **A:** Northern blot probed with A9 probe. **B:** Northern blot probed with GAPDH probe.

3.3.6 Monoclonal antibody specific for the A9 protein.

The hybridoma supernatants obtained from the immunised mice were tested for specific antibody using an ELISA. The initial ELISA was performed on 258 hybridoma supernatants. This was originally performed using the thioredoxin-A9 protein as the coating protein. Controls used in the ELISA were pre-immunised serum and tail bleed from the immunised mice. Clones were selected on the basis of the OD readings being comparable with the positive control. Tables 3.1 and 3.2 show a typical ELISA result from one of the assays performed. From this particular assay four of the hybridomas were used for the second round of screening, 6E1, 6G8, 6A11 and 2A1. The initial ELISA that was carried out resulted in 26 putative anti-A9 positive clones. Samples that were positive for the recombinant thioredoxin-A9 fusion protein were retested on ELISA plates coated with recombinant thioredoxin. Those that were positive for thioredoxin-A9 and negative for thioredoxin on its own were considered positive for A9. From the hybridomas tested, six appeared to react specifically with the A9 protein. The majority of hybridomas contained antibody against thioredoxin only. The six potential A9 antibody positive hybridoma supernatants were tested by immunofluorescence assay using A9-CHO cells. Two hybridoma supernatants were positive by fluorescence, 6E1 and 6G8 (fig. 3.10). Some non-specific staining was observed in CHO cells incubated with pre-immunised mouse serum in both untransfected (UTF) and A9-CHO cells. However the level and intensity was very low. 6G8 was identified as an IgG₂ while 6E1 was identified as an IgM antibody. Unfortunately 6G8 did not grow in subsequent cultures. Therefore, 6E1 remained as the principle A9-specific murine monoclonal antibody for further studies.

	1	2	3	4	5	6	7	8	9	10	11	12
A		Pre-immune	Pre-immune	6A3	6A3	5F12	5F12	4F8	4F8	2A4	2A4	
B		TB	TB	6G8	6G8	5D11	5D11	4D8	4D8	2A1	2A1	
C		1A11	1A11	6F11	6F11	5H9	5H9	4C6	4C6	1B6	1B6	
D		1C12	1C12	6F12	6F12	5H7	5H7	4B4	4B4	1H4	1H4	
E		1E12	1E12	6A11	6A11	5D8	5D8	3H11	3H11	1B1	1B1	
F		2B6	2B6	6B8	6B8	5B8	5B8	3B10	3B10	1D6	1D6	
G		5G1	5G1	6H3	6H3	5D6	5D6	3C5	3C5	1D10	1D10	
H		6E1	6E1	6F3	6F3	4F11	4F11	3G3	3G3	2A1	2A1	

Table 3.1: A typical ELISA using hybridoma supernates. Table shows the orientation of the ELISA plate and which supernates were used in the assay. Pre-immune serum was taken from pre-immunised mice and was used as a negative control. TB= Tail-bleeds from mice after immunisation and was used as a positive control.

	1	2	3	4	5	6	7	8	9	10	11	12
A		0.010	0.021	0.029	0.062	0.057	0.042	0.007	0.012	0.022	0.073	
B		2.741	2.110	2.414	1.987	0.047	0.054	0.009	0.021	0.837	0.753	
C		0.039	0.020	0.062	0.054	0.006	0.010	0.054	0.065	0.037	0.021	
D		0.004	0.008	0.066	0.042	0.045	0.037	0.044	0.087	0.191	0.241	
E		0.06	0.068	2.023	2.132	0.050	0.045	0.024	0.021	0.070	0.039	
F		0.063	0.043	0.054	0.075	0.013	0.024	0.066	0.087	0.241	0.354	
G		0.028	0.045	0.108	0.154	0.004	0.010	0.005	0.012	0.014	0.031	
H		1.555	1.468	0.023	0.054	0.035	0.086	0.020	0.037	0.020	0.052	

Table 3.2: A typical ELISA showing the OD readings at 492nm using neat supernatant of the samples shown in Table 3.1.

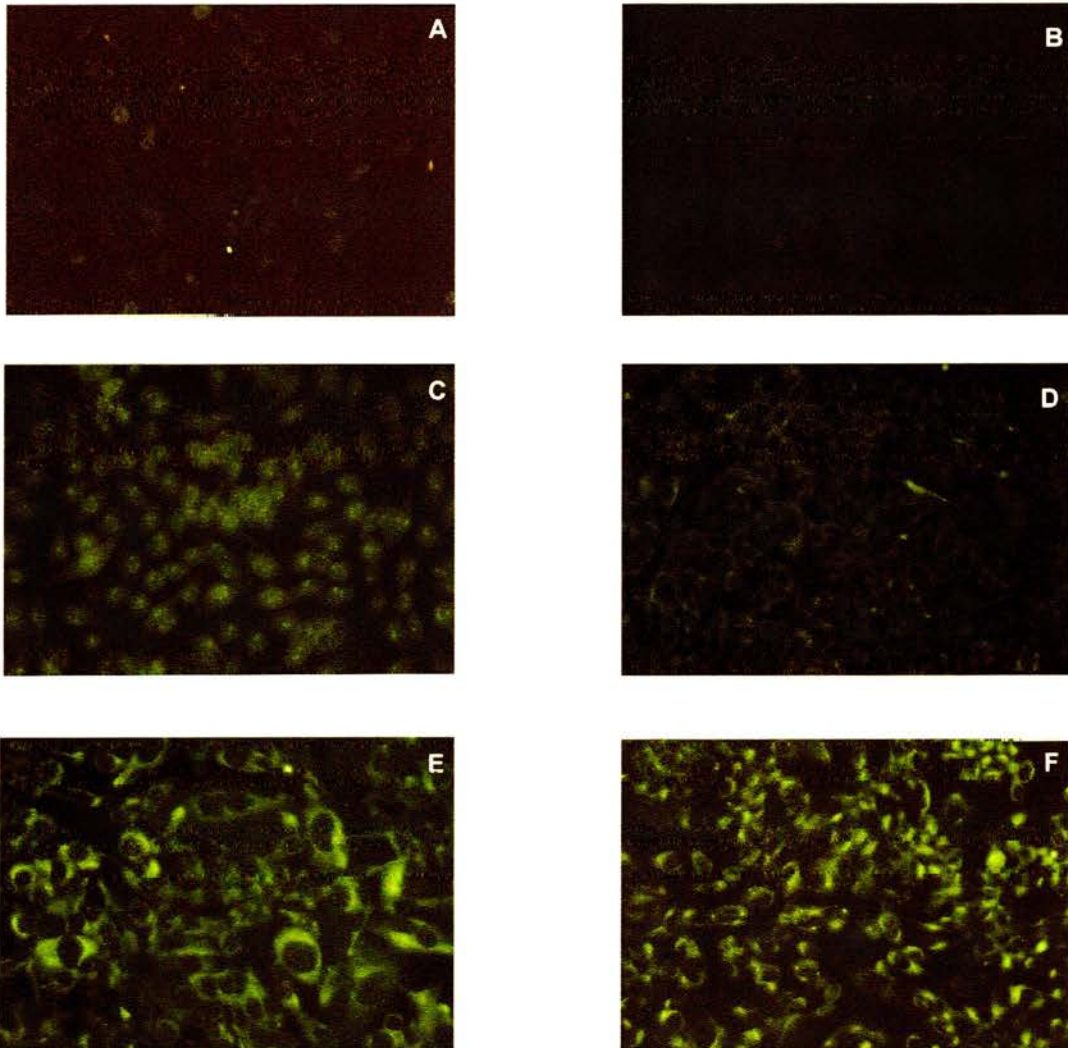


Fig 3.10. Fluorescence images of A9-CHO and UTF CHO cells (photographs were taken using equal time exposures, x 400 magnification). All cells were fixed in ice-cold acetone, incubated with the appropriate primary antibody followed by incubation with goat, anti-mouse-FITC (1:75).

A) A9-CHO cells incubated with pre-immunised mouse serum (1:200).

B) Untransfected CHO cells incubated with pre-immunised mouse serum (1:200).

C) Untransfected CHO cells incubated with 6G8 anti-A9 monoclonal antibody supernatant (neat).

D) Untransfected CHO cells incubated with 6E1 anti-A9 monoclonal antibody supernatant (neat).

E) A9-CHO cells incubated with 6G8 anti-A9 monoclonal antibody supernatant (neat).

F) A9-CHO cells incubated with 6E1 anti-A9 monoclonal antibody supernatant (neat).

3.3.7 Purification of mouse antiserum 6E1 using an anti-mouse IgM column

The supernatant from the 6E1 hybridoma cells was collected and fractionated on an anti-mouse IgM column. Bound IgM proteins were eluted from the column using low pH. However, the yield of antibody collected from the column was very poor as shown in fig. 3.11. Consequently, the supernatant from the hybridoma cells was partially purified using ammonium sulphate precipitation and the antibody from this was used in the fluorescence studies.

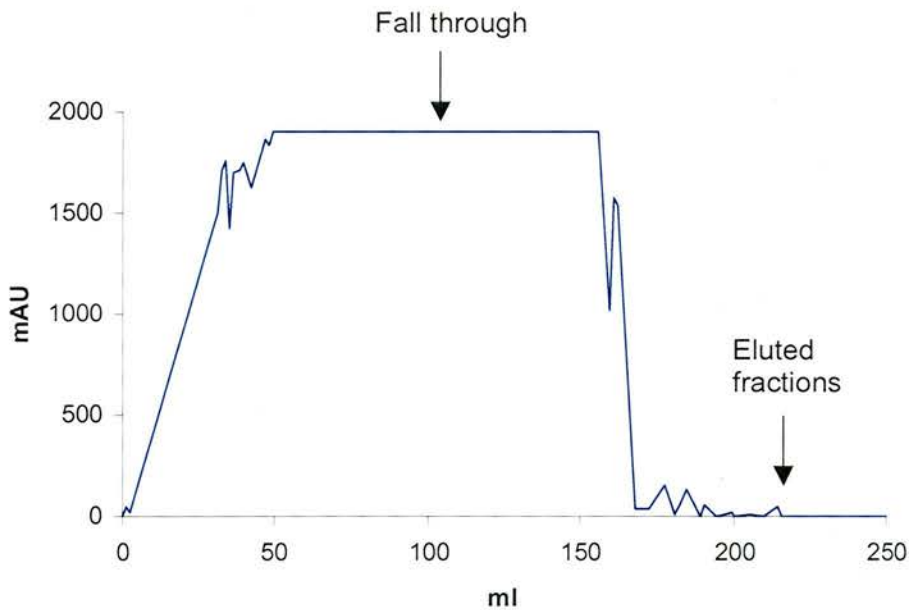


Fig. 3.11. Antiserum to thioredoxin-A9 purified on an anti-IgM-sepharose column. IgM fractions were eluted from the column using a Glycine elution buffer and detected by a shift in absorbance at 280nm. (x-axis is the volume of eluted fractions, y-axis is the absorbance units at 280nm.)

3.3.8 Detection of AIHV-1 A9 protein in transfected CHO cells

Using 6E1 anti-A9 serum that had been partially purified by ammonium sulphate precipitation, A9 vBcl-2 protein was detected in A9-CHO cells (Fig 3.12A).

Localisation of the antibody appeared to be in the cytoplasm. When the antibody was incubated with untransfected CHO cells, a very low intensity of non-specific labelling was observed (fig. 3.12B). Therefore, partially purified 6E1 anti-A9 serum was specific to A9 protein.

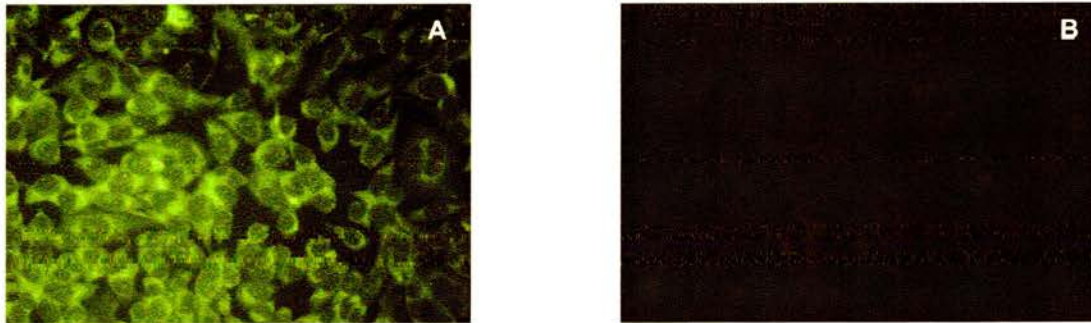


Fig 3.12. Fluorescent images of CHO cells labelled with anti-A9 and control antibody. (All photographs were taken using equal exposure times, x 400 magnification). All cells were fixed in ice-cold acetone, incubated with the appropriate primary antibody followed by goat anti-mouse-FITC (1:75).

A) A9-CHO cells protein labelled with ammonium sulphate enriched 6E1 antibody (1:500).

B) UTF CHO cells labelled with ammonium sulphate enriched 6E1 antibody (1:500).

3.3.9 Rabbit polyclonal antiserum reacts with A9 vBcl-2 recombinant protein

Rabbits were immunised with thioredoxin-A9 purified fusion protein (as described in section 2.7.4). The immunised rabbit serum was tested by western blot analysis along with normal rabbit serum for the presence of antibodies to the recombinant thioredoxin-A9 fusion protein and also to the β -galactosidase-A9 fusion protein.

The antiserum reacted with the 30kDa band of thioredoxin-A9 fusion protein and the 116kDa β -galactosidase-A9 fusion protein (fig. 3.13). From fig. 3.13 it can be seen that the antiserum also reacts with the thioredoxin empty vector. The antibody therefore reacted with the A9 protein because the serum reacted with β -galactosidase-A9 fusion protein, which does not contain any thioredoxin. Therefore, the western blot analysis shows that the polyclonal rabbit antiserum had specificity for both A9 and thioredoxin and could be used as an anti-A9 antibody.

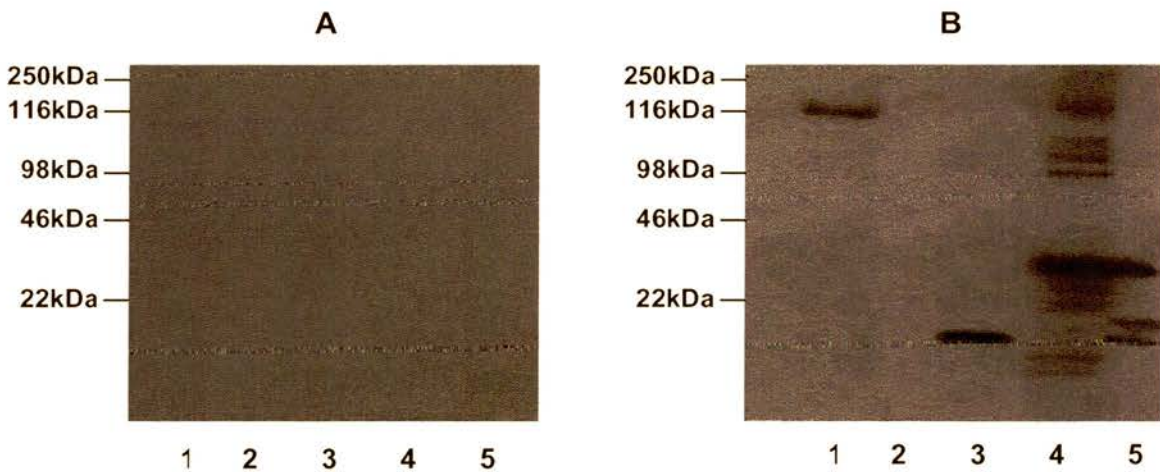


Fig. 3.13. Western blot analysis of rabbit antibody specific for the A9 protein.

1: β -galactosidase-A9 fusion protein.

2: β -galactosidase.

3: Thioredoxin.

4: Thioredoxin-A9 fusion protein.

5: Cleaved thioredoxin-A9 fusion protein.

A: Incubated with normal rabbit serum (1:1000), followed by goat, anti-rabbit-HRP (1:2000).

B: Incubated with anti-A9 rabbit serum, 163 (1:1000), followed by goat, anti-rabbit-HRP (1:2000).

3.3.10 Rabbit anti-A9 serum reacts with the A9 protein expressed by CHO cells

CHO cells expressing A9 protein (A9-CHO) were incubated with antiserum from rabbit 163. Rabbit 163 serum was used as the primary antibody (at a dilution of 1:500). The secondary conjugate was goat anti-rabbit-biotin (1:500) and finally the tertiary conjugate was streptavidin-FITC (1:75). Normal rabbit serum was used as a control (1:2000).

A field of 200 cells was randomly counted and determined if A9 was being expressed or not. Positive immunofluorescence was detected in 58% of A9-CHO incubated with anti-A9 rabbit serum (fig 3.14A).

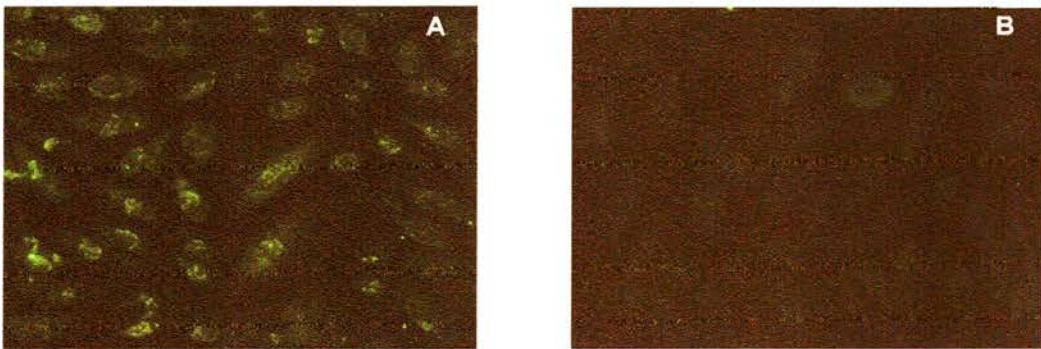


Fig. 3.14. Fluorescent images of A9-CHO cells incubated with serum from an immunised rabbit. (Pictures taken with the same exposure time, x 400 magnification). Cells were fixed in ice-cold acetone, incubated with the appropriate primary antibody, followed by goat anti-rabbit-biotin (1:500) and finally incubated with streptavidin-FITC (1:75)
A) A9-CHO cells incubated with 163 rabbit anti-A9 sera (1:500).
B) A9-CHO cells incubated with normal rabbit serum (1:1000).

3.3.11 Expression of EBV BHRF1 vBcl-2 in CHO cell lines

EBV BHRF1 vBcl-2 protects cells from apoptosis, and therefore has been used throughout this study as a positive control. BHRF1 DNA was transfected into CHO cells (BHRF1-CHO). Immunofluorescence analysis was used to identify the percentage of CHO cells expressing the BHRF1 protein using the anti-BHRF1 mouse monoclonal antibody (clone MAB818) (Chemicon). The secondary conjugate was goat anti-mouse-FITC.

Fig. 3.15 shows that there were no obvious differences between BHRF1-CHO cells incubated with anti-BHRF1 antibody (fig. 3.15.A) and those incubated with normal mouse serum (fig. 3.15.B). It was decided to proceed with the BHRF1-CHO cells as they were surviving the plasmid selectable marker selection and hence assumed a good level of transfection had occurred. This was confirmed by apoptosis assays carried out (discussed in chapter 5).

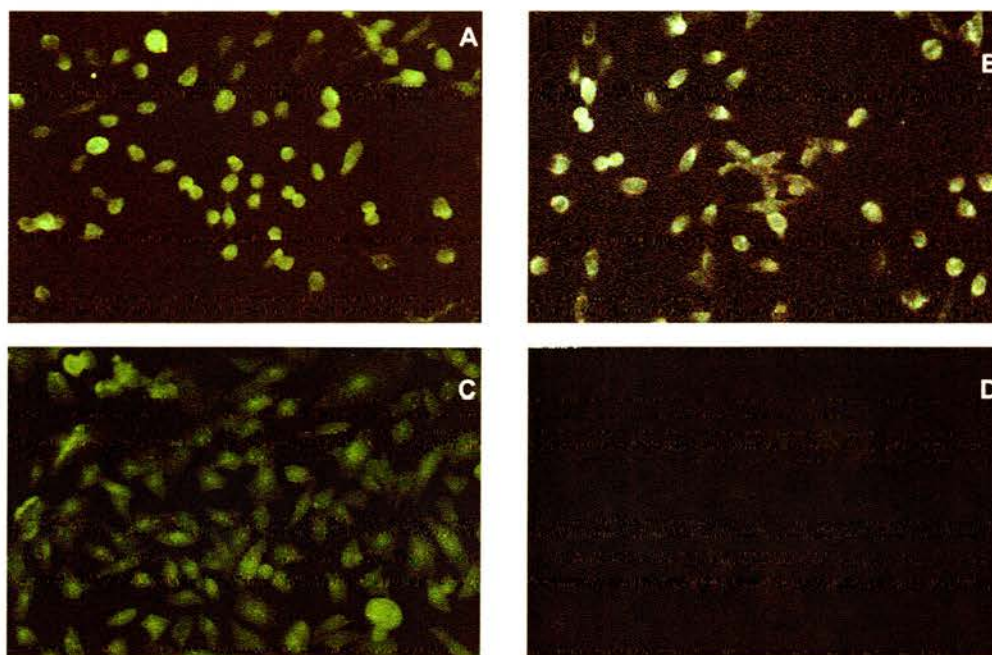


Fig. 3.15. Reaction of anti-BHRF1 with CHO cells expressing BHRF1 protein and in UTF CHO cells. (All pictures taken with the same exposure time, X 400 magnification). All cells were fixed in ice-cold acetone, followed by incubation in the appropriate primary antibody and finally incubate with goat anti-mouse-FITC (1:75).
A: BHRF1-CHO cells incubated with an anti-BHRF1 antibody (1:1000).
B: BHRF1-CHO cells incubated with normal mouse serum (1:1000).
C: Untransfected CHO cells incubated with anti-BHRF1 antibody (1:1000).
D: Untransfected CHO cells incubated with normal mouse serum (1:1000).

3.4 Discussion

The A9 gene product predicted amino acid sequence showed limited homology to the Bcl-2 family of apoptosis regulatory proteins. A9 vBcl-2 possessed the highly conserved Bcl homology (BH) 1 domain and the transmembrane (TM) domain. The BH1 domain is required for the interaction between Bax and anti-apoptotic proteins Bcl-x_L and Bcl-2 (Borner *et al.*, 1994). It has been suggested that the transmembrane domain, which is present in some anti- and pro-apoptotic Bcl-2 family members, localises Bcl-2 family members to membranes such as those of the mitochondria, endoplasmic reticulum and the nucleus (Krajewski *et al.*, 1993).

When this work was initially started, the A9 protein was unique as it was the only Bcl-2 family member identified so far to contain only one of the four known BH domains. However, since starting this research, work has been published on the MHV-68 Bcl-2 homologue. Sequence analysis performed on MHV-68 vBcl-2 protein has demonstrated that it contains only the BH1 domain and was shown to a bone-fide functional Bcl-2 protein (Roy *et al.*, 2000).

A9 protein shows 33% amino acid identity to human Bcl-w. Bcl-w is an anti-apoptotic protein that co-immunoprecipitates with the pro-apoptotic Bcl-2 family members, Bax, Bak, Bad and Bik (Holmgreen *et al.*, 1999). The level of amino acid identity is very low compared to other viral Bcl-2 homologues. For example, it only shares around 10% identity to BHRF1. However, all viral Bcl-2 homologues that have been sequenced share sequence identity within the BH1 domain and TM domain. As would be expected for two viruses that are closely related, the AIHV-1 A9 and the OvHV-2 O9 shared the greatest sequence identity in this study.

The work performed in this section described the expression of recombinant protein and the production of both rabbit and mouse antibodies. The production of recombinant A9 protein by various methods was successful. The GST-A9 fusion protein was mainly insoluble and not a useful reagent. Insolubility is often due to the presence of strongly hydrophobic regions of the protein (Smith & Johnson, 1988). An attempt was made to solubilise the protein by deleting the hydrophobic TM. The TM domain of Bcl-2 proteins has been shown to be involved in the import and insertion of the protein into the mitochondrial outer membrane and can also direct the protein to other membrane sites (Nguyen *et al.*, 1994). Expression of the truncated A9 protein lacking

the TM domain also resulted in a mainly insoluble protein. However, the GST-A9 fusion protein did solubilise in 8M urea. This resulted in an inhibition of binding to glutathione sepharose used for purification. Due to the insolubility of the GST-A9 protein and the inability to purify it with glutathione sepharose, an alternative expression system was tried.

Colleagues in the laboratory had previously successfully produced soluble thioredoxin fusion proteins. Due to problems that had been encountered with the GST fusion protein the TM domain was removed from the A9 gene upon amplification. As previously stated the TM domain enable the Bcl-2 family members to insert into membranes (Hockenberry et al., 1990; Gonzalez et al., 1995). It has been demonstrated that the TM domain is not essential in the prevention of apoptosis, as deleting this domain does not alter the level of protection against apoptosis (Hockenberry et al., 1993; Borner et al., 1994). This was acceptable for the immunisation of the animals, although the truncated gene could not be used in localisation studies. The thioredoxin-A9 fusion protein was successfully expressed as a soluble protein and purified using ThioBond™ affinity resin and electroelution from gels. Murine monoclonal antibodies, 6E1 and 6G8 specific for A9 protein were successfully produced in mice immunised with thioredoxin-A9 protein. These were isotyped IgM (6E1) and IgG₂ (6G8) respectively. However, 6G8 did not grow well in tissue culture. Therefore, 6E1 was chosen for the remaining work. An attempt to purify 6E1 IgM antibody was made using an anti-IgM column. However, the yield of IgM recovered from the column was very poor. It is possible that the integrity of the immunoglobulin was lost in the low pH elution protocol that was used. Due to the poor yield of purified IgM being recovered, it was decided to use a different antibody.

The rabbit polyclonal anti-A9 antibody was shown to react with both thioredoxin-A9 and β -galactosidase-A9 fusion proteins. It also reacted with thioredoxin expressed from the empty pTrxFus vector. However, this reactivity to thioredoxin was expected as the antiserum was raised against a thioredoxin-A9 fusion protein. This rabbit polyclonal anti-A9 was used for the remaining work of this study, as it recognised A9 vBcl-2 by fluorescence and western blot analysis.

A9-CHO cells were shown to express A9 protein through immunofluorescence analysis. Unfortunately it was not possible to determine the level of expression by

BHRF1-CHO cells. Further work needed to be carried out to develop this technique, unfortunately this was not possible due to time constraints. It was therefore assumed that since the transfected cells were surviving selection a proportion of the cells had been transfected and were expressing BHRF1. BHRF1-CHO cells were used throughout this study as a positive control as EBV BHRF1 vBcl-2 has been shown to protect cells from apoptosis (Khanim et al., 1997).

Chapter 4

ORF A9 expression in AIHV-1-infected bovine turbinate cells and LGL cell lines

4.1 Introduction

The objective of this study was to examine the expression of A9 in various cells during the virus life cycle. This section also examines where in the cell the A9 protein localises.

There are three strains of AIHV-1 used commonly in MCF laboratory research. Two are based on: C500, which was first isolated from an infected ox (Plowright *et al.*, 1975). This has two different forms: C500 low passage, which is cell-associated and virulent, C500 high passage, which is cell-free and attenuated with respect to inducing disease in susceptible animals. The third strain of the virus is WC11. This was isolated from a blue wildebeest and is cell-free and attenuated (Plowright *et al.*, 1960; Wright *et al.*, 2003). To determine whether A9 was expressed as an immediate early, early or late viral gene, the metabolic inhibitors cycloheximide and phosphonoacetic acid were used. Early and late gene transcription requires *de novo* protein translation and can be suppressed by cycloheximide, which inactivates host cell ribosomes. Therefore, immediate early genes were detected in the presence of cycloheximide. Late gene expression follows replication of the virus genome and drugs that inhibit virus replication prevent the expression of late genes. Phosphonoacetic acid inhibits DNA polymerase and therefore was used to harvest early gene transcripts.

Infected cell lines can be derived from lymphoid tissues of MCF-affected animals. These cell lines can be maintained for months and sometimes years and display large granular lymphocyte (LGL) characteristics. Part of this study was to determine if the A9 gene was expressed in AIHV-1 infected LGLs, as it is unclear which viral genes were expressed in these cell lines. Therefore, RNA was extracted from infected rabbit LGLs and A9-specific RT-PCR was performed.

The localisation of the A9 protein in cells was determined by confocal microscopy. Many of the Bcl-2 family members that have been characterised so far localise at the mitochondrial membrane (Riparbelli *et al.*, 1995). As demonstrated in chapter 3, the A9 gene is stably-expressed in CHO cells. To identify where in the cell the A9 protein localises the stably-transfected CHO cells were transiently

transfected with mitochondrial green fluorescent protein (mtGFP) (Rizzuto *et al.*, 1995).

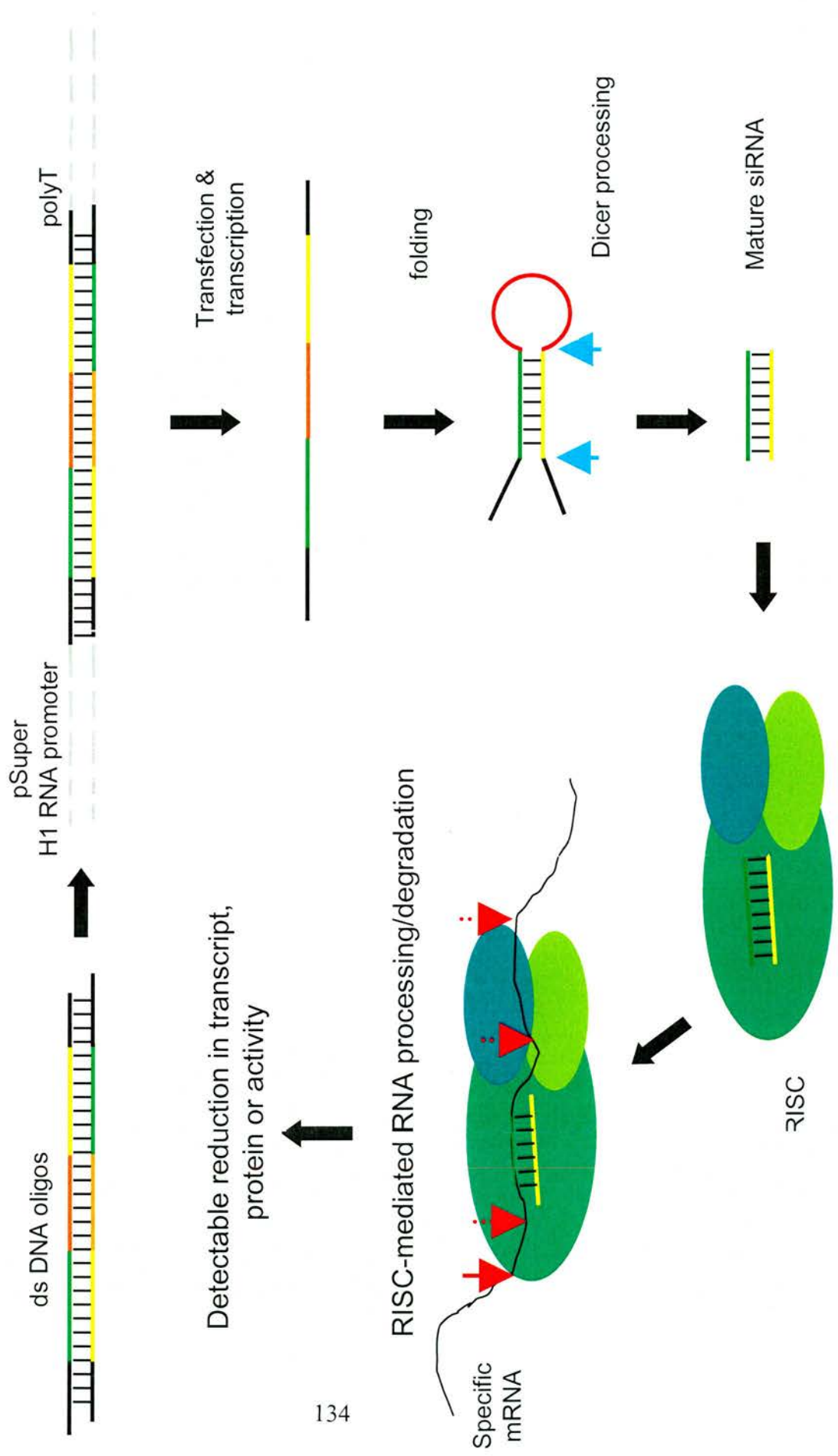
RNA interference (RNAi) is a mechanism of sequence-specific, post-transcriptional gene silencing initiated by dsRNA homologous to the gene that is being suppressed. The mechanism was first described in *Caenorhabditis elegans* (Fire *et al.*, 1998) and was shown to protect against invasion by foreign genes, but has subsequently been described in insects, plants, fungi and vertebrates (Reviewed in Agami, 2002).

During the RNAi process long dsRNA is degraded into 19-23 nucleotide (nt) siRNA and then is recruited into an RNA-induced silencing complex (RISC) to degrade corresponding mRNA (Hammond *et al.*, 2000). In mammalian cells siRNA molecules are capable of specifically silencing gene expressing and has become a novel technique to probe for gene function. In this study the retroviral plasmid pSUPER-retro (Oligoengine) was used. This vector directs the stable synthesis of siRNA in mammalian cells and should result in the efficient long-term down regulation of specific gene expression. The plasmid contains an ampicillin resistance gene to aid selection of transformed *E. coli* and a puromycin resistance gene to aid the selection of transfected cells. siRNA precursor molecules are transcribed from a 64-mer insert by RNA polymerase II. The transcript contains two inverted copies of the intended siRNA target (19-mer sequences) separated by a loop to allow the formation of a RNA duplex. After transcription this hairpin molecule is cleaved by the DICER enzyme *in vivo* to produce mature siRNA (fig 4.1). A9-CHO and UTF CHO cells were stably transfected with pSUPER-A9 and transfectants were selected with puromycin.

Therefore, the specific objectives in this study were:

- Determine when the A9 gene was expressed in the virus life cycle.
- Determine if the A9 gene was expressed in LGL cell lines.
- Determine where in the cell the vBcl-2 localises.
- To silence the A9 gene in A9-CHO cells by siRNA.

Fig. 4.1. siRNA production by the pSUPER system. Double stranded DNA oligonucleotides were designed using an online design system (www.oligoengine.com). **(A)** The annealed oligonucleotides were ligated into the pSUPER-retro vector and then transfected into mammalian cells. **(B)** siRNA precursor molecules are transcribed by RNA polymerase II. **(C)** The transcript is separated by a loop to allow the formation of a RNA duplex. **(D)** The hairpin molecule is cleaved by the DICER enzyme to produce mature siRNA. **(E)** The mature siRNA is recruited in a RNA-induced silencing complex (RISC) to **(F)** degrade corresponding mRNA. This should result in a reduction in transcript of mRNA, protein or activity.



4.2 Materials and Methods

4.2.1 Treatment and infection of BT cells

BT cells were seeded in 225cm² flasks (Costar UK Ltd) and allowed to grow until confluent.

Immediate early (IE) transcripts were detected by incubating the cells with 100µg of cycloheximide (Sigma) for 30 mins, virus was added and the cells were harvested after 8hrs (Wakeling *et al.*, 2001).

Early (E) transcripts were detected by incubating the cells with 100µg/ml of phosphonoacetic acid (ICN Biomedicals Inc) for 2 hrs (Seal *et al.*, 1991) then virus was added and cells were harvested after 24 hrs.

Late (L) transcripts were detected by adding virus to the BT cells with no treatment and the cells were harvested after 24 hrs.

Cells were harvested and the RNA was extracted as described in section 2.4.1. Virus titres used are shown in table 4.1.

Virus	Titre Used (TCID ₅₀)
C500 low passage	10 ^{-5.75}
C500 high passage	10 ^{-5.91}
WC11	10 ^{-5.74}

Table 4.1: Virus titres used in the expression experiment. The titre of each virus preparation used to infect BT cells is shown.

4.2.2 Northern blot analysis of A9 gene expression

The cells were harvested at the appropriate time points using RNA extraction buffer. RNA was extracted from the BT cells as described in section 2.4.1. 10µg of each RNA sample was loaded onto MOPS/formaldehyde gels and run at 100V for 1 hr. RNA was transferred onto nitrocellulose (section 2.4.2). A DNA probe was labelled and the membrane was hybridised as described in section 2.4.2. The

membrane was probed with either an A9 or GAPDH ³²P labelled probe. GAPDH was used as a control to determine if the RNA remained intact.

4.2.3 Expression of A9 gene in LGLs

RNA was extracted from LGLs as described in section 2.4.1. RT-PCR was performed (as described in section 2.4.3.) to determine if A9 was being expressed in the LGLs. Primers used in this section of the study were GAPDH5, GAPDH3, GFPBclF and GFPBclR (as described in appendix 2.1). The annealing temperature was 55°C.

4.2.4 Localisation of the A9 proteins in transfected CHO cells

A9-CHO cells were seeded in 8 well chamber slides at a density of 1×10^5 cells/ml with 200µl of cell suspension added into each well and incubated at 37°C, 5% CO₂ in air atmosphere for 24 hrs. A9-CHO cells were transiently-transfected with 0.2µg of mtGFP (as described in section 2.2.7). After 48 hrs, indirect immunofluorescence analysis was performed (as described in section 2.2.9). Briefly, cells were fixed in ice-cold acetone for 10 mins, blocked with normal goat serum (1:40), incubated with anti-A9 rabbit antibody, 162 (1:500) and detected with goat anti-rabbit-TRITC conjugate (1:75). Control incubations took place with A9-CHO cells incubated with normal rabbit serum (1:1000).

Cells were examined by confocal analysis (as described in section 2.2.10).

4.2.5 Expression of A9 protein in LGLs

An aliquot of LGLs (2×10^5 cells) from AIHV-1 infected rabbits and lymphoid cells grown in culture from healthy rabbits (2×10^5 cells) were cytocentrifuged onto glass microscope slides using a cytospin 3 machine (Shandon). Cells were fixed in ice-cold acetone for 10 mins then washed in PBS and stored at -20°C until required. The indirect immunofluorescence test was carried out as described in section 2.2.9. Non-specific binding sites on the LGLs were blocked with normal goat serum (1:40), before incubating with either anti-A9 rabbit polyclonal, 162 antibody (1:500) or normal rabbit serum (1:1000), followed by anti-rabbit biotin conjugate (1:500) and finally streptavidin-FITC conjugate (1:75). Cells

were examined using an Olympus BX50 microscope (Olympus) using a blue (NB) filter at 470-490nm.

4.2.6 siRNA expression

The mammalian expression vector, pSUPER (Oligoengine) was used for the expression of siRNA in A9-CHO cells. Target sequences were selected using the on-line design system for pSUPER vectors at www.oligoengine.com, which incorporates siRNA design principles established by Elbashir *et al.*, 2001. The gene-specific insert specifies a 19-mer sequence corresponding to nucleotides 125857-125875 (TGGATTTTCCTGCAGCCAC) (Ensser *et al.*, 1997). Additional restrictions were added to optimise the transcription and specific termination of the transcript in pSUPER, as well as its correct folding and processing by the DICER nuclease.

The selected sequence was produced as two complementary 64-mer DNA oligonucleotides which carry two inverted copies of the 19-mer target sequence separated by a 9bp loop sequence to promote correct cleavage by the DICER nuclease and terminal overhangs to facilitate cloning between the *Bgl*III and *Hind*III sites of the pSUPER-retro vector. The A9-specific 64-mer oligonucleotides were annealed by heating a mixture of 3µg of each oligonucleotides to 95°C then cooling slowly to 4°C. The annealed oligonucleotides were then 5'-phosphorylated by treatment with Polynucleotide kinase (Promega) in the presence of 0.1mM ATP. After heat-inactivation of the enzyme, the annealed 64-mer duplex was ligated into *Bgl*III and *Hind*III digested pSUPER-retro and transferred into *E. coli* 'SURE 2' cells (Stratagene).

Plasmid DNA from single colonies were checked for inserts by restriction analysis with *Eco*RI and *Hind*III and positive clones were confirmed by DNA sequencing.

Three clones were selected for further study:

Clone 16, which had the expected sequence.

Clone 22, which had a single base substitution in the A9-specific stem.

Clone 31, which had a base substitution in the loop region.

These three constructs, plus pSUPER-retro vector with no insert were transfected into A9-CHO cells (as described in section 2.2.7). Stable puromycin-resistant cell lines were established from each transfection and RNA was isolated from these cultures (as described in section 2.4.1).

The influence of the pSUPER constructs was examined by northern blot analysis (as described in section 2.4.2).

4.2.7 FACS analysis of rabbit cells

Cells were washed and re-suspended in FACS wash buffer (2% (v/v) FBS, 0.05% (w/v) sodium azide in PBS) to a density of 5×10^5 /ml. In rounded-bottomed 96-well plates, cells were incubated with 50 μ l of the desired primary antibody (see table 4.2) prepared in FACS wash buffer for 30 mins on ice. The cells were centrifuged at 250 x g for 5 mins and the supernatant removed. The pellets were washed twice in FACS wash buffer. The fluorescein-isothiocyanate (FITC) conjugated secondary antibody (rabbit-anti-mouse, 1:50 in FACS wash buffer) (DAKO) was added to cells and mixed thoroughly. This mixture was incubated on ice for 30 mins in the dark. After a further two washes the cells were fixed in 1% (w/v) paraformaldehyde in wash buffer and transferred to FACS tubes (Falcon 2054, Becton Dickinson).

Data acquisition and analysis was performed with a two laser four-colour FACS Calibur flow cytometer and Cell Quest software (Becton Dickinson). 10,000 cells were acquired for each sample with linear amplification for forward (FWS) and side (SSC) scatter and logarithmic amplification for FITC green fluorescence (FL-1). Lymphocytes were distinguished on the basis of FWS/SSC profile. Small and large lymphocytes were distinguished on the basis of the FWS/SSC ratio.

Specificity	mAb	Specificity	Ref.
CD4	KEN-4	T cells/ helper cells	Kotani <i>et al.</i> , 1993
CD5	KEN-5	T cells & subset of B cells	Kotani <i>et al.</i> , 1993
CD8	12C7	T cells/cytotoxic cells	De Smet <i>et al.</i> , 1983
CD43	L11/135	All T cells	Jackson <i>et al.</i> , 1983
IgM	NRBM	B cells	
RLA-DR	RDR34	R-DR (Class II)	Spieker-Polet <i>et al.</i> , 1990

Table 4.2. Selected markers and their use.

4.3 Results

4.3.1 Expression of A9 gene in the lytic virus life cycle

The temporal pattern of ORF A9 expression during the infection of BT cells with or without cycloheximide or phosphonoacetic acid treatment was investigated by Northern blot analysis. Chemical inhibitors were used to establish the stage of the lytic cycle at which A9 gene expression occurred: immediate early (IE), early (E) or late (L).

Fig. 4.2A shows the result of Northern blot analysis with control GAPDH labelled probe. All the Northern RNA samples showed a GAPDH product. This indicated that the RNA samples were intact and the gel was loaded with equivalent amounts of RNA. Fig. 4.2B shows the results of Northern blot analysis with the A9 probe. A9 mRNA expression was detected as an early and late virus gene in cells infected with all three viruses. A9 is therefore expressed as an early-late gene but not as an immediate early gene in the life cycle of both of the attenuated viruses and the virulent C500 virus. The uninfected control cells did not show any expression at any of the time points.

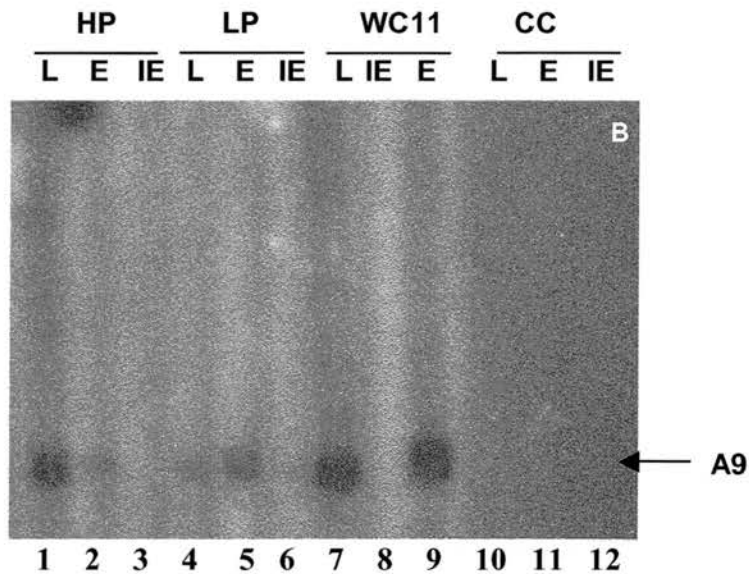
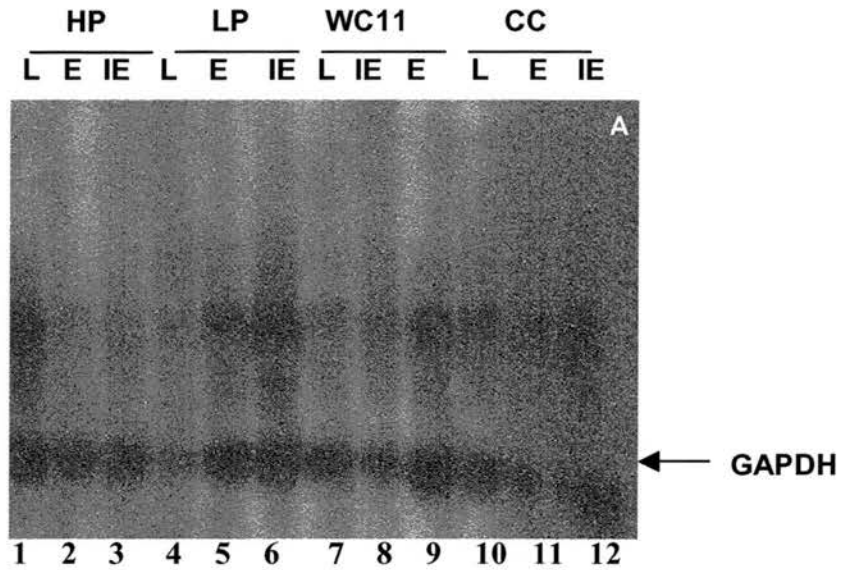


Fig. 4.2. Northern blot analysis of GAPDH and ORF A9 expression. RNA samples were obtained from BT cells infected with high passage (HP) C500 cell-free and attenuated AIHV-1, Low passage (LP) C500 cell-associated and virulent AIHV-1 and WC11 cell-free and attenuated AIHV-1. Cell controls (CC) were treated with chemical inhibitors but not infected with virus. **1:** HP Late. **2:** HP Early. **3:** HP Immediate early. **4:** LP Late. **5:** LP Early. **6:** LP Immediate early. **7:** WC11 Late. **8:** WC11 Immediate early. **9:** WC11 Early. **10:** CC Late. **11:** CC Early. **12:** CC Immediate early. **A:** Northern blot probed with a GAPDH probe. **B:** Northern blot probed with A9 probe. Immediate early mRNA expressed in the presence of cycloheximide. Early mRNA in presence of phosphonoacetic acid, late mRNA no chemical inhibitors.

4.3.2 Cellular localisation of the A9 protein

To determine the cellular localisation of the A9 protein, A9-CHO cells were used. The A9-CHO cells were transiently transfected with mtGFP and the cells were harvested after 24 hrs. mtGFP uses a fragment that encodes for the precursor of subunit VIII of cytochrome c oxidase that targets the mitochondria. Therefore, once transfected into cells, should target the mitochondria (Rizzuto et al., 1995). In this assay mtGFP protein displayed a fluorescence signal in both the nucleus and mitochondria (fig. 4.3). However this signal was significantly higher in the nucleus. This pattern of distribution was not consistent with the localisation that is normally observed with mitochondrial staining. The faint staining in the cytoplasm is possibly consistent with mitochondrial localisation however, due to the high fluorescence observed in the nucleus it is difficult to draw definite conclusions. The cells were also incubated with either anti-A9 rabbit polyclonal (162) (fig 4.3 A&B) or normal rabbit serum (Fig 4.3 C&D). Staining with the anti-A9 antibody was dispersed throughout the cytoplasm but seemed brighter in the cytoplasm. When the A9-CHO cells were incubated with a control normal rabbit serum, a uniform background was observed that was less intense in comparison to the cells incubated with the anti-A9 antibody (fig. 4.3 C&D). Fig 4.3B was further analysed shown in fig 4.4.

As shown in fig. 4.4B A9 vBcl-2 (red fluorescence) is seen throughout the cytoplasmic region of the cells and higher fluorescence is not visible in any particular region. A proportion of the mtGFP transfected cells express mtGFP (green fluorescence) following transient transfection (fig 4.4A). There is strong staining in the nucleus but no staining of mitochondria from mtGFP. Fig.4.4D shows some co-localisation of mtGFP with anti-A9, however as staining with the anti-A9 antibody is observed throughout the cell and the mtGFP localises to the nucleus, it is not possible to conclude that A9vBcl-2 is co-localising with the mitochondrial marker. These results indicate that further work needs to be carried out to determine whether the A9 protein localises in the mitochondria and pro-apoptotic signals influence the localisation.

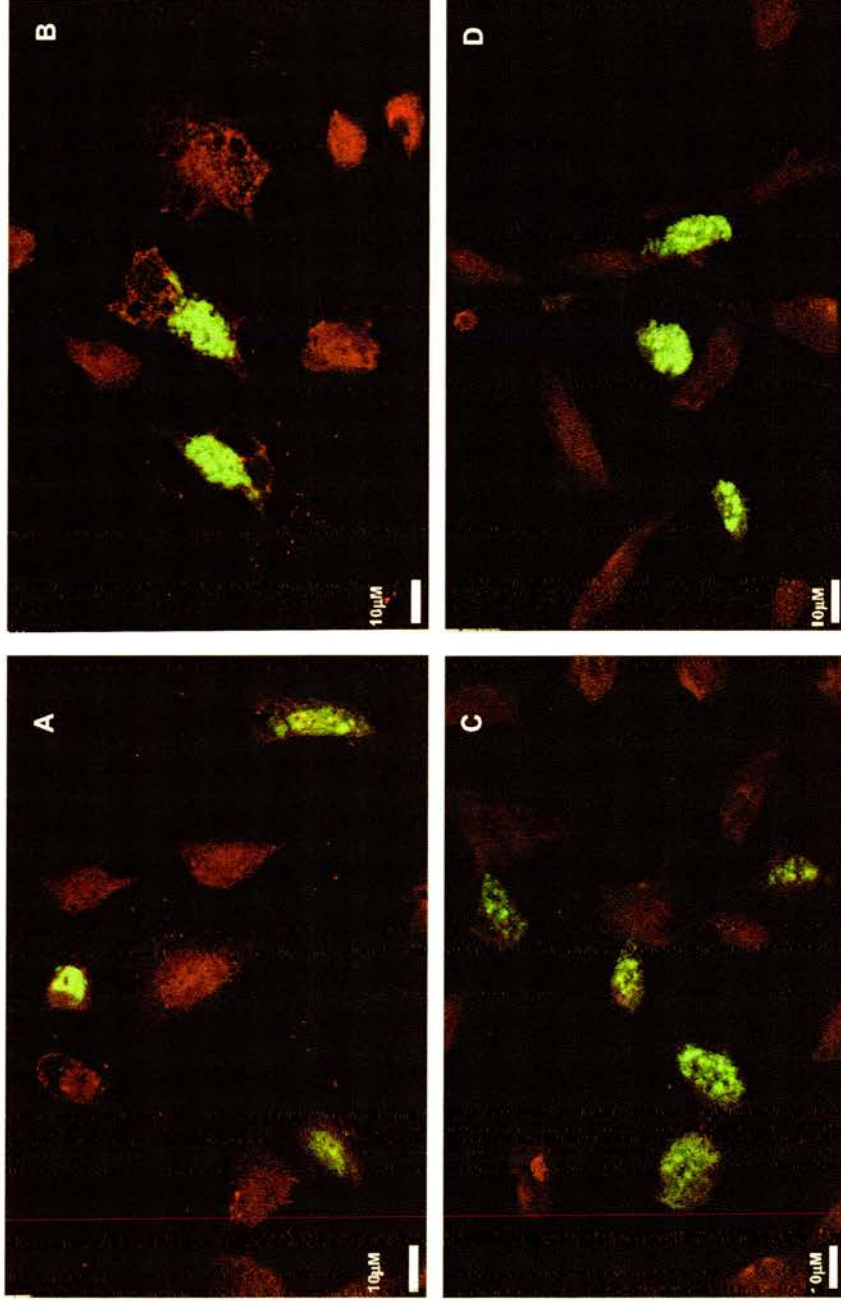


Fig 4.3. Confocal microscopy images of A9-CHO cells. A9-CHO cells were transiently-transfected with mtGFP, fixed with ice-cold acetone and immunofluorescence analysed using anti-A9 rabbit antibody (1:500) or normal rabbit serum (1:1000), followed by a secondary anti-rabbit-TRITC (1:500). **(A) & (B)** Cells incubated with anti-A9 rabbit antibody. **(C) & (D)** Cells incubated with normal rabbit serum. Green fluorescence indicates mtGFP labelling. Red fluorescence indicates TRITC labelling.

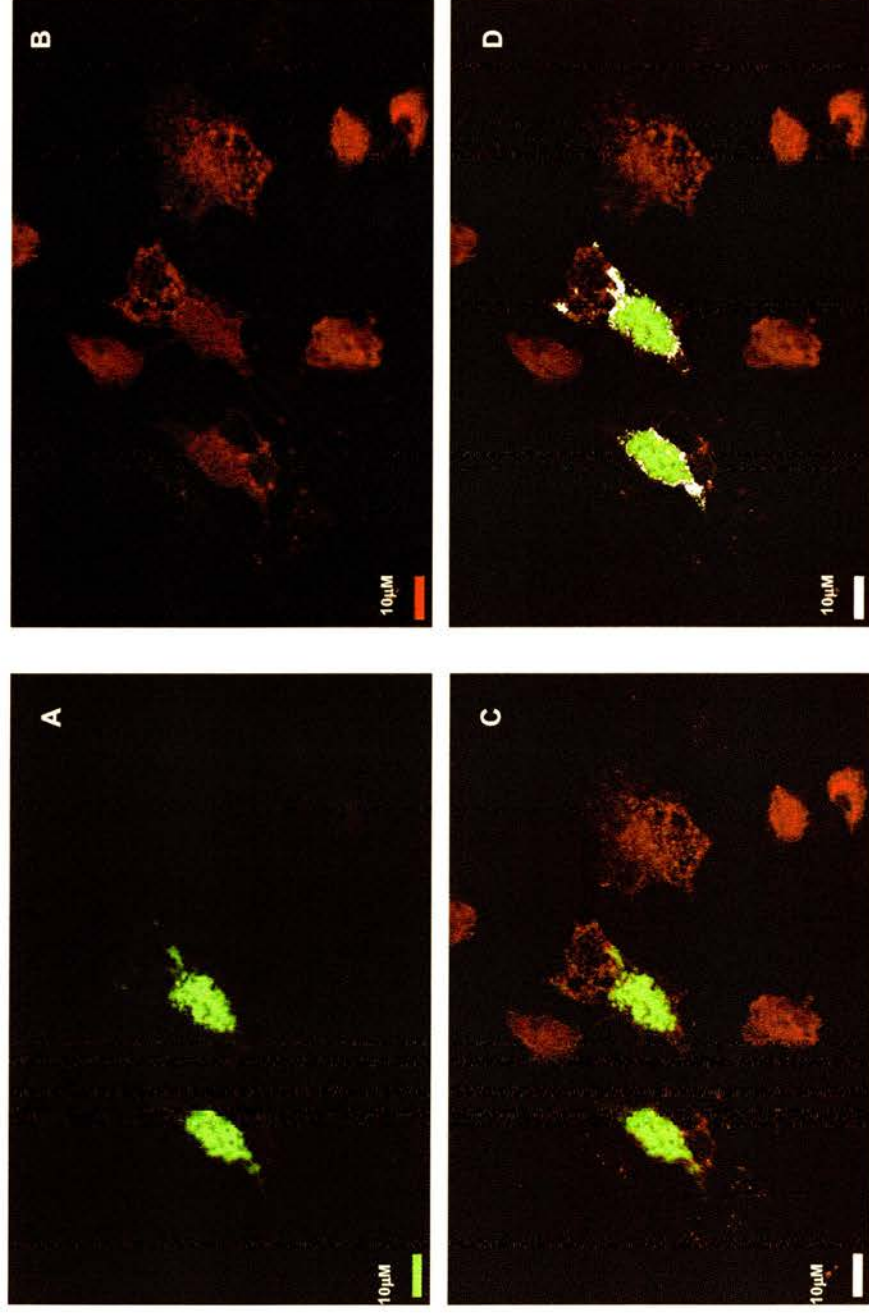


Fig. 4.4. Cellular localisation of A9. A9-CHO cells were transiently transfected with mtGFP, fixed with ice-cold acetone and subjected to immunofluorescence analysis using anti-A9 rabbit antibody (1:500) followed by a secondary anti-rabbit-TRITC (1:50).

A: mtGFP fluorescence.

B: Staining with anti-A9 antibody.

C: mtGFP and anti-A9 images overlapped.

D: Co-localisation of mtGFP and A9 (white shading shows areas of co-localisation). Green fluorescence indicates mtGFP labelling. Red fluorescence indicates anti-A9 labelling.

4.3.3 Phenotypic analysis of AIHV-1 LGL T cells

A rabbit was infected with AIHV-1 C500 HP and the LGL cell line BJ2590 was established (see section 2.2.1) and phenotyped by FACS analysis (see section 4.2.7). Lymphoid tissue was also taken from an uninfected rabbit and cells cultured from this (referred to as uninfected lymphocyte cells (ULC)). ULC were used as control cells and phenotyped by FACS analysis.

The results (table 4.3) show the phenotype of the cell culture at day 6, when A9 is expressed and day 56 of culture when the cell line has been established. ULC phenotype analyses of around the same days have also been shown.

The phenotypic analysis of the rabbit cell line was determined using a number of anti-rabbit CD antibodies (summarised in table 4.2). Cells were characterised with monoclonal antibodies against CD4 (thymocytes and helper/inducer T-cell subset), CD5 (T-cells and a subset of B-cells), CD8 (thymocytes and cytotoxic/suppressor T-cell subset), CD43 (T-cells) rabbit IgM (B cells) and D-related rabbit leukocyte antigen (RLA-DR) (rabbit MHC II DR alpha and beta chains).

The results of the phenotype analysis are summarised in table 4.3. None of the cells expressed surface IgM indicating that none of the cells phenotyped were B cells. At day 6 of culture of the lymphoid tissue the cell line BJ2590 were CD4⁻ (98%), CD5⁺ (98%), CD8⁺ (85%) and CD43⁺ (99%). Cells expressed RLA-DR (98%) indicating that these T cells were activated. Once the cell line BJ2590 had been established in culture these cells were still CD4⁻ (99%), CD5⁺ (93%), CD8⁺ (83%) and CD43⁺ (86%). Cells still expressed RLA-DR (73%) indicating that these were activated T cells.

The ULC line at day 6 of culture was CD4⁻ (>99%), CD5⁻ (<1%) and CD43⁺ (94%). A proportion (12%) of the cells were CD8⁺. However the cells were RLA-DR⁻ indicating that these were not activated T cells. Once the ULC had been established at day 59 these cells were CD4⁻ (>99%), CD5⁻ (>99%) and RLA-DR⁻ (>99%). A proportion of the cells were CD8⁺ (6%) and CD43⁺ (63%). The results presented here show that the cell line BJ2590 had T cell phenotype. Some sample FACS profiles are illustrated in fig 4.5.

Cell line	Day in culture	CD5 (%)	CD8 (%)	CD4 (%)	CD43 (%)	RLA-DR (%)	μ -chain
BJ2590	6	98	85	2	99	98	<1
BJ2590	56	93	83	1	86	73	<1
ULC	6	<1	12	<1	94	<1	<1
ULC	59	<1	6	<1	63	<1	<1

Table 4.3. Detection of cell surface markers on rabbit MCF cell lines. BJ2590 is an established cell line from an AIHV-1-infected rabbit. Uninfected lymphoid cell (ULC) line was established from lymphoid tissues taken from a uninfected healthy rabbit.

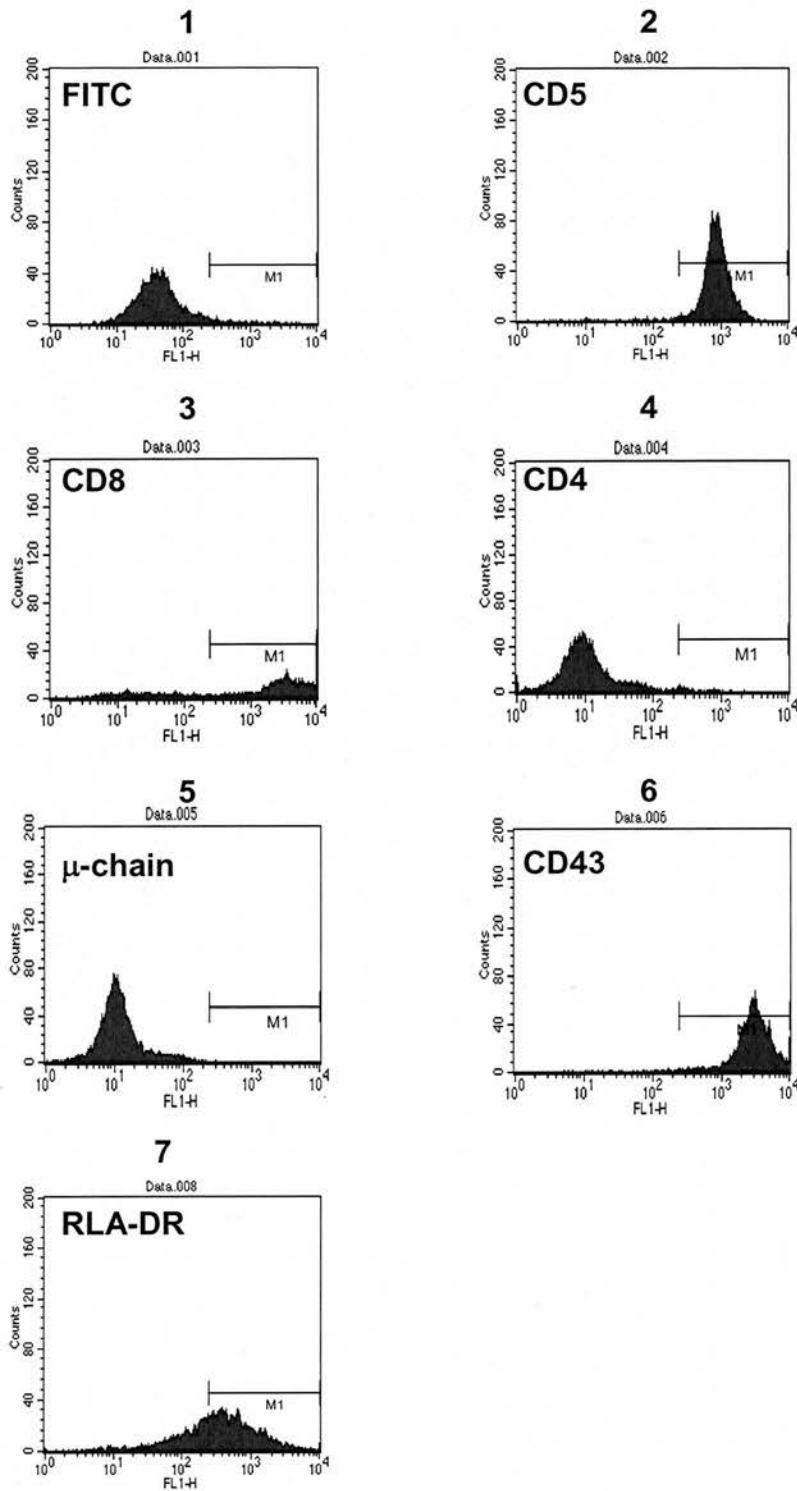


Fig 4.5. FACS profile for rabbit LGL cell line BJ2590 (day 6 of culture of lymphoid tissue).
1) FITC conjugate alone. 2) anti-CD5. 3) anti-CD8. 4) anti-CD4. 5) anti- μ chain. 6) anti-CD43. 7) anti-RLA-DR.

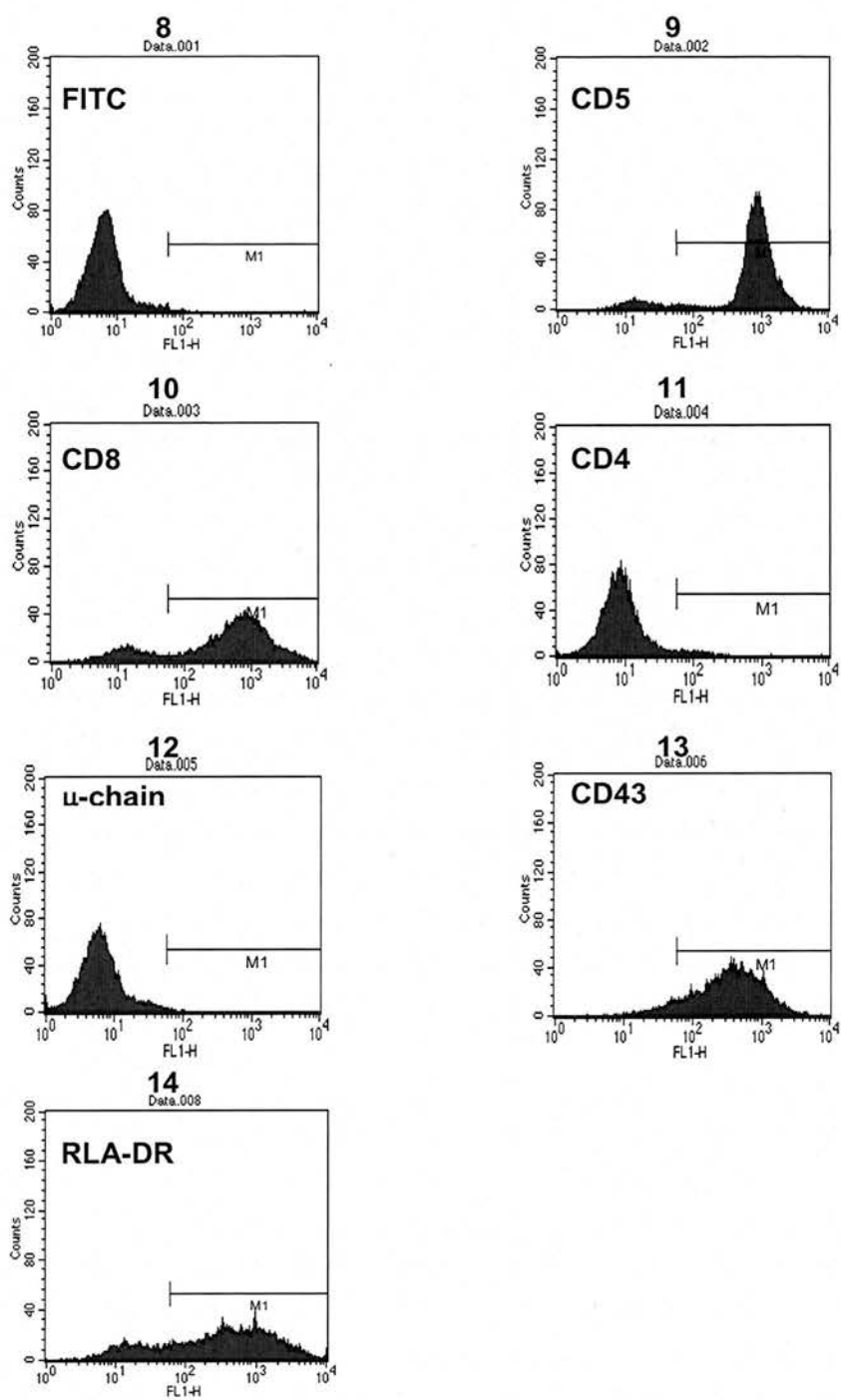


Fig 4.5 (continued): FACS profile for rabbit LGL cell line BJ2590 (day 56 of culture of lymphoid tissue).
 8) FITC conjugate alone. 9) anti-CD5. 10) anti-CD8. 11) anti-CD4. 12) anti-m chain. 13) anti-CD43. 14) anti-RLA-DR.

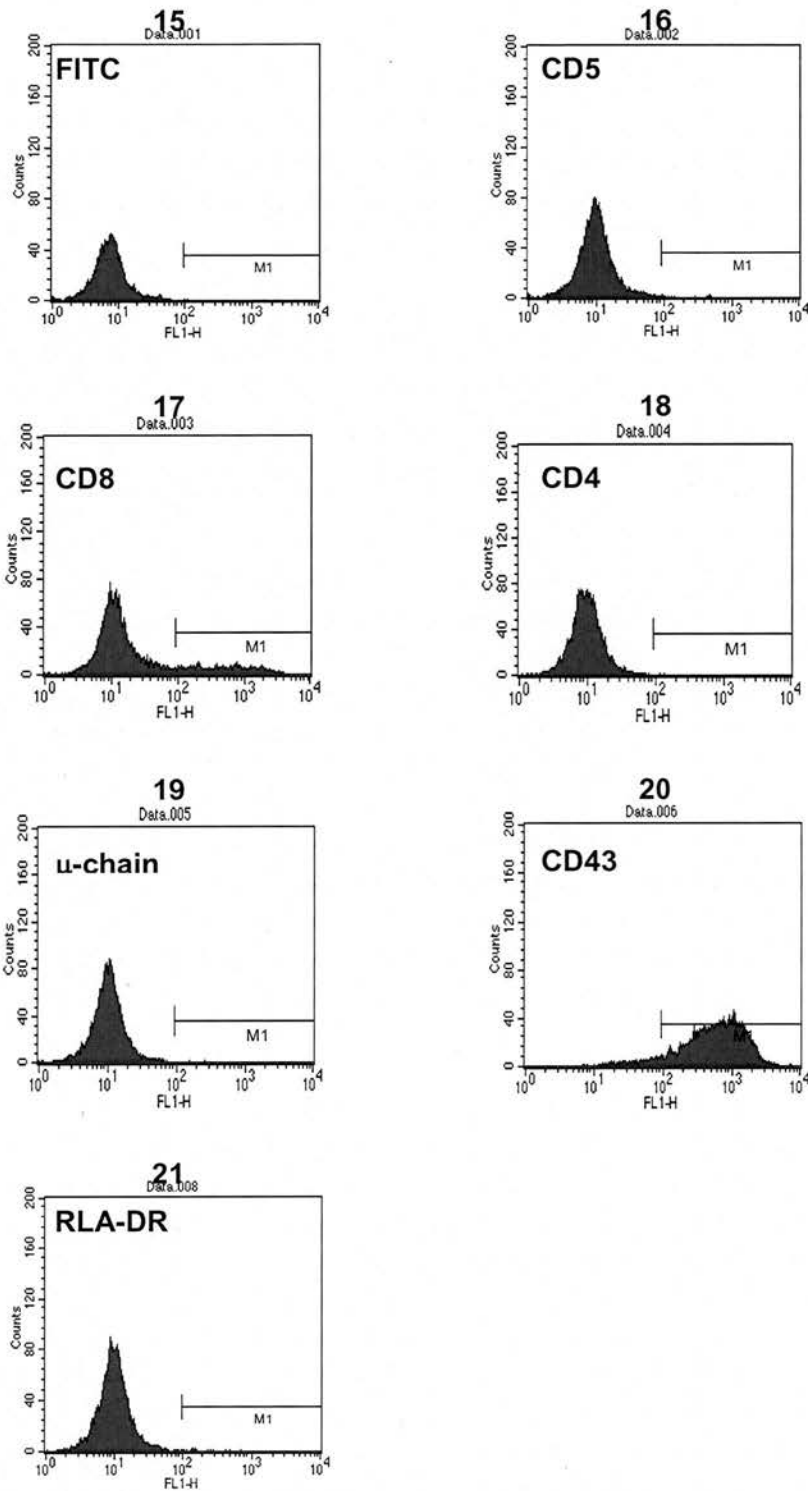


Fig 4.5 (continued): FACS profile for uninfected rabbit LGL cell line (day 6 of culture of lymphoid tissue).

15) FITC conjugate alone. **16)** anti-CD5. **17)** anti-CD8. **18)** anti-CD4. **19)** anti-m chain. **20)** anti-CD43. **21)** anti-RLA-DR.

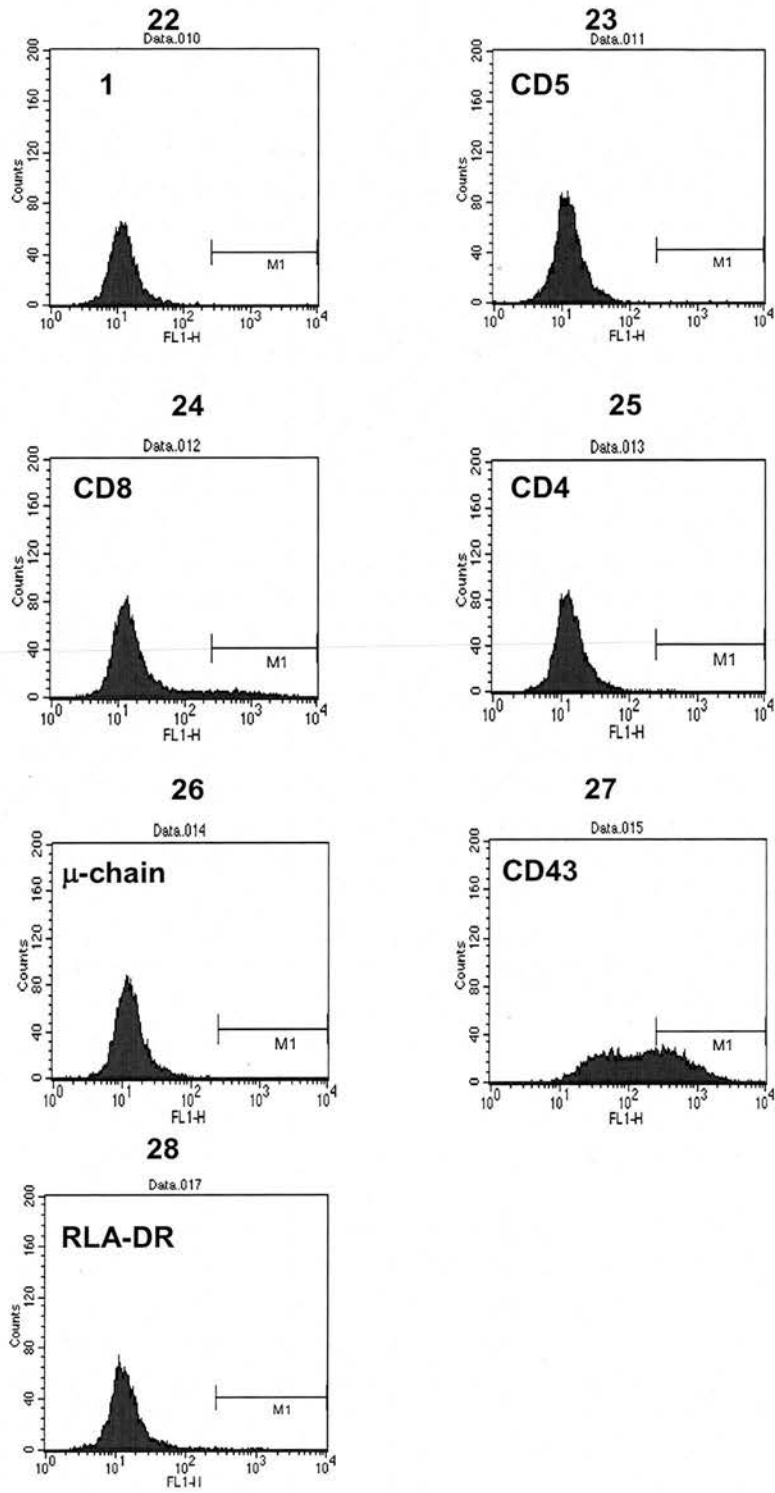


Fig 4.5 (continued): FACS profile for uninfected rabbit LGL cell line (day 59 of culture of lymphoid tissue).

22) FITC conjugate alone. **23)** anti-CD5. **24)** anti-CD8. **25)** anti-CD4. **26)** anti-m chain. **27)** anti-CD43. **28)** anti-RLA-DR.

4.3.4 Expression of A9 gene in LGL cell lines

To determine if the A9 gene was expressed in AIHV-1-infected LGLs produced as a consequence of viral infection, RNA was extracted from the LGL cell line BJ2590 and subjected to RT-PCR analysis.

Fig. 4.6 shows the results of RT-PCR analysis with GAPDH primers. All RT-PCR samples exhibited a 950bp GAPDH product. Water was used as a negative control and it did not show any product. This indicated that the RNA samples were intact and that the reverse transcriptase reactions had worked.

Fig. 4.7 shows the results of RT-PCR analysis with A9 primers. A 500bp product corresponding to the A9 gene was detected in samples from day 4, 8 and 13 of culture of lymphoid tissue but not thereafter. To determine that there was no contaminating viral DNA present in the samples, PCR using A9 specific primers was carried out on the RNA samples without prior RT treatment (fig 4.7, lanes 9-12).

This suggests that A9 is expressed in LGL cell lines at an early stage of LGL establishment in culture of lymphoid tissue from MCF-affected rabbits.

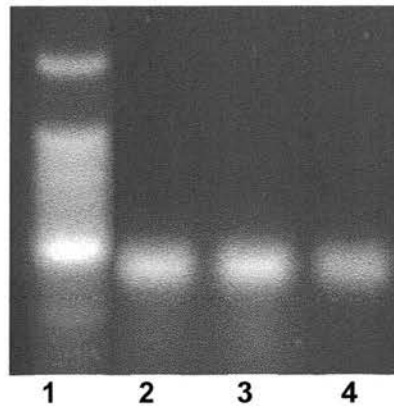


Fig. 4.6. RT-PCR GAPDH-specific primers. RNA was obtained from AIHV-1-infected LGLs at various time points after initiation of cultures. **1:** Markers. **2:** AIHV-1-infected LGLs day 4. **3:** AIHV-1-infected LGLs, day 8. **4:** AIHV-1-infected LGLs day 13.

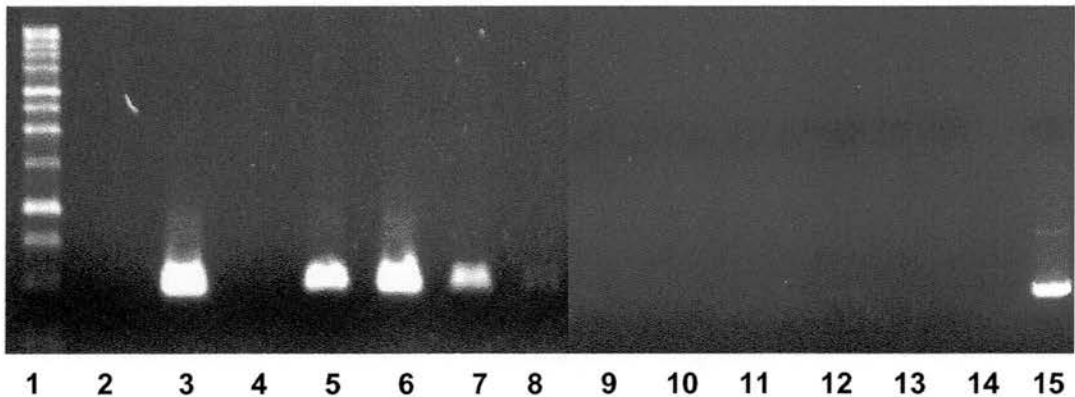


Fig. 4.7. RT-PCR analysis using ORF A9 specific primers. RNA samples were obtained from AIHV-1-infected LGLs. **1:** 1kb marker. **2:** Water. **3:** ORF A9 positive DNA. **4:** Uninfected lymphoid cells. **5:** AIHV-1-infected LGL day 4. **6:** AIHV-1-infected LGL day 8. **7:** AIHV-1-infected LGL day 13. **8:** AIHV-1-infected LGLs day 21. **9:** RT -ve AIHV-1-infected LGL day 4. **10:** RT -ve AIHV-1-infected LGL day 8. **11:** RT -ve AIHV-1-infected LGL day 13. **12:** RT -ve AIHV-1-infected LGLs day 21. **13:** Water. **14:** Negative (no primer). **15:** ORF A9 DNA.

4.3.5 Immunofluorescence analysis of A9 expression in AIHV-1-infected LGL T cell lines.

To detect expression of A9 protein in AIHV-1-infected rabbit LGL T cells, anti-A9 rabbit polyclonal antibody, 163, was used in immunofluorescence studies on acetone-fixed cytocentrifuged preparations. Immunofluorescence analysis was carried out on cells taken at day 6 of culture as these had been shown to express the A9 gene by RT-PCR analysis.

Immunofluorescence analysis using the rabbit polyclonal antibody showed positive fluorescence in a proportion of the cells (fig. 4.8A), which was brighter than that seen in assays using AIHV-1 infected LGLs stained with normal rabbit serum (fig. 4.8B). However, a similar level of fluorescence was observed in control uninfected cells stained with normal rabbit serum (fig. 4.8D). These results may indicate that the expression of A9 is at a low level, which is difficult to detect. More work is required to further clarify this and to show whether A9 expression could be detected in AIHV-1 infected LGLs using the anti-A9 antibody.

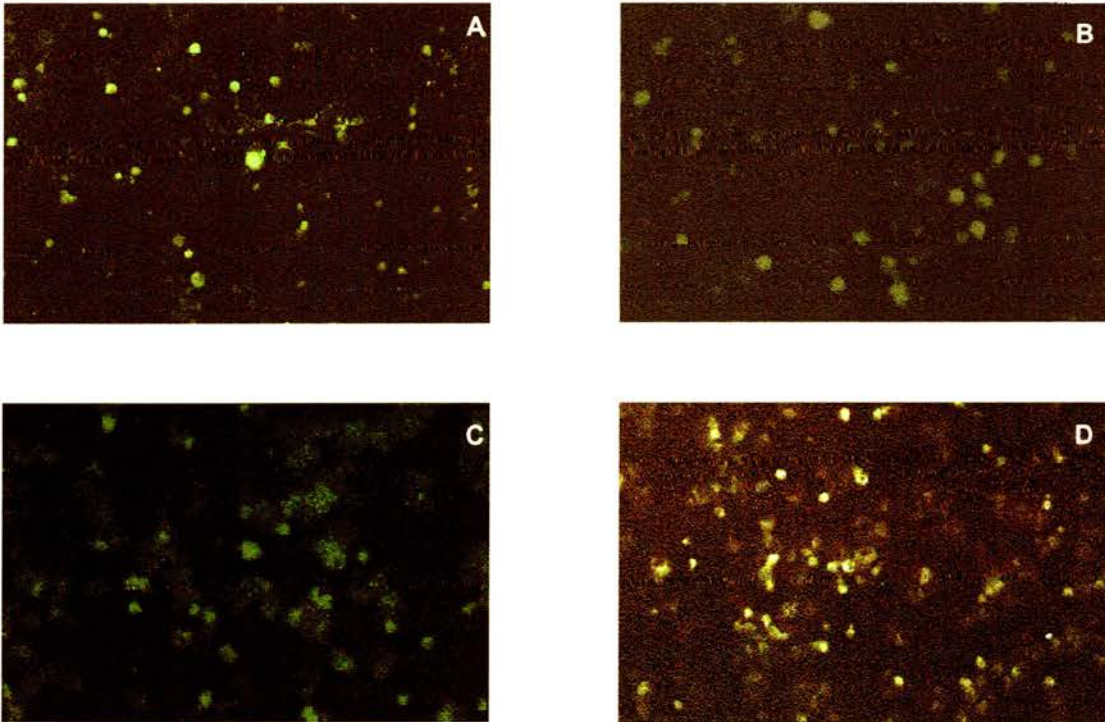


Fig. 4.8. Immunofluorescence analysis of LGL T cells. (All pictures taken with the same exposure time, x 400 magnification). Cells were fixed using ice cold acetone and incubated with the appropriate primary antibody followed by incubation with anti-rabbit biotin conjugate (1:500) and finally incubated with streptavidin-FITC (1:75).

A: AIHV-1-infected LGL incubated with anti-A9 rabbit polyclonal antibody (163) (1:500).

B: AIHV-1 infected LGL's incubated with normal rabbit serum (1:1000).

C: Uninfected lymphoid cells incubated with anti-A9 rabbit polyclonal antibody (163) (1:500).

D: Uninfected lymphoid cells incubated with normal rabbit serum (1:1000).

4.3.6. Attempts to silence the A9 gene by RNA interference

In order to determine whether the expression of A9 in A9-CHO cells could be inhibited, co-stable transfection of A9-specific siRNA was attempted.

The siRNA was produced as described in section 4.2.6. There were four constructs used in this study. There were:

Construct 16: Correct sequence

Construct 22: Had a single base substitution in the A9-specific stem.

Construct 31: had a base substitution in the loop region.

pSUPER empty vector

Fig. 4.9 shows the results of northern blot analysis with an A9 probe on A9-CHO cells that had been transfected with A9-specific siRNA constructs. A9 mRNA expression was detected in all of the transfected A9-CHO cell lines indicating that the mRNA expression has not been diminished by siRNA. A9 mRNA expression was not reduced in the presence of the correct sequence siRNA or in any of the mutated siRNA oligonucleotides. The blot was analysed quantitatively using a phosphor imager (Amersham) to examine if there were any differences in the signal between any of the cell lines. However there was no obvious correlation between the construct that had been transfected with the siRNA and A9-CHO cells.

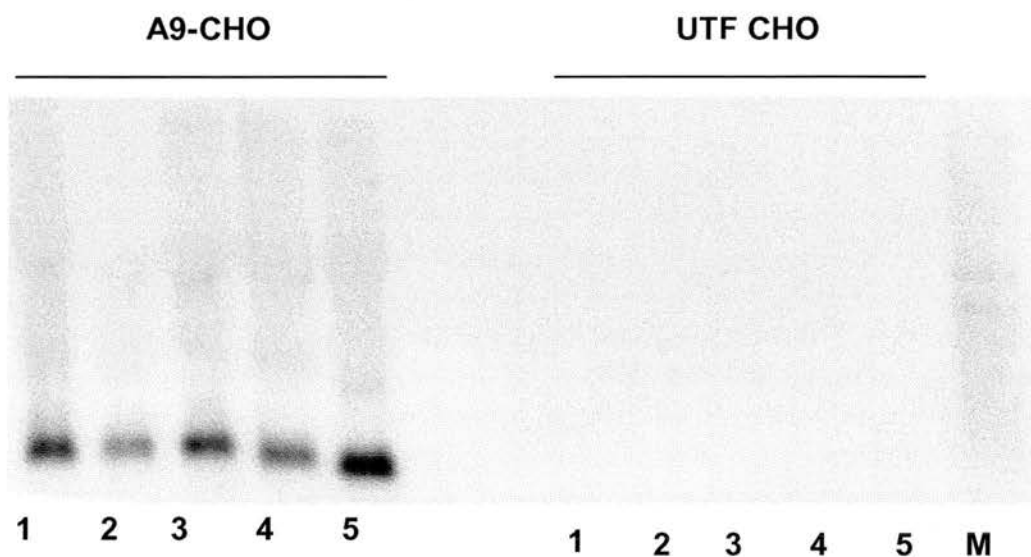


Fig. 4.9. Northern blot analysis of RNA interference of A9 expression. RNA was extracted from UTF and A9-CHO cells. **1:** Construct 31, mutated loop region **2:** Construct 22, mutated A9-specific stem. **3:** Construct 16, expected sequence. **4:** pSUPER empty vector. **5:** CHO cells not transfected with pSuper vector. **M:** RNA markers.

4.4 Discussion

ORF A9 mRNA was expressed as an early through to late viral gene but not as an immediate early gene during the productive phase of the virus life cycle in AIHV-1-infected BT cells. This was the case with all three virus isolates tested, C500 low passage cell-associated and virulent, C500 high passage cell-free and attenuated and WC11 cell-free and attenuated.

The C500 strain of the virus was first isolated from an infected ox with MCF (Plowright *et al.*, 1975). The virus when initially cultured is virulent and cell-associated, however after prolonged passage in culture the virus becomes attenuated and cell-free. This switch from cell-associated to cell free is associated with a loss of pathogenicity for cattle and rabbits (i.e. the disease is not induced. The loss of pathogenicity is due to genome re-arrangement (Wright *et al.*, 2003). There are two genes that are probably affected by the re-arrangement, these are ORF 50 and ORF A6. Others that may also be affected are ORF 48 and A7. In OvHV-2 the O7 homologue encodes a virus glycoprotein therefore it would seem likely that A7 encodes a virus glycoprotein (Wright *et al.*, 2003). This study has demonstrated that although the genome is re-arranged the A9 gene is still expressed. The re-arrangement of the C500 genome does not bring about any changes in the position of the A9 gene or the surrounding genes. This would therefore suggest that A9 is not involved in the pathogenesis of the disease as it is expressed in both the cell-associated and virulent strain and the cell-free and attenuated strain.

This result is consistent with similar studies with other gammaherpesviruses. The MHV-68 ORF M11 vBcl-2 transcript was observed in mouse fibroblast cells where expression was inhibited by cycloheximide treatment but not by phosphonoacetic acid. Therefore it is also an early-late expressed viral gene in the productive phase of the virus life cycle (Roy *et al.*, 2000). The Bcl-2 homologue that is present in KSHV is an early gene in the lytic life cycle (Sun *et al.*, 1999). Early genes generally encode for factors that are required for virus replication. This would suggest that the Bcl-2 homologue is required for virus replication and the establishment of the productive virus life cycle. The latent life cycle has not been defined in MCF viruses therefore no study can be performed to define this at the present time.

A LGL cell line was established from an AIHV-1-infected rabbit. Previous studies have demonstrated these cells to be predominantly T cells based on the presence of cell surface antigens CD4, CD5 and CD8 (Burrells & Reid, 1991; Schock *et al.*, 1998). In this study the cell line BJ2590 was CD4⁻, CD5⁺, CD8⁺ and CD43⁺. This work is in agreement with previous phenotypic work carried out on experimentally infected rabbit LGL cell lines (Reid *et al.*, 1983; Schock & Reid, 1996, Swa *et al.*, 2001). The absence of surface IgM suggests that this culture did not contain B cells.

The AIHV-1 infected LGL cell line established in this study exhibited the morphology of large granular T lymphocytes. They are not B cells as they are IgM negative. The cell line had a cytotoxic cell phenotype and expressed virus genes. These aspects are common features of all LGL cell lines (Swa, 2001).

ORF A9 mRNA was found to be expressed on days 4, 8 and 13 of LGL establishment in culture. However, it was not identified after day 13 in the cells used in this study. This is in contrast with earlier work (carried out at the Moredun Research Institute- Harry Wright, unpublished data), which found that ORF A9 mRNA was expressed 2-3 months after the establishment of two AIHV-1-infected LGL T cell lines (H. Wright, personal communication). It is possible that A9 is required at certain stages of the virus life cycle and this differs amongst cell populations. For example, the A9 gene product appears from the BT study to be required for the establishment of the lytic cycle and may not be required once the lytic phase of the virus cycle is established. The replicative state of the virus in the LGL is unknown and the latent state of the virus is not well characterised in MCF viruses. By examining the latent state of the virus it may lead to a better understanding of the LGLs and their role.

The results of the immunofluorescence assay did not show conclusively whether A9 was expressed at the protein level in AIHV-1 infected LGL cultures at day 6. This may have been due to the level of expression in the LGL cell lines or that the technique needed to be further optimised for the antibodies and cell lines used. This was not possible due to time constraints. It is also possible that the antibodies and cell lines used in this assay derived from the same species, therefore this could lead to a higher background fluorescence being observed. The high

background fluorescence observed could be a reflection of this use of rabbit antibodies with rabbit derived cell lines. Another factor to be considered is the cells are a mixed population at this timepoint therefore the level of expression of the virally infected LGL may be low. A possible alternative to the immunofluorescence assay could be the use of FACS analysis using the anti-A9 antibody, this would possibly give a quantitative result of the expression of A9 at a protein level. The detection, by RT-PCR, of A9 mRNA in AIHV-1-infected LGL T cells at the same stage, supports the view that the A9 gene is likely to be expressed in LGLs. In previous studies, LGL T cell lines have been shown to contain both viral DNA and protein (Swa, 2001) ORF 50, A6 and A7 were found to be expressed at low levels. These three genes encode viral transactivators and a viral glycoprotein suggesting that replicating virus was likely to be present. More recently, OvHV-2-infected LGL T cells from rabbits were shown to contain genome structures characteristic of both latently-infected cells and cells with virus undergoing productive replication (Rosbottom *et al.*, 2002). It could therefore be possible that in AIHV-1-infected LGL T cells, the virus may be latent in some cells and undergoing a lytic phase of the virus life cycle in others. Thus A9 may be expressed in a small proportion of the LGL population, especially if its expression were restricted to the lytic phase. This remains to be determined.

The co-localisation assay carried out in this study did not conclusively reveal the localisation of the A9 gene product. The transfection of mtGFP into the A9-CHO cells displayed labelling of the nucleus of some cells. The mtGFP construct uses a fragment encoding the amino-terminal of the precursor of subunit VIII of cytochrome c oxidase (COX) (Rizzuto *et al.*, 1995). COX catalyses the transfer of electrons from cytochrome c to dioxygen, which is coupled to the translocation of protons across the inner mitochondrial membrane (Ferguson-Miller & Babcock, 1996). In mammals the enzyme consists of 13 subunits per COX monomer, of which three are mitochondrial and ten are nuclear coded (Grossman & Lomax, 1997). When expressed in HeLa cells the mtGFP fusion protein was confined to the mitochondria (Rizzuto *et al.*, 1995). However, in this study CHO cells were used and it is possible that the localisation of mtGFP in these cells did not match that observed in HeLa cells. Therefore, further analysis will be needed to define the

cellular localisation of A9. This could be carried out using another mitochondrial marker such as Mitotracker that has been shown to localise in the mitochondria of CHO cells (Khodjakov *et al.*, 1998).

The vBcl-2 homologue present in EBV (BHRF1) also localised to the mitochondria in EBV genome-positive cell lines (Hickish *et al.*, 1994). Similarly the adenovirus protein E1B19K, that possesses homology to Bcl-2, localised to mitochondria (Perez & White, 2000). The fact that other viral Bcl-2 homologues localise to the mitochondria suggests that the A9 protein may also localise in this organelle. Localisation of A9 may involve its association with other viral or host proteins, either constitutively or following some stimulus. The CHO transfectant system used here may not have provided the correct binding partners for the stimulus to induce localisation. However, further is required to clarify this. If A9 was associated with the mitochondria cells infected with AIHV-1 it might be bind to pro-apoptotic Bcl-2 proteins, preventing them from inserting into the mitochondria and allowing the virus to establish a productive life cycle by extending the life of the target cells.

An initial experiment was carried out to silence the A9 gene in A9-CHO by RNA interference showed no decrease in A9 expression. The reasons for this could be that the siRNA sequence may not be optimal for significant interference with A9-expression. This could be due to features of the siRNA duplex- its processing from the pSUPER transcript, its sensitivity to other nuclease or its ability to activate the silencing complex.

Alternatively the target site of the A9 RNA may not be accessible due to secondary structure or there may be other sequence-based factors required for efficient gene silencing.

There may also have been problems with the transfection and/or expression of the retroviral pSUPER constructs, as the transcription of the hairpin RNA was not assayed in these cells.

The main reason for the lack of RNA silencing is that only a single siRNA molecule was tested in the study. The current opinion in this field is that more than one siRNA molecule is required. However, the design system that was used to generate target sequences only selected one sequence.

However, colleagues in the laboratory are currently developing this technique.

In conclusion this study has demonstrated that A9 is expressed as an early through to late viral gene. It has also shown that at RNA level A9 is expressed at day 6 in culture in virally infected LGLs.

Chapter 5

The apoptotic function of ORF A9 encoding protein

5.1 Introduction

In order to survive within the host, viruses often have to evade the host immune response. Following infection with a virus, cells can enter the apoptotic pathway as a means of limiting virus replication. In addition, one mechanism by which cytotoxic T lymphocytes and natural killer cells kill virus-infected cells is by inducing apoptosis via secretion of cytokines such as TNF, the release of perforin and granzymes or the activation of Fas in the target cell (reviewed in Alcami & Koszinowski, 2000). Many viruses inhibit apoptosis by deploying mechanisms such as inhibiting Fas or TNF receptor pathways or expressing caspase inhibitors, IAP proteins and anti-apoptotic Bcl-2 homologues.

In this study the main objective was to determine if A9 vBcl-2 had anti-apoptotic properties, by observing whether A9-CHO cells were protected after delivery of an apoptotic stimulus (cis-platin).

CHO cells expressing EBV BHRF1 (BHRF1-CHO) were used as a positive control. EBV BHRF1 has been shown to protect human epithelial cells from cis-platin induced apoptosis (Khanim *et al.*, 1997). As a transfection control, CHO cells containing an inactive ovine interferon gamma gene (IFN γ) were used. The transfected cell line does not express IFN- γ (for the remainder of this study it will be referred to as control CHO) (Graham *et al.*, 1995). Finally, untransfected (UTF) CHO cells were used as a second negative control. A9 cDNA-transfected CHO cells (A9-CHO) were used in the apoptosis assays and immunofluorescence assays.

To determine the percentage of CHO cells expressing BHRF1 or A9, immunofluorescence analysis was carried out using the anti-BHRF1 mouse antibody and the anti-A9 rabbit antibody respectively (as described in section 3.3.9 and 3.3.10).

There are several assays available to determine if cells are undergoing apoptosis. These include determining the morphology of the cell, DNA fragmentation, assays of the activity of apoptotic pathway enzymes and flow cytometry to identify changes in cell DNA content (Chiarugi *et al.*, 2002). The assays that will be used in this study analyse the activity of the apoptotic enzyme caspase-3, changes in cell morphology and DNA fragmentation.

“Diff-quick” (Dade Behring) staining allows a quick and simple method to identify morphological changes that arise due to apoptosis. The cells are stained with the Diff-quick reagents. Staining allows changes in cell morphology to be observed by light microscopy. In ‘healthy’ cells the nucleus has a dark appearance with the cytoplasmic region lightly stained. However, in apoptotic cells the overall staining of the cell is visibly darker.

DNA fragmentation occurs during apoptosis due to the activation of specific endonucleases that cut DNA between nucleosomes. The DNA can be extracted from the cells and its fragmentation is analysed by agarose gel electrophoresis. In apoptotic cells typical ‘DNA-laddering’ is observed. This assay was chosen as it is a simple assay that gives a clear qualitative indication of apoptosis.

The final assay chosen was the caspase-3 assay. As described in chapter 1 (section 1.5.2) caspase-3 is an executioner caspase that once cleaved and activated initiates apoptosis. Caspase-3 is activated as a result of the cleavage of inactive pro-caspase-3, caspase-9 or caspase-8. Caspase-9 is activated as a result of the formation of the apoptosome complex, while caspase-8 is activated following FADD activation.

The caspase 3 assay uses the caspase-3 fluorogenic substrate N-Acetyl-Asp-Glu-Val-Asp-7-amido-4-methylcoumarin (Ac-DEVD-AMC) that can be used to identify and quantify caspase-3 activity. Caspase-3 cleaves after the tetrapeptide, releasing the fluorescent AMC, which can be quantified in cell lysates by ultraviolet spectrofluorometry. Apoptotic cell lysates will contain an active caspase-3 yield with a high emission in comparison to non-apoptotic cell lysates. The assay was chosen as it gives a quantitative indication of an early stage of apoptosis.

The cytotoxic drug cis-diamminedichloroplatinum II (cis-platin) has been successfully used to induce apoptosis in CHO cells in other studies (Khanim *et al.*, 1997). Thus, cis-platin was used in this study to induce apoptosis. The specific mechanisms that activate an apoptotic response to cis-platin are not well characterised. However, it is thought that cis-platin damages the DNA. This in turn leads to the induction of the p53 apoptosis system which involves mitochondrial apoptosis and the Bcl-2 family of proteins (Jamieson & Lippard, 1999).

5.2 Materials and Methods

5.2.1 Cells used

CHO cell lines were used throughout this study. UTF (negative control), CHO cells transfected with an inactive ovine IFN γ gene (control CHO) (Graham *et al.*, 1995), CHO cells transfected with EBV BHRF1 (BHRF1-CHO, positive control) and CHO cells transfected with A9 cDNA (A9-CHO). All cells were maintained in GMEM supplemented with 7.5% (v/v) dFBS. Prior to the induction of apoptosis the serum concentration was reduced to 2% (v/v). Apoptosis was induced as described in section 2.8.2. Briefly the various CHO cell lines were incubated with 25 μ M of cis-platin with for 3 hrs. The media was removed and fresh media was added. Cells were analysed 24, 48 and 72 hrs after treatment with cis-platin.

5.2.2 Viability assay

The assay was set up in 35mm² petri dishes; at a concentration of 3×10^5 cells/ml with 1.5ml of cell suspension being added to each petri dish. UTF CHO cells and A9-CHO cells were used in this assay. Apoptosis was induced in cells using cis-platin as described in section 2.8.2. The viability assay was performed as described in section 2.2.6. A sample of cells (200) was counted; live and dead cells were counted in a haemocytometer and the results were expressed as the percentage of cells surviving.

5.2.3 Frequency of cells expressing proteins

To determine the numbers of cells expressing either EBV BHRF1 or A9 vBcl-2, immunostaining of the cells was performed as described in section 2.2.9. A9-CHO cells were incubated with the anti-A9 rabbit polyclonal antibody, 163 (1:500), followed by incubation with anti-rabbit-biotin conjugate (1:500) and finally streptavidin-FITC (1:75). BHRF1-CHO cells were incubated with an anti-BHRF1 mouse monoclonal antibody (1:1000) followed by incubation with goat anti-mouse-FITC (1:75). A sample of cells, 200, was counted and the number expressing the protein of interest was determined. The results were expressed as the percentage of cells expressing the protein of interest.

5.2.4 Caspase-3 Assay

The assay was as described in section 2.8.4. The results were analysed using a fluorescent plate reader (CytoFluor series 4000, Perspective Biosystems) and expressed as relative fluorescent units (RFU). Statistical analysis was performed using the Student's t-test.

5.2.5 Diff-quick Assay

The assay was as described in section 2.8.5. Samples of cells (200) were counted using light microscopy. The results were expressed as the number pyknotic cells compared to healthy cells and statistical analysis was by Student's t-test.

5.2.6 DNA Fragmentation assay

The assay was performed as described in section 2.8.3. The results were using agarose gel electrophoresis to show typical "DNA laddering".

5.3 Results

5.3.1 Frequency of CHO cells expressing A9 and BHRF1

The frequency of CHO cells expressing AIHV-1 A9 was determined at the start of the assays using immunofluorescence staining with an anti-A9 antibody (as described in section 3.3.9). In A9-CHO, 58 % of the cells expressed the A9 protein. Due to time constraints the protocol to optimise the anti-BHRF1 antibody could not be developed to the full extent however, since the BHRF1-CHO were surviving selection it was assumed that the BHRF1-CHO cells contained the BHRF1 gene.

5.3.2 Viability Assay

UTF CHO cells and A9-CHO cells were used to investigate the optimum concentration of cis-platin that should be used to induce apoptosis using cell viability as a read-out. Cells were treated with various concentrations of cis-platin. From fig. 5.1 it can be observed that at higher concentrations of cis-platin (75 μ M and 100 μ M) both UTF CHO and A9-CHO cells were all dead at 72 hrs, indicating that cis-platin is toxic at this concentration and that the A9 gene product could not inhibit apoptosis induced by this dose. At the lowest concentration (25 μ M) of cis-platin there was a significant difference ($p=0.004$) between UTF-CHO (57%) and A9-CHO (78%) cells surviving at 72 hrs, while at 50 μ M an effect was also seen, although it was not significant in this case.

Therefore, it was decided to use a concentration of 25 μ M of cis-platin since this was the only concentration that gave a significant value.

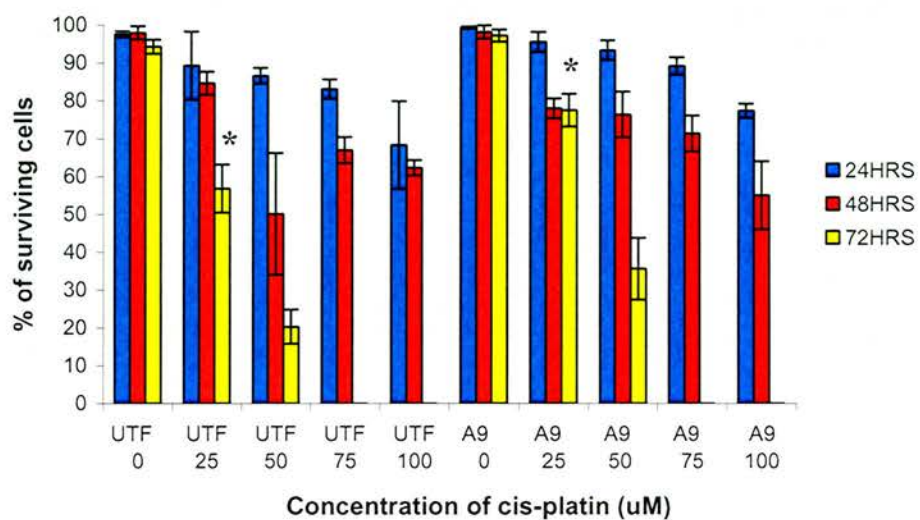


Fig. 5.1. The percentage of surviving cells after incubation with various doses of cis-platin at various time points throughout the assay. Asterisks denote significant differences comparing one to the other, where $p=0.004$. Error bars indicate the standard deviation.

5.3.3 Diff-Quik Assay

All CHO cells were incubated with cis-platin and analysed 24, 48 and 72 hrs after treatment. Fig. 5.2. shows that healthy (non-apoptotic) cells exhibited dark staining around the nucleus and light staining around the cytoplasm. However, in cells undergoing pyknosis, the cells rounded up and a characteristic cytoplasm was no longer obvious. Overall the staining of the apoptotic cells was very dark/intense. Fig. 5.3 summarises the merged to results. The assay was repeated twice with cells set up in triplicate in each assay.

Fig 5.3. shows that at time points 24, 48 and 72 hrs after treatment with cis-platin there were significant differences ($p=0.02$, 0.01 and 0.04 respectively) in the number of pyknotic cells with more pyknotic UTF-CHO cells compared to A9-CHO cells. When the A9-CHO cells were compared with control CHO cells at each time point (24, 48 and 72 hrs) there were also significant differences ($p=0.01$, 0.01 and 0.02) with more control CHO cells undergoing pyknosis compared to A9-CHO cells.

At 24 hrs after treatment there is no significant difference ($p>0.05$) between BHRF1-CHO cells and UTF-CHO cells. However at time points 48 and 72 hrs after treatment with cis-platin there are significantly ($p=0.02$ and 0.04 respectively) more pyknotic UTF-CHO cells compared to BHRF1-CHO cells. At each time point (24, 48 and 72 hrs) after treatment with cis-platin there are significantly ($p=0.003$, 0.002 and 0.01 respectively) less pyknotic BHRF1-CHO cells compared to control CHO cells.

The results of this assay show that A9 protects CHO cells from cis-platin induced apoptosis.

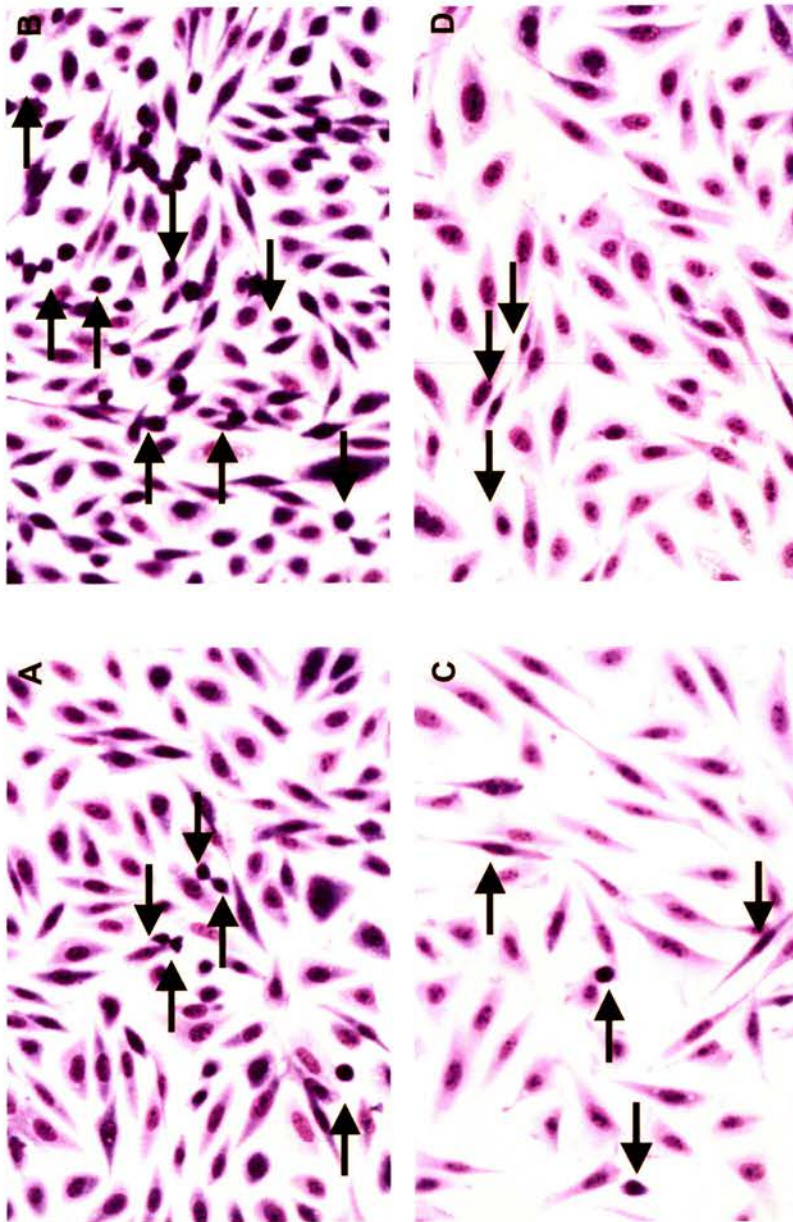


Fig 5.2. CHO cells 24hrs after treatment with 25 μ M cis-platin stained with the Diff-quick staining method. **A)** UTF CHO cells **B)** Control CHO cells **C)** CHO cells transfected with EBV BHRF1 **D)** CHO cells transfected with AIHV-1 A9. (x 400 magnification.) Arrows show a pyknotic cell.

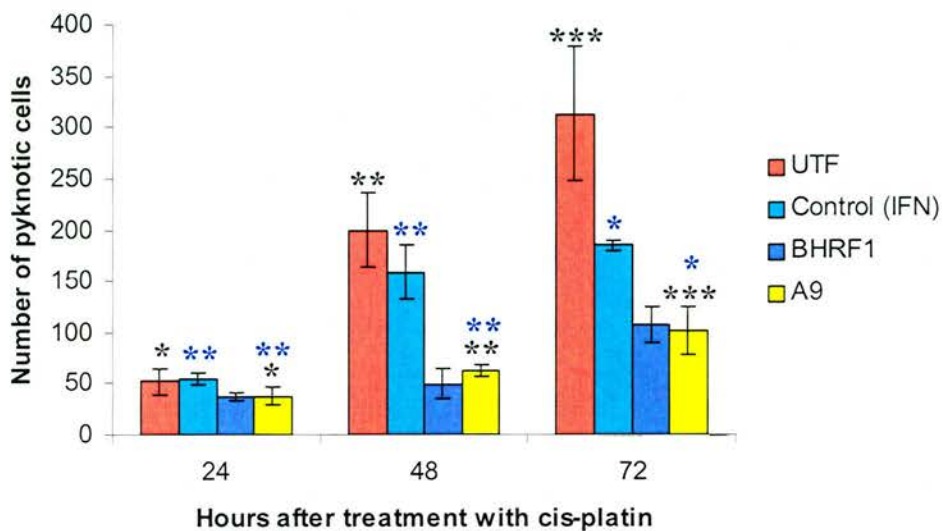


Fig. 5.3. The number of pyknotic cells at various time points after incubation with 25 μ M cis-platin. Pyknotic cells detected with Diff-quick assay. Asterisk shows significant differences between A9-CHO cell and other cell lines. Where * denotes p=0.02, ** denotes p=0.01 and *** denotes p=0.04. Number of cells counted was 400. Error bars indicated the standard deviation.

5.3.4 DNA Fragmentation Assay

During apoptosis, DNA is cleaved between nucleosomes to produce fragments in multiples of around 185bp. This can be analysed using agarose gel electrophoresis to show a typical “DNA-ladder”. DNA was extracted from CHO cells that had been incubated in the presence or absence of cis-platin.

In UTF and control CHO cells, laddering is faintly seen after 24 hrs of treatment with cis-platin. By 48 hrs after treatment, DNA fragmentation is clearly visible (fig. 5.4.). This contrasts with the CHO cells transfected with the Bcl-2 homologues BHRF1 and A9. Both show only very faint laddering after 48 hrs of cis-platin treatment although this is more evident after 72 hrs (fig. 5.4.) but not as marked as in controls. This demonstrates that A9 has anti-apoptotic activity (most clearly seen 48 hrs after cis-platin treatment) and appears to be as qualitatively efficient as BHRF1 in protecting cells from cis-platin induced DNA fragmentation.

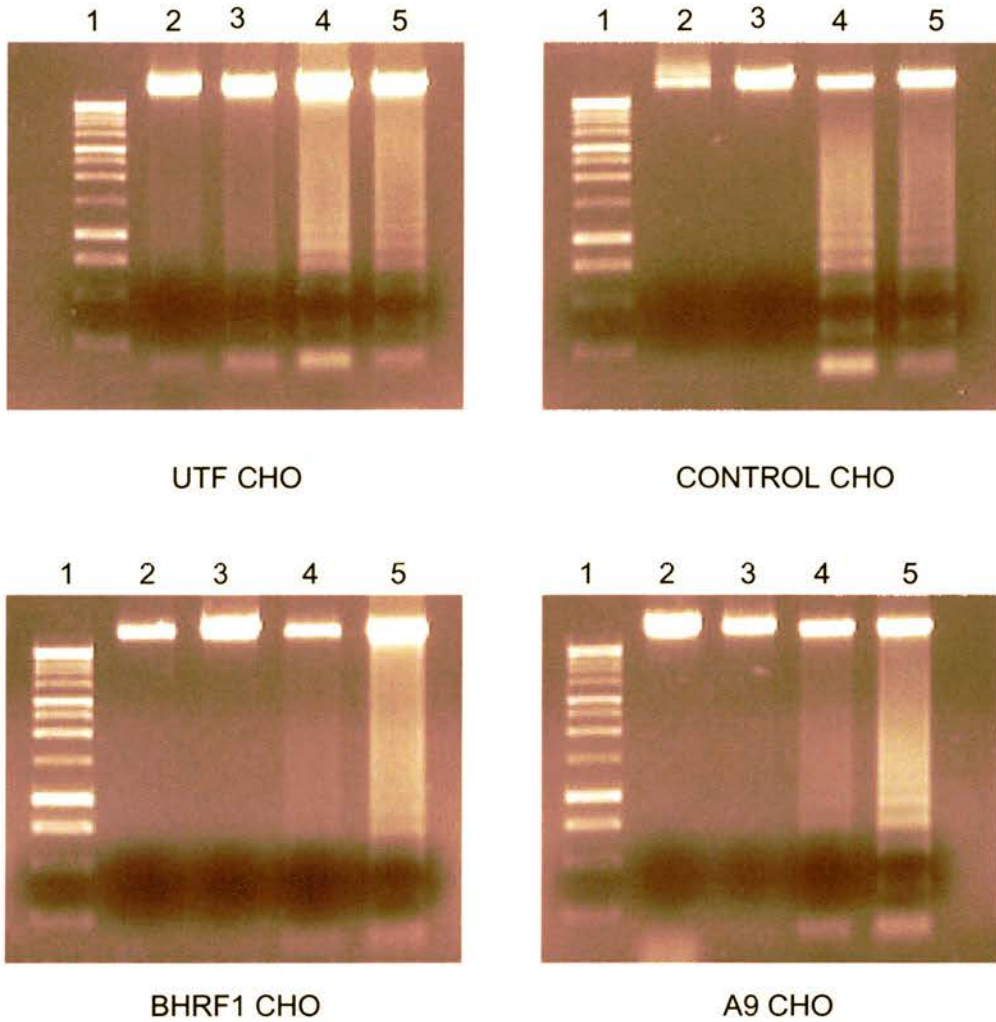


Fig 5.4. Agarose gel electrophoresis showing typical “DNA laddering” associated with apoptosis.

1: 1kb markers.
 2: DNA extracted from CHO cells without cis-platin.
 3: DNA extracted from CHO cells 24 hrs after treatment with cis-platin.
 4: DNA extracted from CHO cells 48 hrs after treatment with cis-platin.
 5: DNA extracted from CHO cells 72 hrs after treatment with cis-platin.

5.3.5 Caspase-3 Assay

The caspase-3 assay looks at the activation of caspase-3, an executioner caspase, in CHO cells undergoing cis-platin-induced apoptosis. The assay was carried out in duplicate, the results shown are the average of the two experiments. The error bars shown on fig. 5.5 show the standard deviation.

Fig. 5.5 shows that at 72 hrs after treatment with cis-platin there was significantly more ($p=0.05$) caspase-3 activity in UTF CHO cells compared to A9-CHO cells. At each timepoint selected in this assay there is more caspase-3 activity in UTF and control CHO cells compared to A9-CHO cells.

Fig. 5.5 shows that there is also significantly more ($p=0.003$) caspase-3 activity in UTF CHO cells than in BHRF1-CHO cells at 72 hrs.

The result of this assay shows that there is less caspase-3 activity in both BHRF1 and A9-CHO cells compared to both control and UTF CHO cells, which suggests that there are less apoptotic cells.

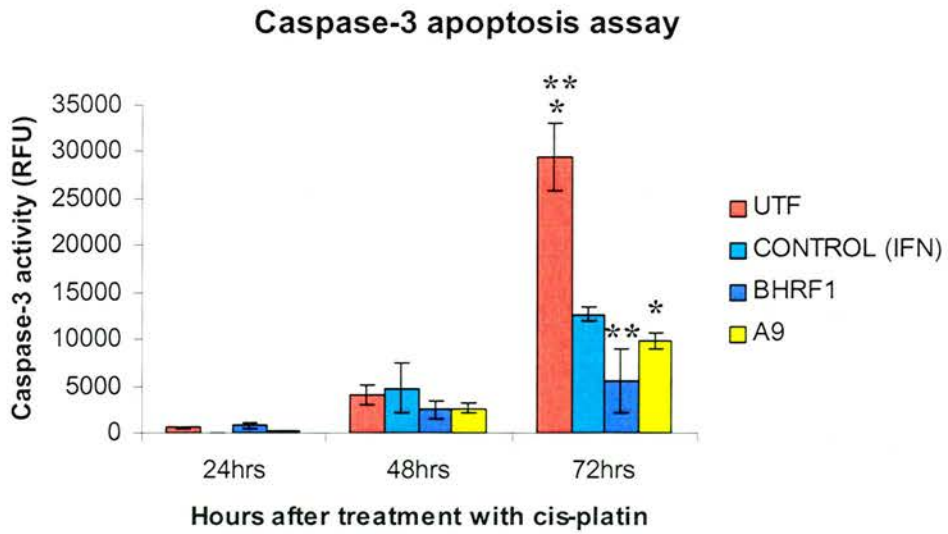


Fig. 5.5. Caspase-3 apoptosis assay. Figure shows the level of caspase-3 activity at various time points after incubation with 25 μ M cis-platin. Where asterisk denotes $*p=0.05$, and $**$ denotes $p=0.003$. Error bars indicate the standard deviation.

5.4 Discussion

The A9 vBcl-2 gene product exhibited anti-apoptotic activity in CHO cells stimulated with cis-platin, as measured in a range of apoptosis assays.

The proportion of cells expressing BHRF1 in BHRF1-CHO cells could not be determined since the assay needed to be optimised. However, it was assumed that the level of expression in both A9-CHO and BHRF1-CHO was comparable.

Cis-platin binds to DNA through nitrogen atoms on DNA base pairs to form cis-platin-DNA adducts. The formation of these adducts causes the purine nitrogen to destack and the DNA helix become kinked (Jamieson & Lippard, 1999). The mechanism by which apoptosis is induced is largely unknown although there are two mechanisms that have been proposed. The first is that high mobility group (HMG) proteins that bind to the cis-platin-DNA adducts are transcription factors. This complex may interfere with the transcription machinery, which in turns induces apoptosis. The second proposed mechanism is that these adducts may not be identified by the repair mechanism. Therefore, DNA repair would occur at a slower rate and lead to the interference with normal cellular functions and induce cell death (Jamieson & Lippard, 1999)

The assays that were chosen for this study were selected to represent different stages of apoptosis. The early stages of apoptosis were examined through the caspase-3 assay. The caspase-3 assay looks at the activation of caspase-3 (an executioner caspase) in cells that have been treated with cis-platin. Once caspase-3 is activated, it cleaves key regulatory or structural proteins - in particular it activates apoptotic nucleases such as caspase activated deoxyribonuclease (CAD) as well as activating upstream death cascades including the release of cytochrome c from mitochondria (Vaughan et al., 2002).

One of the biochemical hallmarks of apoptosis is the activation of specific endonucleases that cleave the DNA between nucleosomes, which can be detected by agarose gel electrophoresis (Wyllie, 1980). This is a relatively late indicator of apoptosis. However, it does provide a benchmark qualitative result in comparison to the other assays performed in this study that provide more quantitative results. The

Diff-quick assay detects morphological changes in the cells that take place during apoptosis and is therefore also a late indicator of apoptosis (Loo & Rillema, 1998). These assays were chosen because they were quick, simple and should be easy to interpret.

The AIHV-1 A9 gene product and EBV BHRF1 gene product protected CHO cells from cis-platin-induced apoptosis in all of these assays. The level of protection was comparable in both the diff-quick and DNA extraction assay. This would suggest that BHRF1 and A9 act at a similar level and fashion. This is similar to results obtained previously with EBV BHRF1 (Khanim *et al.*, 1997), where EBV BHRF1 transiently-transfected into both Cos-1 and SVK fibroblast cells protected them against cis-platin-induced apoptosis. The BHRF1 gene product also protected epithelial cells from apoptosis induced by a variety of stimuli such as TNF, anti-Fas and serum deprivation (Kawanishi, 1997). Similar results have been obtained with other gammaherpesviruses. For example, the vBcl-2s present in MHV-68 and KSHV have anti-apoptotic activity (Sarid *et al.*, 1997; Roy *et al.*, 2000).

The A9 gene product, by exhibiting anti-apoptotic properties would prevent virus-infected cells from undergoing apoptosis and this in turn would allow the virus to replicate and establish a productive life cycle. The results presented here suggest that A9 vBcl-2 is anti-apoptotic and could function by associating with pro-apoptotic proteins produced as a result of infection and thereby prevent them from inducing an apoptotic pathway for the elimination of AIHV-1.

Many viruses, including KSHV, EHV-2, some poxviruses and some adenoviruses have devised mechanisms to inhibit the Fas and TNFR pathways that lead to cell death (Telford *et al.*, 1995; Shisler *et al.*, 1997; Shisler & Moss, 2001, Sun *et al.*, 2003). These viruses encode proteins that have sequence similarity with the death effector domain (DED) motif that is found in FADD. These viral proteins block the recruitment of cell factors to the receptor that have been induced by the TNF and Fas pathways (Hu *et al.*, 1997; Thome *et al.*, 1997). Viruses including baculoviruses and poxviruses express proteins that block the caspase cascade by interfering with proteases such as caspase-8 (Datta *et al.*, 1997). Many viruses are found to possess homologues to the Bcl-2 family of protein including all gammaherpesviruses sequenced so far and African swine fever virus. This suggests

that the prevention of apoptosis is important to viruses and that viruses with large genomes may employ multiple strategies to ensure the survival of infected cells.

Chapter 6

Identifying binding partners of the A9 protein

6.1 Introduction

In chapter 5, the A9 gene product was shown to protect CHO cells from cis-platin-induced apoptosis. The mechanism by which the anti-apoptotic Bcl-2 family members prevent apoptosis is still relatively unknown although there are some theories (Schendel *et al.*, 1997; Desagher *et al.*, 1999; Tsujimoto & Shimizu, 2000). Many believe that the anti-apoptotic family members bind pro-apoptotic family members and prevent them from attaching to the mitochondrial membrane to induce apoptosis (reviewed in Harris & Thompson, 2000).

To determine if the A9 protein binds to pro-apoptotic family members (or other binding partners) in the same way as other anti-apoptotic Bcl-2 family members, protein-protein interactions of the A9 protein were investigated. This was attempted first by immunoprecipitation studies using A9-CHO cells and transiently-A9-transfected *Cos-1* cells. The second method that was used in this study to identify binding partners was tandem affinity purification (TAP). The TAP method is a protein tag-based affinity purification that was originally designed for use in yeast (Rigaut *et al.*, 1999). When compared to other epitope tags such as *myc*- or hemagglutinin- (HA-), TAP is reported to give better yields of affinity-purified proteins, along with a lower background of non-specifically associated proteins (Caspary *et al.*, 1999; Bouveret *et al.*, 2000) that can mask important functional partners. The TAP tag comprises two immunoglobulin-binding domains of protein A from *Staphylococcus aureus*, a cleavage site for the tobacco etch virus (TEV) protease, and a calmodulin-binding peptide (CBP). The original method involved the fusion of the TAP tag to the target gene and the replacement of the construct into the correct site in the yeast genome, which leads to the tagged protein being expressed from its natural promoter. Fusion proteins and associated components in complexes were recovered from cell extracts by affinity purification on an IgG column (Rigaut *et al.*, 1999). After washing, TEV protease was added to release bound proteins. Eluents were incubated with calmodulin-coated agarose beads in the presence of calcium. This second affinity-purification removed TEV protease as well as any traces of contaminants that remained after the first purification step. Bound proteins were released by EGTA, as this is a stronger calcium chelator than calmodulin (Rigaut *et al.*, 1999, Forler *et al.*, 2003).

In the work described here the TAP-tagged fusion constructs were made using the pZome-C retroviral vector (Cellzome) in which the tagged protein is expressed from the retroviral LTR promoter. The constructs were transfected into CHO cells and stably transfected cell were selected with puromycin. TAP-tagged transfected cells were harvested and TAP was performed. The purified eluents were separated by electrophoresis and proteins were detected by silver staining. Any unique protein bands detected were excised and analysed by the use of mass spectrometry.

Therefore, the objectives of this study were:

- Identify binding partners by immunoprecipitation.
- Generate TAP-tagged fusion proteins in *E. coli*.
- Identify A9 vBcl-2 binding partners through TAP.

6.2 Material and Methods

6.2.1 Expression of A9 mRNA analysed by Northern blot analysis

RNA was extracted from A9-CHO and control CHO cells as described in section 2.4.1. Northern blot analysis was performed as described in section 2.4.2. The membrane was probed with an A9 probe.

6.2.2 Immunoprecipitation of Bcl-2 proteins

Attempts to immunoprecipitate A9 protein from cell lysates using specific antibodies at the dilutions indicated (table 6.1) were as described in section 2.6.2. Immunoprecipitated samples were analysed by electrophoresis (as described in section 2.5.1). Proteins were detected by Coomassie blue staining, silver staining or western blot analysis (as described in section 2.5.2 and 2.5.3).

Antibody	Dilution
Anti-A9 6E1 (mouse monoclonal)	1:500
Anti-A9 6G8(mouse monoclonal)	1:500
Anti-A9 163 (rabbit polyclonal)	1:1000

Table 6.1. Antibodies and dilution used.

6.2.3 Construction of TAP-tagged fusion in *E. coli*

TAP-tagged fusions were constructed in the p-Zome-C and pZome-PGK-C vectors (Cellzome) as described in section 2.6.1.1.

6.2.4 Immunostaining of TAP-tagged fusion proteins in transfected CHO cells

The A9-CHO cells were used in an immunofluorescence assay as described in section 2.2.9. Briefly, the cells were washed with warm PBS, fixed in 1% paraformaldehyde in PBS for 10 mins and then washed again with PBS, . Non-specific binding sites were blocked with normal goat serum (1:40) in PBS for 1hr at 37°C. The primary antibody was anti-Bcl-2 rabbit polyclonal antibody 163 (1:500) in PBS, followed by incubation the secondary with goat anti-rabbit biotin (1:500) conjugate in PBS and detection was by streptavidin-FITC (1:75) conjugate. Cells

were incubated for 1 hr at 37°C for each incubation. Control reactions were set up by incubating cells with normal rabbit serum (1:100). Cells were mounted in Mowiol and examined using a fluorescent microscope.

6.2.5 Expression of TAP-tagged fusion proteins

Cells expressing TAP-tagged fusion proteins were grown in 225cm² cell culture flasks until confluent. The cells were harvested as described in section 2.6.1.3. Supernatant material was analysed by electrophoresis (as described in section 2.5.1). Proteins were detected by western blot analysis (as described in section 2.5.3) using peroxidase anti-peroxidase (PAP) (1:200) (Sigma) to detect Ig-binding protein A domain or anti-A9 rabbit polyclonal 163 (1:1000) or anti-A9 mouse monoclonal 6E1 (1:1000) followed by incubation with anti-rabbit-HRP (DAKO, 1:2000) conjugate; or anti-mouse-HRP (DAKO, 1:2000) conjugate. Bound HRP-antibody complexes were detected by treating blots with the enhanced chemoluminescence (ECL) reagent (Amersham International) according to the manufacturer's instructions, and exposure to Hyperfilm ECL (Amersham International) for 10-60sec before development.

6.2.6 Purification of TAP-tagged fusion proteins

TAP-tagged fusion proteins were subjected to tandem affinity purification as described in section 2.6.1.4.

6.2.7 Preparing samples for mass spectrometry analysis

Protein bands were excised from a stained polyacrylamide gel and cut up into small pieces. The gel pieces were transferred into a clean 1.5ml micro-centrifuge tube and covered with 100mM Ammonium bicarbonate/50% (v/v) Acetonitrile. This was incubated for 15 mins at room temperature with vortexing. The supernatant was removed and discarded. This was repeated three times until the stain was completely removed from the gel pieces. The gel pieces were dehydrated with 100% (v/v) Acetonitrile for 10 mins, the supernatant was removed and the gel pieces placed in a vacuum centrifuge for 20 mins to remove excess acetonitrile. To the gel pieces, 10mM DTT in 100mM Ammonium bicarbonate was added to cover them,

and incubated at room temperature for 5 mins. The gel pieces were then incubated at 56°C for 1hr. The supernatant was removed and 55mM Iodoacetamide in 100mM ammonium bicarbonate was added to cover the gel pieces. This was incubated at room temperature in the dark for 30 mins. The supernatant was removed and the gel pieces were incubated with 100mM ammonium bicarbonate/50% (v/v) acetonitrile for 15 mins with vortexing. This supernatant was removed and this wash was repeated three times. The gel pieces were again dehydrated with 100% Acetonitrile for 10mins. The Acetonitrile was removed and the gel pieces were dried by vacuum centrifugation for 20mins. To the gel pieces, sequence-grade modified trypsin (Promega) at 10ng/μl in 25mM Ammonium bicarbonate was added and incubated for 15 mins. The gel pieces were incubated at 37°C for at least 16 hrs. Alpha cyano-4-hydroxycinnamic acid (CHCA) was used as a matrix at 10mg/ml in 50% (v/v) acetonitrile/0.1% (v/v) TFA and 0.5μl of the supernatant around the gel pieces was mixed with 0.5μl of matrix for spotting onto a MALDI target..

6.2.8 Mass Spectrometry

The samples were analysed using an Applied Biosystems Voyager DE-PRO Matrix Assisted Laser Desorption Ionisation-Time of Flight (MALDI-TOF) Mass Spectrometer. Using the manufacturers guidelines a standard peptide mass fingerprint covering the 600-5000 Daltons range was obtained in the reflectron mode. Once a mass spectrum was obtained for the protein sample of interest, the peptide information provided was entered into the MS-FIT database search software. The MS-FIT software works by matching the mass spectrometry data with proteins in a sequence database whose tryptic peptide masses best fit the data.

6.3 Results

6.3.1 Attempting immunoprecipitation of binding proteins for A9 vBcl-2 in CHO cells

A9 protein expression was identified in A9-CHO cells (as described in section 3.3.9). This demonstrated that 58% of A9-CHO cells expressed the A9 protein.

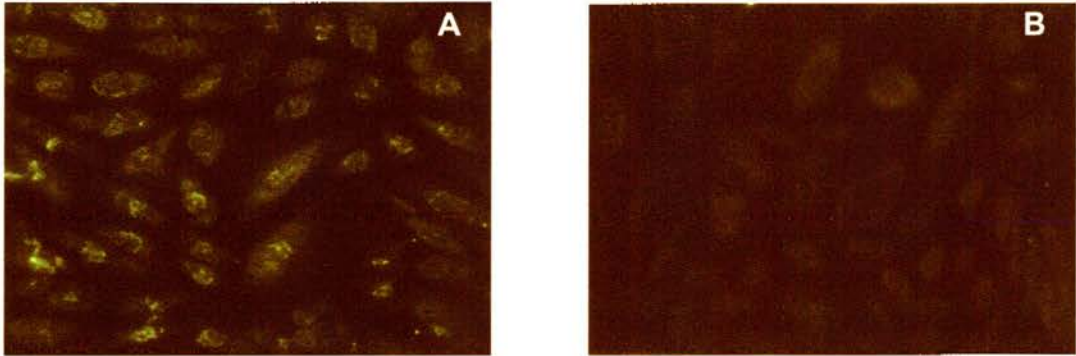


Fig. 6.1. Fluorescent images of A9-CHO cells incubated with serum from rabbit (pictures taken with the same exposure time, x 400 magnification).

Cells were fixed with ice-cold acetone, incubated with the appropriate primary antibody, then with anti-rabbit-biotin (1:500) and then finally incubated with streptavidin-FITC (1:75).

A) A9-CHO cells incubated with 163 rabbit anti-A9 sera (1:500).

B) A9-CHO cells incubated with normal rabbit serum (1:1000).

A9-CHO and UTF CHO cell lysates were incubated with monoclonal antibodies 6E1 and 6G8 to precipitate A9 and any bound proteins. The immunoprecipitated complexes were analysed using SDS-PAGE electrophoresis on a 7-20% gradient gel. Proteins were detected by Coomassie blue staining. As shown in fig. 6.2, no protein band was detected at the correct size of 19kDa with either mouse monoclonal antibody. The immunoprecipitation was repeated using UTF-CHO lysates and A9-CHO lysates with mouse monoclonal antibody 6E1 and with the rabbit polyclonal antibody 163. The proteins were detected by Coomassie blue staining. However, as shown in fig. 6.3. no band of the correct size was detected in the Coomassie blue-stained gel. From these experiments it would appear that the A9 protein was not immunoprecipitated by this method using available anti-A9 antibodies.

6.3.2. Attempts to immunoprecipitate A9 vBcl-2-binding partners from Cos-1 cells

To determine whether cell type would make a difference in identifying binding partners *Cos-1* cells were transiently transfected with pEE14-A9 construct. Cells were harvested 48hrs after transfection. Cell lysates were incubated with the rabbit polyclonal antibody, 163. A control immunoprecipitation experiment was also carried out using normal rabbit serum at the same concentration. The immunoprecipitated lysates were analysed by western blotting using 163 anti-A9 antibody. As shown in fig 6.4. there was no difference between lysates incubated with 163 anti-A9 antibody or with normal rabbit serum. Therefore, no A9 binding partners could be identified by immunoprecipitation.

Fig 6.2. SDS-Page gel of immunoprecipitated CHO lysate proteins. Proteins detected by Coomassie blue staining. **1:** A9-CHO cells immunoprecipitated with mouse monoclonal 6G8. **2:** UTF CHO cells immunoprecipitated with mouse monoclonal 6G8. **3:** A9-CHO cells immunoprecipitated with mouse monoclonal 6E1. **4:** UTF CHO cells immunoprecipitated with 6E1.

Fig. 6.3. Immunoprecipitated lysate proteins detected by Coomassie blue staining. **1:** A9-CHO cells incubated with 6E1 antibody. **2:** UTF CHO cells incubated with 6E1 antibody. **3:** A9-CHO cells incubated with normal rabbit serum. **4:** UTF CHO cells incubated with normal rabbit serum

Fig. 6.4. Immunoprecipitated lysates detected by western blotting. **1:** A9 transfected Cos-1 cells incubated with 163 antibody. **2:** UTF Cos-1 cells incubated with 163 antibody. **3:** A9 transfected Cos-1 cells incubated with normal rabbit serum. **4:** UTF Cos-1 cells incubated with normal rabbit serum

Fig. 6.2.

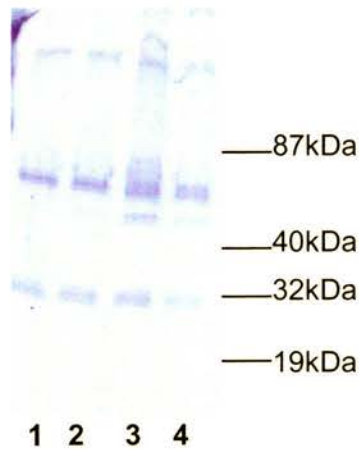


Fig. 6.3.

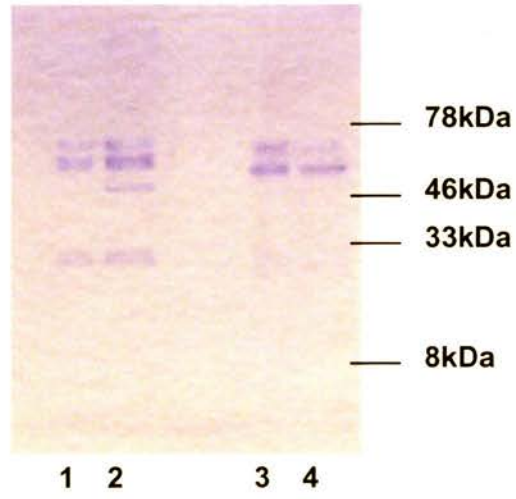
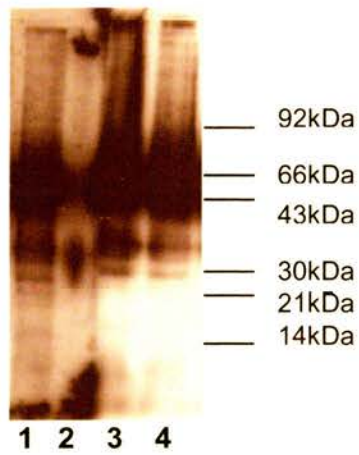


Fig.6.4.



6.3.3 Generation of TAP- A9 and BHRF1 CHO cells

In this study the retroviral vector, pZome-C (Cellzome, fig.2.1) was used to express TAP-A9 in CHO cells. Initially complete sequence was not available for this vector and the restriction map implied that it contained a unique *NcoI* site. A9, with a C-terminal *NcoI* site for protein fusion was cloned into this vector, but restriction mapping and subsequent analysis revealed that a second *NcoI* site was present in the SV40 promoter region of pZome-C. Therefore this pZome construct did not contain the TAP tag or the SV40 promoter.

Therefore the entire SV40 promoter was replaced with the murine phosphoglycerate kinase (PGK) promoter, which does not contain a *NcoI* site. The cloned A9 and BHRF1 genes were then inserted into the pZome-PGK-C vector at the *NcoI* site. The constructs were stably transfected into CHO cells and transfectants were selected with puromycin.

6.3.4 Immunostaining of TAP-A9 fusion protein in CHO cells

In order to check vBcl-2 protein expression, the transfected TAP-A9 CHO cells were analysed by immunofluorescence using the anti-Bcl-2 rabbit polyclonal antibody 163.

Fig. 6.5. shows immunofluorescence carried out on the TAP-tagged transfected cell lines. This figure shows that there does not seem to be differences in the staining pattern or intensity of the staining between cells incubated with anti-A9 antibody (fig. 6.5.A) and TAP-A9 CHO cells incubated with normal rabbit serum (fig. 6.5.B). There were also no differences noted in cell transfected with the empty construct (fig. 6.5.C&D). This was disappointing, however, since the cells were surviving selection media it was decided to carry on and assume that some of the cells did contain the A9-TAP construct.

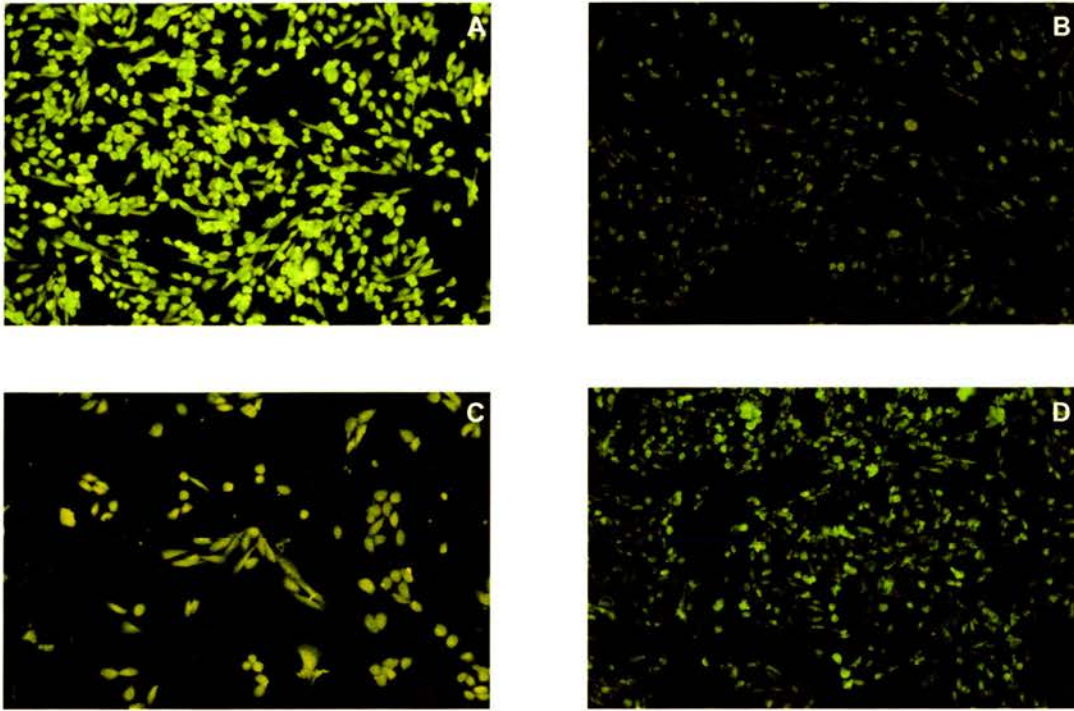


Fig. 6.5. Immunofluorescence analysis of TAP-tagged transfected CHO cell lines.

Cells were fixed in 1% paraformaldehyde, permeabilised with ice-cold acetone, incubated with the appropriate antibody, incubated with goat anti-rabbit-biotin (1:500) and finally incubated with streptavidin-FITC (1:75).

A: TAP-A9 CHO cells incubated with anti-A9 antibody (163) (1:500).

B: TAP-A9 CHO cells incubated with normal rabbit serum (1:1000)

C: CHO cells transfected with the empty pZome-PGK-C plasmid, incubated with anti-A9 antibody (163) (1:500)

D: CHO cells transfected with the empty pZome-PGK-C plasmid incubated with normal rabbit serum (1:500).

6.3.5 Detection of TAP-A9 proteins in CHO cells

Cells expressing the TAP-A9 CHO cells were grown in 225cm² cell culture flasks until confluent. The cells were harvested (see section 2.6.1.3.), lysates collected and analysed by gel electrophoresis. Proteins were detected by Western blot using the appropriate antibody. As shown in fig. 6.6, a protein band, 30kDa, in the empty pZome proteins was detected with the peroxidase anti-peroxidase (PAP) antibody. However, no protein band corresponding to the expected size of A9-TAP tagged fusion protein could be detected. Immunofluorescence analysis indicated that cells were expressing protein. The inability to detect A9 by western blot using a variety of antibodies was unfortunate but it was decided to proceed with the TAP protocol to see if this would reveal any protein-protein interactions.

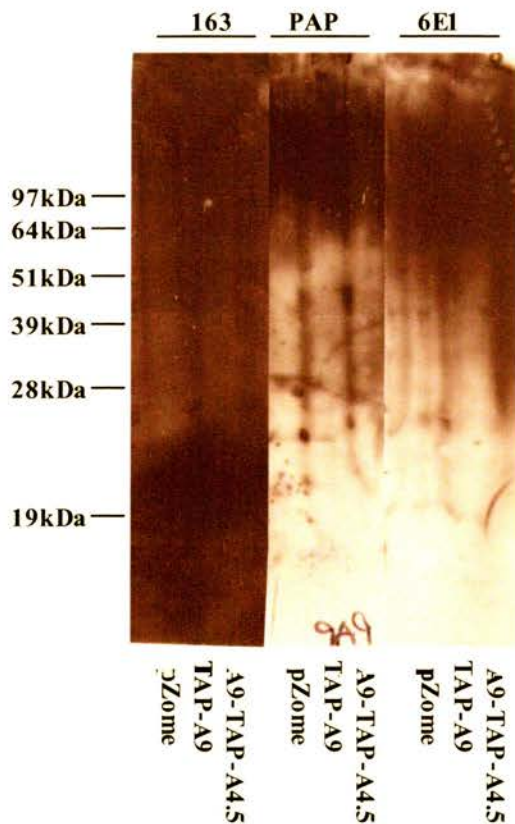


Fig. 6.9. Western blot analysis of TAP-tagged fusion proteins. The TAP tagged fusion proteins were extracted from the cells, proteins were detected using anti-Bcl-2 antibodies 163 and 6E1 and also PAP.

6.3.6 Identification of possible TAP-A9 vBcl-2 and TAP-BHRF1 vBcl-2 binding partners

Both aqueous and detergent-soluble extracts were harvested from CHO cells and used in the TAP protocol. The lysates were analysed by electrophoresis on 12% SDS-PAGE gels. Proteins were detected by silver staining. Fig 6.7. shows that there are a number of bands that could correlate to Bcl-2 family members due to their molecular weight being similar to known Bcl-2 family members. Bands 1, 3 and 4 were common to the TAP cells. Fig 6.7. shows that in lane 6 a band (5) can be observed in the detergent-soluble lysate that has a molecular weight of approximately 30kDa. Another protein band (2) of interest was observed in lane 4. This had an approximate molecule weight of 40kDa. All the selected bands were excised using sharp clean scalpels and destained. The bands were used in mass spectrometry analysis.

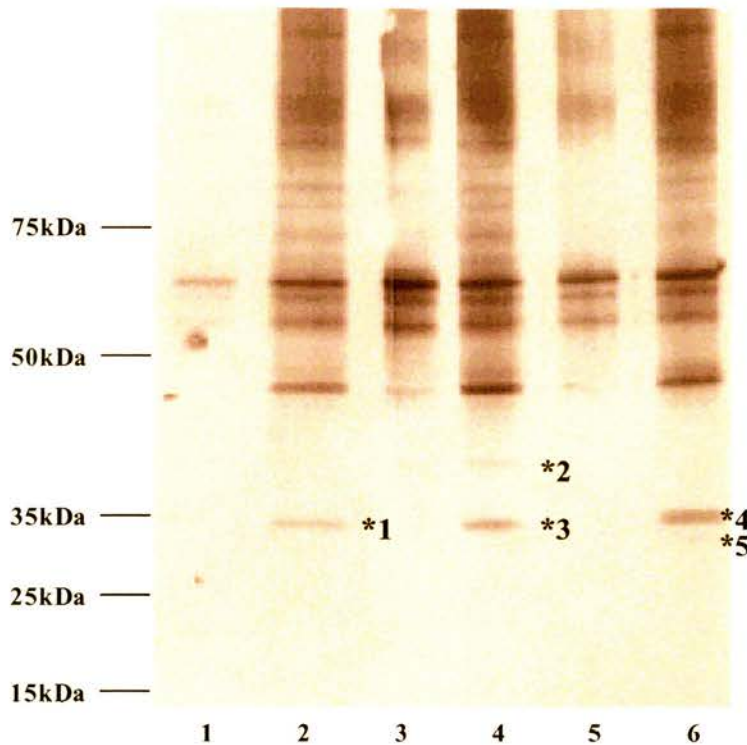


Fig. 6.7. Silver stained gel of TAP-purified proteins from cell lysates. Lane 1: Purified lysates from TAP-CHO cells, detergent-soluble. 2: Purified lysate from TAP-CHO cells, supernatant. 3: Purified lysate from TAP-tagged BHRF1-CHO cells, detergent-soluble. 4: Purified lysate from TAP-tagged BHRF1-CHO cells, supernatant. 5: Purified lysate from TAP-tagged A9-CHO cells, detergent-soluble. 6: Purified lysate from TAP-tagged A9-CHO cells, supernatant. Asterisks denote bands that had been excised from the gel for MALDI mass spectrometry analysis.

6.3.7 MALDI/Mass spectrometry analysis of protein bands

Mass spectrometry was used to determine the masses of tryptic peptides that had been excised from the SDS-PAGE gel using MS-FIT database. Known peptide contaminant masses e.g. from trypsin and keratin were removed before the database search was performed. Fig. 6.8 demonstrates a typical mass spectrum that was obtained from the purified samples. The peptide masses (denoted in red) were entered into the database search. The peptide masses did not match well with any known database entries.

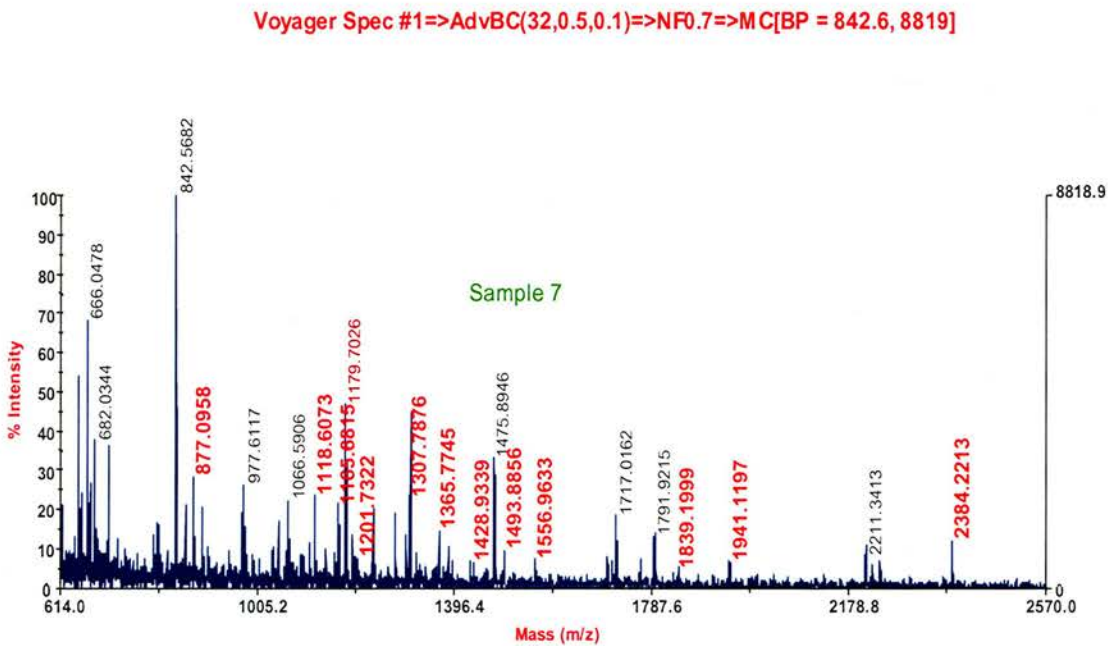


Fig. 6.8. Mass spectrum of purified samples. A typical mass spectrum obtained from the purified lysates. Red denotes masses used in database search. Black denotes common masses that were removed due to contamination (e.g. keratin and trypsin). The x-axis represents the total mass of peptide while the y-axis represents the intensity of the peaks, which in this case is low.

6.4 Discussion

In this study, cellular binding partners for A9 vBcl-2 could not be identified. This is in spite of fluorescence evidence for the expression of A9 protein in A9-CHO cells. Due to time constraints a full evaluation of the new TAP technology could not be performed.

Classical immunoprecipitation did not identify any cellular binding partners for A9 vBcl-2. This could be due to an inability of the A9 antibody to immunoprecipitate or the conditions for immunoprecipitation not being optimal.

The TAP technique was used in preliminary experiments to look for A9 protein-cellular protein interaction. The TAP-technique has been adapted for use in mammalian cells by a variety of groups (Cox *et al.*, 2002; Michela *et al.*, 2002). In this study the retroviral plasmid pZome-C was used. Unfortunately the complete sequence of the pZome-C plasmid was not available initially. After the A9 gene was cloned into the pZome-C retroviral plasmid a second *NcoI* site was discovered in the SV40 promoter. Therefore, the first constructs that were produced did not contain the TAP tag or the SV40 promoter.

The problem could have been corrected by two methods: 1: re-clone the Bcl-2 genes with new flanking *BamHI* sites into this alternate pZome-C cloning site or 2: alter the pZome-C vector by removing the second *NcoI* site. The first method was discarded, as other genes being investigated in this study possessed internal *BamHI* sites, therefore it was decided to delete the second *NcoI* site. Simple filling in of the *NcoI* was not possible because this has been documented to cause a ten-fold reduction in mRNA synthesis from the promoter (Khalili *et al.*, 1986). Therefore the entire SV40 promoter was replaced with the murine phosphoglycerate kinase (PGK) promoter, which does not contain a *NcoI* site.

Immunofluorescence analysis was carried out on the TAP-tagged transfected cell lines. However, this proved to be inconclusive with its results. No differences could be detected between cells incubated with anti-A9 antibody and normal rabbit serum. This is probably due to the TAP tag comprising of two immunoglobulin-binding domains of protein A. Therefore, non-specific antibodies would still bind to this domain, resulting in visible staining in immunofluorescence analysis. It was decided to proceed with the purification of the TAP-tagged proteins with the

assumption that if cells were surviving the selection process then most would be transfected with the TAP-tagged construct.

From the TAP-A9 CHO and TAP-BHRF1 CHO cells a number of proteins were isolated by the TAP procedure. Some of these were excised and analysed by mass spectrometry. No significant peptide matches could be determined from the database searched. However, there was very little material to work with. The bands that were excised from the gels could be artefact since a few of the bands that were excised were present in the empty construct. Two of the bands that were excised were specific to A9 and BHRF1 respectively. However, these bands again showed no specific peptide matches, this could be due to contaminating proteins or due to silver staining being non-quantitative, a band would be present but very little protein would actually be present in the sample. The spectra from the mass spectrometry had peptide peaks with low signal intensity. The presence of peaks for contaminating trypsin and keratin in most of the spectra suggest that the signal/noise ratio is low.

Another factor that could influence a lack of peptide match is the lack of database entries available for hamster proteins (CHO cells). Relatively few database entries are available compared to mouse or human for example. Therefore, this part of the study was slightly flawed and on hindsight, the construct should have been transfected into cells that have a larger database such as mouse or human cells. However, it was hoped that conserved proteins may have shared enough tryptic peptides to hit by hamster mass spectrometry profiles.

The TAP-tag protocol was adapted by using lysis buffers with or without detergent. The lysis buffer used can play an important role. Therefore in this experiment, two different lysis buffers were used. While it was clear that these led to different protein profiles after purification, neither approach identified clear A9 binding partners. The results shown in fig 6.7 suggest that both BHRF1- and A9-specific binding partners might be identified by this system if more protein were available and the TAP technique was subjected to other manipulations.

Unfortunately, a larger scale purification was not possible due to time constraints.

Another technique that could have been used was the yeast two-hybrid system. This technique has been used to identify novel partners for proteins that have a known function and to identify the function of a novel protein by identifying well-characterised interacting partners. The yeast two-hybrid system is a rapid, inexpensive technique that is simple to perform (reviewed in Toby & Golemis, 2001).

However, false-positive and false-negative results, the lack of information about stoichiometry and the limited set of conditions that are testable are disadvantages that have to be considered. The TAP method allows the native purification of protein complexes (Rigaut *et al.*, 1999). The purified complex can then be used for protein identification, functional or structural studies. The initial results described here although disappointing, have encouraged further development of the technology in this laboratory to apply to other viral ORFs to identify binding partners.

Chapter 7

General Discussion

In this study, the principal outcomes can be summarised as follows:

Alcelaphine herpesvirus-1 A9 open reading frame was shown to have predicted polypeptide homology to the cellular Bcl-2 family proteins involved in the regulation of apoptosis. The A9 vBcl-2 protein was expressed and antibodies produced. In a series of apoptosis assays, the A9 vBcl-2 was shown to be anti-apoptotic. A9 mRNA was expressed as an early through to late viral gene in the productive phase of the virus life cycle. In large granular lymphocytes that grow out in culture from the tissues of MCF-affected animals, A9 mRNA was detected. Finally, intracellular binding partners for the A9 protein were sought but none were characterised. The conclusion is that the A9 vBcl-2 is a functional viral anti-apoptotic molecule that functions throughout the productive phase of the virus life cycle. This would have the effect of prolonging the life of infected target cells to allow viral replication.

Sequence analysis of ORF A9 showed that it shared homology with the Bcl-2 family of apoptosis regulatory proteins. In particular, it shared 33% amino acid identity to human Bcl-w. The cellular Bcl-2 family of proteins is conserved from worms through to humans (Hengartner, 2000) however; they generally share only around 20-45% amino acid identity to one another. The viral Bcl-2 homologues that have been examined share 20-30% identity to one another (reviewed in Hardwick & Bellows, 2003). For example, BHRF1 shares 38% primary sequence homology with human Bcl-2. The KSHV Bcl-2 homologue shares 58.7% amino acid similarity to human Bcl-2 (Sarid *et al.*, 1997).

Bcl-w is an anti-apoptotic protein that binds to the pro-apoptotic proteins Bax, Bak, Bad and Bik (Holmgren *et al.*, 1999). One proposed model for the prevention of apoptosis by Bcl-w is that the protein, which is normally loosely associated with the mitochondrial membrane, becomes tightly associated with the membrane following an apoptotic stimulus. This tight association is triggered by the heterodimerisation with pro-apoptotic BH3-only proteins such as Bik and Bid. This would effectively neutralise apoptosis. It has also been shown that upon an apoptotic stimulus, the C-terminal arm of Bcl-w is released and binds to Bax, preventing it from inserting into the mitochondrial membrane (Wilson-Annan *et al.*, 2003) thus preventing apoptosis.

From its predicted amino acid sequence, A9 vBcl-2 protein exhibited homology with only one of the four known Bcl-2 homology (BH) domains of Bcl-2 family members, namely BH1. A9 vbcl2 also has a transmembrane domain. When this work was initially started, ORF A9 product was the only Bcl-2 homologue to have only one BH domain. However, subsequent work carried out with MHV-68 has shown that the gene product of ORF M11 is a vBcl-2 that possesses only the BH1 domain and that it has anti-apoptotic activity (Roy *et al.*, 2000).

The BH1 domain is important for the function of the cellular anti-apoptotic Bcl-2s (Borner *et al.*, 1994b; Yin *et al.*, 1994). Within this domain there is a conserved sequence, NWGR. Mutational studies substituted the glycine¹⁴⁵ residue with alanine. This resulted in the loss of anti-apoptotic function suggesting that the glycine residue is essential for the death-protective role of Bcl-2 (Yin *et al.*, 1994). Substitution of the glycine¹⁸⁵ residue with alanine also resulted in the inability of Bcl-2 to heterodimerise with Bax. However Bcl-2 was still able to form homodimers (Yin *et al.*, 1994).

The Bcl-2 homologue present in African swine fever, ORF A179L, contains two of the four BH domains (BH1 and BH2). When the glycine¹⁸⁵ residue in the BH1 domain was mutated to alanine, the death-protective function was abolished (Revilla *et al.*, 1997).

The AIHV-1 A9 protein contains a HWGR sequence that is part of the conserved NWGR sequence. The conserved glycine residue that is essential for anti-apoptotic activity in other Bcl-2s is also present in the A9 protein, which suggests the A9 protein might have a death-protective role, which has been demonstrated true in this thesis. As this is the only BH domain present in A9, it would be the site in which heterodimerisation occurs with pro-apoptotic Bcl-2 family members such as Bax and Bak. However, no binding partners could be found in this study to confirm this.

The BH2 domain of Bcl-2 family members is also associated with anti-apoptotic activity. Deletion of this domain results in the loss of anti-apoptotic activity (Yin *et al.*, 1994). Specifically, deletion of the GWDA sequence in the BH2 domain of Bcl-2 resulted in the elimination of anti-apoptotic activity. Deletion of the sequence also resulted in the inability of Bcl-2 to heterodimerise with Bax (Yin *et*

al., 1994). Since the BH2 domain is poorly conserved in A9 to the extent that it is unlikely to be functional, A9 vBcl-2 would not be expected to heterodimerise with Bax or other pro-apoptotic proteins through this domain.

The BH3 domain is essential for pro-apoptotic activity. This domain allows protein-protein interactions between pro- and anti-apoptotic proteins (Reed, 1998). The A9 protein does not have an identifiable BH3 domain, indicating that A9 would be unlikely to have any role in inducing apoptosis.

The BH4 domain is anti-apoptotic and has been shown to bind proteins outside the Bcl-2 family that are involved in apoptosis, for example, Raf1, ced4 and calcineurin (Wang *et al.*, 1994; Shibasaki *et al.*, 1997; Huang *et al.*, 1998). The BH4 domain is not conserved in A9 vBcl-2, indicating it may only bind to Bcl-2 family members through the BH1 domain and not to non-Bcl-2 proteins involved in apoptosis.

In summary, AIHV-1 A9 vBcl-2 has a BH1 domain that would be important in mediating an anti-apoptotic function, but does not have any of the other BH domains that would allow this function to be regulated by cellular Bcl-2 family or other apoptosis regulatory proteins. This would be important in maintaining the anti-cell death state in virus-infected cells to allow virus replication and virion production.

The transmembrane (TM) domain is found in many Bcl-2 family members and enables them to insert into cell membranes. More often than not these localise to the mitochondrial membrane (Hockenberry *et al.*, 1990; Gonzalez *et al.*, 1995). The TM domain is not involved in any of the protective functions of the protein, as deleting this domain does not alter the level of death-protection (Hockenberry *et al.*, 1993; Borner *et al.*, 1994a). However, deletion of the TM domain abolishes their ability to localise to the mitochondrial membrane (Nguyen *et al.*, 1993; Nguyen *et al.*, 1994). Many pro-apoptotic Bcl-2 family members possess the TM domain that allows their insertion into the mitochondrial membrane after translocation from the cytosol. The A9 protein TM domain would allow the protein to localise to membranes within cells, particularly the mitochondrial membranes, thereby preventing pro-apoptotic members from inserting into these membranes and effecting apoptosis.

The 3D structures of several Bcl-2 family members have been solved, including those of Kaposi's sarcoma herpesvirus (KSHV) and Epstein Barr virus (EBV) (Huang *et al.*, 2002; Huang *et al.*, 2003). These latter two show general similarities to cellular Bcl-2 family members, being α -helical proteins with seven helices. The central α -helix ($\alpha 5$) forms the core of the protein, and is surrounded by $\alpha 3$ and $\alpha 4$ on one side and helices $\alpha 1$, $\alpha 2$ and $\alpha 6$ on the other side. In KSHV Bcl-2, a hydrophobic groove is formed on the surface of the protein from residues in $\alpha 2$, $\alpha 3$, $\alpha 4$ and the N-terminal residue of $\alpha 5$. The EBV BHRF1 vBcl-2 structure is similar although the hydrophobic region is less exposed as $\alpha 3$ crosses closer to the middle of $\alpha 5$. The loop that connects $\alpha 1$ and $\alpha 2$ is shorter in both KSHV Bcl-2 and EBV BHRF1 vBcl-2 compared to human Bcl-x_L.

However, EBV BHRF1 protein shows several differences from other Bcl-2 family members. The protein lacks the NWGR sequence in the BH1 domain on helix $\alpha 5$. The sequence SLGR is found instead. The surface of the BHRF1 differs from other Bcl-2 proteins. The prominent groove found in Bcl-x_L and the KSHV Bcl-2 homologue is not seen in BHRF1. There are also several amino acid changes that make the surface of BHRF1 less hydrophobic than other anti-apoptotic proteins (Huang *et al.*, 2003).

In contrast, the KSHV Bcl-2 homologue does share considerable structural similarity with related cellular Bcl-2 proteins. The sequence NWGR in the BH1 domain is conserved and it would appear to be important in maintaining the fold of the protein (Huang *et al.*, 2002).

Alignment of the A9 protein sequence with a range of vertebrate and viral Bcl-2 family members showed that A9 grouped most closely with the anti-apoptotic Bcl-x_L proteins. The predicted secondary structure of A9 is shown in fig 7.1. The data indicates that the structure of the A9 protein could be very similar to that of both the KSHV Bcl-2 homologue and EBV BHRF1. However, the structure does not contain the seven helices that are seen in cellular Bcl-2 proteins. It appears that the size and position of $\alpha 4$, $\alpha 5$ and $\alpha 6$ helices relative to the BH1 domain may be conserved in the A9 protein. As previously mentioned, the NWGR sequence is replaced with the sequence HWGR in A9. The data would suggest that the hydrophobic groove formed by residues in $\alpha 2$, $\alpha 3$, $\alpha 4$ and the N-terminus of $\alpha 5$ may

be conserved in the A9 protein, as the contributing helices are conserved. The alignment suggests that structural homologues of helices $\alpha 2$ - $\alpha 6$ are present within the N-terminal part of the A9 protein, being truncated and with an extended loop between the equivalents of $\alpha 3$ and $\alpha 4$. As expected, the best region of alignment of both sequence and structure is around the BH1 domain. This suggests that this region is conserved for an anti-apoptotic role of A9 vBcl-2.

3D structure modelling using Bcl-x_L and BHRF1 (Swiss-model: www.expasy.org/swissmod/SWISS-MODEL.html. Peitsch, 1995; Guex & Peitsch, 1997; Schwede *et al.*, 2003) suggests that A9 is more like the Bcl-x_L protein structure, as the 'what-check output structure z-scores' (Hooft *et al.*, 1996) are better for the Bcl-x_L-based model compared to that based on BHRF1. The A9 structure models based independently on Bcl-x_L and BHRF1 suggest that there is an extra loop between $\alpha 3$ and $\alpha 4$ comprising two short β -strands. There are three major differences between Bcl-x_L and the model of A9 (fig. 7.2A):

- The modelled A9 structure has no helix $\alpha 1$ (the white Bcl-x_L $\alpha 1$ helix can be seen running diagonally at the back of the model).
- The N-terminal part of A9 forms a simple strand lying parallel to $\alpha 5$ helix (vertical red strand). This strand may protect the BH1 domain.
- The loop between helices $\alpha 3$ & $\alpha 4$ is extended in A9, and is shown as two short beta strands (red).

Similarly, there are three main differences between the BHRF1 and A9 structures (fig 7.2B):

- The modelled A9 structure has no $\alpha 1$ helix
- The $\alpha 6$ helix is modelled in two parts for A9 (red strand in $\alpha 6$)
- The loop between helices $\alpha 3$ & $\alpha 4$ is extended in A9, and is shown as two short beta strands (red)

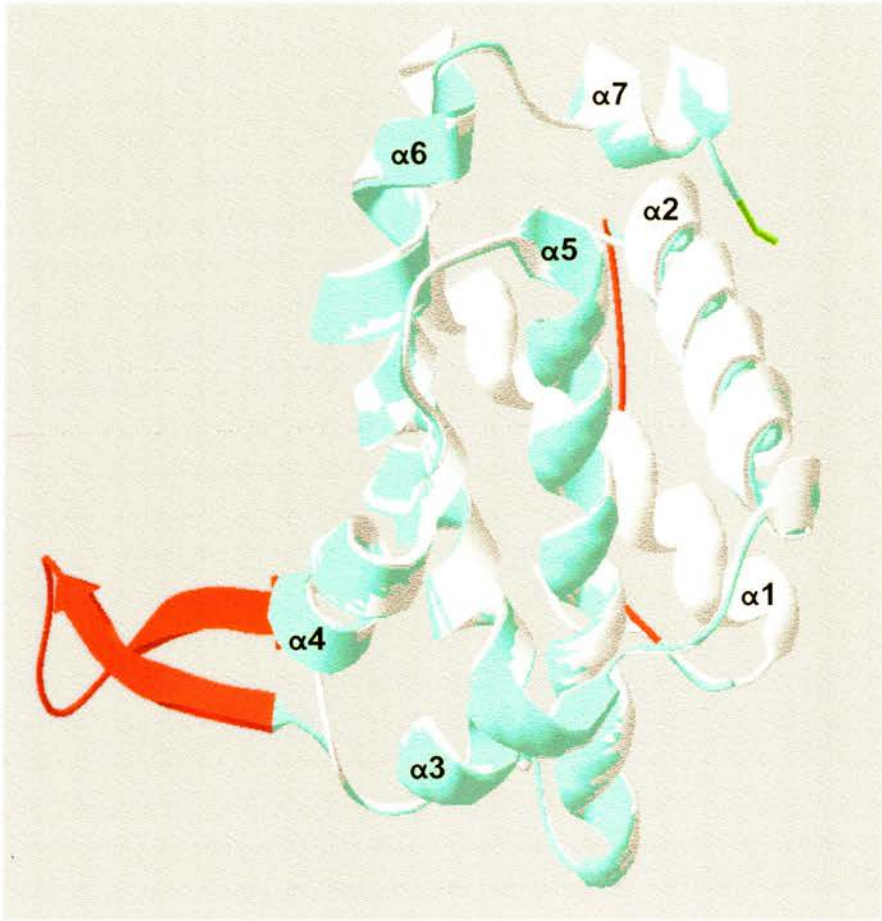


Fig 7.2A. Structure model of A9. Overlaid structural comparison of Bcl-x_L (white) and the model of the A9 structure (blue helices) with the main helices labelled. The majority of the A9 model can superimpose on the Bcl-x_L structure, as seen by the blue/white patching. Small structural variations can be seen where the blue and white structures separate. Red/green represent the A9 model. Three major difference are demonstrated between Bcl-x_L and the model of A9. The model of A9 has no helix α1 (the white bcl-x_L α1 helix can be seen running diagonally at the back of the model). The N-terminal part of A9 form a single strand which lies parallel to α5 helix (vertical red strand). The loop between α3 and α4 helices is extended in A9 and is shown as two short beta strands (red).



Fig. 7.2B. Model of A9 structure. Overlaid structural comparison of BHRF1 (white) and the model of the A9 structure (green/red). The majority of the A9 model can superimpose on the BHRF1 structure, as seen by the green/white patching in most of the structure. Structural variations can be seen where the green and white structures separate and where loops are modelled slightly differently (red). There are three main differences between the BHRF1 structure and the model of A9. The modelled A9 structure does not contain $\alpha 1$ helix. The $\alpha 6$ helix is modelled in two parts for A9 (red strand in $\alpha 6$ helix). The loop between $\alpha 3$ and $\alpha 4$ helices is extended in A9 and is shown as two short beta strands (red)

To summarise, in spite of low overall amino acid identity to other Bcl-2 family members, A9 modelling indicates a structure similar to other Bcl-2 family members, which would present the BH1 domain in a fully functional conformation. Current work within the laboratory is attempting to overproduce A9 vBcl-2 for crystallography X-ray diffraction resolution of its 3D structure.

Since this work was initiated, a second putative Bcl-2 protein has been identified in AIHV-1, namely ORF A4.5 product. The predicted amino acid sequence of this shares 22% sequence identity to a Bcl-2 protein in porcine lymphotropic herpesvirus-1 and 20% amino acid identity to equine herpesvirus-2 E4 (Telford *et al.*, 1995; Ehlers *et al.*, 1999). The A4.5 protein has two conserved BH domains, BH1 and BH2. A second Bcl-2 protein has also been identified in EBV, BamHI 'A' fragment leftward reading frame (BALF1). BALF1 is expressed as an early through to late gene in the lytic cycle of EBV. It also possesses two of the four BH domains, BH1 and BH2 (Marshall *et al.*, 1999). BALF1 does not possess the conserved NWGR sequence present in the BH1 domain. The conserved glycine¹⁸⁵ residue present in the BH1 domain of other Bcl-2 family members is also not present. As previously stated, this residue is essential for anti-apoptotic activity (Yin *et al.*, 1994). However BALF1 does contain a conserved tryptophan¹⁸⁸ residue present in the BH2 domain. Substitution of tryptophan 188 with alanine results in the inability to heterodimerise with the pro-apoptotic protein Bax (Yin *et al.*, 1994). BALF1 heterodimerises with the pro-apoptotic proteins Bak and Bax (Marshall *et al.*, 1999). It has been suggested that BALF1 suppresses the anti-apoptotic function of BHRF1 in virus-infected cells at a later point during infection, when the virus no longer requires a viable cell (Bellows *et al.*, 2002).

The predicted AIHV-1 A4.5 amino acid sequence reveals that it also does not contain the conserved NWGR sequence in the BH1 domain and does not contain the highly conserved glycine residue in BH1 domain. However the sequence demonstrates that the tryptophan¹⁸⁸ residue is present in the BH2 domain. This would suggest that A4.5 might act in a similar fashion to BALF1, forming heterodimers with pro-apoptotic proteins such as Bax and Bak. This would prevent Bax and Bak from associating with the mitochondria and therefore prevent apoptosis.

The transmembrane domain is also missing from the BALF1 protein. BALF1 and BHRF1 do not co-localise, BHRF1 localises to the mitochondria (Hickish *et al.*, 1994) while BALF1 localises in the cytoplasm, which may reflect the lack of a TM domain in BALF1. Once apoptosis has been stimulated, BALF1 fails to localise to mitochondria (Bellows *et al.*, 2002). However, co-immunoprecipitation studies demonstrated that BALF1 and BHRF1 bind to each other (Bellows *et al.*, 2002). BALF1 suppresses Fas-induced and topoisomerase-induced apoptosis in HeLa cells (Marshall *et al.*, 1999). However, BALF1 failed to suppress Sindbis-induced and Bax-induced apoptosis in Rat-1 and B-cell lines (Bellows *et al.*, 2002). A transmembrane domain is not present in A4.5. In summary, the function of AIHV-1 A4.5 vBcl-2 may be similar to that of BALF1. A4.5 may form heterodimers with pro-apoptotic proteins such as Bax and Bak and may also bind A9 protein acting as an antagonist protein, which alone may not be an inhibitor of apoptosis. These hypotheses could be addressed in experiments similar to those described in chapter 6 using the TAP method, and are currently under way in the laboratory.

Apoptosis assays performed on A9-CHO cells treated with cis-platin demonstrated that A9 vBcl-2 inhibited apoptosis. Apoptosis is often seen in response to virus infection and is a potent cellular anti-viral innate response. Therefore, viruses that encode anti-apoptotic Bcl-2 homologues will promote cell survival and enhance virus production. Many of the viral Bcl-2 homologues that have been studied so far protect virus-infected cells from apoptosis. EBV BHRF1 vBcl-2 protects both *Cos-1* and SVK fibroblast cells from cis-platin-induced apoptosis (Khanim *et al.*, 1997). Herpesvirus papio encodes a functional Bcl-2 homologue that protects SVK cells from cis-platin induced apoptosis (Meseda *et al.*, 2000). The Bcl-2 homologue present in KSHV inhibits Sindbis virus-induced apoptosis (Cheng *et al.*, 1997). MHV-68 encodes a functional Bcl-2 homologue (Roy *et al.*, 2000). Therefore A9 vBcl-2 conforms to the anti-apoptotic function of the other known vBcl-2s.

In order to determine the mechanism by which A9 vBcl-2 inhibits apoptosis, protein-protein binding assays were performed. A tandem affinity purification (TAP)-fusion protein system was employed in addition to traditional immunoprecipitation to facilitate the isolation of multiple protein complexes. Much time was

spent working up this technique. Protein bands were identified that bound to TAP-A9 vBcl-2. However, protein could not be characterised, probably due to the small quantity of protein obtained being insufficient for proteolytic degradation and mass spectrometry analysis. The TAP method is currently being refined by colleagues in the laboratory.

However, it is important to point out that others have carried out Bcl-2 protein-binding studies with conflicting results. Co-immuno-precipitation studies with KSHV Bcl-2 and the cellular homologues Bcl-2, Bcl-x_L, Bax and Bak failed to demonstrate heterodimer formation (Cheng *et al.*, 1997). Using the yeast two-hybrid system, it was demonstrated that EBV BHRF1 protein interacted with Bax, Bak and Bik (Hsu *et al.*, 1997). However, others have failed to find interactions between BHRF1 vBcl-2 and Bax, Bak and Bik (Hsu & Hsueh, 1998). BALF1 inhibits the anti-apoptotic function of BHRF1 vBcl-2 and KSHV Bcl-2 but not cellular Bcl-x_L (Bellows *et al.*, 2002). From these results, it is possible that the affinity of binding between Bcl-2 proteins is not strong. This suggests that conditions to identify A9 vBcl-2-binding partners will need to be optimised more carefully.

In this study, A9 vBcl-2 was expressed as an early through to late virus gene during the productive phase of the virus life cycle in culture. Expression at this time coupled to the ability to inhibit apoptosis confers on vBcl-2 an important role in prolonging the life of virus-infected cells to support virus replication and virion production. This is consistent with other viral Bcl-2s that are active during the productive phase of the virus life cycle. For example, the Bcl-2 homologues present in HHV-8, EBV and MHV-68 are also expressed during the productive phase of the virus life cycle (Cheng *et al.*, 1997; Farrell, 1989; Roy *et al.*, 2000).

What is not clear is whether A9 vBcl-2 is active during latent infection. Examples of vBcl-2 expression during latent infection have been described for EBV and MHV-68. EBV infects B-lymphocytes, causes immortalisation and establishes a latent infection. In EBV the two Bcl-2 homologues BALF1 and BHRF1 are dispensable for efficient B-cell immortalisation when deleted individually, however, when they are deleted as a double gene knockout the virus fails to immortalise B-lymphocytes. This suggests that both Bcl-2 homologues are essential to establish a latent infection (Altmann & Hammerschmidt, 2003).

The vBcl-2 present in MHV-68 is not essential for replication during acute infection of mice (even though it is expressed during this phase), as loss of function vBcl-2 mutants replicated as well as wild type virus. This study also found that vBcl-2 was not required for the establishment of latency in splenocytes. However, the MHV-68 vBcl-2 was necessary for reactivation from latency (Gangappa *et al.*, 2002).

Details of the latent state in AIHV-1 and OvHV-2 infection have not yet been defined and so this type of study is currently not possible. These studies would be best performed in the host reservoir species (blue wildebeest for AIHV-1) where both productive and latent states have been strongly implicated. The situation in the MCF-susceptible host is more complex. In this study, A9 vBcl-2 was expressed in an AIHV-1-infected rabbit LGL cell line, and although not detected after 21 days of the development of the cells in culture, work carried out in the laboratory previously had demonstrated that A9 vBcl-2 mRNA was expressed in established AIHV-1+ LGL cell lines (H. Wright, personal communication). It is possible that these lines support both the productive and latent phases of the virus life cycle and it is possible that vBcl-2 may be expressed in one but not the other. LGL lines acquire a uniform phenotype, the majority in cattle (OvHV-2) and rabbits (AIHV-1 and OvHV-2) being T cells with indiscriminate cytotoxic activity. The majority (typically >90%) of the LGLs in any given line express viral antigen detected by immunofluorescence using virus-specific sera (Swa, 2000). Preliminary studies using Gardella gel analysis of viral DNA in LGL cell lines from rabbits infected with AIHV-1 or OvHV-2 and cattle infected with OvHV-2 indicate that the cell lines contain a mixture of lytic-(productive) and latent-infected cells. Gardella analysis discriminates linear from covalently-closed circular viral genomes, which are characteristic of either productive or latent herpesvirus infection respectively. Gardella analysis of OvHV-2-infected LGL cells has demonstrated that in both bovine and rabbit LGL cells, there are both lytic and latent cycle viral genomes present (Rosbottom *et al.*, 2002). However, there is evidence of more productive, lytic infection in the rabbit cell lines compared to the bovine cell line that predominantly contained closed circular viral DNA (Rosbottom *et al.*, 2002; T. Leenadevi, personal communication). These results would suggest that the AIHV-1-infected LGL cell cultures established from

infected rabbits contain a mixture of lytic and latently-infected cells. It is worth noting that in LGL lines virus is cell-associated and virions can only be obtained with difficulty from cell lysates. This would imply that the productive phase of the virus life cycle in these cells is inefficient, even if the cells can be used to transmit the disease. Future studies will reveal whether A9 vBcl-2 is produced during the latent phase of the virus life cycle or not.

Attempts during the course of this study to inhibit A9 vBcl-2 in fibroblasts using siRNA were unsuccessful. It was hoped to express siRNA in a retroviral vector for efficient transduction into LGLs to determine the effect of A9 mRNA knockdown on LGL phenotype and function. For successful siRNA gene expression suppression, several siRNAs per gene are recommended. Only one set was obtainable for A9. However, others in the laboratory are successfully progressing this technology such as we are now confident that we can knock down virus gene expression in LGLs. All of the unique genes of AIHV-1 and OvHV-2 are currently being targeted in this way.

The results of this thesis allow a speculation as to the possible role of A9 vBcl-2 in vivo in the pathogenesis of the disease. Clearly, there is a role in prolonging the life of infected target cells in the reservoir blue wildebeest host in order to support virion production. This is most likely to occur in epithelial cells in young calves. The presence of virus in nasal and ocular secretions in these animals within 9 or so months of birth would support this (Mushi *et al.*, 1981). Such animals are thought to be the source of MCF in pastoralists' cattle grazing areas of wildebeest migration in east-central Africa. In older animals, virus secretion is much reduced although animals are persistently virus DNA positive in their blood cells. This is most likely due to the host immune response inhibiting the productive virus cycle (neutralising antibody and T cells) and applying pressure to maintain a latent state. The cell reservoir for virus latency is not known for AIHV-1 in wildebeest, but is thought to be B cells in sheep with OvHV-2 (Baxter *et al.*, 1997).

In susceptible animals (cattle, experimentally-infected rabbits), MCF is often acute and fatal, with a short time period between the onset of symptoms and death. The reason why only a proportion of a herd of cattle will succumb to such a lethal disease is one of the fascinations of MCF. There is no horizontal spread of the disease though, as cattle are dead-end hosts in this respect. In this scenario, the

pathology is interesting. There is evidence of lymphoproliferation and lymphoblast accumulation in multiple tissues (lymphoid and non-lymphoid). Tissue damage/necrosis can be widespread. However, virus is extremely difficult to detect in affected tissues and viral DNA is in low abundance as detected by either PCR or in situ hybridisation (Tham, 1997). This implies that there are a few virus-infected cells in total and only a few of the accumulating lymphoblasts are virus DNA positive. However, infection may stimulate the accumulation and activation of non-infected lymphocytes. When tissues are cultured from MCF-affected animal tissue, LGLs grow out, virtually all of which contain viral antigens or viral transcripts and are dysregulated compared to normal cell counterparts (Swa *et al.*, 2001). One explanation for this is that virus-infected cells exhibit a growth advantage over other lymphocytes in these cultures. Thus LGLs represent an enriched population of the infected, indiscriminately-cytotoxic cells found in MCF *in vivo*. In the absence of any direct proof, the working hypothesis for MCF in this laboratory is that the disease is due to the action of indiscriminately cytotoxic lymphocytes (mainly T cells) on host tissue. Vasculitis caused by endothelial cell damage may be a major reason for the quick demise of MCF-affected animals.

Against this background, a role for A9 vBcl-2 may be to prolong the life of virus-infected cells *in vivo*, particularly the lymphoblasts. As LGLs from MCF-affected animals will transmit MCF into other susceptible animals when injected intravenously, the assumption is that the productive virus life cycle occurs in the susceptible animals and in lymphoblasts, even if virions are not apparently produced from these cells and the infection is therefore cell-associated. The mixture of lytic and latent virus life cycle stages that are seen in LGLs in culture needs to be confirmed or not with infected cells *in vivo*. In addition, there is a need to resolve whether vBcl-2 is expressed during latency either in maintaining the latent state or involved in reactivation from latency into the productive virus cycle.

The work presented in this study has improved our understanding of the biology of the Bcl-2 homologue present in AIHV-1 and shed light on an aspect of virus pathogenesis. These results form a basis for further work. For example, does A9 play a role in latency during establishment or reactivation? Does A9 form a heterodimer with A4.5? What other Bcl-2 family members do these proteins bind

to? This work provokes continuing and new possibilities of investigation for research in MCF.

References

Abbot,S.D., Rowe,M., Cadwallader,K., Ricksten,A., Gordon,J., Wang,F., Rymo,L., and Rickinson,A.B. (1990) Epstein-Barr virus nuclear antigen 2 induces expression of the virus-encoded latent membrane protein. *J.Virol.* **64**, 2126-2134.

Ablashi,D.V., Schirm,S., Fleckenstein,B., Faggioni,A., Dahlberg,J., Rabin,H., Loeb,W., Armstrong,G., Peng,J.W., Aulakh,G., and . (1985) Herpesvirus saimiri-induced lymphoblastoid rabbit cell line: growth characteristics, virus persistence, and oncogenic properties. *J.Virol.* **55**, 623-633.

Acehan,D., Jiang,X., Morgan,D.G., Heuser,J.E., Wang,X. and Akey,C.W. (2002) Three-dimensional structure of the apoptosome: implications for assembly, procaspase-9 binding, and activation. *Mol.Cell.* **9**, 423-432.

Adams,J.M. and Cory,S. (1998) The Bcl-2 protein family: arbiters of cell survival. *Science* **281**, 1322-1326.

Aeillo, S. Rinderpest: Introduction. In: Merck veterinary manual. Ed 8. Whitehouse Station, NJ: Merck & Co, 1998:542-4.

Agami,R. (2002) RNAi and related mechanisms and their potential use for therapy. *Curr.Opin.Chem.Biol.* **6**, 829-834.

Ahuja,S.K. and Murphy,P.M. (1993) Molecular piracy of mammalian interleukin-8 receptor type B by herpesvirus saimiri. *J.Biol.Chem.* **268**, 20691-20694.

Albrecht,J.C.; Nicholas,J.; Biller,D.; Cameron,K.R.; Biesinger,B.; Newman,C.; Wittmann,S.; Craxton,M.A.; Coleman,H. and Fleckenstein,B. (1992) Primary structure of the herpesvirus saimiri genome. *J.Virol.* **66**, 5047-5058.

Alcami,A. and Koszinowski,U.H. (2000) Viral mechanisms of immune evasion. *Trends Microbiol.* **8**, 410-418.

Altmann, M. and Hammerschmidt, W. (2003) Initiation of latency in infected B-lymphocytes is the third phase of EBV's life cycle. Proceedings of 28th International Herpesvirus Workshop. Abstract 10.01.

Antonsson,B. and Martinou,J.C. (2000) The Bcl-2 protein family. *Exp.Cell Res.* **256**, 50-57.

Arvanitakis,L., Geras-Raaka,E., Varma,A., Gershengorn,M.C., and Cesarman,E. (1997) Human herpesvirus KSHV encodes a constitutively active G-protein-coupled receptor linked to cell proliferation. *Nature* **385**, 347-350.

Ashkenazi,A. and Dixit,V.M. (1998) Death receptors: signaling and modulation. *Science* **281**, 1305-1308.

Bakhshi,A., Jensen,J.P., Goldman,P., Wright,J.J., McBride,O.W., Epstein,A.L., and Korsmeyer,S.J. (1985) Cloning the chromosomal breakpoint of t(14;18) human

lymphomas: clustering around JH on chromosome 14 and near a transcriptional unit on 18. *Cell* **41**, 899-906.

Bankier, A.T., Deininger, P.L., Farrell, P.J., and Barrell, B.G. (1983) Sequence analysis of the 17,166 base-pair EcoRI fragment C of B95-8 Epstein-Barr virus. *Mol.Biol.Med.* **1**, 21-45.

Banyer, J.L., Hamilton, N.H., Ramshaw, I.A., and Ramsay, A.J. (2000) Cytokines in innate and adaptive immunity. *Rev.Immunogenet.* **2**, 359-373.

Barber, G.N. (2001) Host defense, viruses and apoptosis. *Cell Death.Differ.* **8**, 113-126.

Barnard, B.J. and Van de Pypekamp, H.E. (1988) Wildebeest-derived malignant catarrhal fever: unusual epidemiology in South Africa. *Onderstepoort J.Vet.Res.* **55**, 69-71.

Barnard, B.J., Van de Pypekamp, H.F., and Griessel, M.D. (1989) Epizootology of wildebeest-derived malignant catarrhal fever in an outbreak in the north-western Transvaal: indications of an intermediate host. *Onderstepoort J.Vet.Res.* **56**, 135-139.

Barnard, B. J., van der Lugt, J. J. and Mushi, E. Z.. 1994. Malignant Catarrhal Fever,. *In* J. A. Coetzer, G. R. Thomson, and R. C. Tustin (eds.), *Infectious diseases of livestock with special reference to Southern Africa*. Oxford University Press, Cape Town, SA. p. 946-957

Bellows, D.S., Chau, B.N., Lee, P., Lazebnik, Y., Burns, W.H., and Hardwick, J.M. (2000) Antiapoptotic herpesvirus Bcl-2 homologs escape caspase-mediated conversion to proapoptotic proteins. *J.Virol.* **74**, 5024-5031.

Bellows, D.S., Howell, M., Pearson, C., Hazlewood, S.A., and Hardwick, J.M. (2002) Epstein-Barr virus BALF1 is a BCL-2-like antagonist of the herpesvirus antiapoptotic BCL-2 proteins. *J.Virol.* **76**, 2469-2479.

Biron, C.A. (1997) Natural killer cell regulation during viral infection. *Biochem.Soc.Trans.* **25**, 687-690.

Biron, C.A. (1997) Activation and function of natural killer cell responses during viral infections. *Curr.Opin.Immunol.* **9**, 24-34.

Blaskovic, D., Stancekova, M., Svobodova, J., and Mistrikova, J. (1980) Isolation of five strains of herpesviruses from two species of free living small rodents. *Acta Virol.* **24**, 468.

Block, T.M., Deshmane, S., Masonis, J., Maggioncalda, J., Valyi-Nagi, T., and Fraser, N.W. (1993) An HSV LAT null mutant reactivates slowly from latent infection and makes small plaques on CV-1 monolayers. *Virology* **192**, 618-630.

Borner, C., Martinou, I., Mattmann, C., Irmeler, M., Schaerer, E., Martinou, J.C., and Tschopp, J. (1994) The protein bcl-2 alpha does not require membrane attachment, but two conserved domains to suppress apoptosis. *J.Cell Biol.* **126**, 1059-1068.

- Borner,C., Olivier,R., Martinou,I., Mattmann,C., Tschopp,J., and Martinou,J.C. (1994) Dissection of functional domains in Bcl-2 alpha by site-directed mutagenesis. *Biochem. Cell Biol.* **72**, 463-469.
- Boshoff,C., Schulz,T.F., Kennedy,M.M., Graham,A.K., Fisher,C., Thomas,A., McGee,J.O., Weiss,R.A., and O'Leary,J.J. (1995) Kaposi's sarcoma-associated herpesvirus infects endothelial and spindle cells. *Nat.Med.* **1**, 1274-1278.
- Bouveret,E., Rigaut,G., Shevchenko,A., Wilm,M., and Seraphin,B. (2000) A Sm-like protein complex that participates in mRNA degradation. *EMBO J.* **19**, 1661-1671.
- Boya,P., Roques,B., and Kroemer,G. (2001) New EMBO members' review: viral and bacterial proteins regulating apoptosis at the mitochondrial level. *EMBO J.* **20**, 4325-4331.
- Broll,H., Finsterbusch,T., Buhk,H.J., and Goltz,M. (1999) Genetic analysis of the bovine herpesvirus type 4 gene locus for the putative terminase. *Virus Genes* **19**, 243-250.
- Brooks,M.A., Ali,A.N., Turner,P.C., and Moyer,R.W. (1995) A rabbitpox virus serpin gene controls host range by inhibiting apoptosis in restrictive cells. *J.Virol.* **69**, 7688-7698.
- Buell, G. and Panayotos, N. (1986) Mechanism and Practice. In Maximizing Gene expression (Reznikoff, W. and Gold, L., eds) Butterworth Publishers, Boston, MA.
- Burysek,L. and Pitha,P.M. (2001) Latently expressed human herpesvirus 8-encoded interferon regulatory factor 2 inhibits double-stranded RNA-activated protein kinase. *J.Virol.* **75**, 2345-2352.
- Caspary,F., Shevchenko,A., Wilm,M., and Seraphin,B. (1999) Partial purification of the yeast U2 snRNP reveals a novel yeast pre-mRNA splicing factor required for pre-spliceosome assembly. *EMBO J.* **18**, 3463-3474.
- Castro,A.E. and Daley,G.G. (1982) Electron microscopic study of the African strain of malignant catarrhal fever virus in bovine cell cultures. *Am.J.Vet.Res.* **43**, 576-582.
- Cesarman,E., Chang,Y., Moore,P.S., Said,J.W., and Knowles,D.M. (1995) Kaposi's sarcoma-associated herpesvirus-like DNA sequences in AIDS-related body-cavity-based lymphomas. *N.Engl.J.Med.* **332**, 1186-1191.
- Chang,H.Y. and Yang,X. (2000) Proteases for cell suicide: functions and regulation of caspases. *Microbiol.Mol.Biol.Rev.* **64**, 821-846.
- Chen,B.P., Wolfgang,C.D., and Hai,T. (1996) Analysis of ATF3, a transcription factor induced by physiological stresses and modulated by gadd153/Chop10. *Mol.Cell Biol.* **16**, 1157-1168.

- Chen, J., Ueda, K., Sakakibara, S., Okuno, T., Parravicini, C., Corbellino, M., and Yamanishi, K. (2001) Activation of latent Kaposi's sarcoma-associated herpesvirus by demethylation of the promoter of the lytic transactivator. *Proc.Natl.Acad.Sci.U.S.A* **98**, 4119-4124.
- Cheng, E.H., Nicholas, J., Bellows, D.S., Hayward, G.S., Guo, H.G., Reitz, M.S., and Hardwick, J.M. (1997) A Bcl-2 homolog encoded by Kaposi sarcoma-associated virus, human herpesvirus 8, inhibits apoptosis but does not heterodimerize with Bax or Bak. *Proc.Natl.Acad.Sci.U.S.A* **94**, 690-694.
- Chiarugi, V., Cinelli, M., Magnelli, L., and Dello, S.P. (2002) Apoptosis: molecular regulation of cell death and hematologic malignancies. *Mol.Biotechnol.* **20**, 305-314.
- Cho, M.S., Jeang, K.T., and Hayward, S.D. (1985) Localization of the coding region for an Epstein-Barr virus early antigen and inducible expression of this 60-kilodalton nuclear protein in transfected fibroblast cell lines. *J.Virol.* **56**, 852-859.
- Clemens, M.J. and Elia, A. (1997) The double-stranded RNA-dependent protein kinase PKR: structure and function. *J.Interferon Cytokine Res.* **17**, 503-524.
- Cohen, J.I. (2000) Epstein-Barr virus infection. *N.Engl.J.Med.* **343**, 481-492.
- Compton, M.M. and Cidlowski, J.A. (1986) Rapid in vivo effects of glucocorticoids on the integrity of rat lymphocyte genomic deoxyribonucleic acid. *Endocrinology* **118**, 38-45.
- Cossarizza, A., Baccarani-Contri, M., Kalashnikova, G., and Franceschi, C. (1993) A new method for the cytofluorimetric analysis of mitochondrial membrane potential using the J-aggregate forming lipophilic cation 5,5',6,6'-tetrachloro-1,1',3,3'-tetraethylbenzimidazolcarbocyanine iodide (JC-1). *Biochem.Biophys.Res.Commun.* **197**, 40-45.
- Coulter, L.J., Wright, H., and Reid, H.W. (2001) Molecular genomic characterization of the viruses of malignant catarrhal fever. *J.Comp Pathol.* **124**, 2-19.
- Cox, D.M., Du, M., Guo, X., Siu, K.W., and McDermott, J.C. (2002) Tandem affinity purification of protein complexes from mammalian cells. *Biotechniques* **33**, 267-8, 270.
- Crawford, T.B., Li, H., Rosenburg, S.R., Norhausen, R.W., and Garner, M.M. (2002) Mural folliculitis and alopecia caused by infection with goat-associated malignant catarrhal fever virus in two sika deer. *J.Am.Vet.Med.Assoc.* **221**, 813-7, 801.
- Datta, R., Kojima, H., Banach, D., Bump, N.J., Talanian, R.V., Alnemri, E.S., Weichselbaum, R.R., Wong, W.W., and Kufe, D.W. (1997) Activation of a CrmA-insensitive, p35-sensitive pathway in ionizing radiation-induced apoptosis. *J.Biol.Chem.* **272**, 1965-1969.

Dawson,C.W., Dawson,J., Jones,R., Ward,K., and Young,L.S. (1998) Functional differences between BHRF1, the Epstein-Barr virus-encoded Bcl-2 homologue, and Bcl-2 in human epithelial cells. *J.Virol.* **72**, 9016-9024.

De Smet,W., Vaeck,M., Smet,E., Brys,L., and Hamers,R. (1983) Rabbit leukocyte surface antigens defined by monoclonal antibodies. *Eur.J.Immunol.* **13**, 919-928.

Denholm,L.J. and Westbury,H.A. (1982) Malignant catarrhal fever in farmed Rusa deer (*Cervus timorensis*). 1. Clinico-pathological observations. *Aust.Vet.J.* **58**, 81-87.

Desagher,S., Osen-Sand,A., Nichols,A., Eskes,R., Montessuit,S., Lauper,S., Maundrell,K., Antonsson,B., and Martinou,J.C. (1999) Bid-induced conformational change of Bax is responsible for mitochondrial cytochrome c release during apoptosis. *J.Cell Biol.* **144**, 891-901.

Devitt,A., Moffatt,O.D., Raykundalia,C., Capra,J.D., Simmons,D.L., and Gregory,C.D. (1998) Human CD14 mediates recognition and phagocytosis of apoptotic cells. *Nature* **392**, 505-509.

Dimitrov,T., Krajcsi,P., Hermiston,T.W., Tollefson,A.E., Hannink,M. and Wold,W.S. (1997) Adenovirus E3-10.4K/14.5K protein complex inhibits tumor necrosis factor-induced translocation of cytosolic phospholipase A2 to membrane. *J.Virol.* **71**, 2830-2837.

Djerbi,M., Screpanti,V., Catrina,A.I., Bogen,B., Biberfeld,P., and Grandien,A. (1999) The inhibitor of death receptor signaling, FLICE-inhibitory protein defines a new class of tumor progression factors. *J.Exp.Med.* **190**, 1025-1032.

Dowler,K.W. and Veltri,R.W. (1984) In vitro neutralization of HSV-2: inhibition by binding of normal IgG and purified Fc to virion Fc receptor (FcR). *J.Med.Virol.* **13**, 251-259.

Du,C., Fang,M., Li,L. and Wang,X. (2000) Smac, a mitochondrial protein that promotes cytochrome c-dependent caspase activation by eliminating IAP inhibition. *Cell.* **102**, 33-42.

Duboise,S.M., Guo,J., Czajak,S., Desrosiers,R.C., and Jung,J.U. (1998) STP and Tip are essential for herpesvirus saimiri oncogenicity. *J.Virol.* **72**, 1308-1313.

Dupin,N., Diss,T.L., Kellam,P., Tulliez,M., Du,M.Q., Sicard,D., Weiss,R.A., Isaacson,P.G., and Boshoff,C. (2000) HHV-8 is associated with a plasmablastic variant of Castleman disease that is linked to HHV-8-positive plasmablastic lymphoma. *Blood* **95**, 1406-1412.

Edington,N. and PLOWRIGHT,W. (1980) The protection of rabbits against the herpesvirus of malignant catarrhal fever by inactivated vaccines. *Res.Vet.Sci.* **28**, 384-386.

- Ehlers,B., Ulrich,S., and Goltz,M. (1999) Detection of two novel porcine herpesviruses with high similarity to gammaherpesviruses. *J.Gen.Virol.* **80** (Pt 4), 971-978.
- Ehtisham,S., Sunil-Chandra,N.P., and Nash,A.A. (1993) Pathogenesis of murine gammaherpesvirus infection in mice deficient in CD4 and CD8 T cells. *J.Virol.* **67**, 5247-5252.
- El-Deiry,W.S., Tokino,T., Velculescu,V.E., Levy,D.B., Parsons,R., Trent,J.M., Lin,D., Mercer,W.E., Kinzler,K.W. and Vogelstein,B. (1993) WAF1, a potential mediator of p53 tumor suppression. *Cell.* **75**, 817-825.
- Elbashir,S.M., Harborth,J., Lendeckel,W., Yalcin,A., Weber,K., and Tuschl,T. (2001) Duplexes of 21-nucleotide RNAs mediate RNA interference in cultured mammalian cells. *Nature* **411**, 494-498.
- Enari,M., Sakahira,H., Yokoyama,H., Okawa,K., Iwamatsu,A., and Nagata,S. (1998) A caspase-activated DNase that degrades DNA during apoptosis, and its inhibitor ICAD. *Nature* **391**, 43-50.
- Engels,M. and Ackermann,M. (1996) Pathogenesis of ruminant herpesvirus infections. *Vet.Microbiol.* **53**, 3-15.
- Ensser,A., Pflanz,R., and Fleckenstein,B. (1997) Primary structure of the alcelaphine herpesvirus 1 genome. *J.Virol.* **71**, 6517-6525.
- EPSTEIN,M.A. and BARR,Y.M. (1964) CULTIVATION IN VITRO OF HUMAN LYMPHOBLASTS FROM BURKITT'S MALIGNANT LYMPHOMA. *Lancet* **41**, 252-253.
- Fadok,V.A. and Chimini,G. (2001) The phagocytosis of apoptotic cells. *Semin.Immunol.* **13**, 365-372.
- Farrell, P. J. (1989) Epstein-Barr genome. In G. Klein (ed.), *Advances in viral oncology; tumorigenic DNA viruses*, vol. 8. Raven Press, Ltd., New York, N.Y. p.103-132
- Favoreel,H.W., Van de Walle,G.R., Nauwynck,H.J., and Pensaert,M.B. (2003) Virus complement evasion strategies. *J.Gen.Virol.* **84**, 1-15.
- Ferris, D.H., Hamdy, F.M. and Dardiri, A.H. (1976). Detection of African malignant catarrhal fever antigens in cell cultures by immunofluorescence. *Vet. Micro.* **1**: 437-559.
- Fickenscher,H., Bokel,C., Knappe,A., Biesinger,B., Meinl,E., Fleischer,B., Fleckenstein,B., and Broker,B.M. (1997) Functional phenotype of transformed human alphabeta and gammadelta T cells determined by different subgroup C strains of herpesvirus Saimiri. *J.Virol.* **71**, 2252-2263.
- Fickenscher,H. and Fleckenstein,B. (2001) Herpesvirus saimiri. *Philos.Trans.R.Soc.Lond B Biol.Sci.* **356**, 545-567.

- Fingerroth, J.D., Weis, J.J., Tedder, T.F., Strominger, J.L., Biro, P.A., and Fearon, D.T. (1984) Epstein-Barr virus receptor of human B lymphocytes is the C3d receptor CR2. *Proc.Natl.Acad.Sci.U.S.A* **81**, 4510-4514.
- Fiorentino, D.F., Zlotnik, A., Mosmann, T.R., Howard, M., and O'Garra, A. (1991) IL-10 inhibits cytokine production by activated macrophages. *J.Immunol.* **147**, 3815-3822.
- Fire, A., Xu, S., Montgomery, M.K., Kostas, S.A., Driver, S.E., and Mello, C.C. (1998) Potent and specific genetic interference by double-stranded RNA in *Caenorhabditis elegans*. *Nature* **391**, 806-811.
- Flach, E.J., Reid, H., Pow, I., and Klemm, A. (2002) Gamma herpesvirus carrier status of captive artiodactyls. *Res.Vet.Sci.* **73**, 93-99.
- Forler, D., Kocher, T., Rode, M., Gentzel, M., Izaurrealde, E., and Wilm, M. (2003) An efficient protein complex purification method for functional proteomics in higher eukaryotes. *Nat.Biotechnol.* **21**, 89-92.
- Friberg, J., Jr., Kong, W., Hottiger, M.O., and Nabel, G.J. (1999) p53 inhibition by the LANA protein of KSHV protects against cell death. *Nature* **402**, 889-894.
- Fruh, K., Ahn, K., Djaballah, H., Sempe, P., van Endert, P.M., Tampe, R., Peterson, P.A., and Yang, Y. (1995) A viral inhibitor of peptide transporters for antigen presentation. *Nature* **375**, 415-418.
- Gale, J., Korth, M.J.m, Tang, N.M., Tan, S.L., Hopkins, D.A., Dever, T.E., Polyak, S.J., Gretch, D.R. and Katze, M.G. (1997) Evidence that hepatitis C virus resistance to interferon is mediated through repression of the PKR protein kinase by nonstructural 5A protein. *Virology.* **230**, 217-227.
- Galvan, V. and Roizman, B. (1998) Herpes simplex virus 1 induces and blocks apoptosis at multiple steps during infection and protects cells from endogenous inducers in a cell-type-dependent manner. *Proc.Natl.Acad.Sci.* **95**, 3931-3936.
- Gangappa, S., van Dyk, L.F., Jewett, T.J., Speck, S.H., and Virgin, H.W. (2002) Identification of the in vivo role of a viral bcl-2. *J.Exp.Med.* **195**, 931-940.
- Gardella, T., Medveczky, P., Sairenji, T., and Mulder, C. (1984) Detection of circular and linear herpesvirus DNA molecules in mammalian cells by gel electrophoresis. *J.Virol.* **50**, 248-254.
- Gilmore, A.P., Metcalfe, A.D., Romer, L.H., and Streuli, C.H. (2000) Integrin-mediated survival signals regulate the apoptotic function of Bax through its conformation and subcellular localization. *J.Cell Biol.* **149**, 431-446.
- Glykofrydes, D., Niphuis, H., Kuhn, E.M., Rosenwirth, B., Heeney, J.L., Bruder, J., Niedobitek, G., Muller-Fleckenstein, I., Fleckenstein, B., and Ensser, A. (2000) Herpesvirus

saimiri vFLIP provides an antiapoptotic function but is not essential for viral replication, transformation, or pathogenicity. *J.Virol.* **74**, 11919-11927.

Godden-Kent,D., Talbot,S.J., Boshoff,C., Chang,Y., Moore,P., Weiss,R.A., and Mittnacht,S. (1997) The cyclin encoded by Kaposi's sarcoma-associated herpesvirus stimulates cdk6 to phosphorylate the retinoblastoma protein and histone H1. *J.Virol.* **71**, 4193-4198.

Goltz,M., Ericsson,T., Patience,C., Huang,C.A., Noack,S., Sachs,D.H., and Ehlers,B. (2002) Sequence analysis of the genome of porcine lymphotropic herpesvirus 1 and gene expression during posttransplant lymphoproliferative disease of pigs. *Virology* **294**, 383-393.

Gong,M.and Kieff,E. (1990) Intracellular trafficking of two major Epstein-Barr virus glycoproteins, gp350/220 and gp110. *J.Virol.* **64**, 1507-1516.

Gonzalez-Garcia,M., Garcia,I., Ding,L., O'Shea,S., Boise,L.H., Thompson,C.B., and Nunez,G. (1995) bcl-x is expressed in embryonic and postnatal neural tissues and functions to prevent neuronal cell death. *Proc.Natl.Acad.Sci.U.S.A* **92**, 4304-4308.

Goodbourn,S., Didcock,L., and Randall,R.E. (2000) Interferons: cell signalling, immune modulation, antiviral response and virus countermeasures. *J.Gen.Virol.* **81**, 2341-2364.

Goshima,Y., Ito,T., Sasaki,Y., and Nakamura,F. (2002) Semaphorins as signals for cell repulsion and invasion. *J.Clin.Invest* **109**, 993-998.

Gottlieb,R.A. (2000) Mitochondria: execution central. *FEBS Lett.* **482**, 6-12.

Gottlieb,T.M. and Oren,M. (1998) p53 and apoptosis. *Semin.Cancer.Biol.* **8**, 359-368.

Graham,S.P., Jones,G.E., MacLean,M., Livingstone,M., and Entrican,G. (1995) Recombinant ovine interferon gamma inhibits the multiplication of Chlamydia psittaci in ovine cells. *J.Comp Pathol.* **112**, 185-195.

Green,D. and Kroemer,G. (1998) The central executioners of apoptosis: caspases or mitochondria? *Trends Cell Biol.* **8**, 267-271.

Green,D.R. and Reed,J.C. (1998) Mitochondria and apoptosis. *Science* **281**, 1309-1312.

Gross,A., McDonnell,J.M., and Korsmeyer,S.J. (1999) BCL-2 family members and the mitochondria in apoptosis. *Genes Dev.* **13**, 1899-1911.

Guex,N. and Peitsch,M.C. (1997) SWISS-MODEL and the Swiss-PdbViewer: an environment for comparative protein modeling. *Electrophoresis* **18**, 2714-2723.

Haig,D.M. (2001) Subversion and piracy: DNA viruses and immune evasion. *Res.Vet.Sci.* **70**, 205-219.

Haig,D.M., Thomson,J., McInnes,C.J., Deane,D.L., Anderson,I.E., McCaughan,C.A., Imlach,W., Mercer,A.A., Howard,C.J., and Fleming,S.B. (2002) A comparison of the anti-inflammatory and immuno-stimulatory activities of orf virus and ovine interleukin-10. *Virus Res.* **90**, 303-316.

Hamdy,F.M., Dardiri,A.H., Mebus,C., Pierson,R.E., and Johnson,D. (1978) Etiology of malignant catarrhal fever outbreak in Minnesota. *Proc.Annu.Meet.U.S.Anim Health Assoc.* 248-267.

Hammond,S.M., Bernstein,E., Beach,D., and Hannon,G.J. (2000) An RNA-directed nuclease mediates post-transcriptional gene silencing in *Drosophila* cells. *Nature* **404**, 293-296.

Handley,J.A., Sargan,D.R., Herring,A.J., and Reid,H.W. (1995) Identification of a region of the alcelaphine herpesvirus-1 genome associated with virulence for rabbits. *Vet.Microbiol.* **47**, 167-181.

Hardwick,J.M. and Bellows,D.S. (2003) Viral versus cellular BCL-2 proteins. *Cell Death.Differ.* **10 Suppl 1**, S68-S76.

Harris,M.H. and Thompson,C.B. (2000) The role of the Bcl-2 family in the regulation of outer mitochondrial membrane permeability. *Cell Death.Differ.* **7**, 1182-1191.

Hartman,P.S. (1991) Transillumination can profoundly reduce transformation frequencies. *Biotechniques* **11**, 747-748.

Heemels,M.T. and Ploegh,H. (1995) Generation, translocation, and presentation of MHC class I-restricted peptides. *Annu.Rev.Biochem.* **64**, 463-491.

Henderson,S., Huen,D., Rowe,M., Dawson,C., Johnson,G., and Rickinson,A. (1993) Epstein-Barr virus-coded BHRF1 protein, a viral homologue of Bcl-2, protects human B cells from programmed cell death. *Proc.Natl.Acad.Sci.U.S.A* **90**, 8479-8483.

Hengartner,M.O. (2000) The biochemistry of apoptosis. *Nature* **407**, 770-776.

Heuschele,W.P., Nielsen,N.O., Oosterhuis,J.E., and Castro,A.E. (1985) Dexamethasone-induced recrudescence of malignant catarrhal fever and associated lymphosarcoma and granulomatous disease in a Formosan sika deer (*Cervus nippon taiouanus*). *Am.J.Vet.Res.* **46**, 1578-1583.

Hickish,T., Robertson,D., Clarke,P., Hill,M., di Stefano,F., Clarke,C., and Cunningham,D. (1994) Ultrastructural localization of BHRF1: an Epstein-Barr virus gene product which has homology with bcl-2. *Cancer Res.* **54**, 2808-2811.

Hinchcliff, K. W., Radostits, O. M., Gay, C. C. and Blood D. C. (2000) Veterinary medicine: a textbook of the diseases of cattle, sheep, pigs, goats and horses, p. 1081-1085. Harcourt Publishers Limited, London, United Kingdom.

Hockenbery,D., Nunez,G., Milliman,C., Schreiber,R.D., and Korsmeyer,S.J. (1990) Bcl-2 is an inner mitochondrial membrane protein that blocks programmed cell death. *Nature* **348**, 334-336.

Hockenbery,D.M., Oltvai,Z.N., Yin,X.M., Milliman,C.L., and Korsmeyer,S.J. (1993) Bcl-2 functions in an antioxidant pathway to prevent apoptosis. *Cell* **75**, 241-251.

Holmgren,S.P., Huang,D.C., Adams,J.M., and Cory,S. (1999) Survival activity of Bcl-2 homologs Bcl-w and A1 only partially correlates with their ability to bind pro-apoptotic family members. *Cell Death.Differ.* **6**, 525-532.

Holmgren,A. (1985) Thioredoxin. *Annu.Rev.Biochem.* **54**, 237-271.

Hooft,R.W., Vriend,G., Sander,C., and Abola,E.E. (1996) Errors in protein structures. *Nature* **381**, 272.

Hsu,S.Y., Kaipia,A., McGee,E., Lomeli,M., and Hsueh,A.J. (1997) Bok is a pro-apoptotic Bcl-2 protein with restricted expression in reproductive tissues and heterodimerizes with selective anti-apoptotic Bcl-2 family members. *Proc.Natl.Acad.Sci.U.S.A* **94**, 12401-12406.

Hsu,S.Y. and Hsueh,A.J. (1998) A splicing variant of the Bcl-2 member Bok with a truncated BH3 domain induces apoptosis but does not dimerize with antiapoptotic Bcl-2 proteins in vitro. *J.Biol.Chem.* **273**, 30139-30146.

Hu,S., Vincenz,C., Buller,M., and Dixit,V.M. (1997) A novel family of viral death effector domain-containing molecules that inhibit both CD-95- and tumor necrosis factor receptor-1-induced apoptosis. *J.Biol.Chem.* **272**, 9621-9624.

Huang,C.A., Fuchimoto,Y., Gleit,Z.L., Ericsson,T., Griesemer,A., Scheier-Dolberg,R., Melendy,E., Kitamura,H., Fishman,J.A., Ferry,J.A., Harris,N.L., Patience,C., and Sachs,D.H. (2001) Posttransplantation lymphoproliferative disease in miniature swine after allogeneic hematopoietic cell transplantation: similarity to human PTLN and association with a porcine gammaherpesvirus. *Blood* **97**, 1467-1473.

Huang,D.C., Adams,J.M., and Cory,S. (1998) The conserved N-terminal BH4 domain of Bcl-2 homologues is essential for inhibition of apoptosis and interaction with CED-4. *EMBO J.* **17**, 1029-1039.

Huang,Q., Petros,A.M., Virgin,H.W., Fesik,S.W., and Olejniczak,E.T. (2002) Solution structure of a Bcl-2 homolog from Kaposi sarcoma virus. *Proc.Natl.Acad.Sci.U.S.A* **99**, 3428-3433.

Huck, R. Shand, A., A. Allsop, P. J. and Paterson, A. B. (1961) Malignant Catarrh of Deer. *Vet. Rec.* **73**:457-465.

Hunter,J.J. and Parslow,T.G. (1996) A peptide sequence from Bax that converts Bcl-2 into an activator of apoptosis. *J.Biol.Chem.* **271**, 8521-8524.

Inman,M., Perng,G.C., Henderson,G., Ghiasi,H., Nesburn,A.B., Wechsler,S.L., and Jones,C. (2001) Region of herpes simplex virus type 1 latency-associated transcript sufficient for wild-type spontaneous reactivation promotes cell survival in tissue culture. *J.Virol.* **75**, 3636-3646.

Jackson,S., Chused,T.M., Wilkinson,J.M., Leiserson,W.M., and Kindt,T.J. (1983) Differentiation antigens identify subpopulations of rabbit T and B lymphocytes. Definition by flow cytometry. *J.Exp.Med.* **157**, 34-46.

Jackson,S.A. and DeLuca,N.A. (2003) Relationship of herpes simplex virus genome configuration to productive and persistent infections. *Proc.Natl.Acad.Sci.U.S.A* **100**, 7871-7876.

Jacoby,R.O., Reid,H.W., Buxton,D., and Pow,I. (1988) Transmission of wildebeest-associated and sheep-associated malignant catarrhal fever to hamsters, rats and guinea-pigs. *J.Comp Pathol.* **98**, 91-98.

Jamieson,E.R. and Lippard,S.J. (1999) Structure, Recognition, and Processing of Cisplatin-DNA Adducts. *Chem.Rev.* **99**, 2467-2498.

Javier,R.T., Stevens,J.G., Dissette,V.B., and Wagner,E.K. (1988) A herpes simplex virus transcript abundant in latently infected neurons is dispensable for establishment of the latent state. *Virology* **166**, 254-257.

Jenner,R.G., Alba,M.M., Boshoff,C., and Kellam,P. (2001) Kaposi's sarcoma-associated herpesvirus latent and lytic gene expression as revealed by DNA arrays. *J.Virol.* **75**, 891-902.

Jenner,R.G. and Boshoff,C. (2002) The molecular pathology of Kaposi's sarcoma-associated herpesvirus. *Biochim.Biophys.Acta* **1602**, 1-22.

Jessup ,D.A. (1985) Malignant catarrhal fever in a free-ranging black-tailed deer (*Odocoileus hemionus columbianus*) in California. *J.Wildl.Dis* **21**, 167-169.

Johannsen,E., Koh,E., Mosialos,G., Tong,X., Kieff,E., and Grossman,S.R. (1995) Epstein-Barr virus nuclear protein 2 transactivation of the latent membrane protein 1 promoter is mediated by J kappa and PU.1. *J.Virol.* **69**, 253-262.

Jung,J.U., Stager,M., and Desrosiers,R.C. (1994) Virus-encoded cyclin. *Mol.Cell Biol.* **14**, 7235-7244.

Kagi,D., Ledermann,B., Burki,K., Zinkernagel,R.M. and Hengartner,H. (1995) Lymphocyte-mediated cytotoxicity in vitro and in vivo: mechanisms and significance. *Immunol.Rev* **146**, 95-115.

Kam,P.C. and Ferch,N.I. (2000) Apoptosis: mechanisms and clinical implications. *Anaesthesia* **55**, 1081-1093.

Karber,G. (1931) *Arch.Exp.Path. & Pharmacol.* **162**, 480

Kaye,K.M., Izumi,K.M., and Kieff,E. (1993) Epstein-Barr virus latent membrane protein 1 is essential for B-lymphocyte growth transformation. *Proc.Natl.Acad.Sci.U.S.A* **90**, 9150-9154.

Kelekar,A., Chang,B.S., Harlan,J.E., Fesik,S.W., and Thompson,C.B. (1997) Bad is a BH3 domain-containing protein that forms an inactivating dimer with Bcl-XL. *Mol.Cell Biol.* **17**, 7040-7046.

Kelekar,A. and Thompson,C.B. (1998) Bcl-2-family proteins: the role of the BH3 domain in apoptosis. *Trends Cell Biol.* **8**, 324-330.

Kent,J.R., Kang,W., Miller,C.G., and Fraser,N.W. (2003) Herpes simplex virus latency-associated transcript gene function. *J.Neurovirol.* **9**, 285-290.

Kerr,J.F., Wyllie,A.H., and Currie,A.R. (1972) Apoptosis: a basic biological phenomenon with wide-ranging implications in tissue kinetics. *Br.J.Cancer* **26**, 239-257.

Khanim,F., Dawson,C., Meseda,C.A., Dawson,J., Mackett,M., and Young,L.S. (1997) BHRF1, a viral homologue of the Bcl-2 oncogene, is conserved at both the sequence and functional level in different Epstein-Barr virus isolates. *J.Gen.Virol.* **78 (Pt 11)**, 2987-2999.

Kieff, E. and Rickinson (2001). Epstein-Barr Virus and its Replication. In *Fields Virology*, 4th edn, pp. 2343-96. Edited by D. M. K. B.N Fields, P.M. Howley, et al.: Lippincott Williams & Wilkins.

Kluck,R.M., Bossy-Wetzl,E., Green,D.R., and Newmeyer,D.D. (1997) The release of cytochrome c from mitochondria: a primary site for Bcl-2 regulation of apoptosis. *Science* **275**, 1132-1136.

Komano,J., Maruo,S., Kurozumi,K., Oda,T., and Takada,K. (1999) Oncogenic role of Epstein-Barr virus-encoded RNAs in Burkitt's lymphoma cell line Akata. *J.Virol.* **73**, 9827-9831.

Kotani,M., Yamamura,Y., Tamatani,T., Kitamura,F., and Miyasaka,M. (1993) Generation and characterization of monoclonal antibodies against rabbit CD4, CD5 and CD11a antigens. *J.Immunol.Methods* **157**, 241-252.

Kotenko,S.V., Saccani,S., Izotova,L.S., Mirochnitchenko,O.V., and Pestka,S. (2000) Human cytomegalovirus harbors its own unique IL-10 homolog (cmvIL-10). *Proc.Natl.Acad.Sci.U.S.A* **97**, 1695-1700.

Krajewski,S., Tanaka,S., Takayama,S., Schibler,M.J., Fenton,W., and Reed,J.C. (1993) Investigation of the subcellular distribution of the bcl-2 oncoprotein: residence in the nuclear envelope, endoplasmic reticulum, and outer mitochondrial membranes. *Cancer Res.* **53**, 4701-4714.

- Krebs,S., Medugorac,I., Seichter,D., and Forster,M. (2003) RNaseCut: a MALDI mass spectrometry-based method for SNP discovery. *Nucleic Acids Res.* **31**, e37.
- Laemmli,U.K. (1970) Cleavage of structural proteins during the assembly of the head of bacteriophage T4. *Nature* **227**, 680-685.
- Laman,H. and Boshoff,C. (2001) Is KSHV lytic growth induced by a methylation-sensitive switch? *Trends Microbiol.* **9**, 464-466.
- Lange,C., Liehr,T., Goen,M., Gebhart,E., Fleckenstein,B., and Ensser,A. (1998) New eukaryotic semaphorins with close homology to semaphorins of DNA viruses. *Genomics* **51**, 340-350.
- LaVallie, E.R., DiBlasio, E.A., Kovacic, S., Grant, K.L., Schendel, P.F., and McCoy, J.M. (1992) A thioredoxin gene fusion expression system that circumvents inclusion body formation in the *E. coli* cytoplasm. *Bio/technology* **11**: 187-193.
- Lehman,I.R. and Boehmer,P.E. (1999) Replication of herpes simplex virus DNA. *J.Biol.Chem.* **274**, 28059-28062.
- Li,H., Shen,D.T., Knowles,D.P., Gorham,J.R., and Crawford,T.B. (1994) Competitive inhibition enzyme-linked immunosorbent assay for antibody in sheep and other ruminants to a conserved epitope of malignant catarrhal fever virus. *J.Clin.Microbiol.* **32**, 1674-1679.
- Li,H., Shen,D.T., O'Toole,D., Knowles,D.P., Gorham,J.R., and Crawford,T.B. (1995) Investigation of sheep-associated malignant catarrhal fever virus infection in ruminants by PCR and competitive inhibition enzyme-linked immunosorbent assay. *J.Clin.Microbiol.* **33**, 2048-2053.
- Li,H., Zhu,H., Xu,C.J., and Yuan,J. (1998) Cleavage of BID by caspase 8 mediates the mitochondrial damage in the Fas pathway of apoptosis. *Cell* **94**, 491-501.
- Li,H., Zhu,H., Xu,C.J., and Yuan,J. (1998) Cleavage of BID by caspase 8 mediates the mitochondrial damage in the Fas pathway of apoptosis. *Cell* **94**, 491-501.
- Li,H., Hua,Y., Snowden,G., and Crawford,T.B. (2001) Levels of ovine herpesvirus 2 DNA in nasal secretions and blood of sheep: implications for transmission. *Vet.Microbiol.* **79**, 301-310.
- Li,Q., Spriggs,M.K., Kovats,S., Turk,S.M., Comeau,M.R., Nepom,B., and Hutt-Fletcher,L.M. (1997) Epstein-Barr virus uses HLA class II as a cofactor for infection of B lymphocytes. *J.Virol.* **71**, 4657-4662.
- Liggitt,H.D. and DeMartini,J.C. (1980) The pathomorphology of malignant catarrhal fever. I. Generalized lymphoid vasculitis. *Vet.Pathol.* **17**, 58-72.

- Liu,X., Kim,C.N., Yang,J., Jemmerson,R., and Wang,X. (1996) Induction of apoptotic program in cell-free extracts: requirement for dATP and cytochrome c. *Cell* **86**, 147-157.
- Loo,D.T. and Rillema,J.R. (1998) Measurement of cell death. *Methods Cell Biol.* **57**, 251-264.
- Lukac,D.M., Kirshner,J.R., and Ganem,D. (1999) Transcriptional activation by the product of open reading frame 50 of Kaposi's sarcoma-associated herpesvirus is required for lytic viral reactivation in B cells. *J.Virol.* **73**, 9348-9361.
- Lyttle,D.J., Fraser,K.M., Fleming,S.B., Mercer,A.A., and Robinson,A.J. (1994) Homologs of vascular endothelial growth factor are encoded by the poxvirus orf virus. *J.Virol.* **68**, 84-92.
- Mador,N., Goldenberg,D., Cohen,O., Panet,A., and Steiner,I. (1998) Herpes simplex virus type 1 latency-associated transcripts suppress viral replication and reduce immediate-early gene mRNA levels in a neuronal cell line. *J.Virol.* **72**, 5067-5075.
- Mann,K.P., Staunton,D., and Thorley-Lawson,D.A. (1985) Epstein-Barr virus-encoded protein found in plasma membranes of transformed cells. *J.Virol.* **55**, 710-720.
- Marczynska,B., Falk,L., Wolfe,L., and Deinhardt,F. (1973) Transplantation and cytogenetic studies of Herpesvirus saimiri-induced disease in Marmoset monkeys. *J.Natl.Cancer Inst.* **50**, 331-337.
- Marshall,W.L., Yim,C., Gustafson,E., Graf,T., Sage,D.R., Hanify,K., Williams,L., Fingerroth,J., and Finberg,R.W. (1999) Epstein-Barr virus encodes a novel homolog of the bcl-2 oncogene that inhibits apoptosis and associates with Bax and Bak. *J.Virol.* **73**, 5181-5185.
- Matolcsy,A., Nador,R.G., Cesarman,E., and Knowles,D.M. (1998) Immunoglobulin VH gene mutational analysis suggests that primary effusion lymphomas derive from different stages of B cell maturation. *Am.J.Pathol.* **153**, 1609-1614.
- Mattsson,K., Kiss,C., Platt,G.M., Simpson,G.R., Kashuba,E., Klein,G., Schulz,T.F., and Szekely,L. (2002) Latent nuclear antigen of Kaposi's sarcoma herpesvirus/human herpesvirus-8 induces and relocates RING3 to nuclear heterochromatin regions. *J.Gen.Virol.* **83**, 179-188.
- McCarthy,N.I., Hazlewood,S.A., Huen,D.S., Rickinson,A.B., and Williams,G.T. (1996) The Epstein-Barr virus gene BHRF1, a homologue of the cellular oncogene Bcl-2, inhibits apoptosis induced by gamma radiation and chemotherapeutic drugs. *Adv.Exp.Med.Biol.* **406**, 83-97.
- McDonnell,J.M., Fushman,D., Milliman,C.L., Korsmeyer,S.J., and Cowburn,D. (1999) Solution structure of the proapoptotic molecule BID: a structural basis for apoptotic agonists and antagonists. *Cell* **96**, 625-634.

- Medveczky,P., Szomolanyi,E., Desrosiers,R.C., and Mulder,C. (1984) Classification of herpesvirus saimiri into three groups based on extreme variation in a DNA region required for oncogenicity. *J.Virol.* **52**, 938-944.
- Melendez,L.V., Daniel,M.D., Garcia,F.G., Fraser,C.E., Hunt,R.D., and King,N.W. (1969) Herpesvirus saimiri. I. Further characterization studies of a new virus from the squirrel monkey. *Lab Anim Care* **19**, 372-377.
- Mettam, R. W. M. (1923). 9th and 10th reports of the director of veterinary education and research. Union of South Africa.
- Meseda,C.A., Arrand,J.R., and Mackett,M. (2000) Herpesvirus papio encodes a functional homologue of the Epstein-Barr virus apoptosis suppressor, BHRF1. *J.Gen.Virol.* **81**, 1801-1805.
- Miller,C.L., Burkhardt,A.L., Lee,J.H., Stealey,B., Longnecker,R., Bolen,J.B., and Kieff,E. (1995) Integral membrane protein 2 of Epstein-Barr virus regulates reactivation from latency through dominant negative effects on protein-tyrosine kinases. *Immunity.* **2**, 155-166.
- Miller,N. and Hutt-Fletcher,L.M. (1988) A monoclonal antibody to glycoprotein gp85 inhibits fusion but not attachment of Epstein-Barr virus. *J.Virol.* **62**, 2366-2372.
- Millhouse,S. and Wigdahl,B. (2000) Molecular circuitry regulating herpes simplex virus type 1 latency in neurons. *J.Neurovirol.* **6**, 6-24.
- Moore,K.W., Vieira,P., Fiorentino,D.F., Trounstein,M.L., Khan,T.A., and Mosmann,T.R. (1990) Homology of cytokine synthesis inhibitory factor (IL-10) to the Epstein-Barr virus gene BCRF1. *Science* **248**, 1230-1234.
- Motyl,T. (1999) Regulation of apoptosis: involvement of Bcl-2-related proteins. *Reprod.Nutr.Dev.* **39**, 49-59.
- Muchmore,S.W., Sattler,M., Liang,H., Meadows,R.P., Harlan,J.E., Yoon,H.S., Nettesheim,D., Chang,B.S., Thompson,C.B., Wong,S.L., Ng,S.L., and Fesik,S.W. (1996) X-ray and NMR structure of human Bcl-xL, an inhibitor of programmed cell death. *Nature* **381**, 335-341.
- Mushi,E.Z. and Rurangirwa,F.R. (1981) Malignant catarrhal fever virus infectivity in rabbit macrophages and monocytes. *Vet.Res.Comm.* **5**, 51-56.
- Mushi,E.Z. and Rurangirwa,F.R. (1981a) Epidemiology of bovine malignant catarrhal fevers, a review. *Vet.Res.Comm.* **5**, 127-142.
- Mushi,E.Z., Jessett,D.M., Rurangirwa,F.R., Rossiter,P.B., and Karstad,L. (1981b) Neutralising antibodies to malignant catarrhal fever herpesvirus in wildebeest nasal secretions. *Trop.Anim Health Prod.* **13**, 55-56.

- Mushi,E.Z. and Wafula,J.S. (1983) Infectivity of cell-free malignant catarrhal fever virus in rabbits and cattle. *Vet.Res. Commun.* **6**, 153-155.
- Nash,A.A. and Sunil-Chandra,N.P. (1994) Interactions of the murine gammaherpesvirus with the immune system. *Curr.Opin.Immunol.* **6**, 560-563.
- Nava,V.E., Cheng,E.H., Veluona,M., Zou,S., Clem,R.J., Mayer,M.L., and Hardwick,J.M. (1997) Herpesvirus saimiri encodes a functional homolog of the human bcl-2 oncogene. *J.Virol.* **71**, 4118-4122.
- Nguyen,M., Branton,P.E., Walton,P.A., Oltvai,Z.N., Korsmeyer,S.J., and Shore,G.C. (1994) Role of membrane anchor domain of Bcl-2 in suppression of apoptosis caused by E1B-defective adenovirus. *J.Biol.Chem.* **269**, 16521-16524.
- Nicholas,J., Cameron,K.R., and Honess,R.W. (1992) Herpesvirus saimiri encodes homologues of G protein-coupled receptors and cyclins. *Nature* **355**, 362-365.
- Oltvai,Z.N., Milliman,C.L., and Korsmeyer,S.J. (1993) Bcl-2 heterodimerizes in vivo with a conserved homolog, Bax, that accelerates programmed cell death. *Cell* **74**, 609-619.
- Palumbo,G.J., Buller,R.M., and Glasgow,W.C. (1994) Multigenic evasion of inflammation by poxviruses. *J.Virol.* **68**, 1737-1749.
- Parry,C.M., Simas,J.P., Smith,V.P., Stewart,C.A., Minson,A.C., Efstathiou,S., and Alcami,A. (2000) A broad spectrum secreted chemokine binding protein encoded by a herpesvirus. *J.Exp.Med.* **191**, 573-578.
- Paulose-Murphy,M., Ha,N.K., Xiang,C., Chen,Y., Gillim,L., Yarchoan,R., Meltzer,P., Bittner,M., Trent,J., and Zeichner,S. (2001) Transcription program of human herpesvirus 8 (kaposi's sarcoma-associated herpesvirus). *J.Virol.* **75**, 4843-4853.
- Peitsch,M.C., Wells,T.N., Stampf,D.R., and Sussman,J.L. (1995) The Swiss-3DImage collection and PDB-Browser on the World-Wide Web. *Trends Biochem.Sci.* **20**, 82-84.
- Perng,G.C., Dunkel,E.C., Geary,P.A., Slanina,S.M., Ghiasi,H., Kaiwar,R., Nesburn,A.B., and Wechsler,S.L. (1994) The latency-associated transcript gene of herpes simplex virus type 1 (HSV-1) is required for efficient in vivo spontaneous reactivation of HSV-1 from latency. *J.Virol.* **68**, 8045-8055.
- Perng,G.C., Slanina,S.M., Yukht,A., Drolet,B.S., Keleher,W., Jr., Ghiasi,H., Nesburn,A.B., and Wechsler,S.L. (1999) A herpes simplex virus type 1 latency-associated transcript mutant with increased virulence and reduced spontaneous reactivation. *J.Virol.* **73**, 920-929.
- Perng,G.C., Jones,C., Ciacci-Zanella,J., Stone,M., Henderson,G., Yukht,A., Slanina,S.M., Hofman,F.M., Ghiasi,H., Nesburn,A.B., and Wechsler,S.L. (2000) Virus-

induced neuronal apoptosis blocked by the herpes simplex virus latency-associated transcript. *Science* **287**, 1500-1503.

Peterson, B.A. and Frizzera, G. (1993) Multicentric Castleman's disease. *Semin. Oncol.* **20**, 636-647.

Pilder, S., Logan, J., and Shenk, T. (1984) Deletion of the gene encoding the adenovirus 5 early region 1b 21,000-molecular-weight polypeptide leads to degradation of viral and host cell DNA. *J. Virol.* **52**, 664-671.

Platt, G.M., Simpson, G.R., Mitnacht, S., and Schulz, T.F. (1999) Latent nuclear antigen of Kaposi's sarcoma-associated herpesvirus interacts with RING3, a homolog of the *Drosophila* female sterile homeotic (fsh) gene. *J. Virol.* **73**, 9789-9795.

Platt, N., Suzuki, H., Kurihara, Y., Kodama, T., and Gordon, S. (1996) Role for the class A macrophage scavenger receptor in the phagocytosis of apoptotic thymocytes in vitro. *Proc. Natl. Acad. Sci. U.S.A* **93**, 12456-12460.

Platt, N., da Silva, R.P., and Gordon, S. (1998) Class A scavenger receptors and the phagocytosis of apoptotic cells. *Biochem. Soc. Trans.* **26**, 639-644.

Plowright, W., Ferris, R.D., and Scott, G.R. (1960) Blue wildebeest and the aetiological agent of bovine malignant catarrhal fever. *Nature* **188**, 1167-1169.

Plowright W., MacAdam, R.F. and Armstrong J.A. (1963). Growth and characterisation of the virus of bovine malignant fever in east Africa. *J. Gen. Micro.* **39**: 253-266.

Plowright, W. (1965) Malignant catarrhal fever in East Africa. I. Behaviour of the virus in free-living populations of Blue wildebeest (*Gorgon taurinus taurinus*, burchell). *Res. Vet. Sci.* **35**, 56-68.

Plowright, W. (1967) Malignant catarrhal fever in East Africa 3. Neutralizing antibody in free-living wildebeest. *Res. Vet. Sci.* **8**, 129-136.

Plowright, W. (1968) Malignant Catarrhal Fever. *J. Am. Vet. Med. Assoc.* **152**:795-806.

Plowright, W., Kalunda, M., Jessett, D.M., and Herniman, K.A. (1972) Congenital infection of cattle with the herpesvirus causing malignant catarrhal fever. *Res. Vet. Sci.* **13**, 37-45.

Plowright, W., Herniman, K.A., Jessett, D.M., Kalunda, M., and Rampton, C.S. (1975) Immunisation of cattle against the herpesvirus of malignant catarrhal fever: failure of inactivated culture vaccines with adjuvant. *Res. Vet. Sci.* **19**, 159-166.

Plowright, W. (1990) Malignant catarrhal fever virus, *In* Z. Dinter and B. Morein (eds.), *Virus Infections of Ruminants*. Elsevier Science Publishers B.V., New York. p. 123-150.

- Preston,C.M. (2000) Repression of viral transcription during herpes simplex virus latency. *J.Gen.Virol.* **81**, 1-19.
- Purewal,A.S., Smallwood,A.V., Kaushal,A., Adegboye,D., and Edington,N. (1992) Identification and control of the cis-acting elements of the immediate early gene of equid herpesvirus type 1. *J.Gen.Virol.* **73 (Pt 3)**, 513-519.
- Rajcani,J. and Vojvodova,A. (1998) The role of herpes simplex virus glycoproteins in the virus replication cycle. *Acta Virol.* **42**, 103-118.
- Reed,J.C. (1998) Bcl-2 family proteins. *Oncogene* **17**, 3225-3236.
- Regula,K.M., Ens,K., and Kirshenbaum,L.A. (2003) Mitochondria-assisted cell suicide: a license to kill. *J.Mol.Cell Cardiol.* **35**, 559-567.
- Reid,H.W. and Rowe,L. (1973) The attenuation of a herpes virus (malignant catarrhal fever virus) isolated from hartebeest (*Alcelaphus buselaphus cokei* Gunther). *Res.Vet.Sci.* **15**, 144-146.
- Reid,H.W., Buxton,D., Corrigan,W., Hunter,A.R., McMartin,D.A., and Rushton,R. (1979) An outbreak of malignant catarrhal fever in red deer (*Cervus elephus*). *Vet.Rec.* **104**, 120-123.
- Reid,H.W., Buxton,D., Pow,I., Finlayson,J., and Berrie,E.L. (1983) A cytotoxic T-lymphocyte line propagated from a rabbit infected with sheep associated malignant catarrhal fever. *Res.Vet.Sci.* **34**, 109-113.
- Reid, H.W. and Buxton, D. (1984). Malignant catarrhal fever. Proceedings of the Royal Society of Edinburgh **82**: 261-273.
- Reid, H. W. and D. Buxton. (1989) Malignant Catarrhal Fever and the Gammaherpesvirinae of Bovidae, p. 116-162. In G. Wittmann (ed.), Herpesvirus Diseases of Cattle, Horses, and Pigs. Kluwer Academic Publishers, Boston.
- Reid,H.W., Buxton,D., Pow,I., and Finlayson,J. (1989) Isolation and characterisation of lymphoblastoid cells from cattle and deer affected with 'sheep-associated' malignant catarrhal fever. *Res.Vet.Sci.* **47**, 90-96.
- Reid,H.W. and Bridgen,A. (1991) Recovery of a herpesvirus from a roan antelope (*Hippotragus equinus*). *Vet.Microbiol.* **28**, 269-278.
- Reid, H. W. (2000). Malignant Catarrhal Fever. *Infectious diseases review* **2**, 20 - 22.
- Reyes,R.A. and Cockerell,G.L. (1998) Increased ratio of bcl-2/bax expression is associated with bovine leukemia virus-induced leukemogenesis in cattle. *Virology* **242**, 184-192.

- Rigaut,G., Shevchenko,A., Rutz,B., Wilm,M., Mann,M., and Seraphin,B. (1999) A generic protein purification method for protein complex characterization and proteome exploration. *Nat.Biotechnol.* **17**, 1030-1032.
- Rigaut,G., Shevchenko,A., Rutz,B., Wilm,M., Mann,M., and Seraphin,B. (1999) A generic protein purification method for protein complex characterization and proteome exploration. *Nat.Biotechnol.* **17**, 1030-1032.
- Roberge,C.J., Poubelle,P.E., Beaulieu,A.D., Heitz,D., and Gosselin,J. (1996) The IL-1 and IL-1 receptor antagonist (IL-1Ra) response of human neutrophils to EBV stimulation. Preponderance of IL-Ra detection. *J.Immunol.* **156**, 4884-4891.
- Robertson,E.S., Grossman,S., Johannsen,E., Miller,C., Lin,J., Tomkinson,B., and Kieff,E. (1995) Epstein-Barr virus nuclear protein 3C modulates transcription through interaction with the sequence-specific DNA-binding protein J kappa. *J.Virol.* **69**, 3108-3116.
- Roitt I., Brostoff J. and Male D. (1998). *Immunology* (5th Edition). Roitt I, Brostoff J. and Male (eds.). Mosby International Ltd, London.
- Roizman, B. a. K., D.M. (2001a). Herpes simplex viruses and their replication. In *Fields virology*, 4th edn, pp. 2399-2459. Edited by D. M. Knipe, Howley, P.M., Griffin, D.E., Martin, M.A., Lamb, R.A., Roizman, B., Straus, S.E.: Lippincott Williams and Wilkins.
- Roizman, B. a. P., P.E. (2001b). The Family Herpesviridae: A Brief Introduction. In *Fields Virology*, pp. 2381 - 2395. Edited by D. M. Knipe, Howley, P.M., Griffin, D.E., Lamb, R.A., Martin, M.A., Roizman, B. Straus, S.E.: Lippincott Williams & Wilkins.
- Rosbottom,J., Dalziel,R.G., Reid,H.W., and Stewart,J.P. (2002) Ovine herpesvirus 2 lytic cycle replication and capsid production. *J.Gen.Virol.* **83**, 2999-3002.
- Rosl,F. (1992) A simple and rapid method for detection of apoptosis in human cells. *Nucleic Acids Res.* **20**, 5243.
- Rossiter,P.B. (1981) Immunofluorescence and immunoperoxidase techniques for detecting antibodies to malignant catarrhal fever in infected cattle. *Trop.Anim Health Prod.* **13**, 189-192.
- Rossiter,P.B. (1982) Immunoglobulin response of rabbits infected with malignant catarrhal fever virus. *Res.Vet.Sci.* **33**, 120-122.
- Rossiter,P.B. (1983) Antibodies to malignant catarrhal fever virus in cattle with non-wildebeest-associated malignant catarrhal fever. *J.Comp Pathol.* **93**, 93-97.
- Roy,D.J., Ebrahimi,B.C., Dutia,B.M., Nash,A.A., and Stewart,J.P. (2000) Murine gammaherpesvirus M11 gene product inhibits apoptosis and is expressed during virus persistence. *Arch.Virol.* **145**, 2411-2420.

- Rurangirwa,F.R., Mushi,E.Z., and Karstad,L. (1982) Malignant catarrhal fever virus specific secretory IgA in nasal secretions of wildebeest calves. *Comp Immunol.Microbiol.Infect.Dis.* **5**, 429-436.
- Russell,J.H. and Ley,T.J (2002) Lymphocyte-mediated cytotoxicity. *Annu.Rev.Immunol.* **20**,323-70.
- Rweyemamu,M.M., Karstad,L., Mushi,E.Z., Otema,J.C., Jessett,D.M., Rowe,L., Drevemo,S., and Grootenhuis,J.G. (1974) Malignant catarrhal fever virus in nasal secretions of wildebeest: a probable mechanism for virus transmission. *J.Wildl.Dis.* **10**, 478-487.
- Rweyemamu,M.M., Mushi,E.Z., Rowe,L., and Karstad,L. (1976) Persistent infection of cattle with the herpesvirus of malignant catarrhal fever and observations on the pathogenesis of the disease. *Br.Vet.J.* **132**, 393-400.
- Ryan,K.M., Ernst,M.K., Rice,N.R. and Vousden,K.H. (2000) Role of NF-kappaB in p53-mediated programmed cell death. *Nature.* **404**, 892-897.
- Sakahira,H., Enari,M., and Nagata,S. (1998) Cleavage of CAD inhibitor in CAD activation and DNA degradation during apoptosis. *Nature* **391**, 96-99.
- Sample,J., Young,L., Martin,B., Chatman,T., Kieff,E., Rickinson,A., and Kieff,E. (1990) Epstein-Barr virus types 1 and 2 differ in their EBNA-3A, EBNA-3B, and EBNA-3C genes. *J.Virol.* **64**, 4084-4092.
- Sarid,R., Sato,T., Bohenzky,R.A., Russo,J.J., and Chang,Y. (1997) Kaposi's sarcoma-associated herpesvirus encodes a functional bcl-2 homologue. *Nat.Med.* **3**, 293-298.
- Sattler,M., Liang,H., Nettesheim,D., Meadows,R.P., Harlan,J.E., Eberstadt,M., Yoon,H.S., Shuker,S.B., Chang,B.S., Minn,A.J., Thompson,C.B., and Fesik,S.W. (1997) Structure of Bcl-xL-Bak peptide complex: recognition between regulators of apoptosis. *Science* **275**, 983-986.
- Schendel,S.L., Xie,Z., Montal,M.O., Matsuyama,S., Montal,M., and Reed,J.C. (1997) Channel formation by antiapoptotic protein Bcl-2. *Proc.Natl.Acad.Sci.U.S.A* **94**, 5113-5118.
- Schock,A. (1996) PhD thesis. University of Edinburgh.
- Schock,A., Collins,R.A., and Reid,H.W. (1998) Phenotype, growth regulation and cytokine transcription in Ovine Herpesvirus-2 (OHV-2)-infected bovine T-cell lines. *Vet.Immunol.Immunopathol.* **66**, 67-81.
- Schulz,T.F. (1998) Kaposi's sarcoma-associated herpesvirus (human herpesvirus-8). *J.Gen.Virol.* **79 (Pt 7)**, 1573-1591.

Schwede,T., Kopp,J., Guex,N., and Peitsch,M.C. (2003) SWISS-MODEL: An automated protein homology-modeling server. *Nucleic Acids Res.* **31**, 3381-3385.

Seal,B.S., Heuschele,W.P., and Klieforth,R.B. (1989) Prevalence of antibodies to alcelaphine herpesvirus-1 and nucleic acid hybridization analysis of viruses isolated from captive exotic ruminants. *Am.J.Vet.Res.* **50**, 1447-1453.

Seal,B.S., Klieforth,R.B., Welch,W.H., and Heuschele,W.P. (1989) Alcelaphine herpesviruses 1 and 2 SDS-PAGE analysis of virion polypeptides, restriction endonuclease analysis of genomic DNA and virus replication restriction in different cell types. *Arch.Virol.* **106**, 301-320.

Sears,A.E. and Roizman,B. (1990) Amplification by host cell factors of a sequence contained within the herpes simplex virus 1 genome. *Proc.Natl.Acad.Sci.U.S.A* **87**, 9441-9444.

Selman,I.E., Wiseman,A., Wright,N.G., and Murray,M. (1978) Transmission studies with bovine malignant catarrhal fever. *Vet.Rec.* **102**, 252-257.

Sgonc,R. and Wick,G. (1994) Methods for the detection of apoptosis. *Int.Arch.Allergy Immunol.* **105**, 327-332.

Shibasaki,F., Kondo,E., Akagi,T., and McKeon,F. (1997) Suppression of signalling through transcription factor NF-AT by interactions between calcineurin and Bcl-2. *Nature* **386**, 728-731.

Shimizu,S., Konishi,A., Kodama,T., and Tsujimoto,Y. (2000) BH4 domain of antiapoptotic Bcl-2 family members closes voltage-dependent anion channel and inhibits apoptotic mitochondrial changes and cell death. *Proc.Natl.Acad.Sci.U.S.A* **97**, 3100-3105.

Shisler,J., Yang,C., Walter,B., Ware,C.F., and Gooding,L.R. (1997) The adenovirus E3-10.4K/14.5K complex mediates loss of cell surface Fas (CD95) and resistance to Fas-induced apoptosis. *J.Virol.* **71**, 8299-8306.

Shisler,J.L. and Moss,B. (2001) Molluscum contagiosum virus inhibitors of apoptosis: The MC159 v-FLIP protein blocks Fas-induced activation of procaspases and degradation of the related MC160 protein. *Virology* **282**, 14-25.

Simas,J.P. and Efstathiou,S. (1998) Murine gammaherpesvirus 68: a model for the study of gammaherpesvirus pathogenesis. *Trends Microbiol.* **6**, 276-282.

Skulachev,V.P. (1996) Why are mitochondria involved in apoptosis? Permeability transition pores and apoptosis as selective mechanisms to eliminate superoxide-producing mitochondria and cell. *FEBS Lett.* **397**, 7-10.

Slee,E.A., Harte,M.T., Kluck,R.M., Wolf,B.B., Casiano,C.A., Newmeyer,D.D., Wang,H.G., Reed,J.C., Nicholson,D.W., Alnemri,E.S., Green,D.R. and Martin,S.J. (1999)

- Ordering the cytochrome c-initiated caspase cascade: hierarchical activation of caspases-2, -3, -6, -7, -8, and -10 in a caspase-9-dependent manner. *J.Cell.Biol.* **144**, 281-292.
- Smith,D.B. and Johnson,K.S. (1988) Single-step purification of polypeptides expressed in *Escherichia coli* as fusions with glutathione S-transferase. *Gene* **67**, 31-40.
- Spear,P.G., Eisenberg,R.J., and Cohen,G.H. (2000) Three classes of cell surface receptors for alphaherpesvirus entry. *Virology* **275**, 1-8.
- Spieker-Polet,H., Sittisombut,N., Yam,P.C., and Knight,K.L. (1990) Rabbit major histocompatibility complex. IV. Expression of major histocompatibility complex class II genes. *J.Immunogenet.* **17**, 123-132.
- Sturm,R.A., Das,G., and Herr,W. (1988) The ubiquitous octamer-binding protein Oct-1 contains a POU domain with a homeo box subdomain. *Genes Dev.* **2**, 1582-1599.
- Suggs,S.V., Wallace,R.B., Hirose,T., Kawashima,E.H., and Itakura,K. (1981) Use of synthetic oligonucleotides as hybridization probes: isolation of cloned cDNA sequences for human beta 2-microglobulin. *Proc.Natl.Acad.Sci.U.S.A* **78**, 6613-6617.
- Sun,Q., Matta,H., and Chaudhary,P.M. (2003) The human herpes virus 8-encoded viral FLICE inhibitory protein protects against growth factor withdrawal-induced apoptosis via NF-kappa B activation. *Blood* **101**, 1956-1961.
- Sunil-Chandra,N.P., Arno,J., Fazakerley,J., and Nash,A.A. (1994) Lymphoproliferative disease in mice infected with murine gammaherpesvirus 68. *Am.J.Pathol.* **145**, 818-826.
- Sutton,V.R., Davis,J.E., Cancilla,M., Johnstone,R.W., Ruefli,A.A., Sedelies,K., Browne,K.A. and Trapani,J.A. (2000) Initiation of apoptosis by granzyme B requires direct cleavage of bid, but not direct granzyme B-mediated caspase activation. *J.Exp.Med.* **192**, 1403-1414.
- Svobodova,J., Blaskovic,D., and Mistrikova,J. (1982) Growth characteristics of herpesviruses isolated from free living small rodents. *Acta Virol.* **26**, 256-263.
- Swa,S. (2001) PhD thesis. University of Edinburgh.
- Swa,S., Wright,H., Thomson,J., Reid,H., and Haig,D. (2001) Constitutive activation of Lck and Fyn tyrosine kinases in large granular lymphocytes infected with the gamma-herpesvirus agents of malignant catarrhal fever. *Immunology* **102**, 44-52.
- Szomolanyi,E., Medveczky,P., and Mulder,C. (1987) In vitro immortalization of marmoset cells with three subgroups of herpesvirus saimiri. *J.Virol.* **61**, 3485-3490.
- Takada,K. and Ono,Y. (1989) Synchronous and sequential activation of latently infected Epstein-Barr virus genomes. *J.Virol.* **63**, 445-449.

- Tanner, J., Weis, J., Fearon, D., Whang, Y., and Kieff, E. (1987) Epstein-Barr virus gp350/220 binding to the B lymphocyte CD3d receptor mediates adsorption, capping, and endocytosis. *Cell* **50**, 203-213.
- Telford, E.A., Watson, M.S., Aird, H.C., Perry, J., and Davison, A.J. (1995) The DNA sequence of equine herpesvirus 2. *J.Mol.Biol.* **249**, 520-528.
- Tham, K.M. (1997) Molecular and clinicopathological diagnosis of malignant catarrhal fever in cattle, deer and buffalo in New Zealand. *Vet.Rec.* **141**, 303-306.
- Thome, M., Schneider, P., Hofmann, K., Fickenscher, H., Meinel, E., Neipel, F., Mattmann, C., Burns, K., Bodmer, J.L., Schroter, M., Scaffidi, C., Krammer, P.H., Peter, M.E., and Tschopp, J. (1997) Viral FLICE-inhibitory proteins (FLIPs) prevent apoptosis induced by death receptors. *Nature* **386**, 517-521.
- Thompson, C.B. (1995) Apoptosis in the pathogenesis and treatment of disease. *Science* **267**, 1456-1462.
- Thornberry, N.A. and Lazebnik, Y. (1998) Caspases: enemies within. *Science* **281**, 1312-1316.
- Tierney, R.J., Steven, N., Young, L.S., and Rickinson, A.B. (1994) Epstein-Barr virus latency in blood mononuclear cells: analysis of viral gene transcription during primary infection and in the carrier state. *J.Virol.* **68**, 7374-7385.
- Toby, G.G. and Golemis, E.A. (2001) Using the yeast interaction trap and other two-hybrid-based approaches to study protein-protein interactions. *Methods* **24**, 201-217.
- Tsujimoto, Y. and Shimizu, S. (2000) Bcl-2 family: life-or-death switch. *FEBS Lett.* **466**, 6-10.
- Tsujimoto, Y. and Shimizu, S. (2002) The voltage-dependent anion channel: an essential player in apoptosis. *Biochimie* **84**, 187-193.
- Turner, A., Bruun, B., Minson, T., and Browne, H. (1998) Glycoproteins gB, gD, and gHgL of herpes simplex virus type 1 are necessary and sufficient to mediate membrane fusion in a Cos cell transfection system. *J.Virol.* **72**, 873-875.
- Usherwood, E.J., Ross, A.J., Allen, D.J., and Nash, A.A. (1996) Murine gammaherpesvirus-induced splenomegaly: a critical role for CD4 T cells. *J.Gen.Virol.* **77 (Pt 4)**, 627-630.
- van Loo, G., Saelens, X., van Gurp, M., MacFarlane, M., Martin, S.J., and Vandenabeele, P. (2002) The role of mitochondrial factors in apoptosis: a Russian roulette with more than one bullet. *Cell Death.Differ.* **9**, 1031-1042.
- van, B., V, Levine, B., Kapadia, S.B., Goldman, J.E., Speck, S.H., and Virgin, H.W. (2002) Critical role for a high-affinity chemokine-binding protein in gamma-herpesvirus-induced lethal meningitis. *J.Clin.Invest* **109**, 905-914.

Vander Heiden, M.G., Chandel, N.S., Williamson, E.K., Schumacker, P.T., and Thompson, C.B. (1997) Bcl-xL regulates the membrane potential and volume homeostasis of mitochondria. *Cell* **91**, 627-637.

Vink, C., Smit, M.J., Leurs, R., and Bruggeman, C.A. (2001) The role of cytomegalovirus-encoded homologs of G protein-coupled receptors and chemokines in manipulation of and evasion from the immune system. *J. Clin. Virol.* **23**, 43-55.

Virgin, H.W., Latreille, P., Wamsley, P., Hallsworth, K., Weck, K.E., Dal Canto, A.J., and Speck, S.H. (1997) Complete sequence and genomic analysis of murine gammaherpesvirus 68. *J. Virol.* **71**, 5894-5904.

Vossen, M.T., Westerhout, E.M., Soderberg-Naucler, C., and Wiertz, E.J. (2002) Viral immune evasion: a masterpiece of evolution. *Immunogenetics* **54**, 527-542.

Wagner, E.K. and Bloom, D.C. (1997) Experimental investigation of herpes simplex virus latency. *Clin. Microbiol. Rev.* **10**, 419-443.

Wang, F., Gregory, C., Sample, C., Rowe, M., Liebowitz, D., Murray, R., Rickinson, A., and Kieff, E. (1990) Epstein-Barr virus latent membrane protein (LMP1) and nuclear proteins 2 and 3C are effectors of phenotypic changes in B lymphocytes: EBNA-2 and LMP1 cooperatively induce CD23. *J. Virol.* **64**, 2309-2318.

Wang, G.H., Bertin, J., Wang, Y., Martin, D.A., Wang, J., Tomaselli, K.J., Armstrong, R.C., and Cohen, J.I. (1997) Bovine herpesvirus 4 BORFE2 protein inhibits Fas- and tumor necrosis factor receptor 1-induced apoptosis and contains death effector domains shared with other gamma-2 herpesviruses. *J. Virol.* **71**, 8928-8932.

Wang, G.H., Garvey, T.L., and Cohen, J.I. (1999) The murine gammaherpesvirus-68 M11 protein inhibits Fas- and TNF-induced apoptosis. *J. Gen. Virol.* **80 (Pt 10)**, 2737-2740.

Wang, H.G., Miyashita, T., Takayama, S., Sato, T., Torigoe, T., Krajewski, S., Tanaka, S., Hovey, L., III, Troppmair, J., Rapp, U.R., and . (1994) Apoptosis regulation by interaction of Bcl-2 protein and Raf-1 kinase. *Oncogene* **9**, 2751-2756.

Welch, H.M., Bridges, C.G., Lyon, A.M., Griffiths, L., and Edington, N. (1992) Latent equid herpesviruses 1 and 4: detection and distinction using the polymerase chain reaction and co-cultivation from lymphoid tissues. *J. Gen. Virol.* **73 (Pt 2)**, 261-268.

Weninger, W., Partanen, T.A., Breiteneder-Geleff, S., Mayer, C., Kowalski, H., Mildner, M., Pammer, J., Sturzl, M., Kerjaschki, D., Alitalo, K., and Tschachler, E. (1999) Expression of vascular endothelial growth factor receptor-3 and podoplanin suggests a lymphatic endothelial cell origin of Kaposi's sarcoma tumor cells. *Lab Invest* **79**, 243-251.

WHO/FAO (1976). World Health Organisation/Food and Agricultural Organisation, Consultation on the WHO/FAO program on comparative virology.

- Widmer, I., Wernli, M., Bachmann, F., Gudat, F., Cathomas, G., and Erb, P. (2002) Differential expression of viral Bcl-2 encoded by Kaposi's sarcoma-associated herpesvirus and human Bcl-2 in primary effusion lymphoma cells and Kaposi's sarcoma lesions. *J. Virol.* **76**, 2551-2556.
- Williams, T., Sale, D., and Hazlewood, S.A. (2001) BHRF1 is highly conserved in primate virus analogues of Epstein-Barr virus. *Intervirology* **44**, 55-58.
- Wilson-Annan, J., O'Reilly, L.A., Crawford, S.A., Hausmann, G., Beaumont, J.G., Parma, L.P., Chen, L., Lackmann, M., Lithgow, T., Hinds, M.G., Day, C.L., Adams, J.M., and Huang, D.C. (2003) Proapoptotic BH3-only proteins trigger membrane integration of prosurvival Bcl-w and neutralize its activity. *J. Cell Biol.* **162**, 877-887.
- Worthington, R.W. and Bigalke, R.D. (2001) A review of the infectious diseases of African wild ruminants. *Onderstepoort J. Vet. Res.* **68**, 291-323.
- Wright, H., Stewart, J.P., Ileri, R.G., Campbell, I., Pow, I., Reid, H.W., and Haig, D.M. (2003) Genome re-arrangements associated with loss of pathogenicity of the gamma-herpesvirus alcelaphine herpesvirus-1. *Res. Vet. Sci.* **75**, 163-168.
- Wu, G., Chai, J., Suber, T.L., Wu, J.W., Du, C., Wang, X. and Shi, Y. (2000) Structural basis of IAP recognition by Smac/DIABLO. *Nature.* **408**, 1008-1012.
- Wyllie, A. (1998) Apoptosis. An endonuclease at last. *Nature* **391**, 20-21.
- Wyllie, A.H., Kerr, J.F., and Currie, A.R. (1980) Cell death: the significance of apoptosis. *Int. Rev. Cytol.* **68**, 251-306.
- Wyllie, A.H. (1997) Apoptosis: an overview. *Br. Med. Bull.* **53**, 451-465.
- Yang, E., Zha, J., Jockel, J., Boise, L.H., Thompson, C.B., and Korsmeyer, S.J. (1995) Bad, a heterodimeric partner for Bcl-XL and Bcl-2, displaces Bax and promotes cell death. *Cell* **80**, 285-291.
- Yates, J., Warren, N., Reisman, D., and Sugden, B. (1984) A cis-acting element from the Epstein-Barr viral genome that permits stable replication of recombinant plasmids in latently infected cells. *Proc. Natl. Acad. Sci. U.S.A* **81**, 3806-3810.
- Yin, X.M., Oltvai, Z.N., and Korsmeyer, S.J. (1994) BH1 and BH2 domains of Bcl-2 are required for inhibition of apoptosis and heterodimerization with Bax. *Nature* **369**, 321-323.
- Yokoyama, A., Tanaka, M., Matsuda, G., Kato, K., Kanamori, M., Kawasaki, H., Hirano, H., Kitabayashi, I., Ohki, M., Hirai, K., and Kawaguchi, Y. (2001) Identification of major phosphorylation sites of Epstein-Barr virus nuclear antigen leader protein (EBNA-LP): ability of EBNA-LP to induce latent membrane protein 1 cooperatively with EBNA-2 is regulated by phosphorylation. *J. Virol.* **75**, 5119-5128.

York, I.A. and Rock, K.L. (1996) Antigen processing and presentation by the class I major histocompatibility complex. *Annu.Rev.Immunol.* **14**, 369-396.

Young, L.S., Dawson, C.W., Clark, D., Rupani, H., Busson, P., Tursz, T., Johnson, A., and Rickinson, A.B. (1988) Epstein-Barr virus gene expression in nasopharyngeal carcinoma. *J.Gen.Virol.* **69 (Pt 5)**, 1051-1065.

Zamzami, N., Marchetti, P., Castedo, M., Decaudin, D., Macho, A., Hirsch, T., Susin, S.A., Petit, P.X., Mignotte, B., and Kroemer, G. (1995) Sequential reduction of mitochondrial transmembrane potential and generation of reactive oxygen species in early programmed cell death. *J.Exp.Med.* **182**, 367-377.

Zdanov, A., Schalk-Hihi, C., Menon, S., Moore, K.W., and Wlodawer, A. (1997) Crystal structure of Epstein-Barr virus protein BCRF1, a homolog of cellular interleukin-10. *J.Mol.Biol.* **268**, 460-467.

Zhang, J., Liu, X., Scherer, D.C., van Kaer, L., Wang, X., and Xu, M. (1998) Resistance to DNA fragmentation and chromatin condensation in mice lacking the DNA fragmentation factor 45. *Proc.Natl.Acad.Sci.U.S.A* **95**, 12480-12485.

Zimmermann, W., Broll, H., Ehlers, B., Buhk, H.J., Rosenthal, A., and Goltz, M. (2001) Genome sequence of bovine herpesvirus 4, a bovine Rhadinovirus, and identification of an origin of DNA replication. *J.Virol.* **75**, 1186-1194.

Zou, H., Henzel, H.W.J., Liu, X., Lutschg, A. and Wang, X. (1997) Apaf-1, a human protein homologous to *C. elegans* CED-4, participates in cytochrome c-dependent activation of caspase-3. *Cell.* **90**, 405-413.

Appendices

Appendix 2.1 Primers used in this study

Primer	Sequence	Annealing temp
5 Bcl Gex	5' TGC TGG TCG ACC TTG CAT GAA AAT GTT GGG 3'	90
3 Bcl Gex T	5' AAT AAA GCG GCC GCG GTA ATT TAT CAA ATGG 5'	88
3 Bcl Gex	5' CCA TTA TTT GCG GCC GCA GTC ATT TCG TTT GAG TGG 3'	104
5pMSBCL	GTG ACA AGC TTC ATG AAA ATG TTG GGA G 3'	78
3pMSBcl	5' TTT CAA AGC TTG TCA TTT CGT TTG AGT GG 3'	80
GAPDH 5	5' CCT TCA TTG ACC TCA ACT ACA T 3'	62
GAPDH 3	5' CCA AAG TTG TCA TGG ATG ACC 3'	62
vbcI-5'	5' GAC GGA TCC ATG AAA ATG TTG GGA GAA CC-3'	86
vbcI2/3'a	5' TTT TGA GCT CTA GTC ATT TCG TTT GAG TGG 3'	80
Y4233	5' GCT GTG GTA CCT TGC CAT GAA AAT GTT GGG A 3'	88
Y4234	5' TAA AAG TCT AGA GGT AAT TTA TCA AAT GGA 3'	76
bcl2ahvF	5' GGA TCC ATG AAA ATG TTG GGA GAA CC 3'	63.2
bclahvR	5' CCA TGG TCG TTT GAG TGG TTC GGA AG 3'	66.4
BHRF1F	5' TCT AGA CCA TGG CCT ATT CAA CAA GGG AG 3'	66.7
BHRF1R	5' CCC GGG TCA GGC CAT GGC GTG TCT TCC TCT GGA GAT AAA TAA AT 3'	75

Appendix 2.2 Commercial Suppliers

Ambion Inc, Ambion (Europe) Ltd, Ermine Business Park, Spitfire Close,
Huntingdon, Cambridgeshire PE29 6XY
www.ambion.com

Difco Laboratories, Detroit, MI

Amersham Biosciences UK Ltd, Amersham Place, Little Chalfont,
Buckinghamshire HP7 9NA
www.amershambiosciences.com

Autogen Bioclear UK Ltd, Holly Ditch Farm, Mile Elm, Cane, Wiltshire SN11 0PY
info@autogenbioclear.com

BDH Laboratory Supplies, Poole UK

Bibby Sterilin Ltd, Tilling drive, Stone Staffs, T15 0SA

Bio-Rad laboratories Ltd, Bio-Rad House, Mayland Avenue, Hemel Hempstead,
Hertfordshire HP2 7TD
www.bio-rad.com

Cellzome AG, 160 Centennial Avenue, Centennial Park, Elstree, Hertfordshire WD6
3SH

Costar UK Ltd, 1 The Valley Centre, Gordon Road, High Wycombe, Bucks, HP13
6EQ

DakoCytomaton Ltd, Denmarl House, Angel Drive Ely, Cambridgeshire CB4 4ET
www.dakocytomaton.com

DYNEX Technologies Ltd, Columbia House, Cloumbia Drive, Worhting, West
Sussex BN13 3HD
www.dynextechnologies.com

ECACC, CAMR, Porton Down, Salisbury, Wiltshire, SP4 0JG
www.ecacc.org.uk

Eurocetus UK Ltd, Harefield, UK

Gibco BRL, Invitrogen Ltd, 3 Fountain Drive, Inchinnan Business Park, Paisley PA4
9RF
www.invitrogen.com

Greiner Labortechnik, Unit 5 Strondwater Business Park, Brunel Wat, Stonehouse,
Gloucestershire, GL10 3SX

Hybaid Ltd, Action Court, Ashford Rd, Ashford, Middlesex

Insight Biotechnonology Ltd, PO Box 520, Wembley, Middlesex HA9 7YN
www.insightbio.com

Invitrogen Ltd, 3 Fountain Drive, Inchinnan Business Park, Paisley PA4 9RF
www.invitrogen.com

Luckham Ltd, Burgesshill, Suffolk, UK

Marvel, Chivers, Dublin, Ireland

Nunc Inc, Fischer Scientific Ltd, Bishop Meadow Rd, Loughborough, LE11 5RG

Nalge Nunc International, Fischer Scientific Ltd, Bishop Meadow Rd,
Loughborough, LE11 5RG
www.fischer.com

Perbio Science UK Ltd, Century House, High St, Tattenhall, Cheshire CH3 9RJ

Promega UK, Delta House, Chilworth Science Park, Southampton,
www.promega.com

QIGEN Ltd, Boundary Court, Gatwick Rd, Crawley, West Sussex
www.QIAGEN.com

R&D Systems Europe Ltd, 19 Barton Lane, Abingdon Science Park, Abingdon, Oxon

Roche Dignostics Ltd, Bell lane, Lewes, East Sussex
www.roche.com

Sigma-Aldrich Company Ltd, Dorset, UK
www.sigmaaldrich.com

Stratagene Europe, GebouwCalifornia, Hogehilweg 15, 1101 CB Amsterdam,
Zuidoost
www.stratagene.com

ThermoShandon, 171 Industry dr, Pittsburgh, PA 15272 USA
www.shandon.com

TPP AG, Zollstrasse 155, 8219 Trasadingen, Switzerland